NATIONAL CENTER FOR EARTHQUAKE ENGINEERING RESEARCH

State University of New York at Buffalo

NCEER-Taisei Corporation Research Program on Sliding Seismic Isolation Systems for Bridges:

Experimental and Analytical Study of a Friction Pendulum System (FPS)

by

M.C. Constantinou, P. Tsopelas, Y-S. Kim and S. Okamoto

State University of New York at Buffalo
Department of Civil Engineering
Buffalo, New York 14260
and
Taisei Corporation
Sanken Building
25-1, HyaKunin-cho 3-chome
Shinjuku-Ku 169
Tokyo, Japan

Technical Report NCEER-93-0020

November 1, 1993

This research was conducted at the State University of New York at Buffalo and Taisei Corporation and was partially supported by the National Science Foundation under Grant No. BCS 90-25010 and the New York State Science and Technology Foundation under Grant No. NEC-91029.

PB94-142775

NCEER-Taisei Corporation Research Program on Sliding Seismic Isolation Systems for Bridges:

Experimental and Analytical Study of a Friction Pendulum System (FPS)

by

M.C. Constantinou[1], P. Tsopelas[2], Y-S. Kim[2] and S. Okamoto[3]

November 1, 1993

Technical Report NCEER-93-0020

NCEER Project Numbers 90-2101 and 91-5411B
and
Taisei Corporation Grant 150-6889A

NSF Master Contract Number BCS 90-25010
and
NYSSTF Grant Number NEC-91029

1 Associate Professor, Department of Civil Engineering, State University of New York at Buffalo
2 Research Assistant, Department of Civil Engineering, State University of New York at Buffalo
3 Research Engineer, Technology Research Center, Taisei Corporation, Yokohama, Japan

NATIONAL CENTER FOR EARTHQUAKE ENGINEERING RESEARCH
State University of New York at Buffalo
Red Jacket Quadrangle, Buffalo, NY 14261

PREFACE

The National Center for Earthquake Engineering Research (NCEER) was established to expand and disseminate knowledge about earthquakes, improve earthquake-resistant design, and implement seismic hazard mitigation procedures to minimize loss of lives and property. The emphasis is on structures in the eastern and central United States and lifelines throughout the country that are found in zones of low, moderate, and high seismicity.

NCEER's research and implementation plan in years six through ten (1991-1996) comprises four interlocked elements, as shown in the figure below. Element I, Basic Research, is carried out to support projects in the Applied Research area. Element II, Applied Research, is the major focus of work for years six through ten. Element III, Demonstration Projects, have been planned to support Applied Research projects, and will be either case studies or regional studies. Element IV, Implementation, will result from activity in the four Applied Research projects, and from Demonstration Projects.

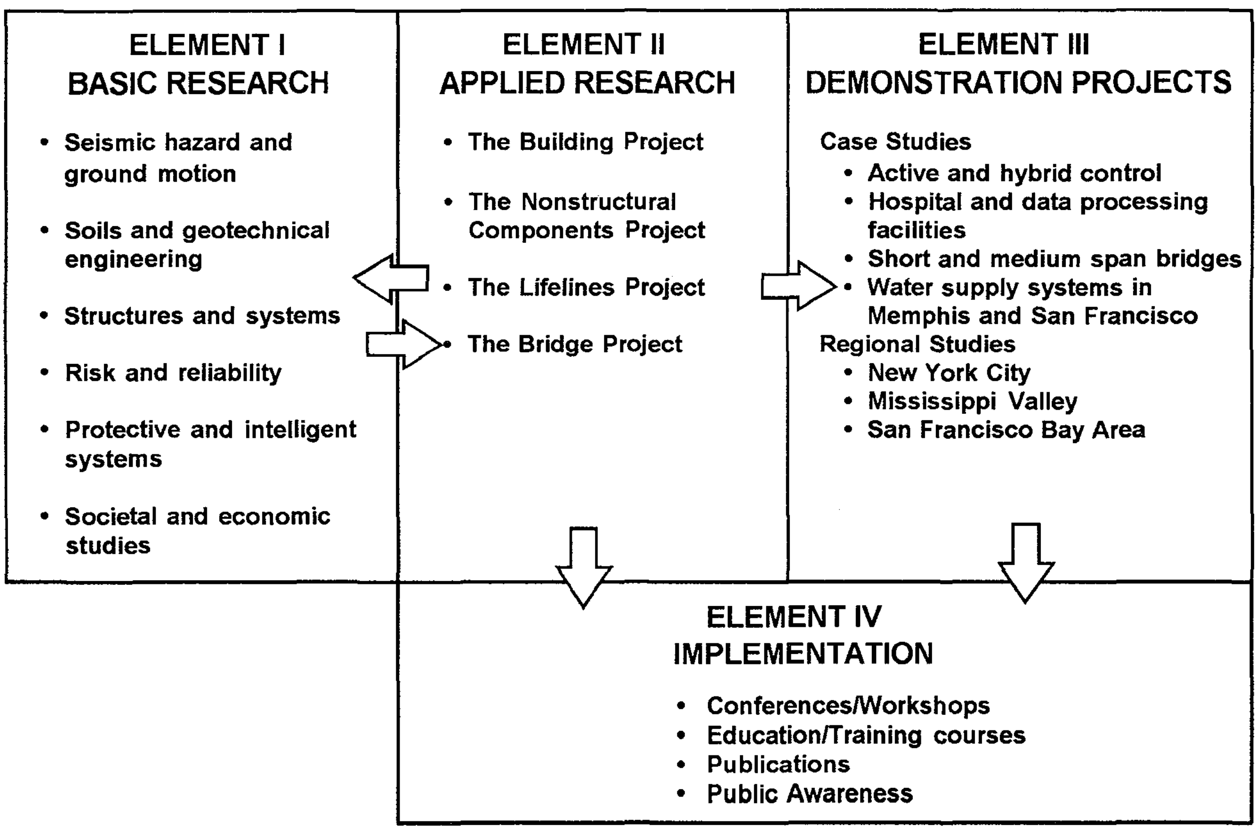

Research tasks in the **Bridge Project** expand current work in the retrofit of existing bridges and develop basic seismic design criteria for eastern bridges in low-to-moderate risk zones. This research parallels an extensive multi-year research program on the evaluation of gravity-load design concrete buildings. Specifically, tasks are being performed to:

1. Determine the seismic vulnerability of bridge structures in regions of low-to-medium seismicity, and in particular of those bridges in the eastern and central United States.

2. Develop concepts for retrofitting vulnerable bridge systems, particularly for typical bridges found in the eastern and central United States.

3. Develop improved design and evaluation methodologies for bridges, with particular emphasis on soil-structure mechanics and its influence on bridge response.

4. Review seismic design criteria for new bridges in the eastern and central United States.

The end product of the **Bridge Project** will be a collection of design manuals, pre-standards and design aids which will focus on typical eastern and central United States highway bridges. Work begun in the **Bridge Project** has now been incorporated into the **Highway Project.**

The **protective and intelligent systems program** constitutes one of the important areas of research in the **Bridge Project**. Current tasks include the following:

1. Evaluate the performance of full-scale active bracing and active mass dampers already in place in terms of performance, power requirements, maintenance, reliability and cost.
2. Compare passive and active control strategies in terms of structural type, degree of effectiveness, cost and long-term reliability.
3. Perform fundamental studies of hybrid control.
4. Develop and test hybrid control systems.

This report describes the results of an experimental study of the behavior of the Friction Pendulum System (FPS) in bridge seismic isolation. Earthquake simulator tests have been performed on a model bridge structure both isolated with Friction Pendulum System bearings and non-isolated. The experimental results demonstrate a marked increase of the capacity of the isolated bridge to withstand earthquake forces under all conditions. Analytical techniques are used to predict the dynamic response of the system and the obtained results are in very good agreement with the experimental results.

PB94-142775

ABSTRACT

This report describes the results of an experimental study of the behavior of the Friction Pendulum System (FPS) in bridge seismic isolation. Earthquake simulator tests have been performed on a model bridge structure both isolated with Friction Pendulum System bearings and non-isolated. The experimental results demonstrate a marked increase of the capacity of the isolated bridge to withstand earthquake forces under all conditions. Analytical techniques are used to predict the dynamic response of the system and the obtained results are in very good agreement with the experimental results.

ACKNOWLEDGEMENTS

Financial support for this project has been provided by Taisei Corporation, Japan and the National Center for Earthquake Engineering Research, Projects No. 902101 and 915411B. The FPS bearings used in the study were supplied by Earthquake Protection Systems, Inc., San Francisco, California.

TABLE OF CONTENTS

TABLE OF CONTENTS (Cont'd)

LIST OF ILLUSTRATIONS

LIST OF ILLUSTRATIONS (Cont'd)

LIST OF ILLUSTRATIONS (Cont'd)

LIST OF ILLUSTRATIONS (Cont'd)

LIST OF ILLUSTRATIONS (Cont'd)

LIST OF ILLUSTRATIONS (Cont'd)

LIST OF ILLUSTRATIONS (Cont'd)

LIST OF ILLUSTRATIONS (Cont'd)

LIST OF ILLUSTRATIONS (Cont'd)

LIST OF TABLES

SECTION 1

INTRODUCTION

Seismic isolation systems are typified by the use of either elastomeric or sliding bearings. Elastomeric isolation systems have been used in the seismic isolation of buildings in Japan and the United States (Buckle 1990, Soong 1992, Kelly 1993). Several other countries, such as New Zealand and Italy among others, have a number of applications of elastomeric isolation systems in buildings (Buckle 1990, Martelli 1993).

Sliding isolation systems in buildings have been widely used in the former Soviet Union, where over 200 buildings are now seismically isolated (Constantinou 1991a, Eisenberg 1992). In Japan, Taisei Corporation constructed three buildings on the TASS sliding isolation system (Kawamura 1988, Constantinou 1991a). In the United States, sliding isolation systems have recently been selected for the retrofit of three buildings (Soong 1992, Kelly 1993). In particular, spherical sliding or FPS bearings (Zayas 1987, Mokha 1990b and 1991) have been selected for the retrofit of the U.S. Court of Appeals building in San Francisco. This historic structure with a floor area of 31500m^2, will be, when completed, the largest base-isolated structure in the U.S. and one of the largest in the world (Soong 1992).

For the first time in the U.S., the isolation system selection for U.S. Court of Appeals was based on technical rating and competitive bidding of elastomeric and sliding isolation systems. Interestingly, the FPS isolation system received the highest technical rating and had the least cost (Palfalvi 1993). This represents a turning point for the implementation of seismic isolation in the U.S. Sliding isolation systems are now regarded as technically equivalent and potentially less expensive than elastomeric isolation systems.

Seismic isolation of bridge structures has been widely implemented in New Zealand and Italy (Buckle 1990, Medeot 1991, Martelli 1993). While in New Zealand the application is exclusively with elastomeric systems, in Italy the application is primarily with sliding systems. Over 150 km of isolated bridge deck in Italy is supported by sliding bearings together with various forms of restoring force and energy dissipation devices (Medeot 1991, Constantinou 1991a).

Japan has over 100 concrete railway bridges of the Shinkansen supported by sliding bearings together with viscous fluid devices, called the KP-stoppers, for restricting displacements within acceptable limits (Buckle 1990, Constantinou 1991a). This system is regarded as an early form of sliding isolation system.

More recently, Japan moved towards a cautious implementation of modern seismic isolation systems in bridges. So far, the application is restricted to only longitudinal isolation using elastomeric systems (Kawashima 1991).

The application of seismic isolation to bridges in the U.S. followed an interesting development. Until 1989, only six bridges were isolated, of which five were retrofit projects in California and one was a new construction in Illinois (Buckle 1990). While the 1989 Loma Prieta earthquake resulted in an accelerated implementation of seismic isolation systems to buildings, this has not been the case in bridges. Rather, we observe a renewed interest and new applications of bridge seismic isolation following the development of specifications for seismic isolation design (ICBO 1991, AASHTO 1991) and the adoption of seismic design guidelines for bridges in the entire U.S. The lack of specifications for the design of seismic isolated structures was regarded as an impediment to the application of the technology (Mayes 1990). Today, 57 bridges of total deck length exceeding 11 km are open to traffic, in the construction process or the design process in the U.S. Interestingly, the majority of these bridges are located in the Eastern United States.

While seismic isolation systems found application to over 200 bridges, large scale testing of bridge isolation systems has been so far limited to three studies which concentrated on elastomeric systems (Kelly 1986, Kawashima 1991) and one specific sliding system (Constantinou 1991a and 1992a). All three studies were restricted to models with rigid piers or abutments and rigid decks. The effects of pier flexibility, pier strength, deck flexibility and distribution of isolation elements could not be studied in these experimental programs. Rather, these effects were studied by analytical techniques and found to be significant (Constantinou 1991a, Kartoum 1992).

The study reported herein concentrates on the Friction Pendulum (or FPS) sliding isolation system. It was carried out as part of the NCEER-Taisei Corporation research project on bridge seismic isolation systems. The study includes a comprehensive testing program utilizing a flexible pier bridge model.

SECTION 2

NCEER-TAISEI CORPORATION RESEARCH PROJECT ON BRIDGE SLIDING SEISMIC ISOLATION SYSTEMS

In 1991, the National Center for Earthquake Engineering Research and Taisei Corporation began a collaborative research project on the development and verification of advanced sliding seismic isolation systems for bridges (Constantinou 1992b). The project included also the study of established sliding isolation systems such as the Friction Pendulum (or FPS) system (Zayas 1987, Mokha 1990b and 1991) and the lubricated sliding bearing/hysteretic steel damper system used in a large number of bridges in Italy (Medeot 1991, Marioni 1991).

The project had two portions: one concentrated on active systems and was carried out at Taisei Corporation and Princeton University, and the other concentrated on passive systems and was carried out at the University at Buffalo and Taisei Corporation. The Buffalo/Taisei portion of the project had the objective of producing a class of advanced passive sliding seismic isolation systems by modifying and/or adapting existing technology. Particular emphasis has been given to the adaptation and use of aerospace and military hardware in either the form of restoring force and damping devices or in the form of high performance composite materials in the construction of sliding bearings. The following systems were experimentally studied:

(1) Flat sliding bearings consisting of PTFE or PTFE-based composites in contact with polished stainless steel (coefficient of sliding friction at high velocity of sliding in the range of 0.07 to 0.15) and in combination with
   - (a) Rubber restoring force devices,
   - (b) Rubber restoring force devices and fluid viscous dampers,
   - (c) Wire rope restoring force devices, and
   - (d) Fluid restoring force/damping devices.

(2) Spherically shaped FPS sliding bearings.

(3) Flat lubricated PTFE-stainless steel sliding bearings in combination with yielding E-shaped mild steel devices.

This report contains the results of the experimental study, interpretation of the results and analytical modeling of the Friction Pendulum (or FPS) isolation system.

SECTION 3

FRICTION PENDULUM (or FPS) SEISMIC ISOLATION SYSTEM

The principles of operation of the FPS bearing have been established by Zayas, 1987 and Mokha 1990b and 1991. Herein, we restate these principles and provide a complete description of the behavior of the bearing which is valid at large displacements.

3.1 Principles of Operation and Mathematical Modeling

A cross section view of an FPS is shown in Figure 3-1. The bearing consists of a spherical sliding surface and an articulated slider which is faced with a high pressure capacity bearing material. The bearing may be installed as shown in Figure 3-1 or upside-down with the spherical surface facing down rather than up. In both installation methods the behavior is identical.

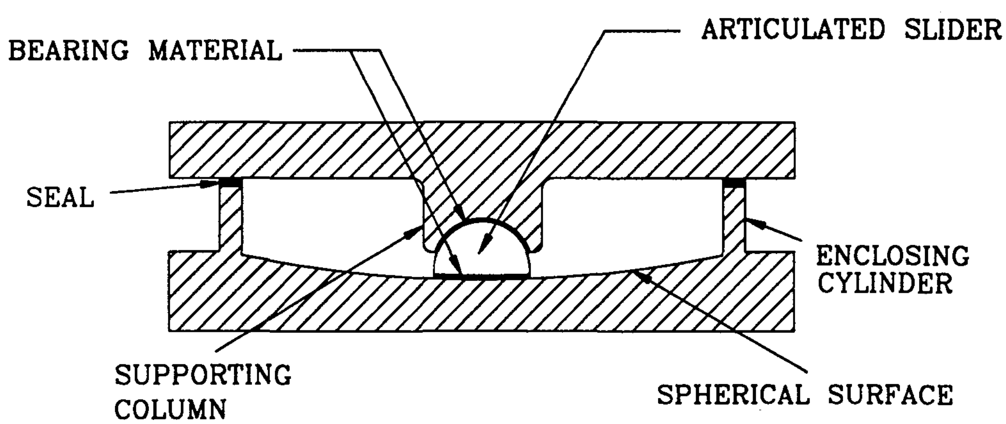

Figure 3-1 FPS Bearing Section

The bearing is constructed of steel with the articulated slider and the spherical sliding surface made of stainless steel. Specifically, the spherical sliding surface consists of highly polished austenitic, type 316 stainless steel. All sliding interfaces, that is those of the articulated slider with the spherical surface and the supporting column, are faced with a high bearing capacity, self lubricating, PTFE-based composite material. The rated load capacity of this material is about 400 MPa (60 ksi). The material is characterized by low friction, low wear and marked insensitivity of its frictional properties to significant temperature changes. It has been used for the last 30 years in applications of the U.S. aerospace and military industry such as commercial and military aircraft, satellite construction, helicopter bearings and actuator systems. It has also been used in industrial applications such as heavy machinery and equipment, cranes etc.

The basic principle of operation of the FPS bearing is illustrated in Figure 3-2. The motion of a structure supported by these bearings is identical to that of pendulum motion with the additional beneficial effect of friction at the sliding interface.

The force needed to produce displacement of the FPS bearing consist of the combination of restoring force during the induced rising of the structure along the spherical surface and of friction force at the sliding interface. The derivation of the force-displacement relation is based on Figure 3-3. The FPS bearing is considered in its deformed position under the action of a lateral force F. The horizontal and vertical components of displacement are respectively given by

$$u = R\sin\theta \tag{3-1}$$

$$v = R(1-\cos\theta) \tag{3-2}$$

where R is the radius of curvature of the spherical sliding surface. From equilibrium of the bearing in the vertical and horizontal directions it is obtained that

$$W - S\cos\theta + F_f\sin\theta = 0 \tag{3-3}$$

$$F - S\sin\theta - F_f\cos\theta = 0 \tag{3-4}$$

where W is the weight carried by the bearing and F_f is the friction force at the sliding interface.

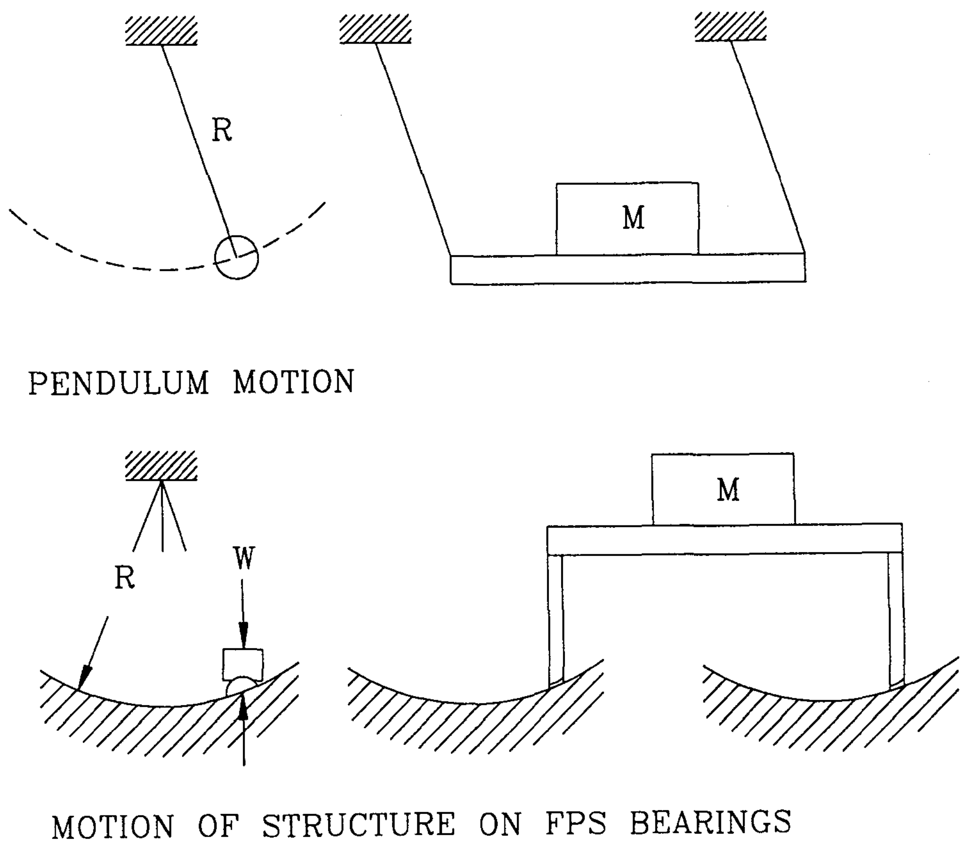

Figure 3-2 Basic Principle of Operation of FPS Bearing

Solution of Equations (3-3) and (3-4) results in

$$F = W\tan\theta + \frac{F_f}{\cos\theta} \tag{3-5}$$

The term Wtanθ represents the restoring force in its most general form (θ may be large), whereas the term F_f / cosθ represents the contribution of friction.

The stiffness of the bearing is derived by dividing the restoring force by the displacement u

$$K = \frac{F}{u} = \frac{W}{R\cos\theta} \tag{3-6}$$

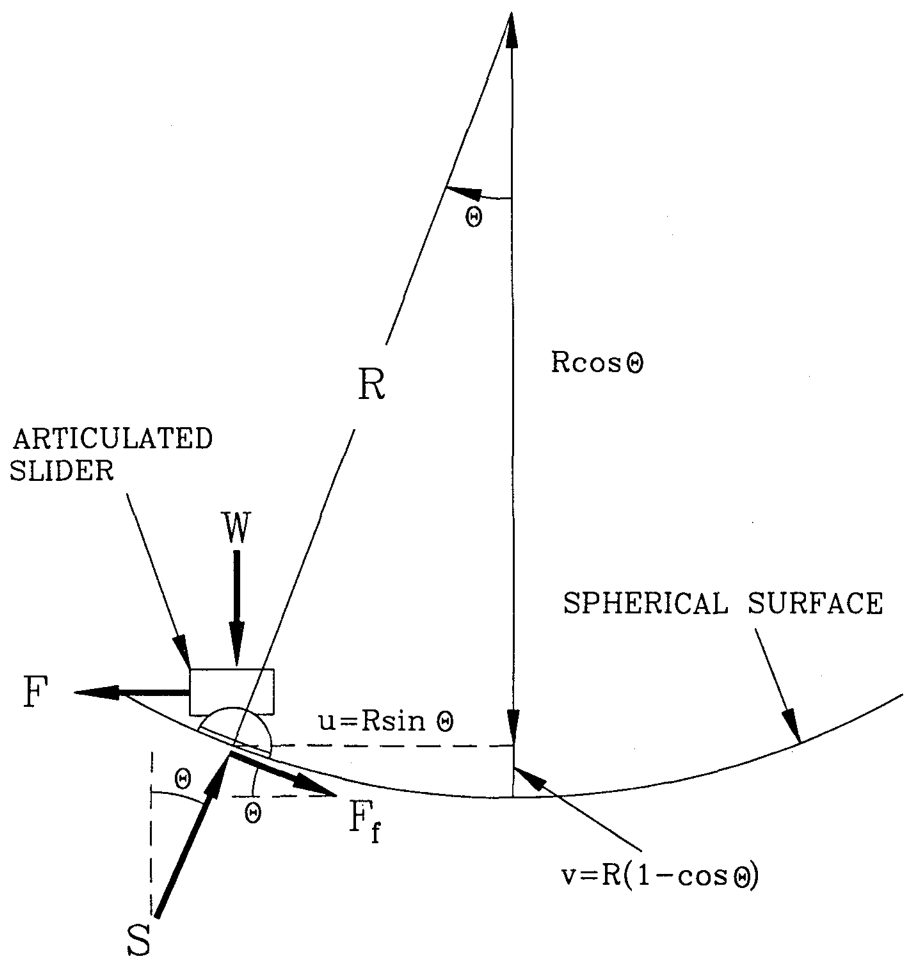

Figure 3-3 Free Body Diagram of FPS Bearing

Accordingly, the force needed to induce a displacement u in the horizontal direction is given in the general case of large θ by

$$F = \frac{W}{R\cos\theta}u + \frac{F_f}{\cos\theta} \tag{3-7}$$

For small values of angle θ, $\cos\theta \approx 1$ and Equations (3-6) and (3-7) take the linearized form

$$K = \frac{W}{R} \tag{3-8}$$

$$F = \frac{W}{R}u + \mu W sgn(\dot{u}) \tag{3-9}$$

in which now the friction force F_f has been replaced by the product of the coefficient of friction μ and weight W. Furthermore, $\dot{u}$ represents the horizontal component of velocity. Equations (3-8) and (3-9) are valid for all practical purposes. FPS bearings are typically designed for displacement u < 0.2 R, so that the error due to linearization of Equations (3-6) and (3-7) is insignificant.

Returning now to Equation (3-8), the period of free vibration is derived

$$T = 2\pi\left(\frac{W}{Kg}\right)^{1/2} = 2\pi\left(\frac{R}{g}\right)^{1/2} \tag{3-10}$$

The period is independent of the mass of the structure and dependent only on the geometry of the bearing. Thus, the period does not change if the weight of the structure changes or is different than assumed.

Furthermore, Equation (3-9) demonstrates that the lateral force is directly proportional to the supported weight. As a result of this significant property, the center of lateral rigidity of the isolation system coincides with the center of mass of the structure. This property makes the FPS bearings particularly effective at minimizing adverse torsional motion in asymmetric structures.

3.2 Properties of FPS Bearings

As with all seismic isolation systems, the intent of isolation is to substantially reduce the seismic forces to the structural system by introducing flexibility and energy absorption capability. The FPS isolation bearings produce this effect while they furthermore have some unique properties. These properties are:

(1) Period of vibration which is independent of the supported mass.

(2) Their lateral force is directly proportional to the weight they carry and, thus, the isolation system force always develops at the center of mass of the supported structure. This property minimizes adverse torsional motions.

(3) They provide rigidity to wind and minor earthquake loads. This is accomplished by the friction in the bearings which do not allow motion until the static friction limit is exceeded.

(4) They have high vertical load capacity and stability. Owing to their unique construction they do not exhibit P-Δ effects at large displacements. Furthermore, the enclosing cylinder of the bearing provides lateral displacement restraint.

(5) Their properties of flexibility and energy absorption capability are not interrelated. The first is entirely controlled by geometry (radius R) and the second is controlled by friction at the sliding interface. This property allows for optimum design of the isolation system.

SECTION 4

MODEL FOR EARTHQUAKE SIMULATOR TESTING

4.1 Bridge Model

The bridge model was designed to have flexible piers so that under non-isolated conditions the fundamental period of the model in the longitudinal direction is 0.25s (or 0.5s in prototype scale).

The bridge model is shown in Figure 4-1. At quarter length scale, it had a clear span of 4.8m (15.7 feet), height of 2.53m (8.3 feet) and total weight of 157.8 kN (35.5 kips). The deck consisted of two AISC W14x90 sections which were transversely connected by beams. Additional steel and lead weights were added to reach the model deck weight of 140kN (31.5 kips), as determined by the similitude requirements. Each pier consisted of two AISC TS 6 x 6 x 5/16 columns with a top made of a channel section which was detailed to have sufficient torsional rigidity. The tube columns were connected to beams which were bolted to a concrete extension of the shake table. In this configuration, the column loads were transferred at a point located 0.57m (1.87 ft) beyond the edge of the shake table. While the overhangs of the concrete shake table extension could safely carry the column load of over 80kN (18 kips), they had some limited vertical flexibility which during seismic testing resulted in vertical motion of the piers and the supported deck.

The piers were designed to have in their free standing cantilever position a period of 0.1s (0.2s in prototype scale) when fully loaded (load cells and bottom part of bearings). Furthermore, the piers were detailed to yield under the combined effects of gravity load (40kN each column) and 50 percent of the gravity load applied as horizontal load at each bearing location. The stiffness of each pier was verified by pulling the piers against each other on the shake table. During the test the piers were also proof-loaded to their rated capacity and the results were used to calibrate the strain gage load cell of each column.

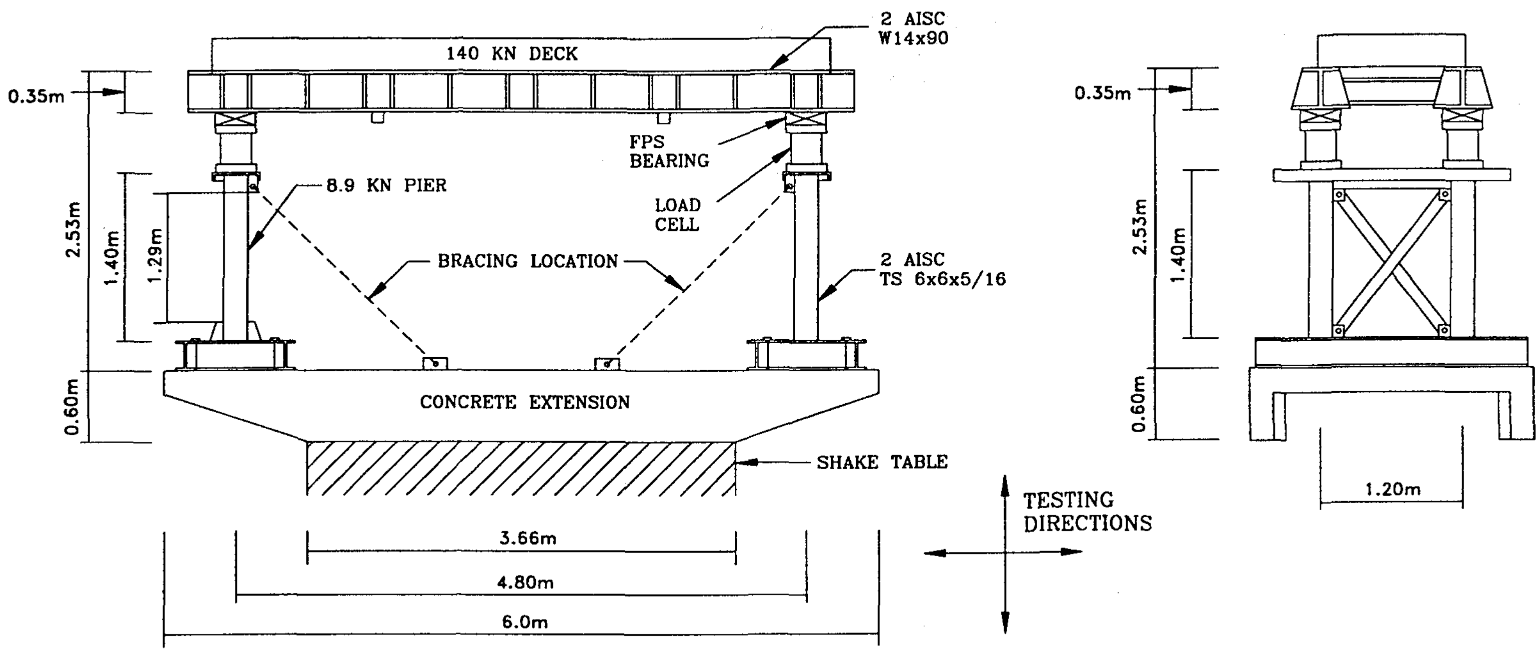

Figure 4-1 Schematic of Quarter Scale Bridge Model

Identification of the model was conducted by exciting the shake table with a 0-20 Hz banded white noise of 0.03g peak acceleration. Acceleration transfer functions of each free standing pier and of the assembled bridge model with all bearings fixed against translational movement (but not rotation) revealed the following properties: fundamental period of free standing pier equal to 0.096s and fundamental period of non-isolated bridge in the longitudinal direction equal to 0.26s. These values are in excellent agreement with the design values of 0.1s and 0.25s, respectively.

Damping in the model was estimated to be 0.015 of critical for the free standing piers and 0.02 of critical for the entire model in its non-isolated condition. Identification tests of the model were also conducted with white noise input of 0.1g peak table acceleration to obtain a fundamental period of 0.25s and corresponding damping ratio of 0.04 of critical. The increased damping was the result of hysteretic action, not in the columns of the model but in the overhangs of the concrete extension of the shake table. During shake table testing of the non-isolated model, the recorded loops of shear force versus displacement of the piers displayed hysteretic action (see section 5). Estimates of damping ratio from these loops were in the range of 0.04 to 0.08 of critical. Thus while the columns of the piers remained elastic, the pier system displayed realistic hysteretic action with equivalent damping ratio of at least 5 percent of critical.

The design of the model bridge was based in the similitude laws for artificial mass simulation (Sabnis 1983). A summary of the scale factors in the model is presented in Table 4-I.

4.2 Friction Pendulum (or FPS) Bearings

The isolation system consisted of four FPS bearings which were located on top of load cells as shown in Figure 4-1. The geometry of the bearing is presented in Figure 4-2, and a view of an open FPS bearing is shown in Figure 4-3. The bearings were installed with the spherical surface facing down. The radius of curvature of the spherical sliding surface was R=558.8mm (22 inches) so that the period of vibration of the isolation system was 1.5s (Equation 3-10). The displacement capacity of the bearing was 89mm (3.5 inches) in all directions.

Table 4-I : Summary of Scale Factors in Bridge Model

QUANTITY	DIMENSION	SCALE FACTOR*
Linear Dimension	L	4
Displacement	L	4
Velocity	LT^{-1}	2
Acceleration	LT^{-2}	1
Time	T	2
Frequency	T^{-1}	0.5
Force	F	16
Stress	FL^{-2}	1
Pressure	FL^{-2}	1
Strain	---	1

* PROTOTYPE / MODEL

Four different materials were used at the sliding interface. All four were self-lubricating PTFE-based composites. They were assigned numbers No.1, 2, 3 and 4. Of these, No.1 was identical to the material used in the bearings of the U.S. Court of Appeals building in San Francisco. The materials were tested under an average bearing pressure (load on bearing divided by the geometrical area of the slider) of 17.2 MPa (2.5 ksi) and 275.6 MPa (40 ksi). This was accomplished by using different articulated sliders with bearing contact areas of diameter equal to 12.7mm and 50.8mm, respectively.

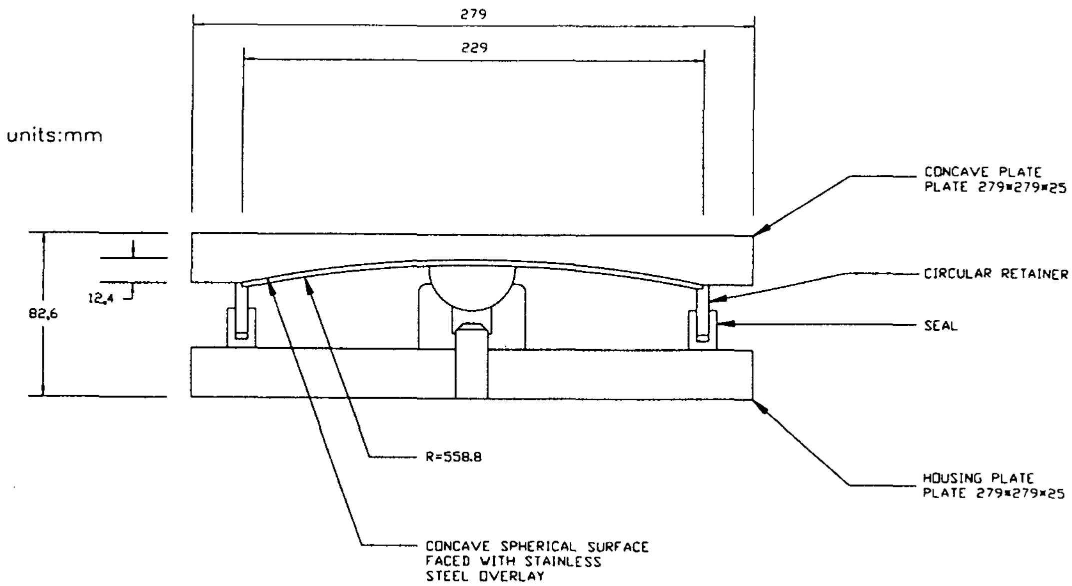

Figure 4-2 Construction of Friction Pendulum System Bearing

The frictional properties of these four materials in contact with polished stainless steel were determined in identification tests prior to and following the seismic testing. In these tests the piers were stiffened by braces (see Figure 4-1) and the deck was connected by rods to a nearby reaction frame. The shake table was then driven in displacement-controlled mode with specified frequency and amplitude of harmonic motion. The lateral force in each bearing was recorded by the supporting load cell. From recorded loops of force versus bearing displacement the friction force was extracted. Division by the normal load, which was also monitored by the load cell, gave the coefficient of sliding friction. Furthermore, the coefficient of friction was extracted from recorded loops of force versus bearing displacement during seismic testing.

The results are presented in Figures 4-4 and 4-5 as function of bearing pressure and velocity of sliding. The coefficient of friction follows the relation proposed by Constantinou 1990a

$$\mu = f_{max} - (f_{max} - f_{min})\exp(-a|\dot{u}|) \qquad (4\text{-}1)$$

where f_{max} is the coefficient of friction at high velocity of sliding, f_{min} is the coefficient

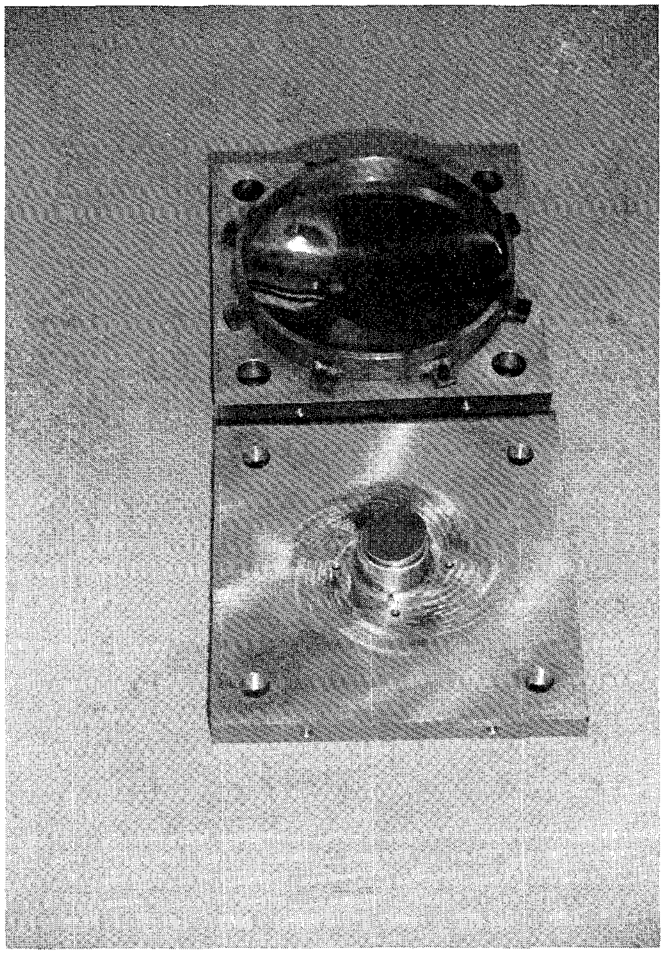

Figure 4-3 View of FPS Bearing

of friction at essentially zero velocity of sliding and a is a parameter controlling the variation of the coefficient with velocity of sliding. Values of the model parameters are presented in Table 4-II. It may be seen in Figures 4-4 and 4-5 that the experimental results agree well with the predictions of the calibrated model of Equation 4-1.

Of interest is to note that all four composite materials had nearly the same frictional properties. In all four, the breakaway (or static) coefficient of friction was found to be always less than f_{max} regardless of the duration of dwell of load which varied between a few minutes and 24 hours.

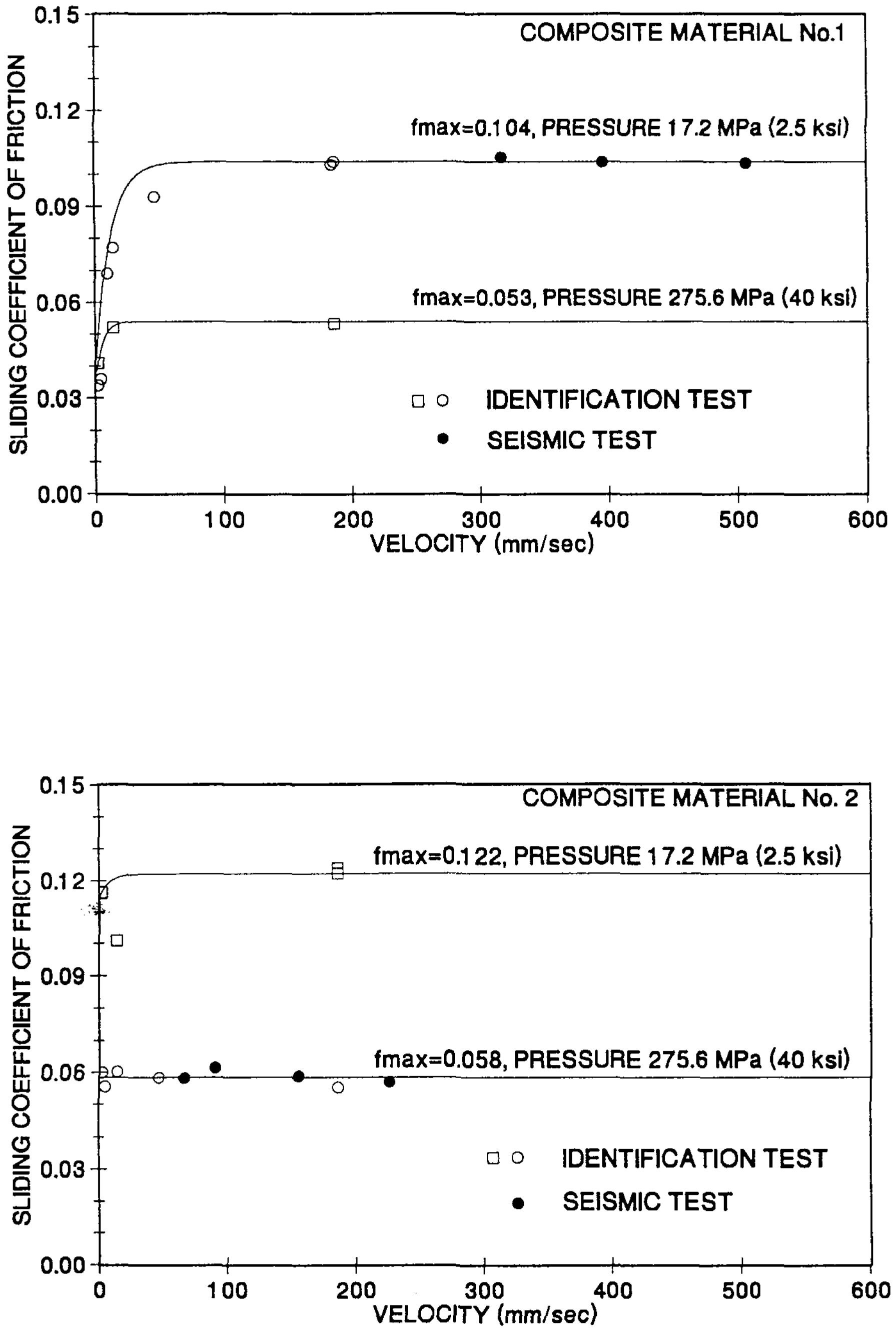

Figure 4-4 **Coefficient of Sliding Friction as Function of Bearing Pressure and Sliding Velocity for Composite Materials No.1 and 2 in Contact with Polished Stainless Steel**

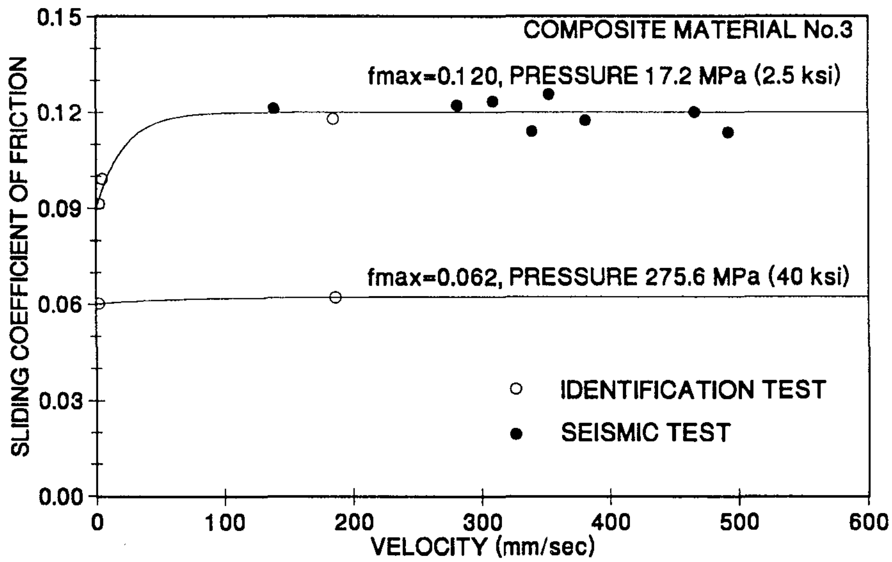

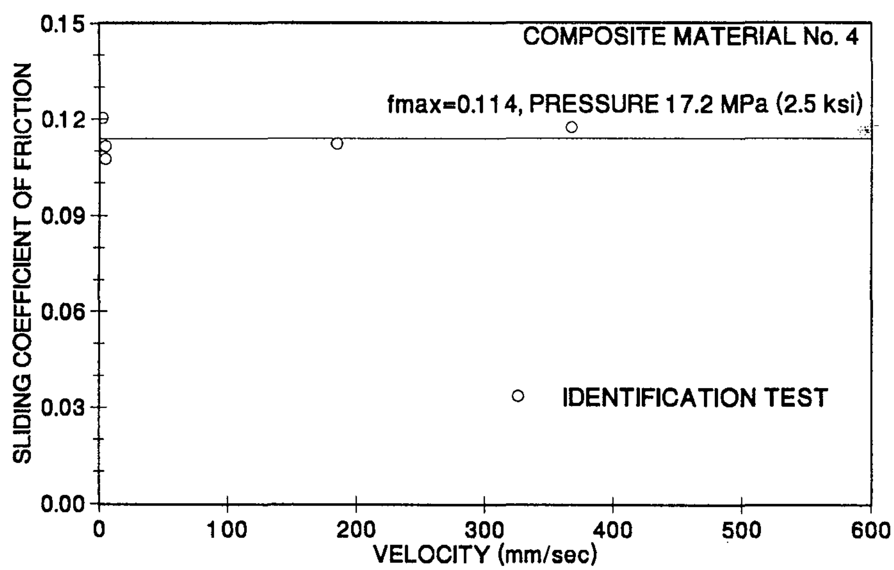

Figure 4-5 **Coefficient of Sliding Friction as Function of Bearing Pressure and Sliding Velocity for Composite Materials No.3 and 4 in Contact with Polished Stainless Steel**

Table 4-II Parameters in Model of Friction

PRESSURE (MPa)	MATERIAL	f_{max}	f_{min}	a (sec/m)	COMMENTS
17.2	No.1	0.104	0.040	83.4	
	No.2	0.122	0.115	127.5	*
	No.3	0.120	0.090	47.0	
	No.4	0.114	0.114	---	*
275.6	No.1	0.053	0.034	199.7	
	No.2	0.058	0.058	---	*
	No.3	0.062	0.062	---	*

* essentially Coulomb friction

4.3 Instrumentation

The instrumentation consisted of load cells, accelerometers and displacement transducers. Figure 4-6 shows the overall instrumentation diagram, whereas Figures 4-7 and 4-8 shows the instrumentation diagrams for accelerometers and displacement transducers, respectively. A list of monitored channels and their corresponding descriptions are given in Table 4-III. A total of 51 channels were monitored.

4.4 Test Program

Testing of the bridge model was performed in five different configurations, as shown in Figure 4-9. These configuration were:

(1) The bearings were locked by side plates to represent a non-isolated bridge. In this configuration, the structure was identified in tests with banded white noise table motion. Furthermore, a selected number of seismic tests was conducted.

(2) Braces were installed to stiffen the piers (see Figure 4-1) and the deck was

connected by stiff rods to a nearby reaction wall. In this configuration, the shake table was driven in displacement-controlled mode with specified frequency and amplitude of harmonic motion. This motion was nearly the motion experienced by the FPS bearings. Loops of bearing horizontal force versus bearing displacement were recorded and used to extract the frictional properties of the FPS bearings.

(3) Both piers were stiffened by braces so that they represented stiff abutments. In this configuration, the model resembled a single span isolated bridge.

(4) The south location pier was stiffened by braces so that it represented a stiff abutment. In this configuration, the model resembled a two-span bridge with two stiff abutments and a centrally located flexible pier. A view of this configuration on the shake table is shown in Figure 4-10.

(5) A configuration with two flexible piers which resembled portion of a multiple span bridge between expansion joints. A view of this configuration on the shake table is shown in Figure 4-11.

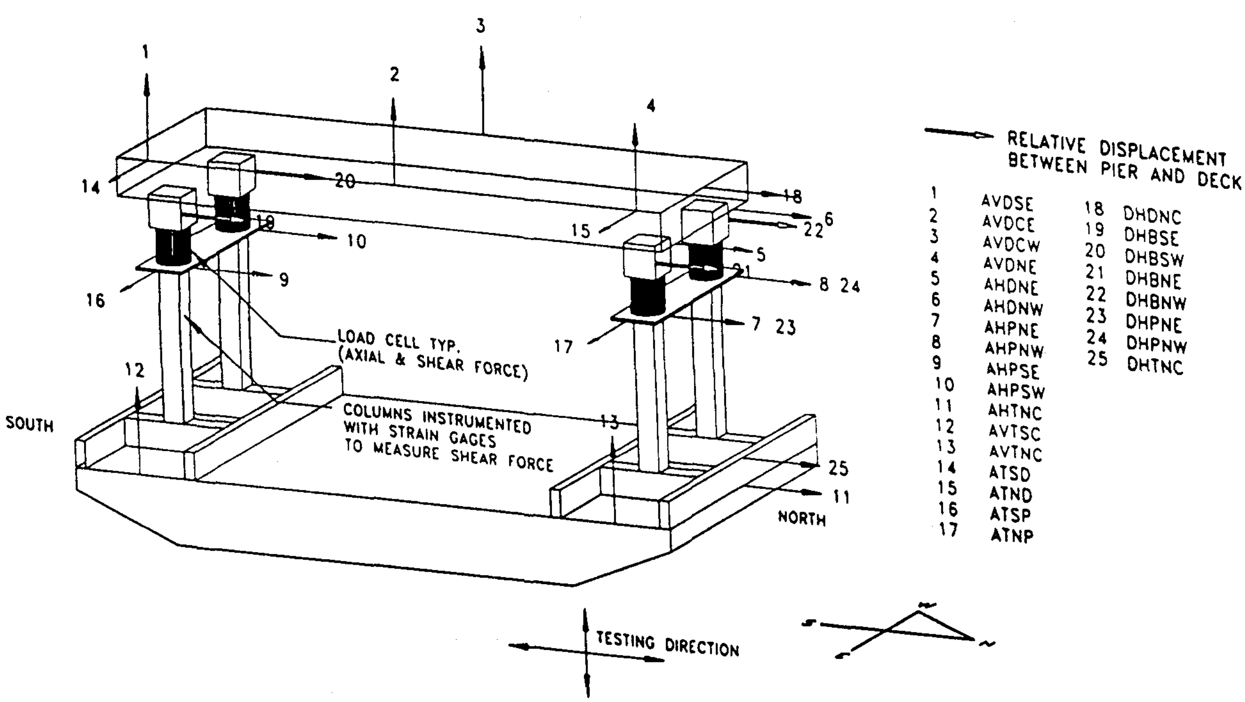

Figure 4-6 Overall Instrumentation Diagram

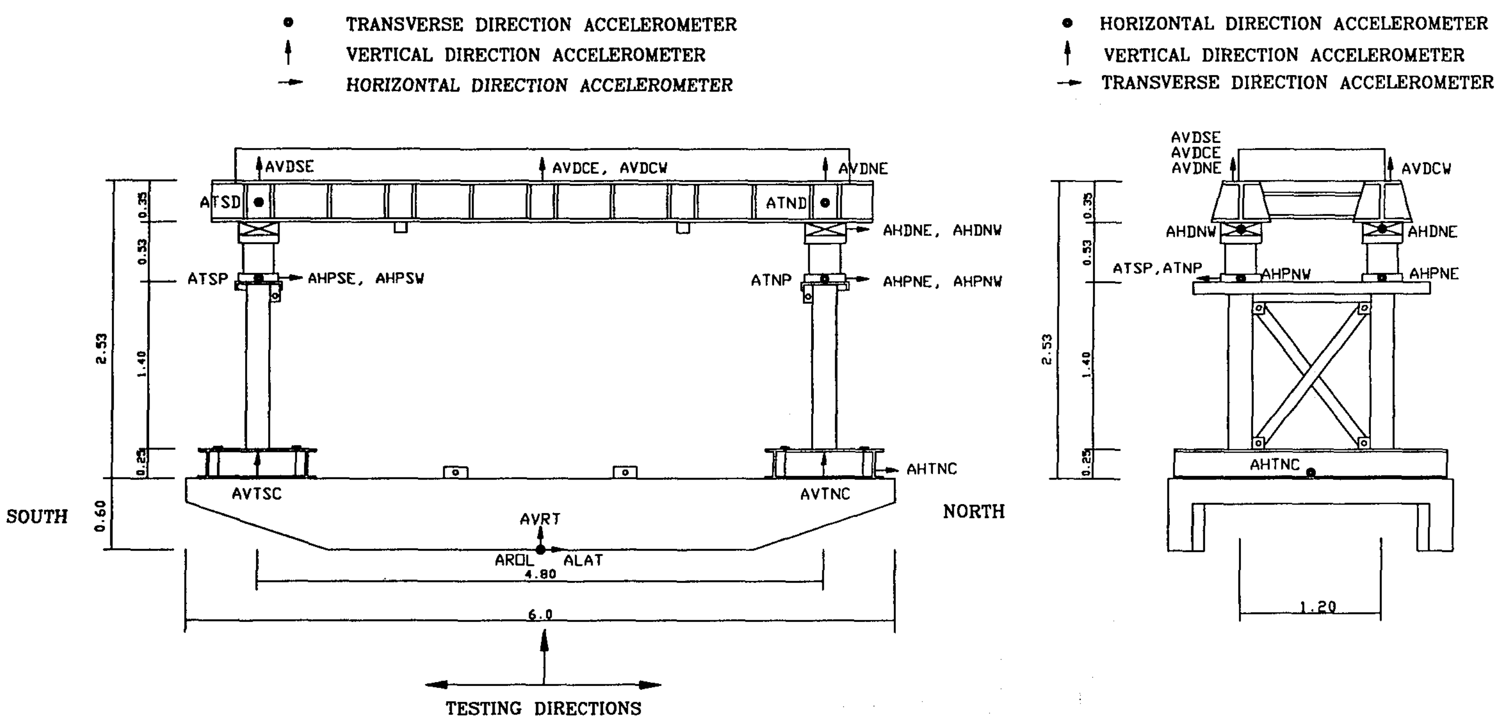

Figure 4-7 Location of Accelerometers (UNITS:m)

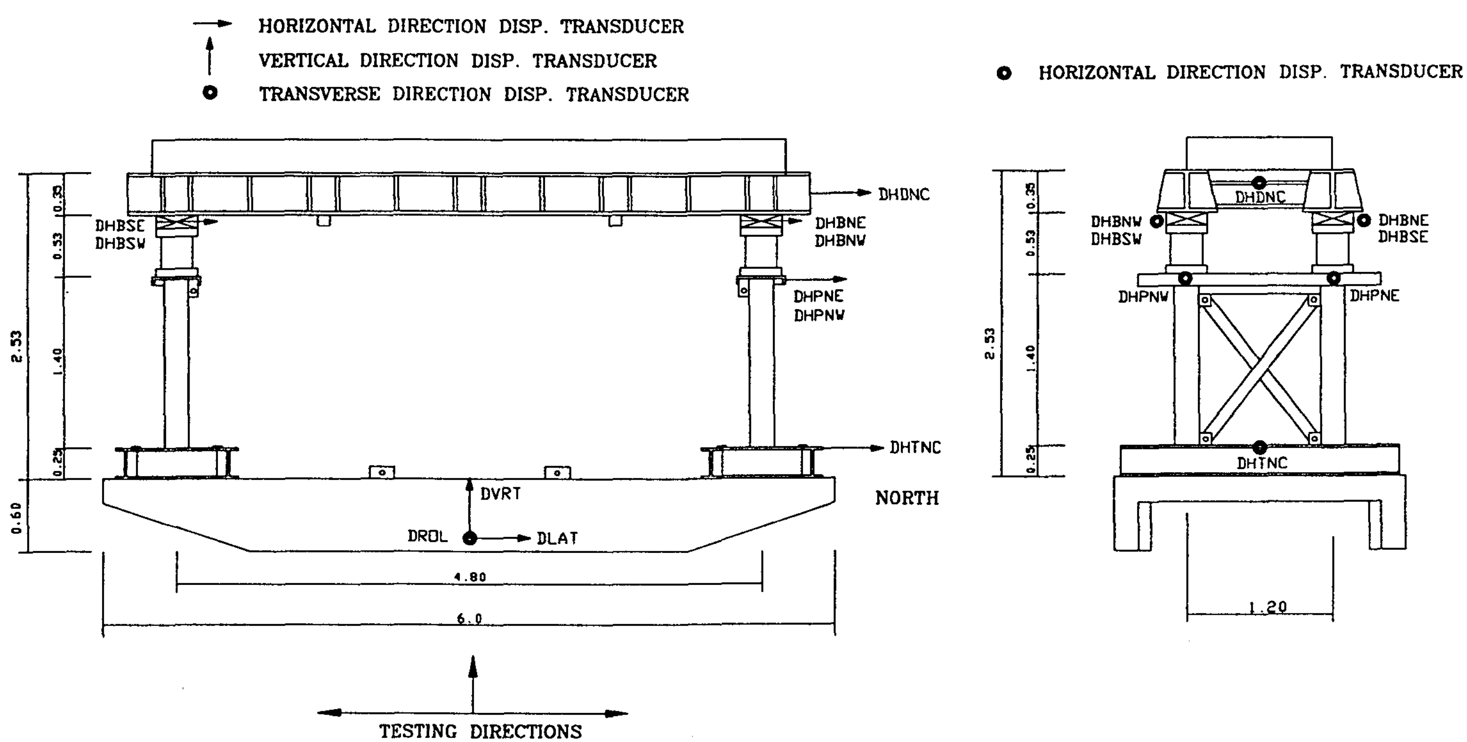

Figure 4-8 Location of Displacement Transducers (UNITS:m)

Table 4-III List of Channels (with reference to Figures 4-6 to 4-8)

CHANNEL	NOTATION	INSTRUMENT	RESPONSE MEASURED
1	AVDSE	ACCL	Deck Vertical Accel.-South East Corner
2	AVDCE	ACCL	Deck Vertical Accel.-East Side at Center
3	AVDCW	ACCL	Deck Vertical Accel.-West Side at Center
4	AVDNE	ACCL	Deck Vertical Accel.-North East Corner
5	AHDNE	ACCL	Deck Horizontal Accel.-North East Corner
6	AHDNW	ACCL	Deck Horizontal Accel.-North West Corner
7	AHPNE	ACCL	Pier Horizontal Accel.-North East
8	AHPNW	ACCL	Pier Horizontal Accel.-North West
9	AHPSE	ACCL	Pier Horizontal Accel.-South East
10	AHPSW	ACCL	Pier Horizontal Accel.-South West
11	AHTNC	ACCL	Table Horizontal Accel.-North Side at Center
12	AVTSC	ACCL	Table Vertical Accel.-South Side at Center
13	AVTNC	ACCL	Table Vertical Accel.-North Side at Center
14	ATSD	ACCL	Deck Transverse Accel.-South Side
15	ATND	ACCL	Deck Transverse Accel.-North Side
16	ATSP	ACCL	Pier Transverse Accel.-South
17	ATNP	ACCL	Pier Transverse Accel.-North
18	DHDNC	DT	Deck Total Horizontal Displ.-North Side Center
19	DHBSE	DT	Bearing Horizontal Displ.-South East
20	DHBSW	DT	Bearing Horizontal Displ.-South West
21	DHBNE	DT	Bearing Horizontal Displ.-North East
22	DHBNW	DT	Bearing Horizontal Displ.-North West
23	DHPNE	DT	Pier Total Horizontal Displ.-North East
24	DHPNW	DT	Pier Total Horizontal Displ.-North West
25	DHTNC	DT	Table Horizontal Displ.-North Side at Center
26	DHBAV	DT	Bearing Horizontal Average Displ.

ACCEL=Accelerometer, DT=Displacement Transducer

Table 4-III (Cont'd)

CHANNEL	NOTATION	INSTRUMENT	RESPONSE MEASURED
27	DLAT	DT	Table Horizontal Displ.
28	ALAT	ACCL	Table Horizontal Accel.
29	DVRT	DT	Table Vertical Displ.
30	AVRT	ACCL	Table Vertical Accel.
31	DROL	DT	Table Rolling Displ.
32	AROL	ACCL	Table Rolling Accel.
33	SX1	LOAD CELL	Shear Bearing Force-South West
34	SX2	LOAD CELL	Shear Bearing Force-South East
35	SX3	LOAD CELL	Shear Bearing Force-North West
36	SX4	LOAD CELL	Shear Bearing Force-North East
37	SCNE	LOAD CELL	Column Shear Force-North East
38	SESE	LOAD CELL	Column Shear Force-South East
39	SCNW	LOAD CELL	Column Shear Force-North West
40	SCSW	LOAD CELL	Column Shear Force-South West
41	N1SW	LOAD CELL	Axial Bearing Force-South West
42	N2SE	LOAD CELL	Axial Bearing Force-South East
43	N3NW	LOAD CELL	Axial Bearing Force-North West
44	N4NE	LOAD CELL	Axial Bearing Force-North East
45	SCN	LOAD CELL	Average Column Shear Force-North
46	SCS	LOAD CELL	Average Column Shear Force-South
47	DHDSW	DT	Deck Total Horizontal Displ.-South West Corner
48	DHDSE	DT	Deck Total Horizontal Displ.-South East Corner
49	LCNE	LOAD CELL	East Friction Force-North East Corner(ID-test)
50	LCNW	LOAD CELL	West Friction Force-North West Corner(ID-Test)
51	LCTOT	LOAD CELL	Average Friction Force(ID-Test)

ACCEL=Accelerometer, DT=Displacement Transducer

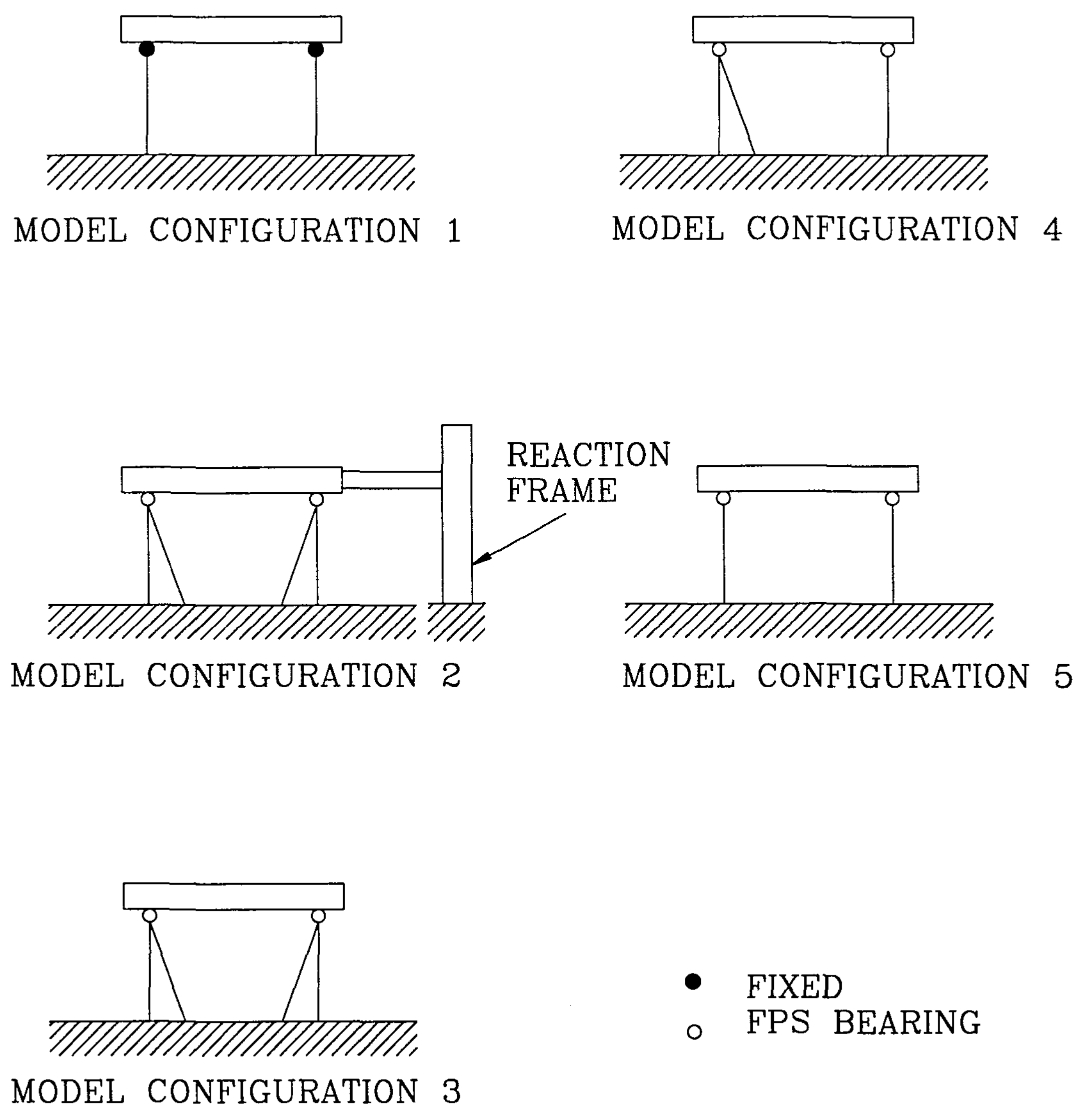

Figure 4-9 Model Configurations in Testing (1:Non-isolated Bridge, 2:Identification of Frictional Properties, 3:Single Span Model, 4:Two-Span Model, 5:Multiple Span Model)

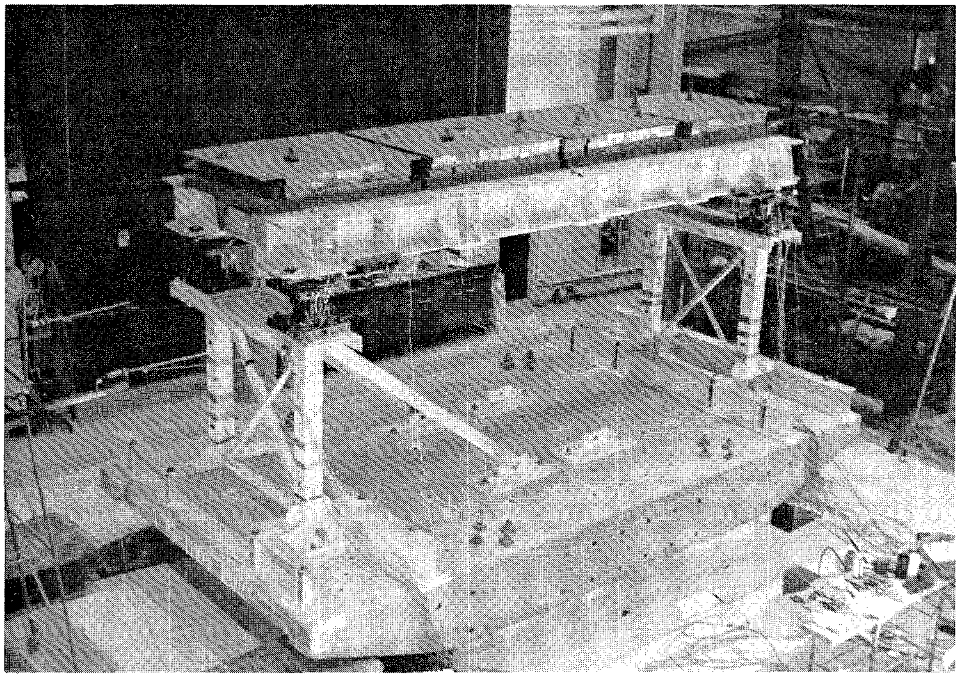

Figure 4-10 View of Bridge Model Configuration with One Flexible Pier and One Stiff Pier

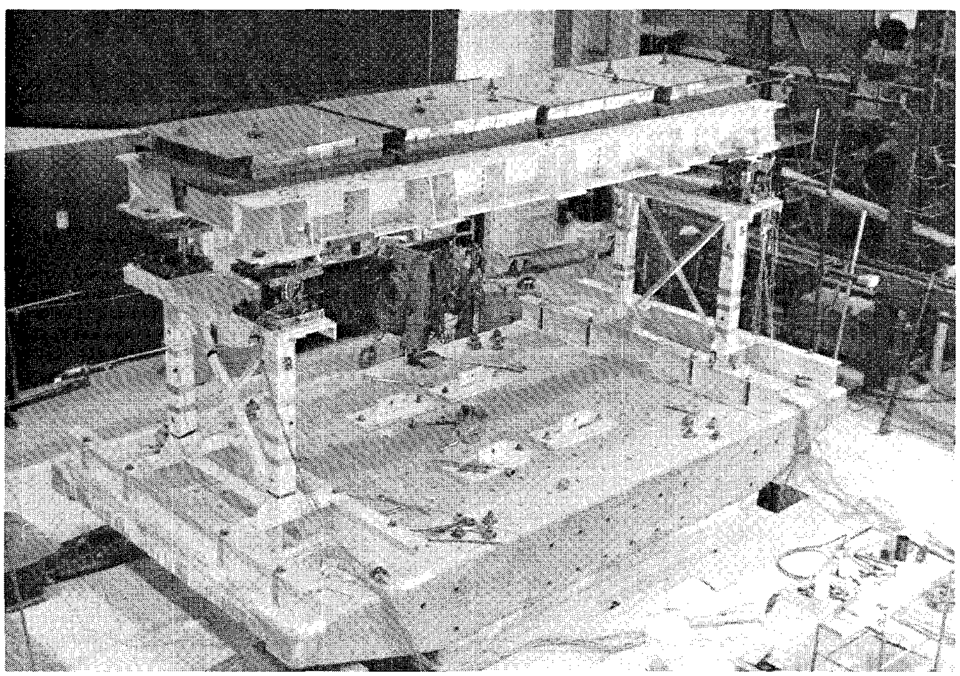

Figure 4-11 View of Bridge Model in Configuration with Two Flexible Piers

A total of 173 earthquake simulation tests were performed on the model bridge. Tests were conducted with only horizontal input and with combined horizontal and vertical input. The earthquake signals and their characteristics are listed in Table 4-IV. The earthquake signals consisted of historic earthquakes and artificial motions compatible with

(a) The Japanese bridge design spectra for level 1 and level 2 and ground conditions 1 (rock), 2 (alluvium) and 3 (deep alluvium) (CERC 1992). In Japan, it is required that bridges are designed for two levels of seismic loading. In level 1 seismic loading, it is required that the bridge remains undamaged and fully elastic. In level 2 seismic loading, inelastic behavior is permitted. Tables 4-V and 4-VI describe the shapes of the 5%-damped acceleration spectra of the Japanese level 1 and 2 motions.

(b) The California Department of Transportation (CalTrans) bridge spectra (Gates 1979). These motions were identical to those used in the testing of another bridge model by Constantinou, 1991a.

(c) Site specific spectra for a location in Boston, Massachusetts.

Each record was compressed in time by a factor of two to satisfy the similitude requirements. Figure 4-12 to 4-31 show recorded time histories of the table motion in tests with input being the earthquake signals of Table 4-IV. The acceleration and displacement records were directly measured, whereas the velocity record was obtained by numerical differentiation of the displacement record. It may be observed that the peak ground motion was reproduced well, but not exactly, by the table generated motion.

Figures 4-12 to 4-31 also show the response spectra of acceleration of the table motions. The 5% damped acceleration spectrum is compared to the spectrum of the target record to demonstrate the good reproduction of the motion by the table.

Table 4-IV Earthquake Motions Used in Test Program and Characteristics in Prototype Scale

NOTATION	RECORD	PEAK ACC. (g)	PEAK VEL. (mm/sec)	PEAK DIS. (mm)
EL CENTRO S00E	Imperial Vally, May 18 1940 Component S00E	0.34	334.5	108.7
TAFT N21E	Kern County, July 21,1952 Component N21E	0.16	157.2	67.1
MEXICO CITY	Mexico City, September 19, 1985 SCT building, Component N90W	0.17	605.0	212.0
PACOIMA S16E	San Fernando, February 9, 1971 Component S16E	1.17	1132.3	365.3
PACOIMA S74W	San Fernando, February 9, 1971 Component S74E	1.08	568.2	108.2
HACHINOHE N-S	Tokachi, Japan, May 16, 1968 Hachinohe, Component N-S	0.23	357.1	118.9
MIYAGIKEN OKI	Miyaki, Japan, June 12, 1978 Ofunato-Bochi, Component E-W	0.16	141.0	50.8
AKITA N-S	Nihonkai Chuubu, Japan, May 23, 1983 Component N-S	0.19	292.0	146.0
JP. L1G1	Artificial Compatible with Japanese Level 1 Ground Condition 1	0.10	215.0	90.0
JP. L1G2	Artificial Compatible with Japanese Level 1 Ground Condition 2	0.12	251.0	69.0
JP. L1G3	Artificial Compatible with Japanese Level 1 Ground Condition 3	0.14	274.0	132.0
JP. L2G1	Artificial Compatible with Japanese Level 2 Ground Condition 1	0.37	864.0	526.0
JP. L2G2	Artificial Compatible with Japanese Level 2 Ground Condition 2	0.43	998.0	527.0
JP. L2G3	Artificial Compatible with Japanese Level 2 Ground Condition 3	0.45	1121.0	700.0
CALTRANS 0.6g A2	Artificial Compatible with CalTrans 0.6g 80'-150' Alluvium Spectrum No.2	0.60	836.4	282.9
CALTRANS 0.6g S2	Artificial Compatible with CalTrans 0.6g 10'-80' Alluvium Spectrum No.2	0.60	765.0	248.9
CALTRANS 0.6g S3	Artificial Compatible with CalTrans 0.6g 10'-80' Alluvium Spectrum No.3	0.60	778.0	438.9
CALTRANS 0.6g R1	Artificial Compatible with CalTrans 0.6g Rock Spectrum No.1	0.60	530.9	443.8
CALTRANS 0.6g R2	Artificial Compatible with CalTrans 0.6g Rock Spectrum No.2	0.60	510.0	274.3
CALTRANS 0.6g R3	Artificial Compatible with CalTrans 0.6g Rock Spectrum No.3	0.60	571.0	342.4
BOSTON 1	Artificial Compatible with a Site in Boston, No. 1	0.15	123.5	26.3
BOSTON 2	Artificial Compatible with a Site in Boston, No. 2	0.15	110.1	25.1
BOSTON 3	Artificial Compatible with a Site in Boston, No. 3	0.15	99.7	21.7

Table 4-V Spectral Acceleration of Japanese Bridge Design Spectra, Level 1

G.C.	Spectral Acceleration (S_{10}) in units of cm/sec^2 as Function of Period T_i in units of seconds		
1	$T_i < 0.1$ $S_{10} = 431T_i^{1/3}$ $S_{10} \geq 160$	$0.1 \leq T_i \leq 1.1$ $S_{10}=200$	$1.1 < T_i$ $S_{10}=220/T_i$
2	$T_i < 0.2$ $S_{10} = 427T_i^{1/3}$ $S_{10} \geq 200$	$0.2 \leq T_i \leq 1.3$ $S_{10}=250$	$1.3 < T_i$ $S_{10}=325/T_i$
3	$T_i < 0.34$ $S_{10} = 430T_i^{1/3}$ $S_{10} \geq 240$	$0.34 \leq T_i \leq 1.5$ $S_{10}=300$	$1.5 < T_i$ $S_{10}=450/T_i$

Table 4-VI Spectral Acceleration of Japanese Bridge Design Spectra, Level 2

G.C.	Spectral Acceleration (S_{20}) in units of cm/sec^2 as Function of Period T_i in units of seconds		
1	$T_i \leq 1.4$ $S_{20} = 700$		$1.4 < T_i$ $S_{20}=980/T_i$
2	$T_i < 0.18$ $S_{20} = 1506T_i^{1/3}$ $S_{20} \geq 700$	$0.18 \leq T_i \leq 1.6$ $S_{20}=850$	$1.6 < T_i$ $S_{20}=1360/T_i$
3	$T_i < 0.29$ $S_{20} = 1511T_i^{1/3}$ $S_{20} \geq 700$	$0.29 \leq T_i \leq 2.0$ $S_{20}=1000$	$2.0 < T_i$ $S_{20}=2000/T_i$

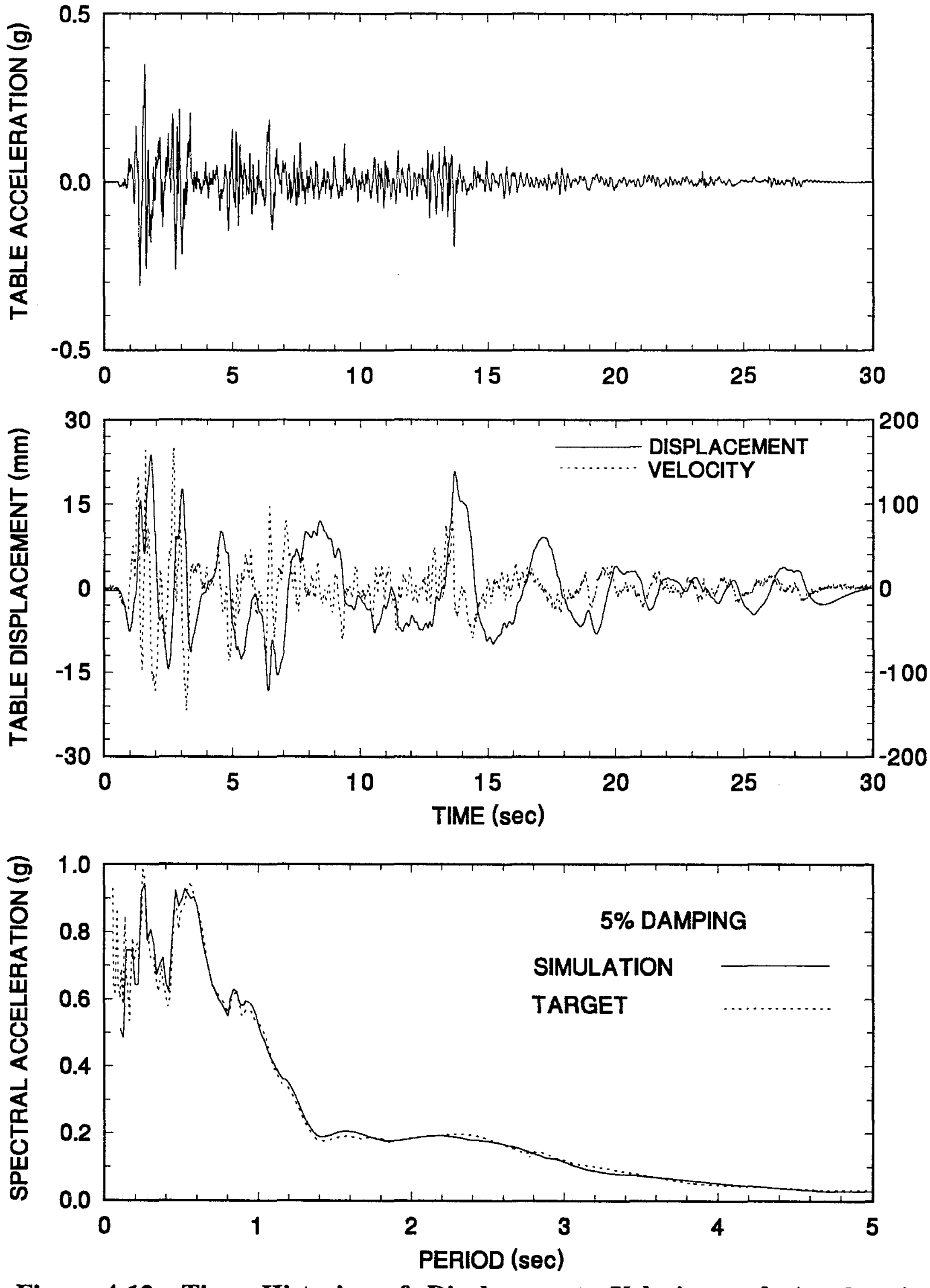

Figure 4-12 **Time Histories of Displacement, Velocity and Acceleration and Acceleration Response Spectrum of Shaking Table Motion Excited with El Centro S00E 100% Motion**

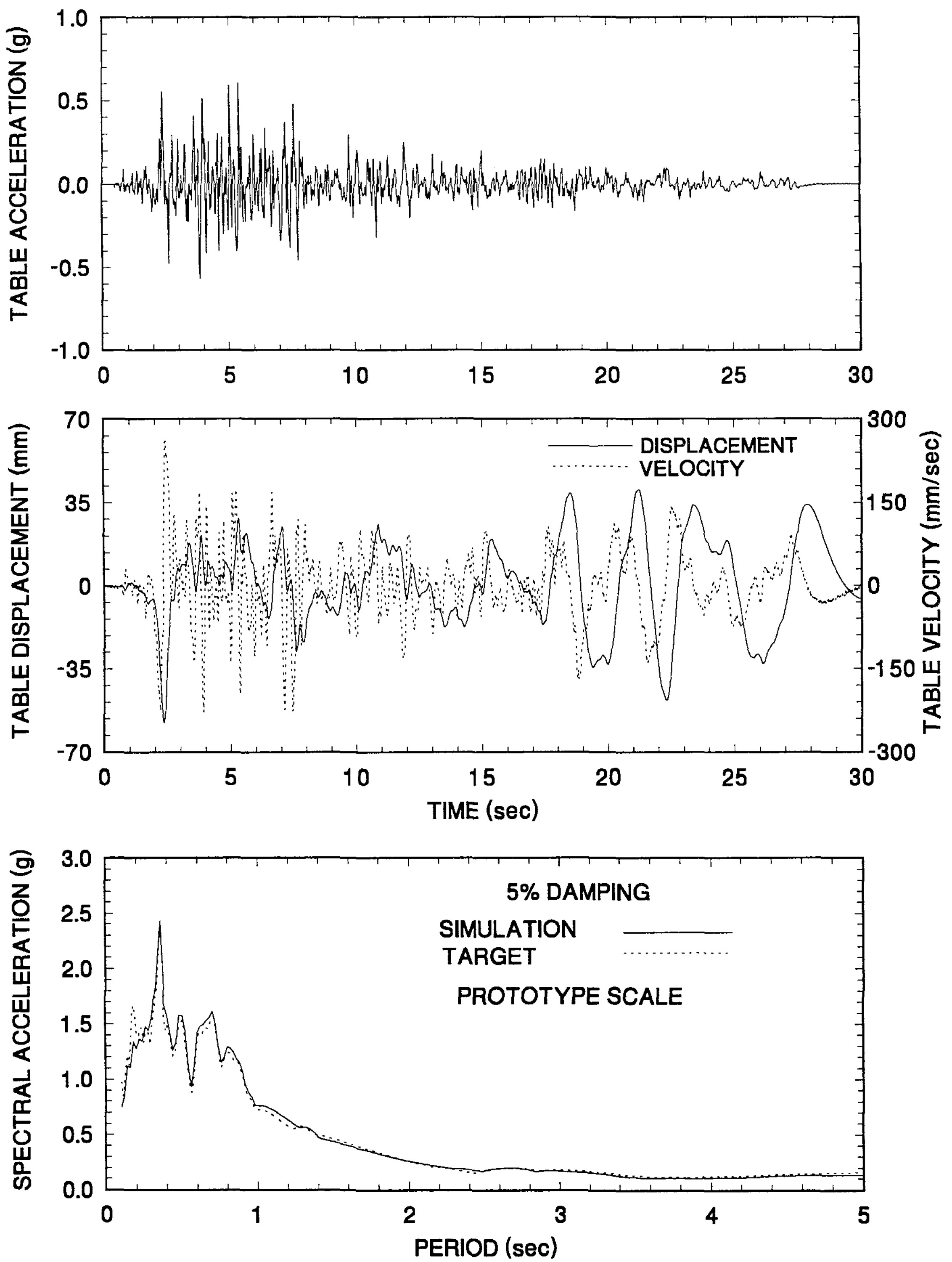

Figure 4-13 Time Histories of Displacement, Velocity and Acceleration and Acceleration Response Spectrum of Shaking Table Motion Excited with Taft N21E 400% Motion

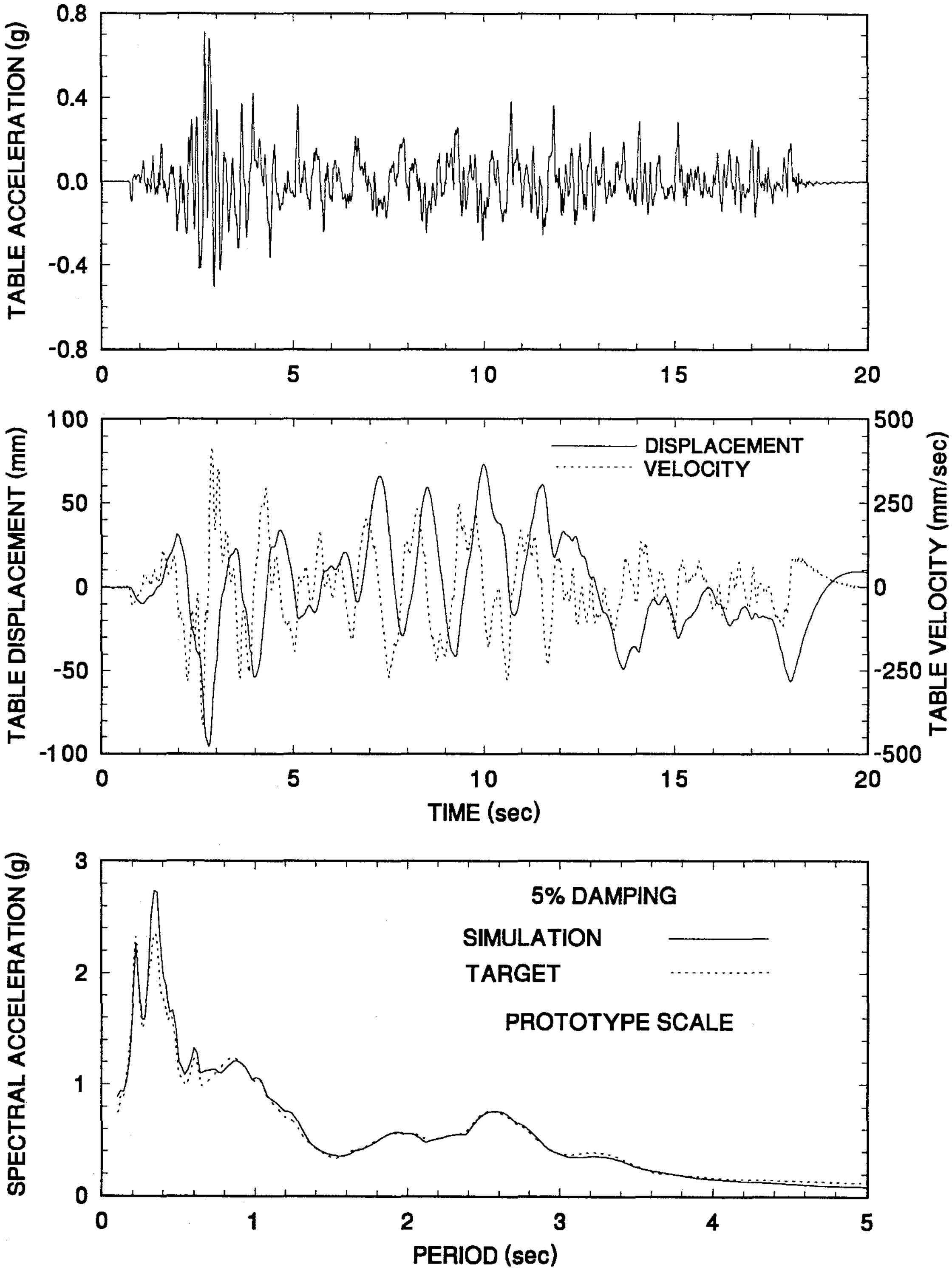

Figure 4-14 Time Histories of Displacement, Velocity and Acceleration and Acceleration Response Spectrum of Shaking Table Motion Excited with Hachinohe N-S 300% Motion

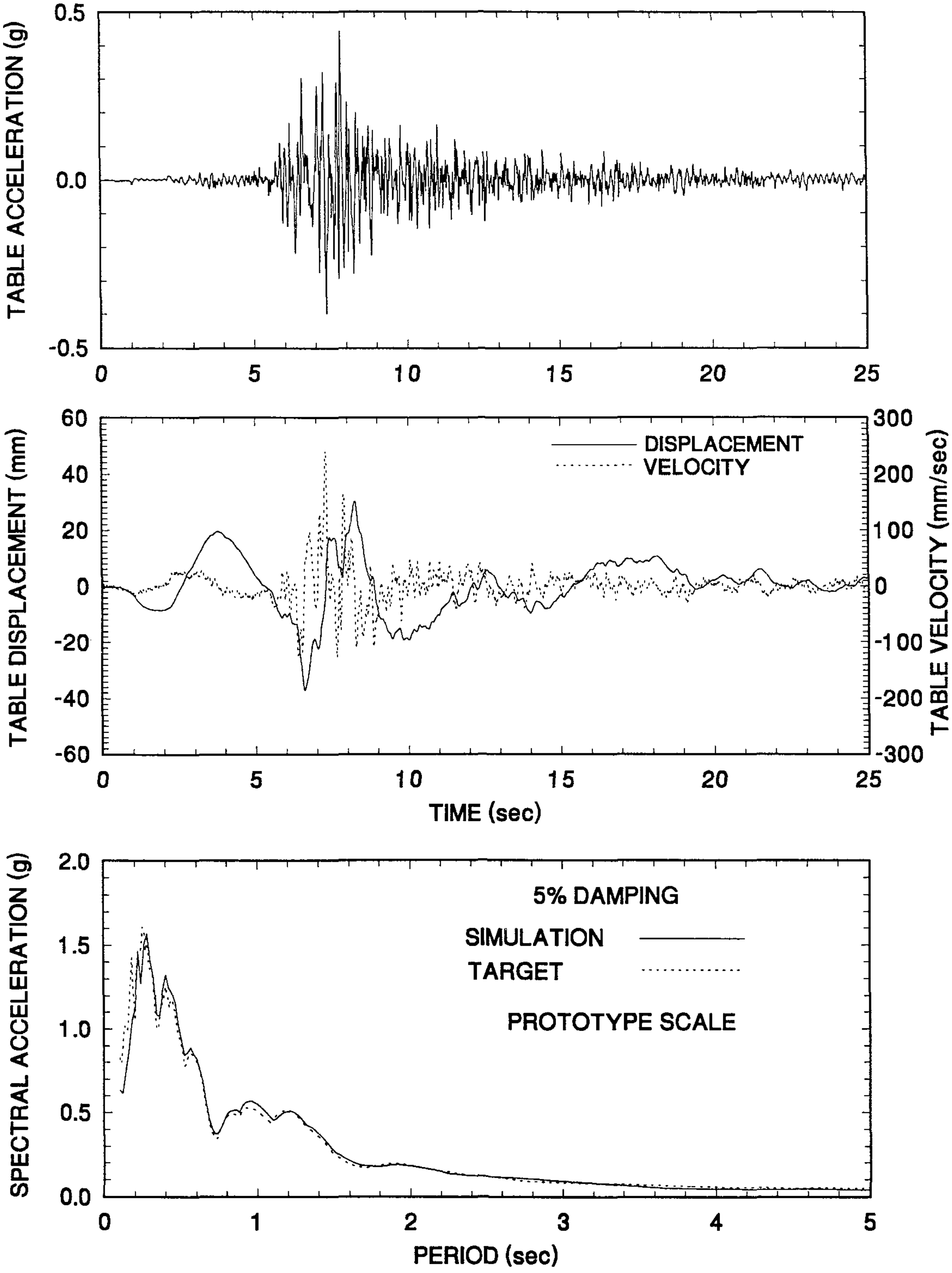

Figure 4-15 **Time Histories of Displacement, Velocity and Acceleration and Acceleration Response Spectrum of Shaking Table Motion Excited with Miyagiken Oki E-W 300% Motion**

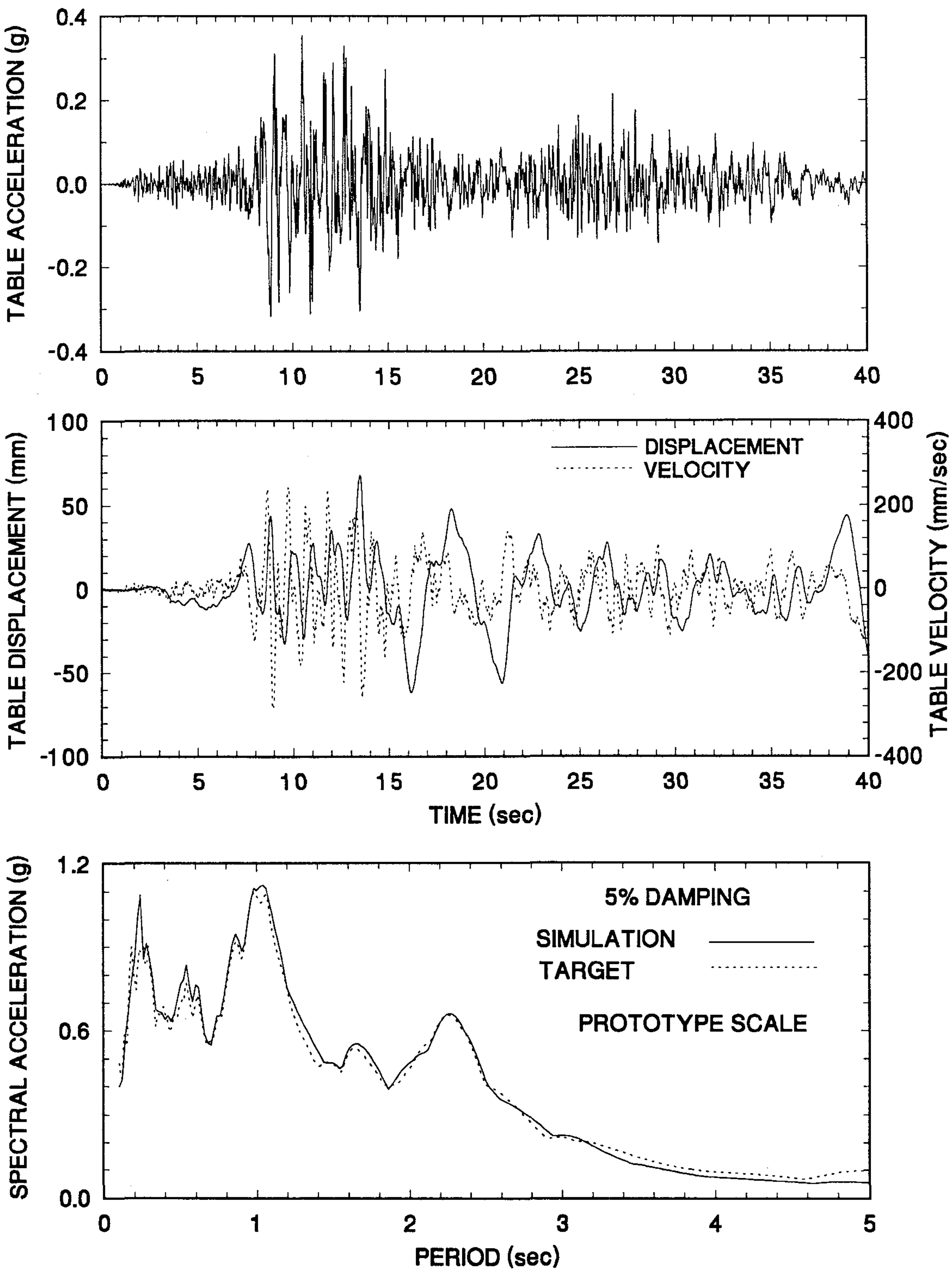

Figure 4-16 Time Histories of Displacement, Velocity and Acceleration and Acceleration Response Spectrum of Shaking Table Motion Excited with Akita N-S 200% Motion

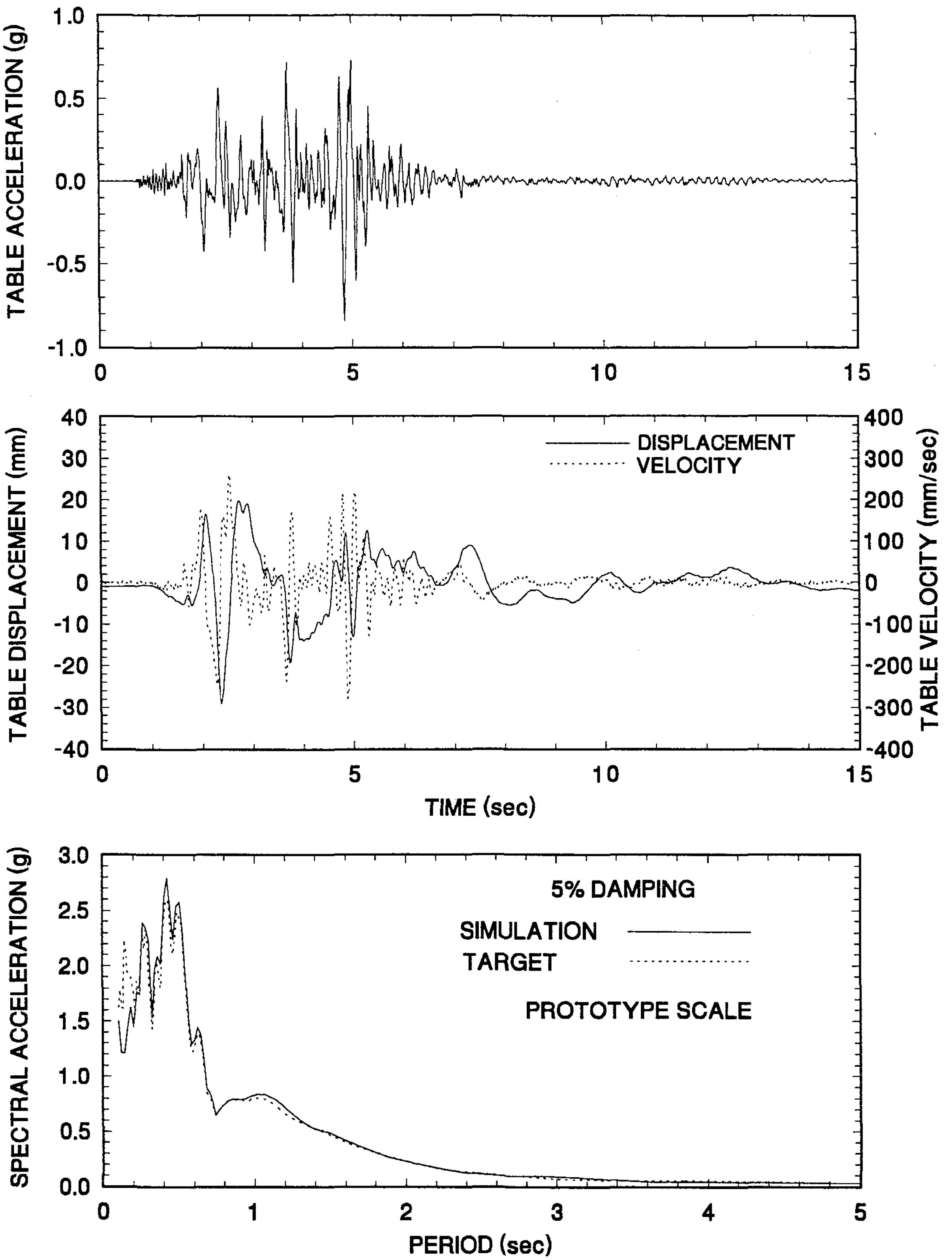

Figure 4-17 Time Histories of Displacement, Velocity and Acceleration and Acceleration Response Spectrum of Shaking Table Motion Excited with Pacoima S74W 100% Motion

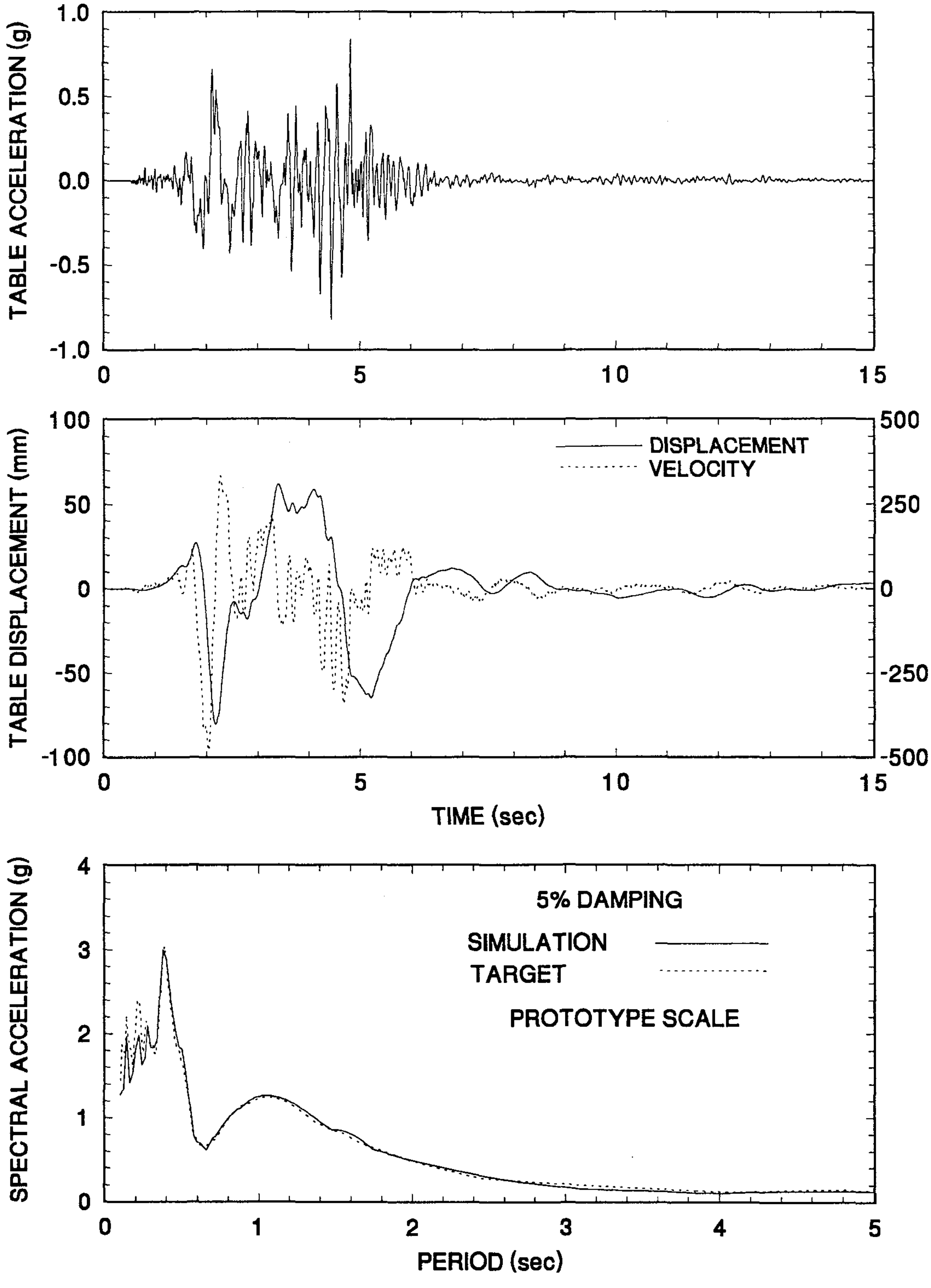

Figure 4-18 Time Histories of Displacement, Velocity and Acceleration and Acceleration Response Spectrum of Shaking Table Motion Excited with Pacoima S16E 100% Motion

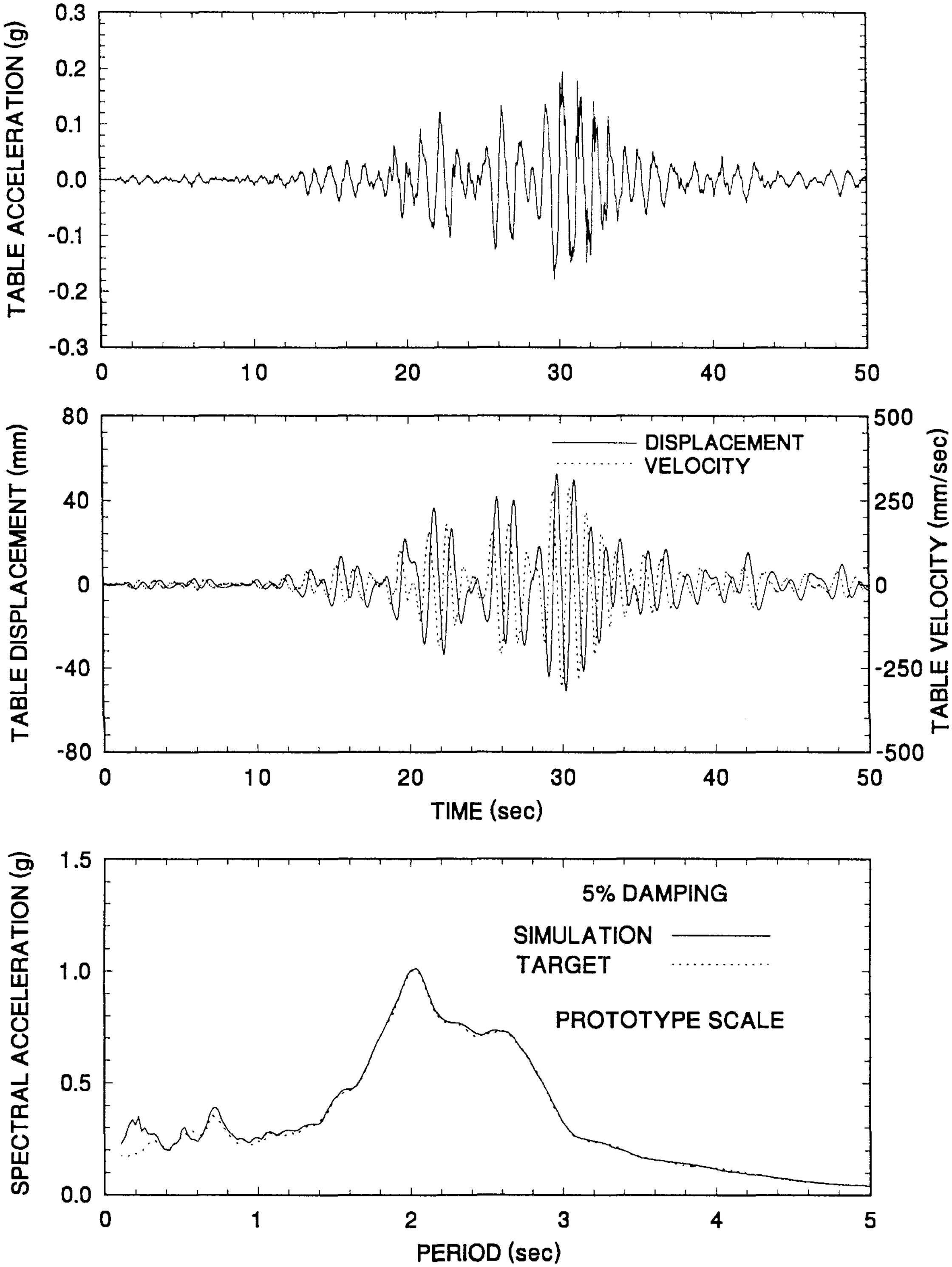

Figure 4-19 Time Histories of Displacement, Velocity and Acceleration and Acceleration Response Spectrum of Shaking Table Motion Excited with Mexico N90W 100% Motion

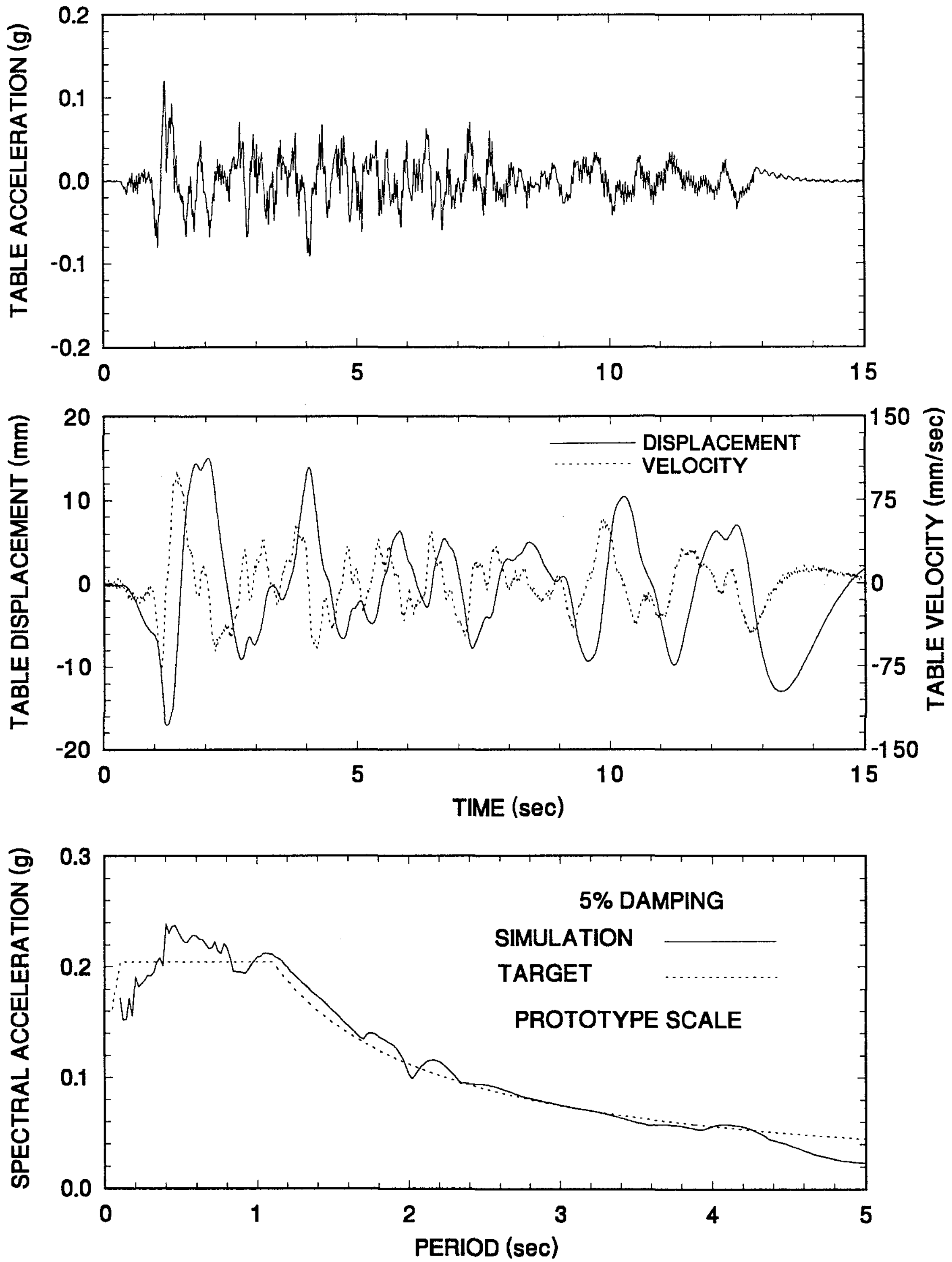

Figure 4-20 Time Histories of Displacement, Velocity and Acceleration and Acceleration Response Spectrum of Shaking Table Motion Excited with JP. Level 1 G.C.1 100% Motion

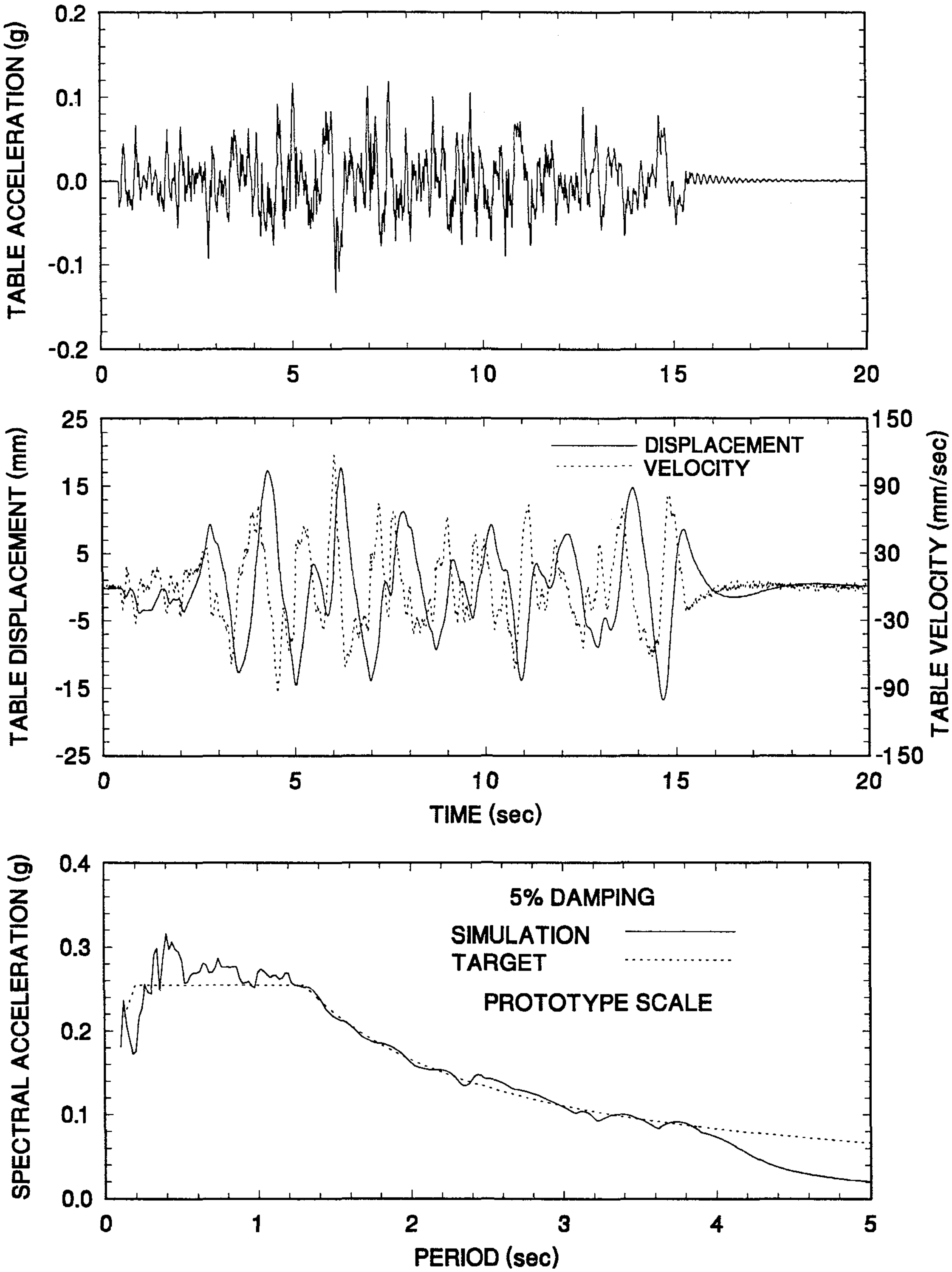

Figure 4-21 Time Histories of Displacement, Velocity and Acceleration and Acceleration Response Spectrum of Shaking Table Motion Excited with JP. Level 1 G.C.2 100% Motion

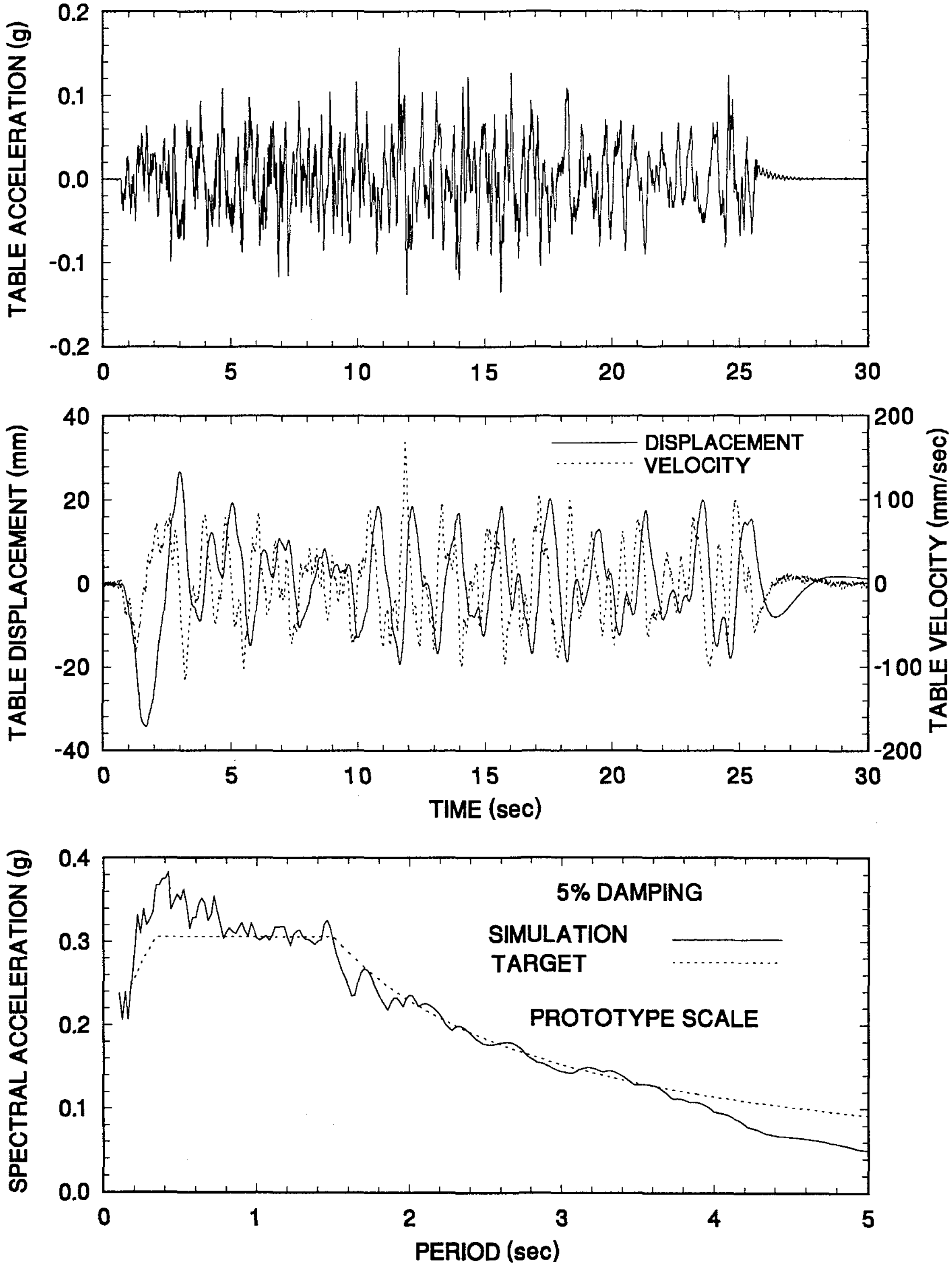

Figure 4-22 Time Histories of Displacement, Velocity and Acceleration and Acceleration Response Spectrum of Shaking Table Motion Excited with JP. Level 1 G.C.3 100% Motion

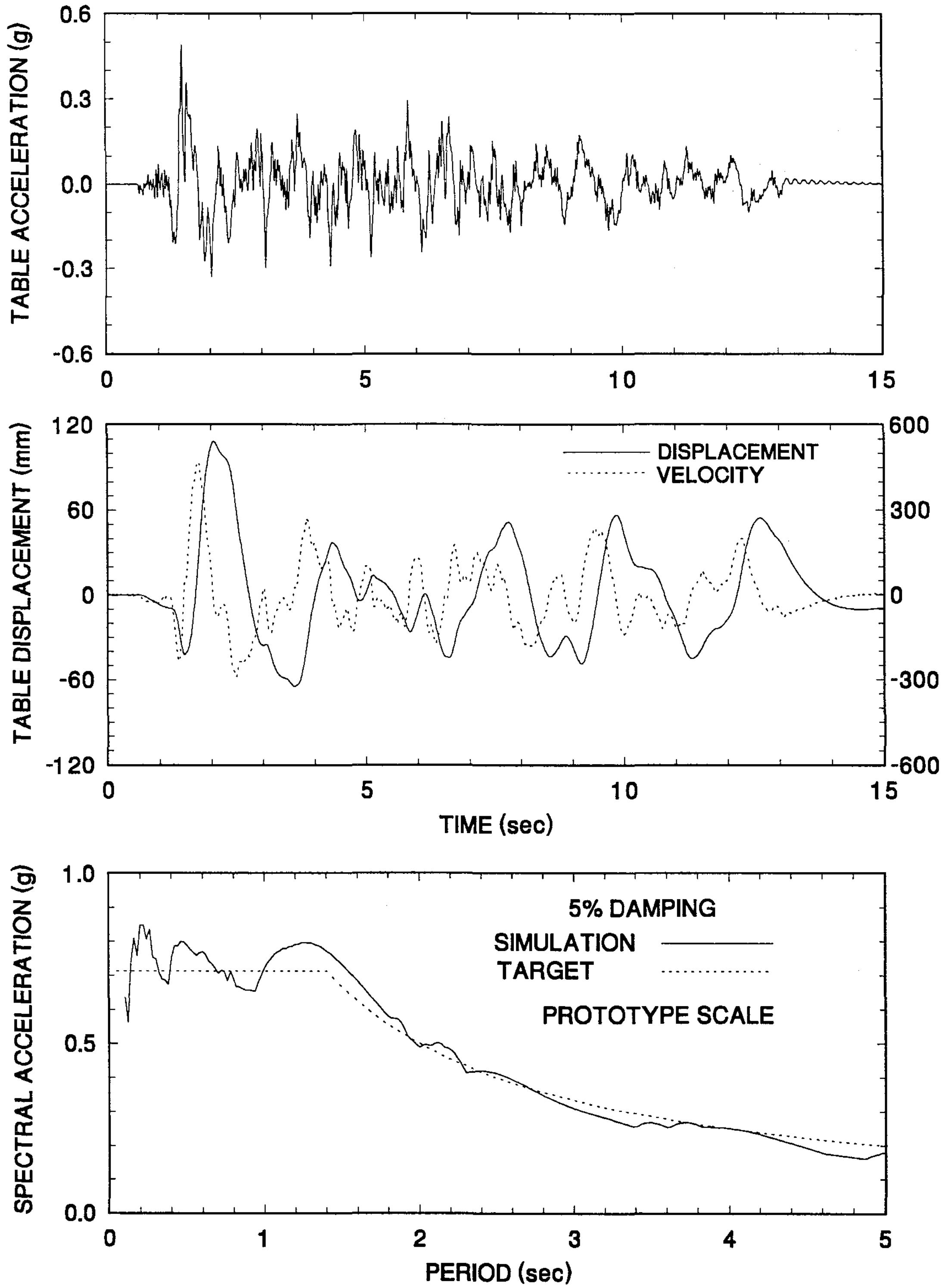

Figure 4-23 Time Histories of Displacement, Velocity and Acceleration and Acceleration Response Spectrum of Shaking Table Motion Excited with JP. Level 2 G.C.1 100% Motion

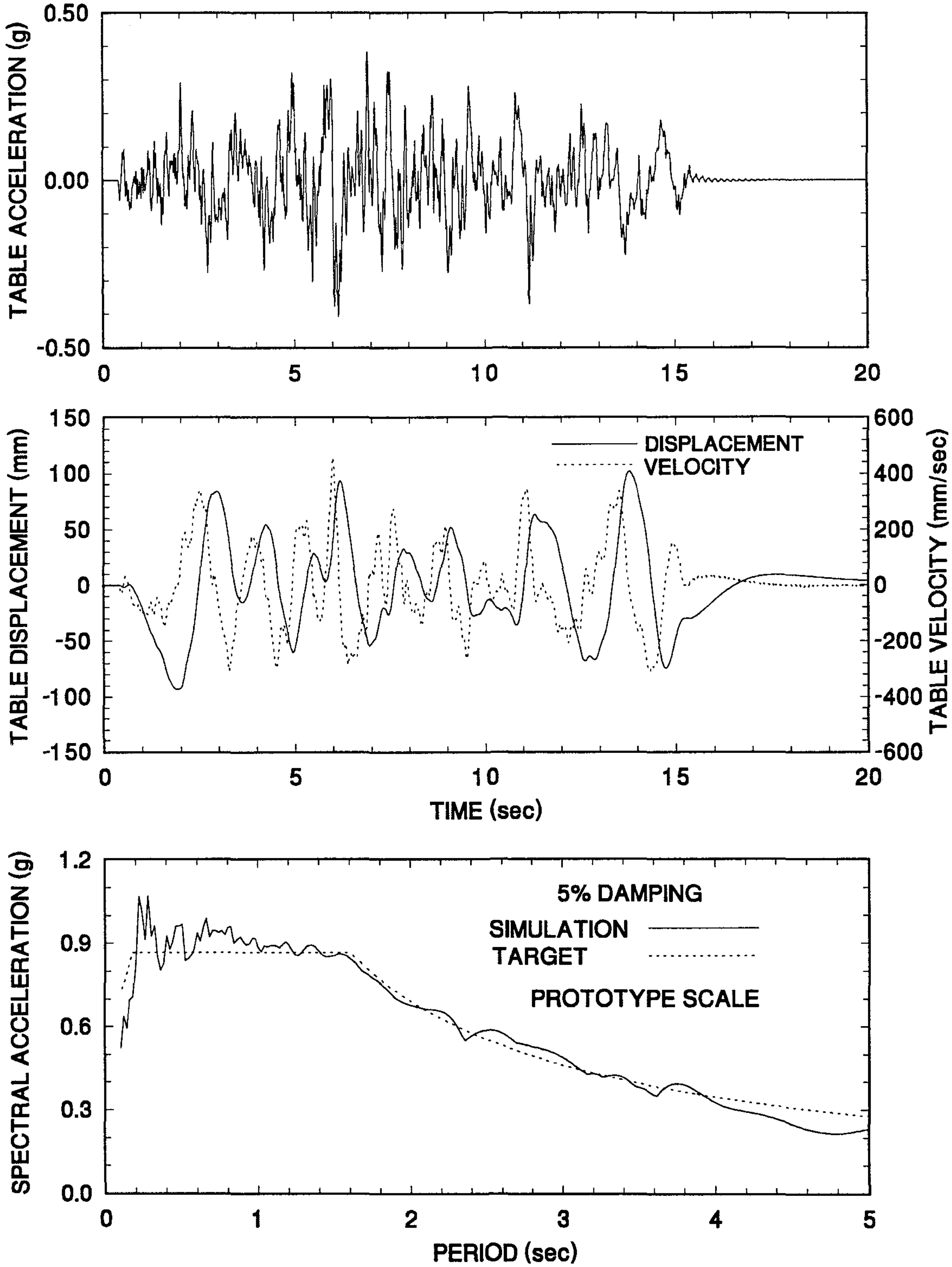

Figure 4-24 Time Histories of Displacement, Velocity and Acceleration and Acceleration Response Spectrum of Shaking Table Motion Excited with JP. Level 2 G.C.2 100% Motion

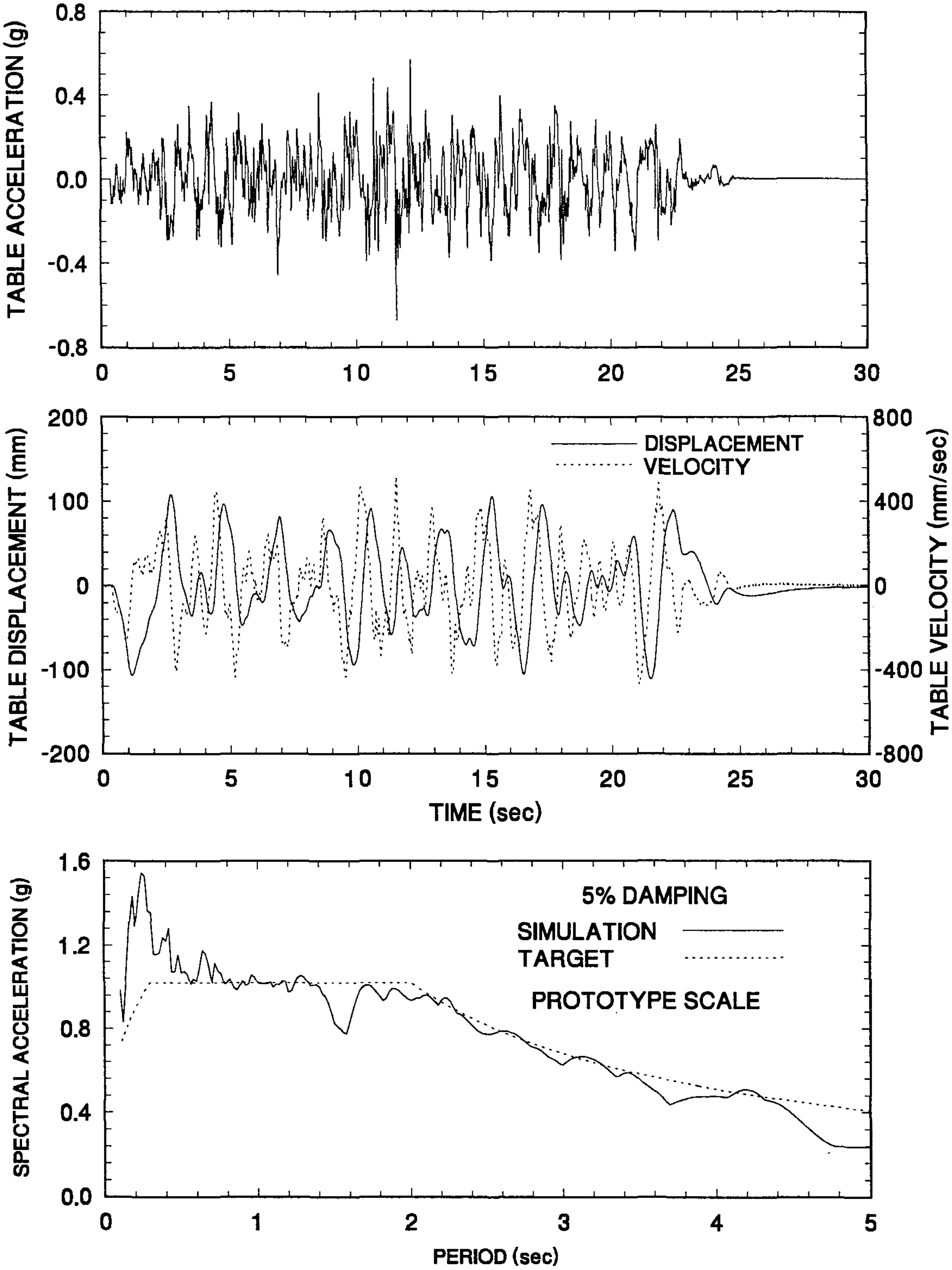

Figure 4-25 Time Histories of Displacement, Velocity and Acceleration and Acceleration Response Spectrum of Shaking Table Motion Excited with JP. Level 2 G.C.3 100% Motion

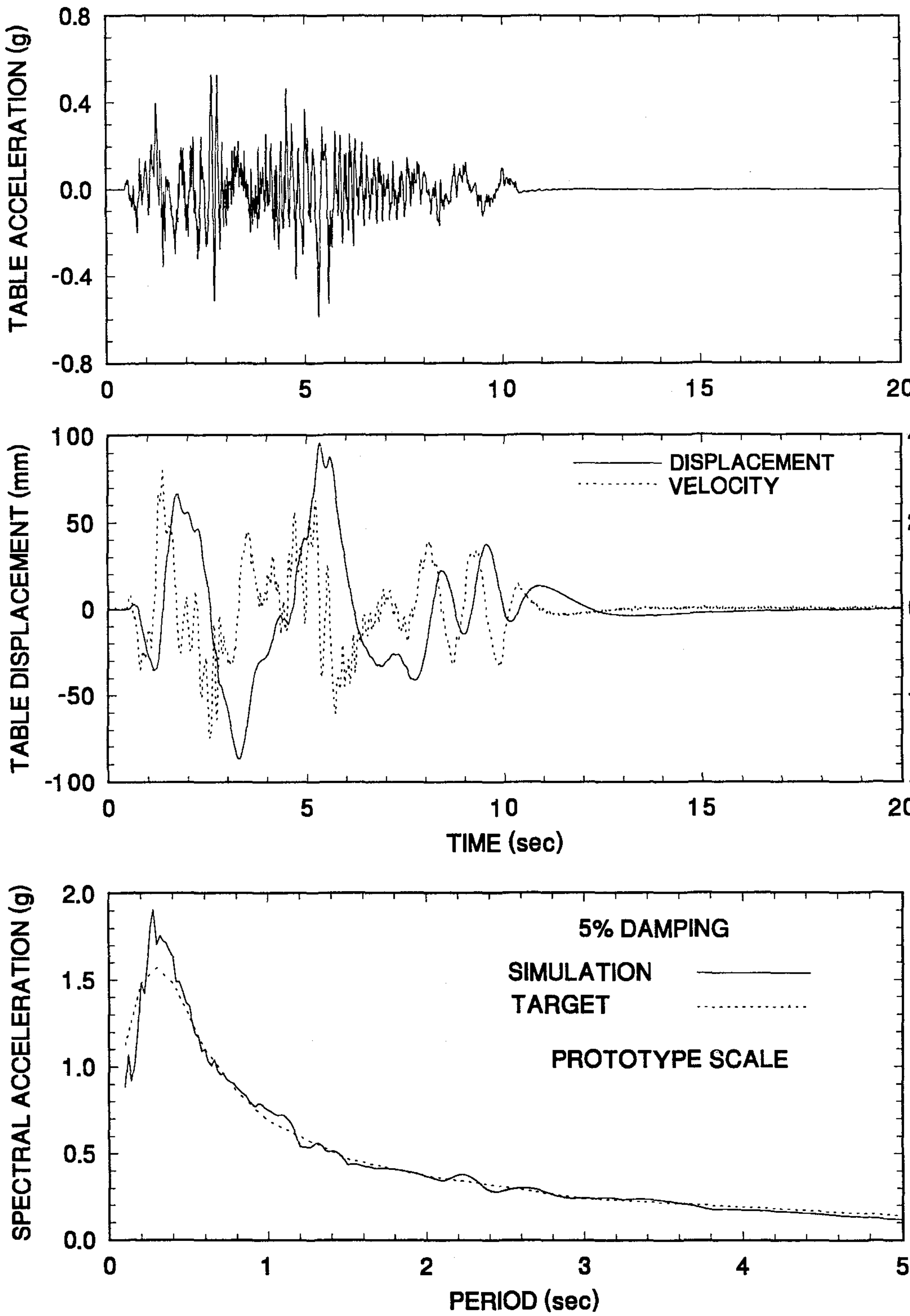

Figure 4-26 Time Histories of Displacement, Velocity and Acceleration and Acceleration Response Spectrum of Shaking Table Motion Excited with CalTrans Rock No.3 0.6g 100% Motion

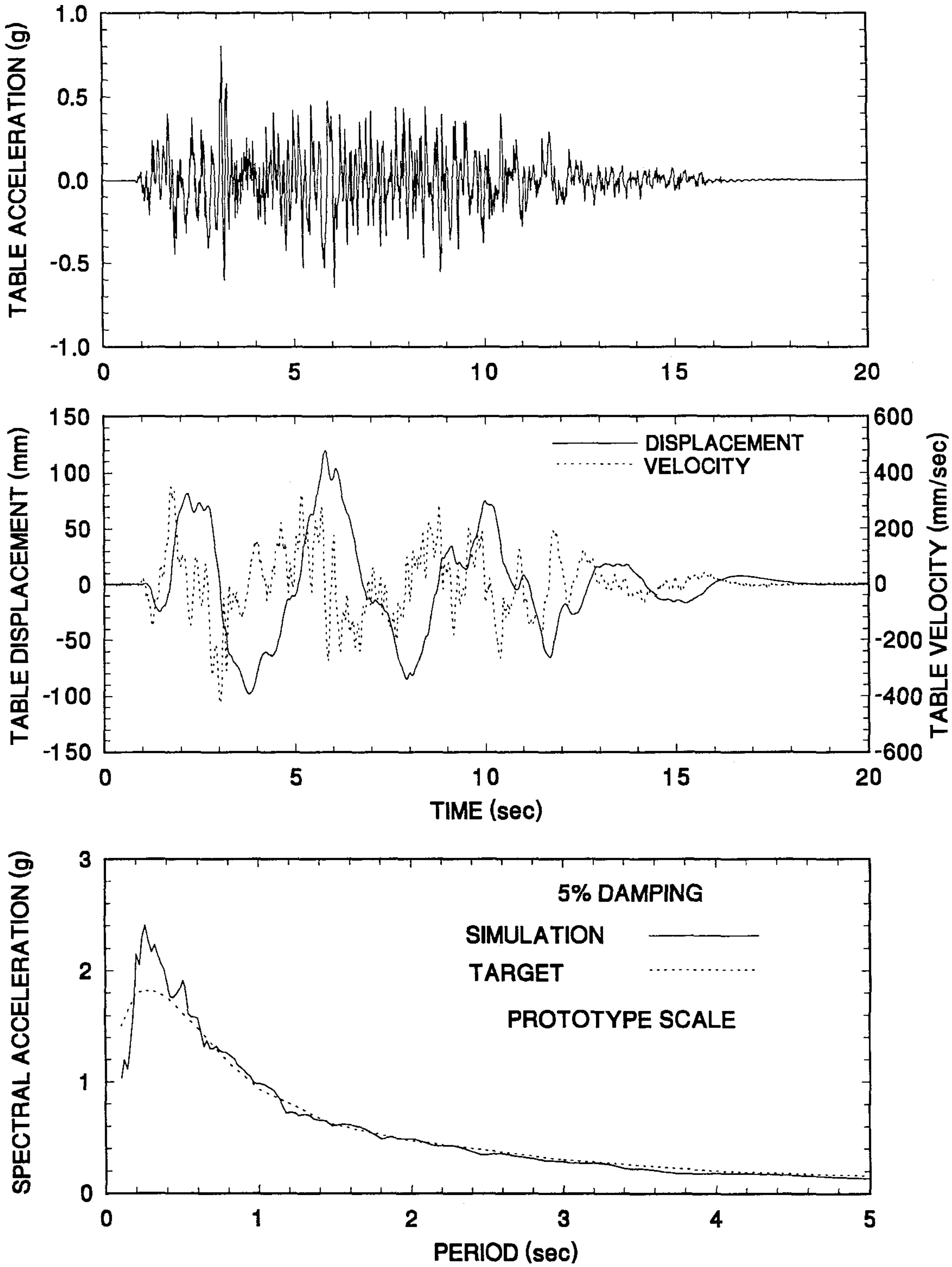

Figure 4-27 Time Histories of Displacement, Velocity and Acceleration and Acceleration Response Spectrum of Shaking Table Motion Excited with CalTrans 10'-80' Alluvium No.3 0.6g 100% Motion

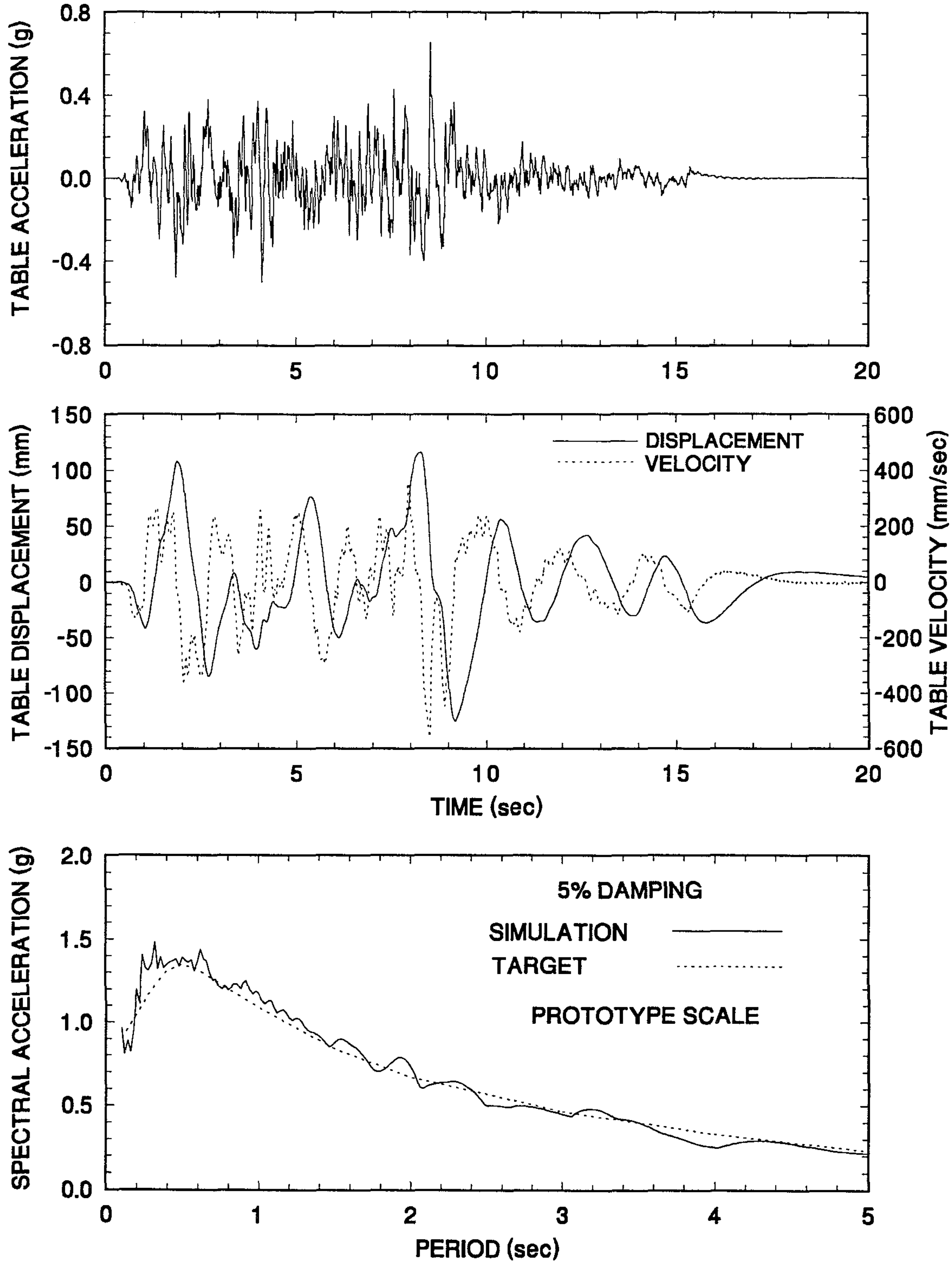

Figure 4-28 Time Histories of Displacement, Velocity and Acceleration and Acceleration Response Spectrum of Shaking Table Motion Excited with CalTrans 80'-150' Alluvium No.2 0.6g 100% Motion

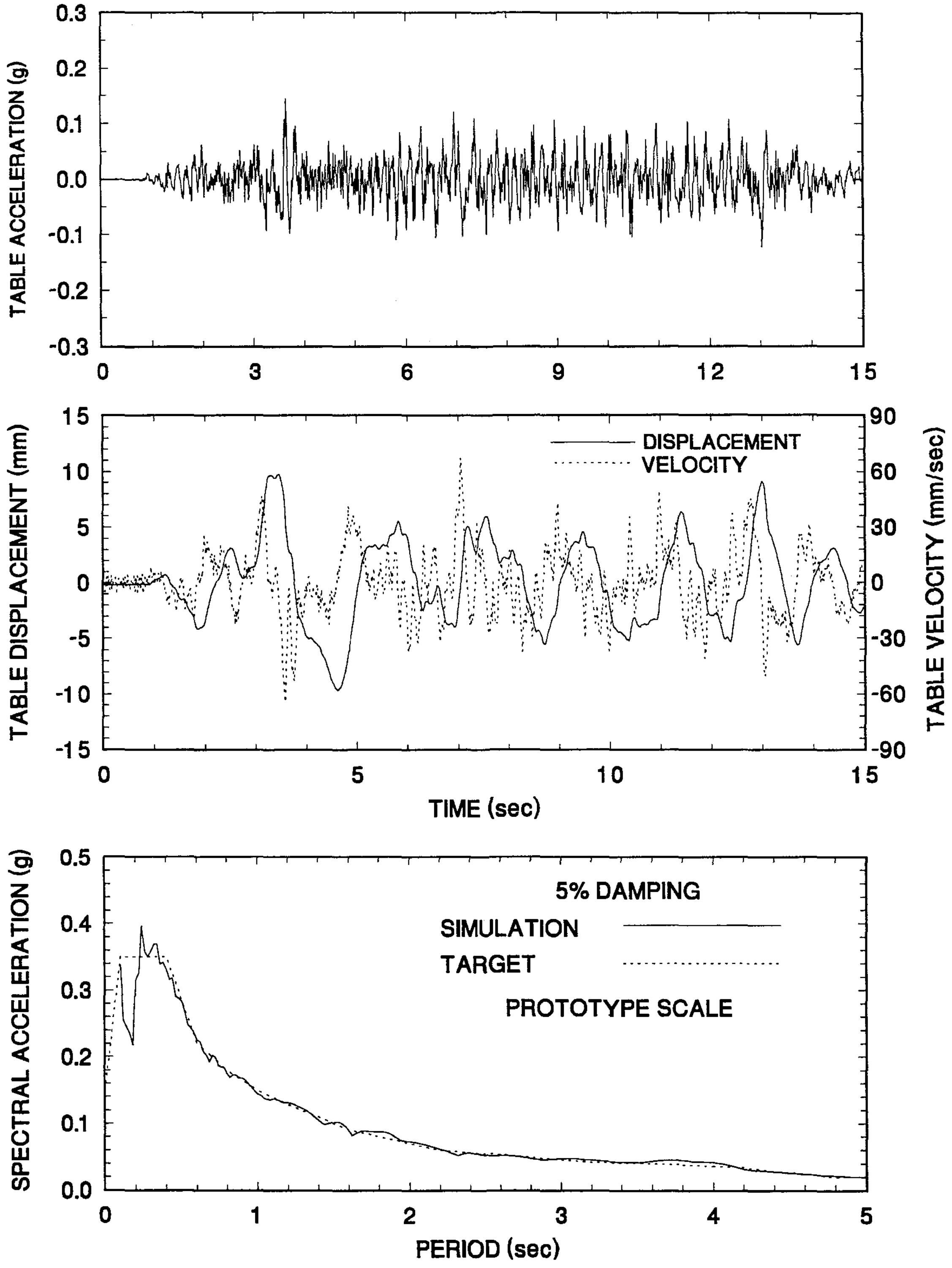

Figure 4-29 Time Histories of Displacement, Velocity and Acceleration and Acceleration Response Spectrum of Shaking Table Motion Excited with Boston 1 100% Motion

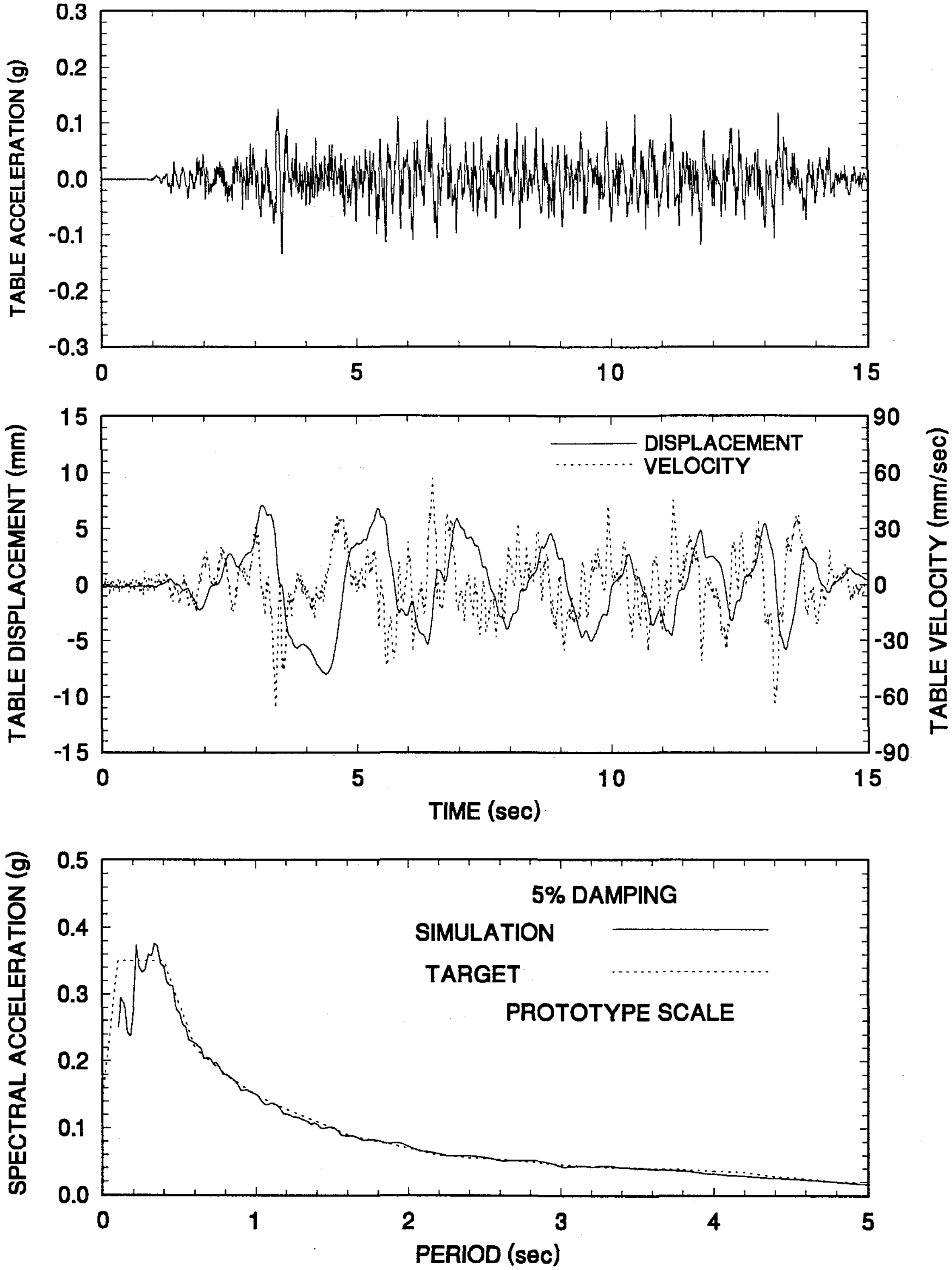

Figure 4-30 Time Histories of Displacement, Velocity and Acceleration and Acceleration Response Spectrum of Shaking Table Motion Excited with Boston 2 100% Motion

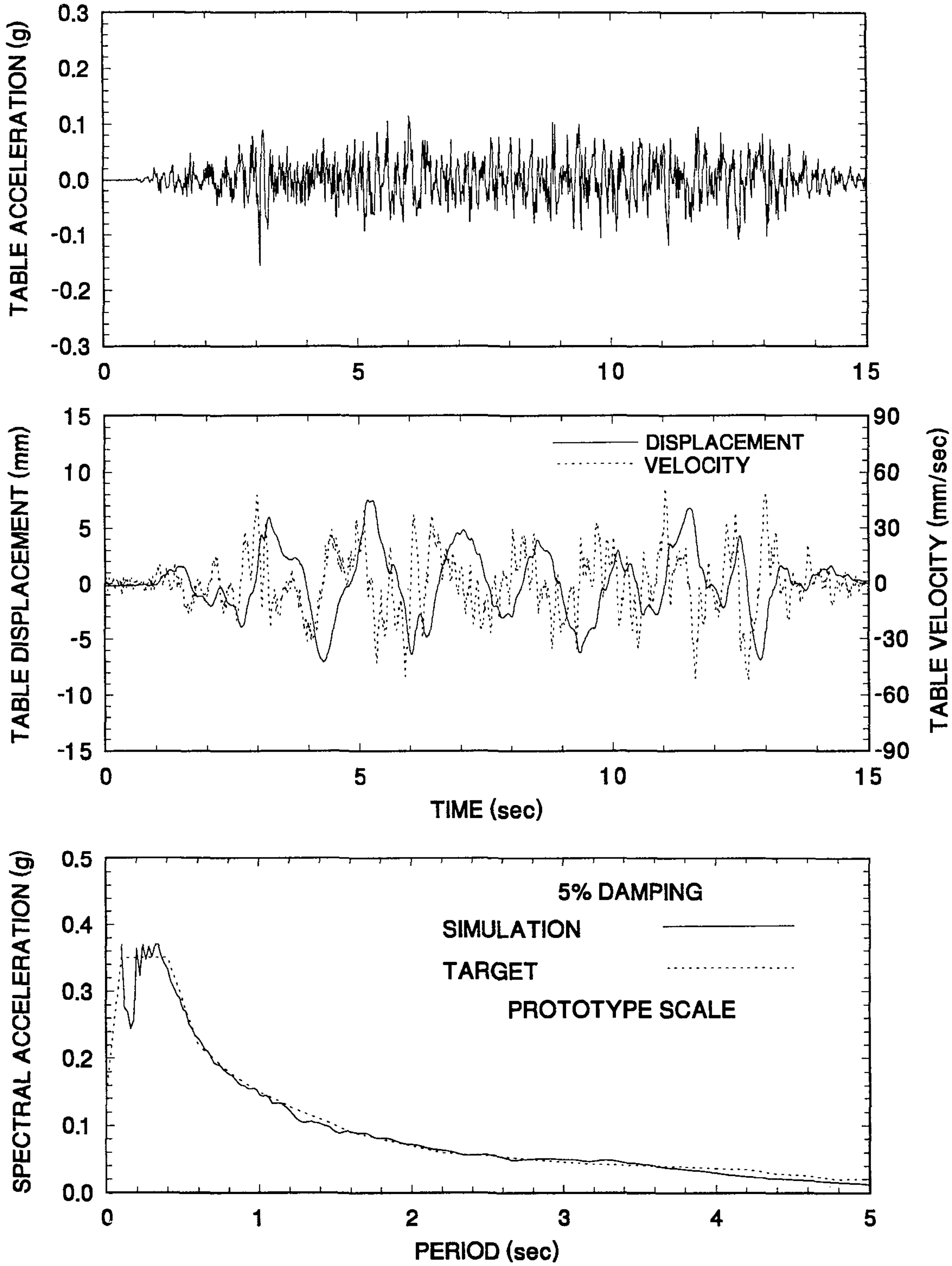

Figure 4-31 Time Histories of Displacement, Velocity and Acceleration and Acceleration Response Spectrum of Shaking Table Motion Excited with Boston 3 100% Motion

SECTION 5

EARTHQUAKE SIMULATOR TEST RESULTS

5.1 Results for Non-isolated Bridge

Testing of the non-isolated bridge (see Figure 4-9, configuration 1) was conducted with only horizontal excitation. The experimental results for the bridge in its non-isolated configuration are summarized in Table 5-I. For each test, the peak values of the table motion in the horizontal direction are given. The displacement and acceleration were directly measured whereas the velocity was determined by numerical differentiation of the displacement record. The peak pier drift is given as a percentage of the pier height which was 1290.3mm. This is the length of the column excluding the stiffeners at the ends (see Figure 4-1). The peak shear force is given as a fraction of the axial load carried by the pier (70 kN each pier).

5.2 Results for Isolated Bridge

Table 5-II lists the earthquake simulation tests and model conditions in the tests of the isolated bridge. The excitation in Table 5-II is identified with a percentage figure which represents a scaling factor on the acceleration, velocity and displacement of the actual record. For example, the figure 200% denotes a motion scaled up by a factor of two in comparison to the actual record.

Table 5-III presents a summary of the experimental results of the isolated bridge. The table includes the following results:

(a) Displacement of bearings located at the south pier (see Figures 4-7 to 4-9). The transducers monitoring the south bearing displacement were continuously monitored and not initialized prior to each test. Thus, the instruments recorded correctly the initial and permanent bearing displacements. Figure 5-1 shows an

Table 5-I Summary of Experimental Results of Non-Isolated Bridge

TEST No.	EXCITATION	PEAK TABLE MOTION			DECK ACCEL.	PIER SHEAR / AXIAL LOAD		PIER DRIFT RATIO (%)	
		DISP. (mm)	VEL. (mm/sec)	ACCEL. (g)	(g)	SOUTH	NORTH	SOUTH	NORTH
FRUN05	EL CENTRO S00E 25%	5.8	40.0	0.095	0.25	0.266	0.271	N/A	0.381
FRUN06	TAFT N21E 50%	7.0	32.7	0.069	0.21	0.230	0.234	N/A	0.315
FRUN07	TAFT N21E 75%	10.5	47.7	0.102	0.25	0.273	0.278	N/A	0.385
FRUN08	JP LEVEL 1 G.C.1 100%	16.6	96.0	0.109	0.21	0.231	0.222	N/A	0.346
FRUN09	JP LEVEL 1 G.C.2 100%	17.3	113.6	0.110	0.26	0.280	0.269	N/A	0.414
FRUN10	JP LEVEL 1 G.C.3 100%	33.7	158.3	0.130	0.33	0.353	0.354	N/A	0.623
FRUN11	AKITA N-S 75%	25.1	108.4	0.138	0.26	0.284	0.283	N/A	0.474
FRUN12	HACHINOHE N-S 50%	15.8	66.0	0.103	0.18	0.200	0.198	N/A	0.311
FRUN13	MIYAGIKEN OKI E-W 75%	8.0	38.0	0.080	0.22	0.242	0.235	N/A	0.384
FRUN14	MEXICO N90W 100%	51.7	303.1	0.169	0.26	0.286	0.284	N/A	0.522
FRUN15	JP LEVEL 2 G.C.1 25%	26.7	114.1	0.104	0.17	0.189	0.181	N/A	0.301
FRUN16	JP LEVEL 2 G.C.2 25%	25.0	109.8	0.098	0.21	0.232	0.225	N/A	0.365
FRUN17	JP LEVEL 2 G.C.3 25%	27.6	116.6	0.117	0.26	0.285	0.283	N/A	0.497
FRUN18	PACOIMA S74W 13%	4.0	36.4	0.103	0.20	0.221	0.214	N/A	0.346
FRUN19	PACOIMA S16E 13%	10.4	63.9	0.095	0.17	0.187	0.186	N/A	0.275
FRUN20	CALTRANS R3 0.6g 20%	23.5	124.8	0.101	0.22	0.227	0.234	N/A	0.389
FRUN21	CALTRANS S3 0.6g 20%	32.1	102.4	0.112	0.31	0.320	0.345	N/A	0.565
FRUN22	CALTRANS A2 0.6g 20%	47.2	128.3	0.104	0.27	0.278	0.298	N/A	0.475

example of bearing displacement time history. The initial displacement is the permanent displacement in the previous test and the initial displacement in the current test.

(b) Maximum travel of bearings located at the North pier. The transducers monitoring the North bearing displacements were initialized prior to each test so that the initial displacement appeared always as zero. Thus, only the maximum travel (MAX.-INIT. in Figure 5-1) could be accurately obtained and not the initial and permanent displacements.

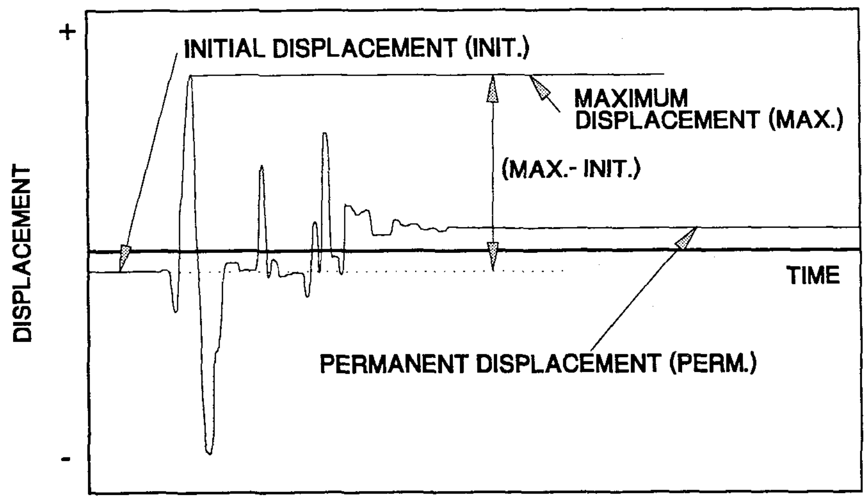

Figure 5-1 Example of Bearing Displacement History

(c) Isolation system shear force normalized by the carried weight (140 kN for total shear force and 70 kN for shear force at each pier). The isolation system shear force is the sum of the horizontal components of bearing forces as recorded by the load cells supporting the bearings.

(d) Pier acceleration. The peak accelerations of the top of the South and North piers are reported.

(e) Deck horizontal acceleration.

(f) Pier shear force normalized by axial load. Each column was instrumented with strain gages to measure the shear force. The reported quantity is the sum of the shear forces in the two columns of each pier divided by the axial load on each pier (140/2=70 kN). It should be noted that the pier shear force is, in general, different than the isolation system shear force. The two forces differ by the inertia force of the accelerating part of the pier between the sliding interface and the location of the strain gages.

(g) Pier drift ratio. This is the displacement of the top of the pier relative to the shake table, divided by the length of the column (1290.3 mm).

During testing of the model bridge in its isolated condition it was observed that the overhangs of the shake table extension, which supported the piers (see Figure 4-1), underwent significant vertical motion even when only horizontal table motion was imposed. The two overhangs did not move vertically in unison. Rather, the motion of the two overhangs was anti-symmetric with the two sides moving with different amplitude and content in frequency. It was concluded that this vertical motion of the overhangs was the combined result of table-structure interaction, vertical flexibility of the overhangs and differences in the vertical stiffness of the overhangs (it was later found that on one side of the concrete table extension the reinforcement was misplaced).

The implications of this phenomenon were to increase the severity of the testing. In effect, in all tests the piers experienced out-of-phase vertical input at their bases. This caused changes in the vertical load carried by the FPS bearings, which in turn affected the stiffness and friction force of the bearings (see Equation 3-9). This explains the differences in the isolation system shear force, pier acceleration and pier shear force and drift between the South and North piers (see Table 5-III). Furthermore, it explains the wavy nature of the recorded force versus displacement loops of the isolation system (see Appendix A).

Table 5-II List of Earthquake Simulation Tests and Model Conditions in Tests of the Isolated Bridge

TEST No.	EXCITATION	PEAK TABLE MOTION			PIER CONDITION		BEARING MATERIAL		BEARING PRESSURE(MPa)		FRICTIONAL PROPERTIES		COMMENTS
		DIS. (mm)	VEL. (mm/s)	ACC. (g)	SOUTH	NORTH	SOUTH	NORTH	SOUTH	NORTH	fmax	fmin	
FPSAR01	EL CENTRO S00E 100%	23.8	166.8	0.350	STIFF	STIFF	No.1	No.1	17.2	17.2	0.104	0.040	
FPSAR02	EL CENTRO S00E 200%	48.0	325.9	0.632	STIFF	STIFF	No.1	No.1	17.2	17.2	0.104	0.040	
FPSAR03	TAFT N21E 100%	14.2	66.0	0.163	STIFF	STIFF	No.1	No.1	17.2	17.2	0.104	0.040	
FPSAR04	TAFT N21E 400%	57.6	261.8	0.606	STIFF	STIFF	No.1	No.1	17.2	17.2	0.104	0.040	
FPSAR05	TAFT N21E 600%	86.2	408.3	0.956	STIFF	STIFF	No.1	No.1	17.2	17.2	0.104	0.040	
FPSAR06	JP LEVEL1 G.C.1 100%	17.1	101.8	0.120	STIFF	STIFF	No.1	No.1	17.2	17.2	0.104	0.040	
FPSAR07	JP LEVEL1 G.C.2 100%	17.7	117.9	0.134	STIFF	STIFF	No.1	No.1	17.2	17.2	0.104	0.040	
FPSAR08	JP LEVEL1 G.C.3 100%	34.4	168.9	0.156	STIFF	STIFF	No.1	No.1	17.2	17.2	0.104	0.040	
FPSAR09	JP LEVEL2 G.C.1 100%	108.4	470.6	0.489	STIFF	STIFF	No.1	No.1	17.2	17.2	0.104	0.040	
FPSAR10	JP LEVEL2 G.C.2 100%	101.6	457.4	0.407	STIFF	STIFF	No.1	No.1	17.2	17.2	0.104	0.040	
FPSAR11	JP LEVEL2 G.C.3 100%	111.7	505.4	0.673	STIFF	STIFF	No.1	No.1	17.2	17.2	0.104	0.040	*
FPSAR12	CALTRANS R3 0.6g 100%	95.9	319.0	0.588	STIFF	STIFF	No.1	No.1	17.2	17.2	0.104	0.040	
FPSAR13	CALTRANS S3 0.6g 100%	119.4	424.6	0.804	STIFF	STIFF	No.1	No.1	17.2	17.2	0.104	0.040	
FPSAR14	CALTRANS A2 0.6g 100%	125.5	559.3	0.653	STIFF	STIFF	No.1	No.1	17.2	17.2	0.104	0.040	
FPSAR15	HACHINOHE N-S 100%	32.3	138.6	0.263	STIFF	STIFF	No.1	No.1	17.2	17.2	0.104	0.040	
FPSAR16	HACHINOHE N-S 300%	95.9	415.3	0.712	STIFF	STIFF	No.1	No.1	17.2	17.2	0.104	0.040	
FPSAR17	AKITA N-S 100%	34.0	144.3	0.193	STIFF	STIFF	No.1	No.1	17.2	17.2	0.104	0.040	
FPSAR18	AKITA N-S 200%	67.9	286.0	0.354	STIFF	STIFF	No.1	No.1	17.2	17.2	0.104	0.040	
FPSAR22	MIYAGIKENOKI E-W 300%	37.1	241.4	0.441	STIFF	STIFF	No.1	No.1	17.2	17.2	0.104	0.040	
FPSAR23	MIYAGIKENOKI E-W 600%	74.2	480.9	1.045	STIFF	STIFF	No.1	No.1	17.2	17.2	0.104	0.040	
FPSAR24	MEXICO N90W 100%	52.5	306.1	0.194	STIFF	STIFF	No.1	No.1	17.2	17.2	0.104	0.040	
FPSAR25	MEXICO N90W 120%	63.0	369.0	0.384	STIFF	STIFF	No.1	No.1	17.2	17.2	0.104	0.040	*
FPSAR26	EL CENTRO S00E 100%	23.9	156.1	0.285	FLEXIBLE	FLEXIBLE	No.1	No.1	17.2	17.2	0.104	0.040	
FPSAR27	EL CENTRO S00E 200%	47.7	324.7	0.620	FLEXIBLE	FLEXIBLE	No.1	No.1	17.2	17.2	0.104	0.040	
FPSAR28	TAFT N21E 100%	14.8	64.6	0.148	FLEXIBLE	FLEXIBLE	No.1	No.1	17.2	17.2	0.104	0.040	

* : DISPLACEMENT RESTRAINER ACTIVATED

Table 5-II Cont'd

TEST No.	EXCITATION	PEAK TABLE MOTION DIS. (mm)	VEL. (mm/s)	ACC. (g)	PIER CONDITION SOUTH	NORTH	BEARING MATERIAL SOUTH	NORTH	BEARING PRESSURE(MPa) SOUTH	NORTH	FRICTIONAL PROPERTIES fmax	fmin	COMMENTS
FPSAR29	TAFT N21E 300%	43.3	198.1	0.510	FLEXIBLE	FLEXIBLE	No.1	No.1	17.2	17.2	0.104	0.040	
FPSAR30	TAFT N21E 400%	57.6	268.8	0.713	FLEXIBLE	FLEXIBLE	No.1	No.1	17.2	17.2	0.104	0.040	
FPSAR31	TAFT N21E 500%	71.6	337.0	0.905	FLEXIBLE	FLEXIBLE	No.1	No.1	17.2	17.2	0.104	0.040	
FPSAR32	TAFT N21E 600%	85.9	408.7	1.067	FLEXIBLE	FLEXIBLE	No.1	No.1	17.2	17.2	0.104	0.040	
FPSAR33	JP LEVEL1 G.C.1 100%	17.4	105.1	0.105	FLEXIBLE	FLEXIBLE	No.1	No.1	17.2	17.2	0.104	0.040	
FPSAR34	JP LEVEL1 G.C.2 100%	17.2	118.5	0.110	FLEXIBLE	FLEXIBLE	No.1	No.1	17.2	17.2	0.104	0.040	
FPSAR35	JP LEVEL1 G.C.3 100%	34.2	160.1	0.118	FLEXIBLE	FLEXIBLE	No.1	No.1	17.2	17.2	0.104	0.040	
FPSAR36	JP LEVEL2 G.C.1 75%	81.2	358.1	0.277	FLEXIBLE	FLEXIBLE	No.1	No.1	17.2	17.2	0.104	0.040	
FPSAR37	JP LEVEL2 G.C.1 100%	108.8	474.8	0.377	FLEXIBLE	FLEXIBLE	No.1	No.1	17.2	17.2	0.104	0.040	
FPSAR38	JP LEVEL2 G.C.2 100%	102.0	454.2	0.415	FLEXIBLE	FLEXIBLE	No.1	No.1	17.2	17.2	0.104	0.040	
FPSAR39	JP LEVEL2 G.C.3 75%	83.7	372.6	0.324	FLEXIBLE	FLEXIBLE	No.1	No.1	17.2	17.2	0.104	0.040	
FPSAR40	JP LEVEL2 G.C.3 90%	97.1	450.4	0.427	FLEXIBLE	FLEXIBLE	No.1	No.1	17.2	17.2	0.104	0.040	*
FPSAR41	CALTRANS R3 0.6g 100%	95.7	315.3	0.608	FLEXIBLE	FLEXIBLE	No.1	No.1	17.2	17.2	0.104	0.040	
FPSAR42	CALTRANS S3 0.6g 100%	119.1	429.5	0.697	FLEXIBLE	FLEXIBLE	No.1	No.1	17.2	17.2	0.104	0.040	
FPSAR43	CALTRANS A2 0.6g 100%	125.3	558.6	0.631	FLEXIBLE	FLEXIBLE	No.1	No.1	17.2	17.2	0.104	0.040	
FPSAR44	HACHINOHE N-S 100%	32.3	143.2	0.226	FLEXIBLE	FLEXIBLE	No.1	No.1	17.2	17.2	0.104	0.040	
FPSAR45	HACHINOHE N-S 300%	96.0	425.9	0.809	FLEXIBLE	FLEXIBLE	No.1	No.1	17.2	17.2	0.104	0.040	
FPSAR46	AKITA N-S 100%	34.1	143.1	0.175	FLEXIBLE	FLEXIBLE	No.1	No.1	17.2	17.2	0.104	0.040	
FPSAR47	AKITA N-S 200%	68.0	291.1	0.352	FLEXIBLE	FLEXIBLE	No.1	No.1	17.2	17.2	0.104	0.040	
FPSAR48	MIYAGIKEN OKI E-W 300%	37.0	234.1	0.452	FLEXIBLE	FLEXIBLE	No.1	No.1	17.2	17.2	0.104	0.040	
FPSAR49	MIYAGIKEN OKI E-W 600%	74.0	478.0	1.115	FLEXIBLE	FLEXIBLE	No.1	No.1	17.2	17.2	0.104	0.040	
FPSAR50	MEXICO N90W 100%	52.6	306.1	0.219	FLEXIBLE	FLEXIBLE	No.1	No.1	17.2	17.2	0.104	0.040	
FPSAR51	PACOIMA S74W 100%	29.2	278.6	0.764	FLEXIBLE	FLEXIBLE	No.1	No.1	17.2	17.2	0.104	0.040	
FPSAR52	PACOIMA S16E 50%	40.7	247.7	0.419	FLEXIBLE	FLEXIBLE	No.1	No.1	17.2	17.2	0.104	0.040	
FPSAR53	TAFT N21E H+V 400%	58.2	272.4	0.684	FLEXIBLE	FLEXIBLE	No.1	No.1	17.2	17.2	0.104	0.040	

* : DISPLACEMENT RESTRAINER ACTIVATED

Table 5-II Cont'd

TEST No.	EXCITATION	PEAK TABLE MOTION DIS. (mm)	VEL. (mm/s)	ACC. (g)	PIER CONDITION SOUTH	NORTH	BEARING MATERIAL SOUTH	NORTH	BEARING PRESSURE(MPa) SOUTH	NORTH	FRICTIONAL PROPERTIES fmax	fmin	COMMENTS
FPSAR54	EL CENTRO S00E H+V 200%	46.7	323.8	0.644	FLEXIBLE	FLEXIBLE	No.1	No.1	17.2	17.2	0.104	0.040	
FPSAR55	TAFT N21E H+V 400%	58.7	273.9	0.590	STIFF	STIFF	No.1	No.1	17.2	17.2	0.104	0.040	
FPSAR56	EL CENTRO S00E H+V 200%	47.0	328.3	0.661	STIFF	STIFF	No.1	No.1	17.2	17.2	0.104	0.040	
FPSAR57	PACOIMA S74W 100%	29.0	278.7	0.841	STIFF	STIFF	No.1	No.1	17.2	17.2	0.104	0.040	
FPSAR58	PACOIMA S16E 50%	40.6	246.6	0.475	STIFF	STIFF	No.1	No.1	17.2	17.2	0.104	0.040	
FPSBR01	EL CENTRO S00E 50%	12.1	81.8	0.184	STIFF	STIFF	No.2	No.2	275.6	275.6	0.058	0.058	
FPSBR02	EL CENTRO S00E 100%	23.9	161.2	0.330	STIFF	STIFF	No.2	No.2	275.6	275.6	0.058	0.058	
FPSBR03	TAFT N21E 100%	14.3	65.8	0.152	STIFF	STIFF	No.2	No.2	275.6	275.6	0.058	0.058	
FPSBR04	TAFT N21E 200%	28.8	127.3	0.296	STIFF	STIFF	No.2	No.2	275.6	275.6	0.058	0.058	
FPSBR05	TAFT N21E 300%	43.2	196.8	0.442	STIFF	STIFF	No.2	No.2	275.6	275.6	0.058	0.058	
FPSBR06	MIYAGIKEN OKI E-W 130%	16.0	104.6	0.185	STIFF	STIFF	No.2	No.2	275.6	275.6	0.058	0.058	
FPSBR10	HACHINOHE N-S 100%	32.2	134.8	0.262	STIFF	STIFF	No.2	No.2	275.6	275.6	0.058	0.058	
FPSBR11	BOSTON 1 100%	9.7	67.2	0.145	STIFF	STIFF	No.2	No.2	275.6	275.6	0.058	0.058	
FPSBR12	BOSTON 2 100%	8.0	65.9	0.134	STIFF	STIFF	No.2	No.2	275.6	275.6	0.058	0.058	
FPSBR13	BOSTON 3 100%	7.5	52.3	0.156	STIFF	STIFF	No.2	No.2	275.6	275.6	0.058	0.058	
FPSCR01	EL CENTRO S00E 200%	48.1	318.6	0.622	STIFF	STIFF	No.3	No.3	17.2	17.2	0.120	0.090	
FPSCR02	TAFT N21E 400%	57.4	265.8	0.606	STIFF	STIFF	No.3	No.3	17.2	17.2	0.120	0.090	
FPSCR03	TAFT N21E 600%	86.0	406.0	0.953	STIFF	STIFF	No.3	No.3	17.2	17.2	0.120	0.090	
FPSCR04	JP LEVEL 2 G.C.1 100%	107.7	469.6	0.522	STIFF	STIFF	No.3	No.3	17.2	17.2	0.120	0.090	
FPSCR05	CALTRANS R3 0.6g 100%	95.5	317.1	0.587	STIFF	STIFF	No.3	No.3	17.2	17.2	0.120	0.090	
FPSCR06	CALTRANS A2 0.6g 100%	125.0	556.9	0.633	STIFF	STIFF	No.3	No.3	17.2	17.2	0.120	0.090	
FPSCR07	HACHINOHE N-S 100%	32.1	137.7	0.252	STIFF	STIFF	No.3	No.3	17.2	17.2	0.120	0.090	
FPSCR08	HACHINOHE N-S 300%	95.8	421.6	0.694	STIFF	STIFF	No.3	No.3	17.2	17.2	0.120	0.090	
FPSCR09	AKITA N-S 200%	67.9	288.0	0.392	STIFF	STIFF	No.3	No.3	17.2	17.2	0.120	0.090	
FPSCR10	MEXICO N90W 100%	52.3	312.2	0.185	STIFF	STIFF	No.3	No.3	17.2	17.2	0.120	0.090	

Table 5-II Cont'd

TEST No.	EXCITATION	PEAK TABLE MOTION DIS. (mm)	VEL. (mm/s)	ACC. (g)	PIER CONDITION SOUTH	NORTH	BEARING MATERIAL SOUTH	NORTH	BEARING PRESSURE(MPa) SOUTH	NORTH	FRICTIONAL PROPERTIES fmax	fmin	COMMENTS
FPSCR11	EL CENTRO S00E 100%	24.7	167.2	0.351	STIFF	STIFF	No.3	No.3	17.2	17.2	0.120	0.090	
FPSCR12	TAFT N21E 200%	28.6	130.3	0.310	STIFF	STIFF	No.3	No.3	17.2	17.2	0.120	0.090	
FPSCR13	TAFT N21E 400%	57.4	264.6	0.608	STIFF	STIFF	No.3	No.3	17.2	17.2	0.120	0.090	
FPSCR14	HACHINOHE N-S 200%	64.0	273.30	0.510	STIFF	STIFF	No.3	No.3	17.2	17.2	0.120	0.090	
FPSCR15	CALTRANS R1 0.6g 100%	118.3	294.2	0.609	STIFF	STIFF	No.3	No.3	17.2	17.2	0.120	0.090	
FPSCR16	CALTRANS R2 0.6g 100%	74.6	270.9	0.555	STIFF	STIFF	No.3	No.3	17.2	17.2	0.120	0.090	
FPSCR17	CALTRANS S2 0.6g 100%	67.5	417.8	0.755	STIFF	STIFF	No.3	No.3	17.2	17.2	0.120	0.090	
FPSCR18	CALTRANS S3 0.6G 100%	118.8	429.8	0.835	STIFF	STIFF	No.3	No.3	17.2	17.2	0.120	0.090	
FPSCR19	AKITA N-S 100%	33.9	145.7	0.197	STIFF	STIFF	No.3	No.3	17.2	17.2	0.120	0.090	
FPSCR20	MIYAGIKEN OKI E-W 200%	24.7	162.2	0.267	STIFF	STIFF	No.3	No.3	17.2	17.2	0.120	0.090	
FPSCR21	MIYAGIKEN OKI E-W 400%	49.4	317.6	0.612	STIFF	STIFF	No.3	No.3	17.2	17.2	0.120	0.090	
FPSCR22	MIYAGIKEN OKI E-W 600%	74.1	476.4	0.989	STIFF	STIFF	No.3	No.3	17.2	17.2	0.120	0.090	
FPSCR23	PACOIMA S74W 100%	29.6	277.4	0.829	STIFF	STIFF	No.3	No.3	17.2	17.2	0.120	0.090	
FPSCR24	EL CENTRO S00E H+V 200%	46.9	327.1	0.655	STIFF	STIFF	No.3	No.3	17.2	17.2	0.120	0.090	
FPSCR25	TAFT N21E H+V 400%	58.6	273.7	0.614	STIFF	STIFF	No.3	No.3	17.2	17.2	0.120	0.090	
FPSCR26	JP LEVEL 2 G.C.2 100%	101.0	454.7	0.402	STIFF	STIFF	No.3	No.3	17.2	17.2	0.120	0.090	
FPSCR27	JP LEVEL 2 G.C.3 75%	83.6	370.3	0.348	STIFF	STIFF	No.3	No.3	17.2	17.2	0.120	0.090	
FPSCR28	JP LEVEL 2 G.C.3 100%	111.4	501.3	0.494	STIFF	STIFF	No.3	No.3	17.2	17.2	0.120	0.090	
FPSCR29	PACOIMA S16E 50%	40.4	239.8	0.501	STIFF	STIFF	No.3	No.3	17.2	17.2	0.120	0.090	
FPSCR30	PACOIMA S16E 75%	60.5	375.7	0.755	STIFF	STIFF	No.3	No.3	17.2	17.2	0.120	0.090	
FPSCR31	PACOIMA S16E 85%	68.4	422.3	0.837	STIFF	STIFF	No.3	No.3	17.2	17.2	0.120	0.090	
FPSCR32	PACOIMA S16E 100%	80.5	493.8	0.963	STIFF	STIFF	No.3	No.3	17.2	17.2	0.120	0.090	*
FPSCR33	JP LEVEL 2 G.C.3 100%	111.3	497.2	0.483	STIFF	FLEXIBLE	No.3	No.3	17.2	17.2	0.120	0.090	* (IMPACT SOUTH ONLY)
FPSCR34	JP LEVEL 2 G.C.3 100% REV	111.5	500.5	0.516	STIFF	FLEXIBLE	No.3	No.3	17.2	17.2	0.120	0.090	* (IMPACT SOUTH ONLY)
FPSCR35	JP LEVEL 2 G.C.2 100%	101.1	452.7	0.400	STIFF	FLEXIBLE	No.3	No.3	17.2	17.2	0.120	0.090	

* : DISPLACEMENT RESTRAINER ACTIVATED

REV : POLARITY REVERSED

Table 5-II Cont'd

TEST No.	EXCITATION	PEAK TABLE MOTION DIS. (mm)	VEL. (mm/s)	ACC. (g)	PIER CONDITION SOUTH	NORTH	BEARING MATERIAL SOUTH	NORTH	BEARING PRESSURE(MPa) SOUTH	NORTH	FRICTIONAL PROPERTIES fmax	fmin	COMMENTS
FPSCR36	JP LEVEL 2 G.C.1 100%	107.7	473.3	0.412	STIFF	FLEXIBLE	No.3	No.3	17.2	17.2	0.120	0.090	
FPSCR37	EL CENTRO S00E 200%	47.6	321.5	0.584	STIFF	FLEXIBLE	No.3	No.3	17.2	17.2	0.120	0.090	
FPSCR38	TAFT N21E 400%	57.4	265.4	0.637	STIFF	FLEXIBLE	No.3	No.3	17.2	17.2	0.120	0.090	
FPSCR39	TAFT N21E 600%	85.9	413.4	1.006	STIFF	FLEXIBLE	No.3	No.3	17.2	17.2	0.120	0.090	
FPSCR40	HACHINOHE N-S 300%	95.9	426.7	0.747	STIFF	FLEXIBLE	No.3	No.3	17.2	17.2	0.120	0.090	
FPSCR41	CALTRANS R1 0.6g 100%	118.4	285.5	0.525	STIFF	FLEXIBLE	No.3	No.3	17.2	17.2	0.120	0.090	
FPSCR42	CALTRANS R2 0.6g 100%	74.6	269.9	0.568	STIFF	FLEXIBLE	No.3	No.3	17.2	17.2	0.120	0.090	
FPSCR43	CALTRANS R3 0.6g 100%	95.5	315.9	0.595	STIFF	FELXIBLE	No.3	No.3	17.2	17.2	0.120	0.090	
FPSCR44	CALTRANS S2 0.6g 100%	67.6	416.2	0.800	STIFF	FELXIBLE	No.3	No.3	17.2	17.2	0.120	0.090	
FPSCR45	CALTRANS S3 0.6g 100%	118.8	427.6	0.737	STIFF	FLEXIBLE	No.3	No.3	17.2	17.2	0.120	0.090	
FPSCR46	CALTRANS A2 0.6g 100%	125.1	558.2	0.646	STIFF	FLEXIBLE	No.3	No.3	17.2	17.2	0.120	0.090	
FPSCR47	AKITA N-S 200%	67.8	289.8	0.350	STIFF	FLEXIBLE	No.3	No.3	17.2	17.2	0.120	0.090	
FPSCR48	MEXICO N90W 100%	52.4	306.5	0.205	STIFF	FLEXIBLE	No.3	No.3	17.2	17.2	0.120	0.090	
FPSCR49	EL CENTRO S00E 200% H+V	46.7	329.6	0.591	STIFF	FLEXIBLE	No.3	No.3	17.2	17.2	0.120	0.090	
FPSCR50	TAFT N21E 400% H+V	58.6	272.6	0.614	STIFF	FLEXIBLE	No.3	No.3	17.2	17.2	0.120	0.090	
FPSCR51	EL CENTRO S00E 100%	23.7	157.9	0.289	FLEXIBLE	FLEXIBLE	No.3	No.3	17.2	17.2	0.120	0.090	
FPSCR52	EL CENTRO S00E 200%	47.6	325.3	0.639	FLEXIBLE	FLEXIBLE	No.3	No.3	17.2	17.2	0.120	0.090	
FPSCR53	TAFT N21E 200%	28.7	129.0	0.346	FLEXIBLE	FLEXIBLE	No.3	No.3	17.2	17.2	0.120	0.090	
FPSCR54	TAFT N21E 400%	57.3	266.3	0.699	FLEXIBLE	FLEXIBLE	No.3	No.3	17.2	17.2	0.120	0.090	
FPSCR55	TAFT N21E 500%	71.5	339.1	0.864	FLEXIBLE	FLEXIBLE	No.3	No.3	17.2	17.2	0.120	0.090	
FPSCR56	CALTRANS R1 0.6g 100%	118.1	284.9	0.568	FLEXIBLE	FLEXIBLE	No.3	No.3	17.2	17.2	0.120	0.090	
FPSCR57	CALTRANS R2 0.6g 100%	74.5	271.6	0.586	FLEXIBLE	FLEXIBLE	No.3	No.3	17.2	17.2	0.120	0.090	
FPSCR58	CALTRANS R3 0.6g 100%	95.4	315.9	0.598	FLEXIBLE	FLEXIBLE	No.3	No.3	17.2	17.2	0.120	0.090	
FPSCR59	CALTRANS S2 0.6g 100%	67.6	420.2	0.785	FLEXIBLE	FLEXIBLE	No.3	No.3	17.2	17.2	0.120	0.090	
FPSCR60	CALTRANS S3 0.6g 100%	118.6	430.9	0.677	FLEXIBLE	FLEXIBLE	No.3	No.3	17.2	17.2	0.120	0.090	

Table 5-II Cont'd

TEST No.	EXCITATION	PEAK TABLE MOTION DIS. (mm)	PEAK TABLE MOTION VEL. (mm/s)	PEAK TABLE MOTION ACC. (g)	PIER CONDITION SOUTH	PIER CONDITION NORTH	BEARING MATERIAL SOUTH	BEARING MATERIAL NORTH	BEARING PRESSURE(MPa) SOUTH	BEARING PRESSURE(MPa) NORTH	FRICTIONAL PROPERTIES fmax	FRICTIONAL PROPERTIES fmin	COMMENTS
FPSCR61	CALTRANS A2 0.6g 100%	125.0	557.2	0.648	FLEXIBLE	FLEXIBLE	No.3	No.3	17.2	17.2	0.120	0.090	
FPSCR62	HACHINOHE N-S 100%	32.2	142.5	0.226	FLEXIBLE	FLEXIBLE	No.3	No.3	17.2	17.2	0.120	0.090	
FPSCR63	HACHINOHE N-S 300%	95.6	427.8	0.764	FLEXIBLE	FLEXIBLE	No.3	No.3	17.2	17.2	0.120	0.090	
FPSCR64	AKITA N-S 100%	34.0	143.5	0.172	FLEXIBLE	FLEXIBLE	No.3	No.3	17.2	17.2	0.120	0.090	
FPSCR65	AKITA N-S 200%	67.7	286.5	0.379	FLEXIBLE	FLEXIBLE	No.3	No.3	17.2	17.2	0.120	0.090	
FPSCR66	MIYAGIKEN OKI E-W 200%	24.8	153.5	0.294	FLEXIBLE	FLEXIBLE	No.3	No.3	17.2	17.2	0.120	0.090	
FPSCR67	MIYAGIKEN OKI E-W 400%	49.2	314.1	0.644	FLEXIBLE	FLEXIBLE	No.3	No.3	17.2	17.2	0.120	0.090	
FPSCR68	MIYAGIKEN OKI E-W 400%	49.1	313.1	0.642	FLEXIBLE	FLEXIBLE	No.3	No.3	17.2	17.2	0.120	0.090	
FPSCR69	PACOIMA S74W 100%	28.8	279.0	0.734	FLEXIBLE	FLEXIBLE	No.3	No.3	17.2	17.2	0.120	0.090	
FPSCR70	JP LEVEL 2 G.C.1 100%	107.5	474.3	0.383	FLEXIBLE	FLEXIBLE	No.3	No.3	17.2	17.2	0.120	0.090	
FPSCR71	JP LEVEL 2 G.C.2 100%	101.1	452.1	0.412	FLEXIBLE	FLEXIBLE	No.3	No.3	17.2	17.2	0.120	0.090	
FPSCR72	JP LEVEL 2 G.C.3 75%	83.8	371.4	0.324	FLEXIBLE	FLEXIBLE	No.3	No.3	17.2	17.2	0.120	0.090	
FPSCR73	JP LEVEL 2 G.C.3 85%	94.4	421.4	0.368	FLEXIBLE	FLEXIBLE	No.3	No.3	17.2	17.2	0.120	0.090	
FPSCR74	PACOIMA S16E 50%	40.7	247.2	0.426	FLEXIBLE	FLEXIBLE	No.3	No.3	17.2	17.2	0.120	0.090	
FPSCR75	PACOIMA S16E 75%	60.7	370.6	0.637	FLEXIBLE	FLEXIBLE	No.3	No.3	17.2	17.2	0.120	0.090	
FPSCR76	PACOIMA S16E 85%	68.7	417.4	0.725	FLEXIBLE	FLEXIBLE	No.3	No.3	17.2	17.2	0.120	0.090	
FPSCR77	EL CENTRO S00E 200% H+V	46.5	329.1	0.658	FLEXIBLE	FLEXIBLE	No.3	No.3	17.2	17.2	0.120	0.090	
FPSCR78	TAFT N21E 400% H+V	58.4	268.6	0.649	FLEXIBLE	FLEXIBLE	No.3	No.3	17.2	17.2	0.120	0.090	
FPSCR79	PACOIMA S16E 100%	80.4	482.2	0.841	FLEXIBLE	FLEXIBLE	No.3	No.3	17.2	17.2	0.120	0.090	
FPSCR80	PACOIMA S16E 100%	80.5	486.4	0.892	STIFF	FLEXIBLE	No.3	No.3	17.2	17.2	0.120	0.090	
FPSCR81	EL CENTRO S00E 200%	47.8	321.6	0.645	STIFF	STIFF	No.3	No.3	17.2	17.2	0.120	0.090	
FPSCR82	TAFT N21E 600%	85.7	409.6	0.969	STIFF	STIFF	No.3	No.3	17.2	17.2	0.120	0.090	
FPSCR83	MEXICO N90W 100%	52.2	304.4	0.196	STIFF	STIFF	No.3	No.3	17.2	17.2	0.120	0.090	
FPSCR84	MEXICO N90W 100%	52.2	304.6	0.218	FLEXIBLE	FLEXIBLE	No.3	No.3	17.2	17.2	0.120	0.090	

Table 5-III Summary of Experimental Results of Isolated Bridge

TEST No.	BEARING DISPLACEMENT (mm)				ISOLATION SYSTEM SHEAR / WEIGHT			DECK ACC. (g)	PIER ACC. (g)		PIER DRIFT RATIO (%)		PIER SHEAR / AXIAL LOAD	
	SOUTH			NORTH										
	INIT.	MAX.	PERM.	MAX.-INIT.	SOUTH	NORTH	TOTAL		SOUTH	NORTH	SOUTH	NORTH	SOUTH	NORTH
FPSAR01	-0.6	12.3	3.1	13.0	0.123	0.125	0.123	0.145	0.483	0.458	0.06	0.05	N/A	N/A
FPSAR02	3.1	40.1	1.7	37.9	0.191	0.160	0.173	0.186	0.793	0.757	0.06	0.04	N/A	N/A
FPSAR03	1.7	-2.0	-0.6	3.7	0.116	0.117	0.114	0.123	0.271	0.276	0.04	0.03	N/A	N/A
FPSAR04	-0.5	-40.4	1.0	39.7	0.202	0.156	0.170	0.183	0.826	0.821	0.06	0.04	N/A	N/A
FPSAR05	1.0	-78.6	-1.2	79.7	0.291	0.211	0.236	0.260	1.183	1.125	0.06	0.05	N/A	N/A
FPSAR06	-1.1	-3.6	-0.5	1.4	0.103	0.110	0.107	0.108	0.143	0.159	0.05	0.02	N/A	N/A
FPSAR07	-0.5	2.1	-0.9	2.5	0.114	0.118	0.112	0.117	0.202	0.212	0.04	0.03	N/A	N/A
FPSAR08	-0.9	-5.8	-0.5	4.9	0.116	0.122	0.118	0.128	0.224	0.269	0.05	0.03	N/A	N/A
FPSAR09	-0.5	-68.1	0.0	67.4	0.231	0.200	0.212	0.226	0.570	0.641	0.06	0.05	N/A	N/A
FPSAR10	0.0	59.3	-11.9	59.3	0.217	0.195	0.206	0.210	0.483	0.470	0.06	0.05	N/A	N/A
FPSAR11	1.2	-86.9	-17.5	87.9	1.195	0.812	0.816	0.823	1.437	1.506	0.37	0.44	N/A	N/A
FPSAR12	-11.6	30.8	2.2	42.3	0.162	0.151	0.153	0.169	0.993	0.914	0.08	0.08	N/A	N/A
FPSAR13	2.2	35.6	1.3	33.0	0.170	0.173	0.170	0.187	1.141	1.194	0.09	0.09	N/A	N/A
FPSAR14	1.3	71.9	-2.1	70.4	0.231	0.215	0.215	0.223	0.793	0.785	0.09	0.07	N/A	N/A
FPSAR15	-2.1	-8.8	-2.2	6.8	0.130	0.127	0.119	0.126	0.365	0.360	0.06	0.05	N/A	N/A
FPSAR16	-2.2	-62.1	-10.0	59.4	0.231	0.195	0.208	0.223	1.013	0.930	0.07	0.08	N/A	N/A
FPSAR17	-8.8	2.8	-1.0	11.7	0.122	0.121	0.119	0.123	0.314	0.324	0.06	0.05	N/A	N/A
FPSAR18	-1.0	45.0	-1.0	45.9	0.182	0.164	0.172	0.180	0.614	0.578	0.09	0.06	N/A	N/A
FPSAR22	-0.2	-15.2	-1.1	15.0	0.150	0.141	0.139	0.160	0.782	0.810	0.08	0.10	N/A	N/A
FPSAR23	-1.1	41.0	-2.5	41.9	0.186	0.183	0.181	0.183	1.543	1.444	0.12	0.10	N/A	N/A
FPSAR24	-2.1	51.1	-4.5	53.0	0.202	0.185	0.178	0.180	0.311	0.269	0.07	0.06	N/A	N/A
FPSAR25	-4.5	87.2	-2.4	90.6	1.285	1.073	0.834	0.832	1.498	1.502	0.67	0.62	N/A	N/A
FPSAR26	-2.6	10.7	0.6	13.2	0.126	0.128	0.125	0.140	0.704	0.667	0.26	0.24	0.182	0.180
FPSAR27	0.6	36.8	2.5	35.9	0.156	0.152	0.154	0.168	1.574	1.198	0.31	0.29	0.219	0.219
FPSAR28	2.5	-4.1	-1.1	6.5	0.117	0.123	0.116	0.120	0.266	0.315	0.22	0.21	0.147	0.144

Table 5-III Cont'd

TEST No.	BEARING DISPLACEMENT (mm)				ISOLATION SYSTEM SHEAR / WEIGHT			DECK ACC. (g)	PIER ACC. (g)		PIER DRIFT RATIO (%)		PIER SHEAR / AXIAL LOAD	
	SOUTH			NORTH										
	INIT.	MAX.	PERM.	MAX.-INIT.	SOUTH	NORTH	TOTAL		SOUTH	NORTH	SOUTH	NORTH	SOUTH	NORTH
FPSAR29	-1.0	-26.9	-1.1	25.8	0.140	0.141	0.135	0.155	0.896	0.929	0.32	0.28	0.211	0.214
FPSAR30	-1.1	-47.9	-2.7	47.0	0.193	0.163	0.177	0.180	1.209	1.196	0.36	0.33	0.243	0.234
FPSAR31	-2.6	-63.1	-3.1	63.5	0.226	0.181	0.202	0.208	1.489	1.448	0.37	0.34	0.270	0.250
FPSAR32	-3.1	-80.6	-3.0	77.9	0.256	0.195	0.220	0.227	1.640	1.637	0.40	0.36	0.258	0.267
FPSAR33	-3.0	-9.7	-0.5	6.2	0.120	0.125	0.122	0.127	0.287	0.309	0.23	0.22	0.151	0.151
FPSAR34	-0.5	-8.1	0.3	7.4	0.121	0.126	0.123	0.129	0.333	0.334	0.24	0.29	0.154	0.154
FPSAR35	0.3	7.8	-2.7	7.3	0.120	0.124	0.122	0.128	0.343	0.371	0.23	0.23	0.159	0.154
FPSAR36	-2.7	-47.6	-1.6	44.9	0.188	0.155	0.171	0.176	0.673	0.727	0.28	0.27	0.200	0.190
FPSAR37	-1.5	70.9	1.0	72.0	0.237	0.213	0.214	0.230	0.839	0.911	0.37	0.33	0.248	0.230
FPSAR38	-4.8	66.8	-5.1	71.0	0.213	0.198	0.202	0.229	1.055	1.060	0.32	0.36	0.266	0.203
FPSAR39	-5.1	54.4	-1.6	59.2	0.200	0.172	0.180	0.194	0.872	0.913	0.28	0.28	0.209	0.193
FPSAR40	-1.6	86.9	-5.1	88.2	0.662	0.602	0.631	0.624	2.191	2.065	1.02	1.04	0.714	0.654
FPSAR41	-5.0	38.1	4.2	43.3	0.172	0.163	0.166	0.182	1.249	1.393	0.34	0.34	0.246	0.243
FPSAR42	4.2	-34.7	-0.0	39.3	0.178	0.171	0.175	0.196	1.877	2.110	0.33	0.35	0.246	0.241
FPSAR43	0.0	78.6	1.5	78.1	0.230	0.221	0.223	0.233	0.897	1.021	0.37	0.32	0.237	0.242
FPSAR44	1.5	-10.5	-1.1	11.8	0.121	0.125	0.122	0.126	0.298	0.314	0.23	0.20	0.152	0.147
FPSAR45	-1.1	-62.5	-11.7	62.3	0.227	0.186	0.202	0.219	1.097	1.125	0.35	0.40	0.306	0.226
FPSAR46	-11.6	6.3	-0.6	17.9	0.121	0.123	0.122	0.126	0.441	0.444	0.23	0.21	0.152	0.151
FPSAR47	-0.5	54.5	0.0	54.7	0.190	0.183	0.186	0.198	0.750	0.729	0.29	0.27	0.204	0.191
FPSAR48	0.0	-12.8	-1.2	12.5	0.126	0.130	0.127	0.144	0.676	0.676	0.26	0.25	0.178	0.171
FPSAR49	-1.1	-41.6	-0.1	40.4	0.184	0.165	0.169	0.180	1.510	1.610	0.37	0.34	0.275	0.242
FPSAR50	-0.4	69.7	-3.4	70.0	0.217	0.204	0.206	0.216	0.545	0.584	0.32	0.32	0.227	0.206
FPSAR51	-3.4	29.5	3.7	32.5	0.170	0.168	0.167	0.175	1.211	1.331	0.33	0.31	0.247	0.244
FPSAR52	2.9	38.1	-7.7	41.4	0.177	0.149	0.162	0.177	0.786	0.798	0.28	0.27	0.196	0.176
FPSAR53	-7.6	-47.9	-3.1	40.2	0.202	0.170	0.182	0.197	1.087	1.107	0.40	0.38	0.238	0.230

Table 5-III Cont'd

TEST No.	BEARING DISPLACEMENT (mm)				ISOLATION SYSTEM SHEAR / WEIGHT			DECK ACC. (g)	PIER ACC. (g)		PIER DRIFT RATIO (%)		PIER SHEAR / AXIAL LOAD	
	SOUTH			NORTH										
	INIT.	MAX.	PERM.	MAX.-INIT.	SOUTH	NORTH	TOTAL		SOUTH	NORTH	SOUTH	NORTH	SOUTH	NORTH
FPSAR54	-3.1	35.7	2.6	38.6	0.156	0.160	0.155	0.182	1.525	1.160	0.42	0.36	0.208	0.237
FPSAR55	2.6	-38.9	1.1	41.4	0.179	0.177	0.166	0.172	0.922	0.819	0.20	0.17	N/A	N/A
FPSAR56	1.1	38.5	1.95	37.3	0.172	0.168	0.160	0.195	0.874	0.921	0.15	0.13	N/A	N/A
FPSAR57	1.9	-37.5	-0.2	39.3	0.174	0.150	0.156	0.181	0.945	0.914	0.06	0.05	N/A	N/A
FPSAR58	0.0	-31.8	-3.3	31.8	0.166	0.149	0.155	0.167	0.532	0.535	0.05	0.04	N/A	N/A
FPSBR01	-0.5	5.0	1.7	5.6	0.070	0.072	0.070	0.082	0.241	0.235	0.03	0.02	N/A	N/A
FPSBR02	1.5	17.6	0.9	16.0	0.083	0.094	0.088	0.097	0.369	0.399	0.04	0.02	N/A	N/A
FPSBR03	1.0	-2.5	-0.5	3.5	0.067	0.071	0.067	0.081	0.235	0.227	0.03	0.02	N/A	N/A
FPSBR04	-0.4	-15.5	-0.5	15.3	0.086	0.087	0.086	0.094	0.406	0.400	0.04	0.03	N/A	N/A
FPSBR05	-0.5	-37.4	-0.5	37.0	0.123	0.119	0.118	0.137	0.571	0.564	0.04	0.03	N/A	N/A
FPSBR06	-0.5	-5.5	-0.5	5.0	0.072	0.076	0.073	0.087	0.235	0.246	0.04	0.03	N/A	N/A
FPSBR10	-0.3	-14.4	-3.7	14.2	0.082	0.082	0.082	0.096	0.316	0.301	0.03	0.02	N/A	N/A
FPSBR11	-3.7	0.6	-0.6	4.4	0.069	0.073	0.071	0.077	0.201	0.215	0.03	0.03	N/A	N/A
FPSBR12	-0.6	-2.7	-1.3	2.2	0.066	0.071	0.068	0.074	0.193	0.201	0.03	0.02	N/A	N/A
FPSBR13	-1.3	2.3	1.0	3.6	0.068	0.073	0.069	0.074	0.213	0.212	0.03	0.02	N/A	N/A
FPSCR01	1.6	36.3	2.9	34.7	0.209	0.188	0.197	0.206	0.878	0.869	0.08	0.04	N/A	N/A
FPSCR02	2.9	-28.0	0.3	30.7	0.190	0.166	0.172	0.193	0.876	0.878	0.07	0.05	N/A	N/A
FPSCR03	0.3	-72.5	0.4	72.8	0.293	0.243	0.251	0.285	1.281	1.283	0.09	0.07	N/A	N/A
FPSCR04	0.4	-59.1	-2.3	59.5	0.243	0.213	0.226	0.246	0.659	0.607	0.09	0.05	N/A	N/A
FPSCR05	-2.3	26.5	2.8	28.8	0.166	0.178	0.168	0.195	0.776	0.844	0.09	0.05	N/A	N/A
FPSCR06	2.5	-44.3	-8.5	46.8	0.218	0.211	0.207	0.214	0.679	0.698	0.08	0.05	N/A	N/A
FPSCR07	-8.5	0.4	-2.0	8.9	0.169	0.151	0.158	0.162	0.364	0.357	0.05	0.04	N/A	N/A
FPSCR08	-2.0	-52.6	-10.8	50.3	0.236	0.214	0.225	0.252	0.876	0.871	0.08	0.06	N/A	N/A
FPSCR09	-10.8	27.8	-3.1	38.6	0.169	0.172	0.170	0.184	0.540	0.484	0.07	0.04	N/A	N/A
FPSCR10	-3.1	-9.5	-2.7	12.6	0.141	0.142	0.140	0.149	0.208	0.193	0.06	0.03	N/A	N/A

Table 5-III Cont'd

TEST No.	BEARING DISPLACEMENT (mm)				ISOLATION SYSTEM SHEAR / WEIGHT			DECK ACC. (g)	PIER ACC. (g)		PIER DRIFT RATIO (%)		PIER SHEAR/ AXIAL LOAD	
	SOUTH			NORTH										
	INIT.	MAX.	PERM.	MAX.-INIT.	SOUTH	NORTH	TOTAL		SOUTH	NORTH	SOUTH	NORTH	SOUTH	NORTH
FPSCR11	-4.7	5.2	-4.8	9.8	0.139	0.147	0.138	0.166	0.519	0.451	0.06	0.04	N/A	N/A
FPSCR12	-4.8	-12.5	-8.7	7.7	0.134	0.143	0.135	0.165	0.486	0.467	0.06	0.05	N/A	N/A
FPSCR13	-8.7	-39.2	-6.8	30.3	0.181	0.163	0.165	0.188	0.862	0.833	0.07	0.05	N/A	N/A
FPSCR14	-6.8	-35.5	-13.8	28.8	0.162	0.157	0.150	0.188	0.710	0.597	0.07	0.05	N/A	N/A
FPSCR15	-13.8	13.4	-4.6	27.1	0.175	0.172	0.158	0.203	0.751	0.686	0.08	0.07	N/A	N/A
FPSCR16	-4.6	10.7	-8.8	15.2	0.154	0.159	0.151	0.172	0.638	0.675	0.07	0.05	N/A	N/A
FPSCR17	-8.8	24.4	-11.7	33.2	0.167	0.175	0.168	0.184	0.824	0.823	0.06	0.06	N/A	N/A
FPSCR18	-9.5	26.4	-8.6	35.9	0.182	0.184	0.176	0.204	1.069	0.934	0.09	0.05	N/A	N/A
FPSCR19	-8.6	-11.8	-9.7	3.3	0.143	0.141	0.137	0.154	0.303	0.287	0.05	0.04	N/A	N/A
FPSCR20	-9.7	-14.9	-8.3	5.2	0.155	0.141	0.144	0.174	0.387	0.387	0.06	0.05	N/A	N/A
FPSCR21	-8.3	-30.7	-9.5	22.5	0.157	0.162	0.159	0.188	0.949	0.890	0.06	0.05	N/A	N/A
FPSCR22	-9.5	31.0	-9.6	40.3	0.199	0.181	0.183	0.206	1.399	1.331	0.08	0.06	N/A	N/A
FPSCR23	-9.6	-46.6	-7.6	37.1	0.188	0.176	0.172	0.211	0.974	0.973	0.06	0.06	N/A	N/A
FPSCR24	-7.6	29.9	-4.8	37.5	0.186	0.177	0.172	0.219	0.874	0.951	0.15	0.13	N/A	N/A
FPSCR25	-4.8	-38.5	-6.3	33.5	0.174	0.195	0.185	0.190	0.961	0.821	0.21	0.17	N/A	N/A
FPSCR26	-6.2	48.0	-13.4	54.1	0.213	0.203	0.207	0.222	0.512	0.517	0.08	0.05	N/A	N/A
FPSCR27	-13.4	17.4	-8.7	30.8	0.189	0.163	0.168	0.183	0.463	0.478	0.07	0.04	N/A	N/A
FPSCR28	-8.7	-82.4	-5.1	73.7	0.249	0.217	0.228	0.238	0.544	0.585	0.09	0.05	N/A	N/A
FPSCR29	-5.1	-32.6	-10.5	27.6	0.164	0.151	0.152	0.174	0.531	0.488	0.08	0.04	N/A	N/A
FPSCR30	-10.5	-69.4	-13.8	58.9	0.245	0.204	0.217	0.246	0.939	0.781	0.06	0.05	N/A	N/A
FPSCR31	-13.8	-79.2	-13.5	65.4	0.260	0.209	0.230	0.250	1.061	0.912	0.07	0.05	N/A	N/A
FPSCR32	-7.7	-94.2	-12.5	86.2	0.488	0.418	0.453	0.484	1.194	1.046	0.13	0.11	N/A	N/A
FPSCR33	-11.5	78.3	-17.4	82.7	0.645	0.289	0.410	0.417	0.612	1.239	0.15	0.44	N/A	0.297
FPSCR34	-17.4	78.8	3.5	95.3	0.784	0.244	0.501	0.531	1.206	0.993	0.27	0.40	N/A	0.268
FPSCR35	-14.0	56.9	-14.6	65.6	0.230	0.201	0.212	0.234	0.511	1.047	0.08	0.33	N/A	0.224

Table 5-III Cont'd

TEST No.	BEARING DISPLACEMENT (mm)				ISOLATION SYSTEM SHEAR / WEIGHT			DECK ACC. (g)	PIER ACC. (g)		PIER DRIFT RATIO (%)		PIER SHEAR / AXIAL LOAD	
	SOUTH			NORTH										
	INIT.	MAX.	PERM.	MAX.-INIT.	SOUTH	NORTH	TOTAL		SOUTH	NORTH	SOUTH	NORTH	SOUTH	NORTH
FPSCR36	-14.6	-76.4	-6.4	57.8	0.240	0.203	0.219	0.238	0.652	0.818	0.07	0.41	N/A	0.251
FPSCR37	-6.4	31.8	-2.5	35.1	0.189	0.157	0.169	0.185	0.914	1.675	0.07	0.30	N/A	0.208
FPSCR38	-2.5	-49.3	-9.2	43.4	0.210	0.145	0.178	0.190	0.962	1.097	0.07	0.30	N/A	0.197
FPSCR39	-9.1	-91.5	-8.5	78.3	0.252	0.217	0.233	0.255	1.311	1.663	0.08	0.42	N/A	0.285
FPSCR40	-8.5	-57.6	-19.2	53.8	0.219	0.221	0.202	0.220	0.732	1.093	0.07	0.39	N/A	0.254
FPSCR41	-19.2	20.8	-7.9	36.6	0.167	0.153	0.150	0.173	0.699	1.339	0.07	0.31	N/A	0.211
FPSCR42	-7.8	13.3	-6.1	19.1	0.147	0.138	0.135	0.163	0.666	0.875	0.07	0.26	N/A	0.176
FPSCR43	-6.1	27.4	-4.6	30.2	0.168	0.162	0.165	0.185	0.915	1.183	0.07	0.29	N/A	0.216
FPSCR44	-4.6	28.1	-9.7	30.5	0.169	0.184	0.156	0.166	0.845	1.237	0.07	0.32	N/A	0.228
FPSCR45	-9.7	33.1	-4.7	38.7	0.201	0.183	0.162	0.184	0.914	1.882	0.07	0.32	N/A	0.233
FPSCR46	-4.7	67.5	-9.2	68.0	0.233	0.243	0.230	0.236	0.740	1.024	0.08	0.39	N/A	0.270
FPSCR47	-9.2	43.9	-6.5	48.3	0.184	0.203	0.191	0.206	0.583	0.748	0.06	0.32	N/A	0.220
FPSCR48	-6.9	-69.2	-11.7	57.8	0.234	0.204	0.207	0.219	0.302	0.531	0.06	0.32	N/A	0.203
FPSCR49	-11.6	33.0	-2.7	41.4	0.189	0.153	0.167	0.213	0.818	1.551	0.15	0.33	N/A	0.214
FPSCR50	-2.7	-53.4	-8.4	47.2	0.201	0.163	0.179	0.195	0.994	1.223	0.20	0.35	N/A	0.195
FPSCR51	-8.4	4.1	-6.3	12.6	0.134	0.134	0.124	0.144	0.850	0.802	0.26	0.27	0.181	0.168
FPSCR52	-6.3	31.9	-4.5	38.0	0.161	0.167	0.163	0.176	1.458	1.234	0.27	0.27	0.189	0.194
FPSCR53	-4.5	-15.2	-8.0	10.8	0.119	0.131	0.123	0.143	0.647	0.706	0.24	0.23	0.163	0.163
FPSCR54	-8.0	-55.0	-10.1	47.8	0.201	0.172	0.184	0.202	1.026	1.101	0.30	0.30	0.201	0.203
FPSCR55	-10.4	-73.1	-10.3	63.9	0.230	0.204	0.217	0.234	1.233	1.316	0.34	0.34	0.230	0.222
FPSCR56	-10.4	-43.7	-10.9	32.7	0.166	0.162	0.161	0.178	1.261	1.525	0.30	0.32	0.225	0.212
FPSCR57	-10.9	15.3	-5.8	25.9	0.132	0.152	0.141	0.156	0.774	0.889	0.26	0.26	0.172	0.176
FPSCR58	-5.8	29.2	-2.1	35.1	0.161	0.166	0.162	0.186	1.116	1.404	0.30	0.34	0.218	0.212
FPSCR59	-2.1	-36.6	-7.5	34.6	0.152	0.162	0.152	0.181	1.195	1.247	0.32	0.29	0.199	0.210
FPSCR60	-7.4	31.6	-7.0	39.2	0.162	0.171	0.160	0.189	1.905	2.046	0.29	0.37	0.207	0.238

Table 5-III Cont'd

TEST No.	BEARING DISPLACEMENT (mm)				ISOLATION SYSTEM SHEAR / WEIGHT			DECK ACC. (g)	PIER ACC. (g)		PIER DRIFT (%)		PIER SHEAR / AXIAL LOAD	
	SOUTH			NORTH										
	INIT.	MAX.	PERM.	MAX.-INIT.	SOUTH	NORTH	TOTAL		SOUTH	NORTH	SOUTH	NORTH	SOUTH	NORTH
FPSCR61	-6.9	67.7	-6.5	74.3	0.219	0.247	0.229	0.246	0.851	0.995	0.39	0.33	0.233	0.265
FPSCR62	-6.5	-18.6	-8.8	12.8	0.127	0.124	0.121	0.131	0.275	0.294	0.22	0.22	0.147	0.142
FPSCR63	-8.8	-67.0	-19.2	59.2	0.218	0.189	0.202	0.236	1.000	1.250	0.34	0.40	0.283	0.222
FPSCR64	-19.2	-1.1	-7.9	17.9	0.121	0.116	0.115	0.124	0.421	0.469	0.22	0.24	0.154	0.137
FPSCR65	-7.9	46.4	-7.0	53.7	0.194	0.201	0.194	0.217	0.711	1.004	0.30	0.32	0.218	0.207
FPSCR66	-7.0	-0.1	-7.0	6.9	0.113	0.122	0.116	0.138	0.472	0.593	0.23	0.26	0.158	0.153
FPSCR67	-7.0	-27.2	-7.8	20.0	0.127	0.135	0.130	0.153	0.839	0.943	0.27	0.26	0.179	0.171
FPSCR68	-7.8	12.2	-7.8	20.0	0.128	0.136	0.131	0.152	0.836	0.943	0.26	0.26	0.180	0.172
FPSCR69	-7.8	-43.6	-3.2	36.5	0.156	0.164	0.160	0.177	1.310	1.423	0.30	0.31	0.218	0.217
FPSCR70	-3.5	-77.9	-4.8	74.1	0.230	0.211	0.221	0.240	0.799	0.961	0.43	0.36	0.240	0.265
FPSCR71	-4.8	58.2	-11.4	62.6	0.212	0.207	0.205	0.252	1.012	1.235	0.32	0.37	0.261	0.211
FPSCR72	-11.4	44.1	-8.5	55.3	0.204	0.190	0.187	0.207	0.749	0.900	0.29	0.32	0.212	0.199
FPSCR73	-8.5	-84.8	-15.5	77.3	0.235	0.223	0.215	0.239	0.833	0.993	0.35	0.36	0.247	0.242
FPSCR74	-15.8	-43.2	-14.6	28.8	0.170	0.139	0.153	0.177	0.691	0.804	0.25	0.28	0.185	0.163
FPSCR75	-14.6	-63.3	-12.2	50.1	0.216	0.181	0.193	0.225	1.047	1.053	0.33	0.34	0.218	0.208
FPSCR76	-12.2	-74.5	-10.8	63.0	0.230	0.198	0.205	0.238	1.107	1.226	0.38	0.38	0.243	0.242
FPSCR77	-10.8	31.7	-4.4	42.7	0.161	0.168	0.160	0.188	1.334	1.230	0.37	0.38	0.186	0.199
FPSCR78	-4.4	-54.0	-9.6	49.7	0.195	0.177	0.182	0.207	1.023	1.209	0.35	0.37	0.204	0.199
FPSCR79	-9.6	-90.4	-9.9	80.3	0.251	0.223	0.231	0.257	1.385	1.584	0.43	0.45	0.287	0.274
FPSCR80	-9.9	-93.9	-13.6	81.1	0.284	0.220	0.240	0.258	1.428	1.194	0.07	0.45	N/A	0.277
FPSCR81	-13.2	33.1	-6.1	46.5	0.173	0.172	0.172	0.191	0.773	0.784	0.06	0.04	N/A	N/A
FPSCR82	-6.1	-87.4	-8.8	81.3	0.268	0.213	0.228	0.262	1.073	1.100	0.06	0.05	N/A	N/A
FPSCR83	-8.8	43.0	-11.9	51.7	0.205	0.187	0.185	0.198	0.279	0.255	0.05	0.04	N/A	N/A
FPSCR84	-11.9	63.9	-10.3	75.7	0.221	0.216	0.206	0.233	0.610	0.684	0.33	0.36	0.231	0.223

5.3 Behavior and Effectiveness of Low Friction Isolation System

Tests were conducted with four different sliding interfaces at low and very high bearing pressures. The four interfaces exhibited similar frictional behavior so that, effectively, testing was conducted at two levels of friction: (a) at low level of friction with f_{max}=0.058, and (b) at medium level of friction with f_{max}=0.10 to 0.12.

The isolation system with low friction (f_{max}=0.058) and isolation period of 1.5s (3s in prototype scale) is appropriate for application in areas of moderate seismicity. Accordingly, tests were primarily conducted with moderate excitation, including artificial motions compatible with spectra for a site in Boston (see test series FPSCR in Table 5-II and 5-III). For such excitations, it would be expected that bearings displacements be small and, thus, the developed restoring forces would be insufficient to re-center the isolated bridge.

The test results are summarized in Table 5-IV where they are compared to the results of the non-isolated bridge. The latter results were either directly obtained in tests or extrapolated from test results of the non-isolated bridge by assuming linear behavior. Evidently, the isolated bridge performs significantly better than the non-isolated bridge. Deck Accelerations (and accordingly forces in the substructure) are lower by factors of the order of 4 to 6, while bearing displacements are of the same order or less than the deck to ground displacement of the non-isolated bridge. Furthermore, the permanent displacement in the FPS bearings is very small and does not accumulate with repeated testing.

Table 5-IV Comparison of Response of Isolated (case of low friction) and Non-isolated Bridge

EXCITATION	ISOLATED (f_{max}= 0.058)			NON-ISOLATED	
	DECK ACCEL. (g)	PEAK BEARING DISPL.(mm)	PERM. BEARING DISPL.(mm)	DECK ACCEL (g)	DISPL. OF DECK W.R.T TABLE (mm)
EL CENTRO S00E 25%	N.A.	N.A.	N.A.	0.250	4.9
EL CENTRO S00E 50%	0.082	5.6	1.7	0.500	9.8 *
EL CENTRO S00E 100%	0.097	16.0	0.9	INELASTIC BEHAVIOR *	
TAFT N21E 75%	N.A.	N.A.	N.A	0.250	5.0
TAFT N21E 100%	0.081	3.5	0.5	0.333	6.6 *
TAFT N21E 200%	0.094	15.3	0.5	INELASTIC BEHAVIOR *	
TAFT N21E 300%	0.137	37.0	0.5	INELASTIC BEHAVIOR *	
MIYAGIKENOKI E-W 75%	N.A.	N.A.	N.A.	0.220	4.9
MIYAGIKENOKI E-W 130%	0.087	5.0	0.5	0.509	11.4
HACHINOHE N-S 50%	N.A.	N.A.	N.A.	0.180	4.0
HACHINOHE N-S 100%	0.096	14.2	3.7	0.360	8.0

*EXTRAPOLATED FROM LOWER AMPLITUDE TESTS AND ASSUMING LINEAR BEHAVIOR WHEN PIER SHEAR FORCE / AXIAL LOAD IS LESS THAN OR EQUAL 0.5

5-4 Effectiveness of Medium Friction Isolation System

The isolation system with medium level friction (f_{max}=0.104 or 0.120) is appropriate for application in areas of strong seismicity. Nevertheless, the system was found to be effective at all levels of input excitation. This is vividly illustrated in Figure 5-2 where the deck acceleration and pier shear force of the isolated and non-isolated bridge models is plotted against the peak table acceleration for all conducted tests. In contrast to the behavior of the non-isolated bridge, the isolated one exhibits a response which is nearly unaffected by the level of input excitation. The deck acceleration is maintained between 0.1 and 0.25g and the pier shear force between 0.1W and nearly 0.25W (W = axial load carried by pier), while the table acceleration varies between 0.1 and nearly 1g. This demonstrates the significant benefits offered by seismic isolation.

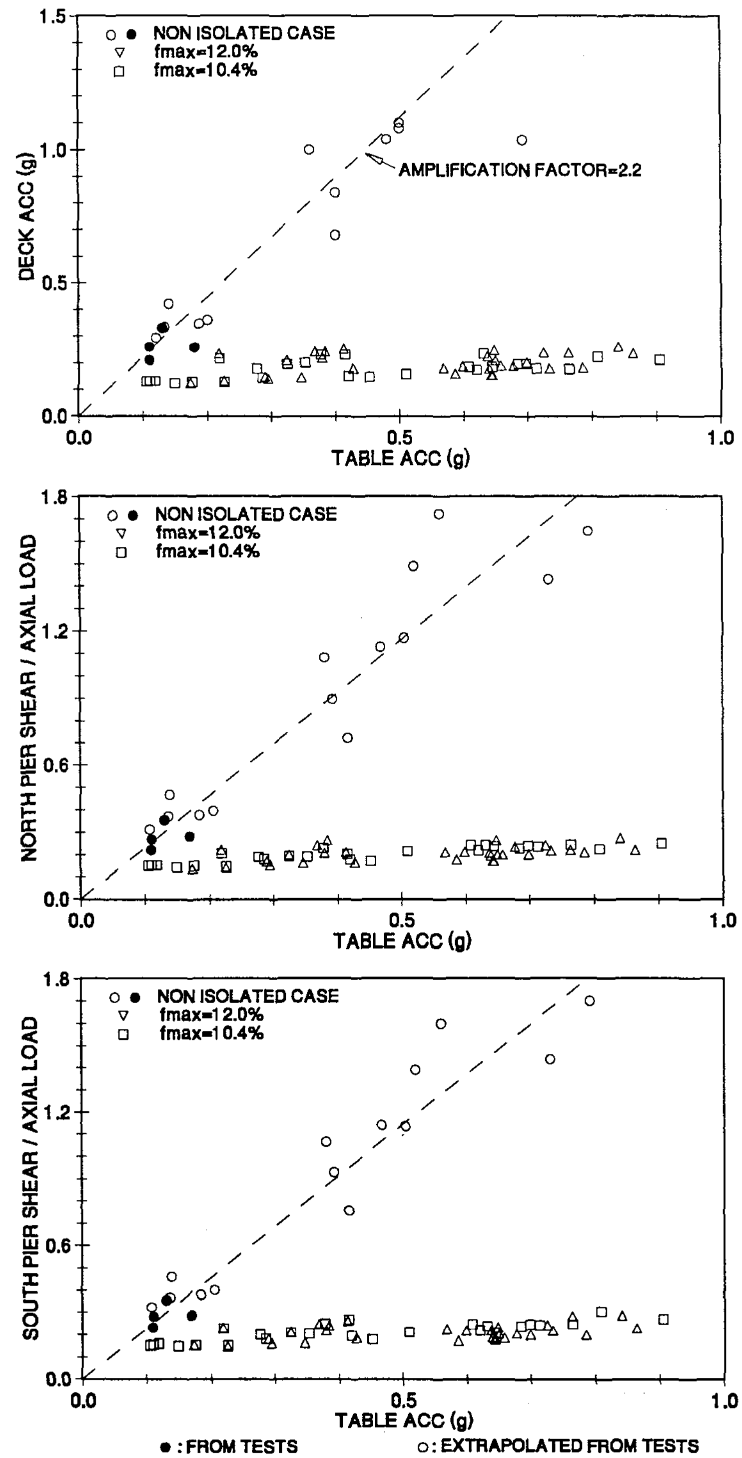

Figure 5-2 **Comparison of Response of Medium Friction Isolated Bridge to Response of Non-isolated Bridge (Flexible Pier Case)**

Figures 5-3 and 5-4 depict the response of the isolated bridge as a function of increasing intensity of specific earthquake motions. It may be observed that the deck acceleration is only marginally affected by the intensity of the input motion. This desirable behavior is achieved with relatively small bearing displacements which are less or about the same as the table displacement.

The experimental results demonstrate the benefits offered by the medium friction isolation system in strong seismic excitation. It may be, however, argued that an isolation system designed for optimum performance in strong seismic excitation might be ineffective in weak seismic excitation. Indeed, this is the case in elastomeric isolation systems with strain dependent properties (Maison, 1992). For example, high damping rubber exhibits significantly more stiffness at low shear strains in comparison to shear strains exceeding 100%.

Exactly the reverse is true for the FPS system. The stiffness, being controlled by the radius of curvature of the spherical sliding interface, is unaffected by the amplitude of motion. Furthermore, the coefficient of sliding friction is velocity dependent so that in weak excitation the sliding velocity is low and, accordingly, the mobilized friction force is less than the one mobilized in strong excitation (see Figure 4-4, material No.1 at low bearing pressure).

Figures 5-5 to 5-7 provide evidence for the performance of the medium friction isolation system at low level excitation. The figures compare the response of the isolated bridge (case of flexible piers, bearing material No.1 at low pressure with f_{max}=0.104) to that of the non-isolated bridge for the Japanese level 1 input motion. The effectiveness of the isolation system in these weak motions is clearly evident in the recorded loops of pier shear force versus pier drift. Shear force and drift in the piers of the isolated bridge are approximately half of those in the non-isolated bridge. Moreover, the insensitivity of the isolated bridge to the frequency content of input (ground conditions 1 through 3) is noted in the recorded loops of Figures 5-5 to 5-7.

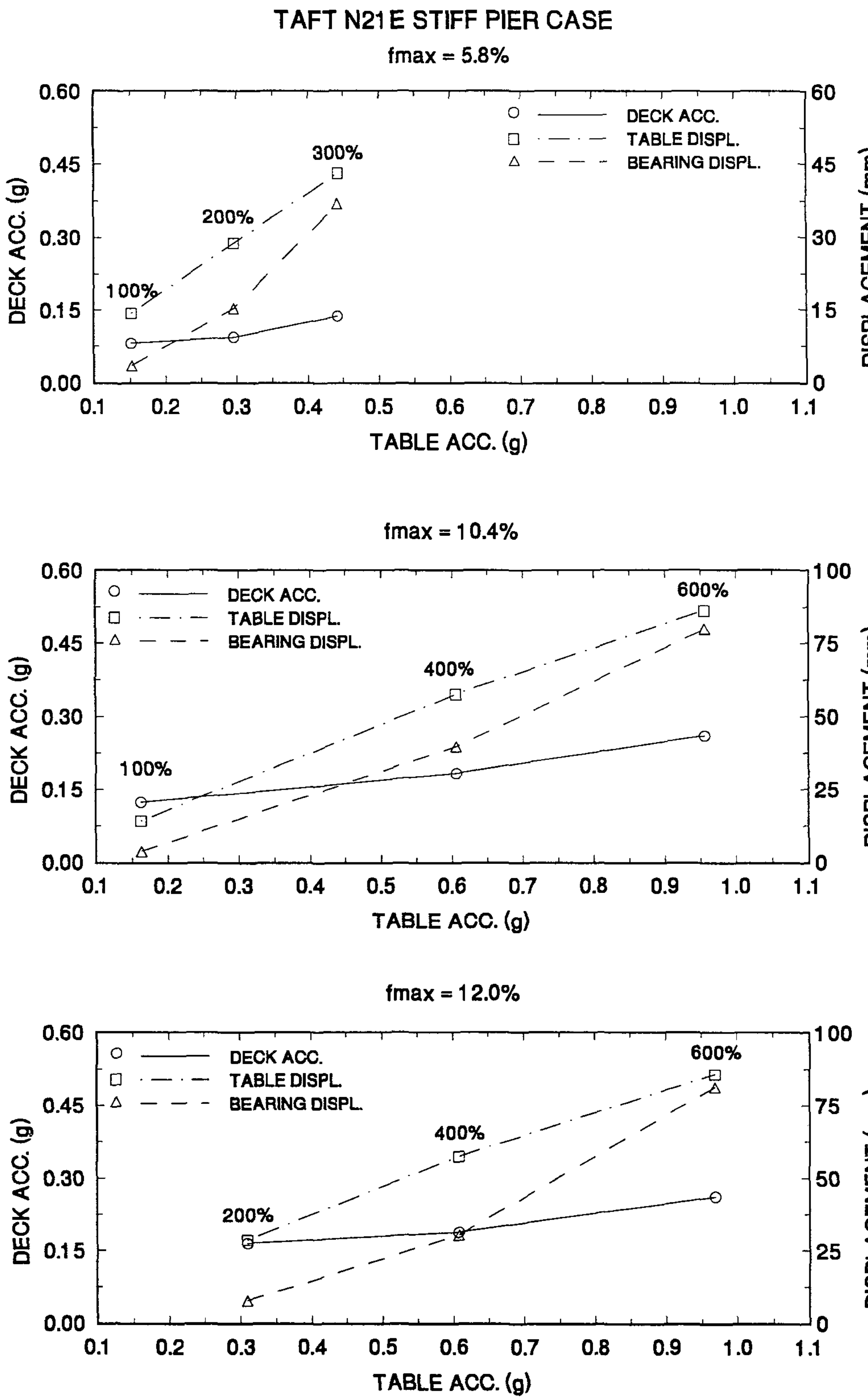

Figure 5-3 **Response of Isolated Bridge Model under Taft Input with Increasing Intensity.**

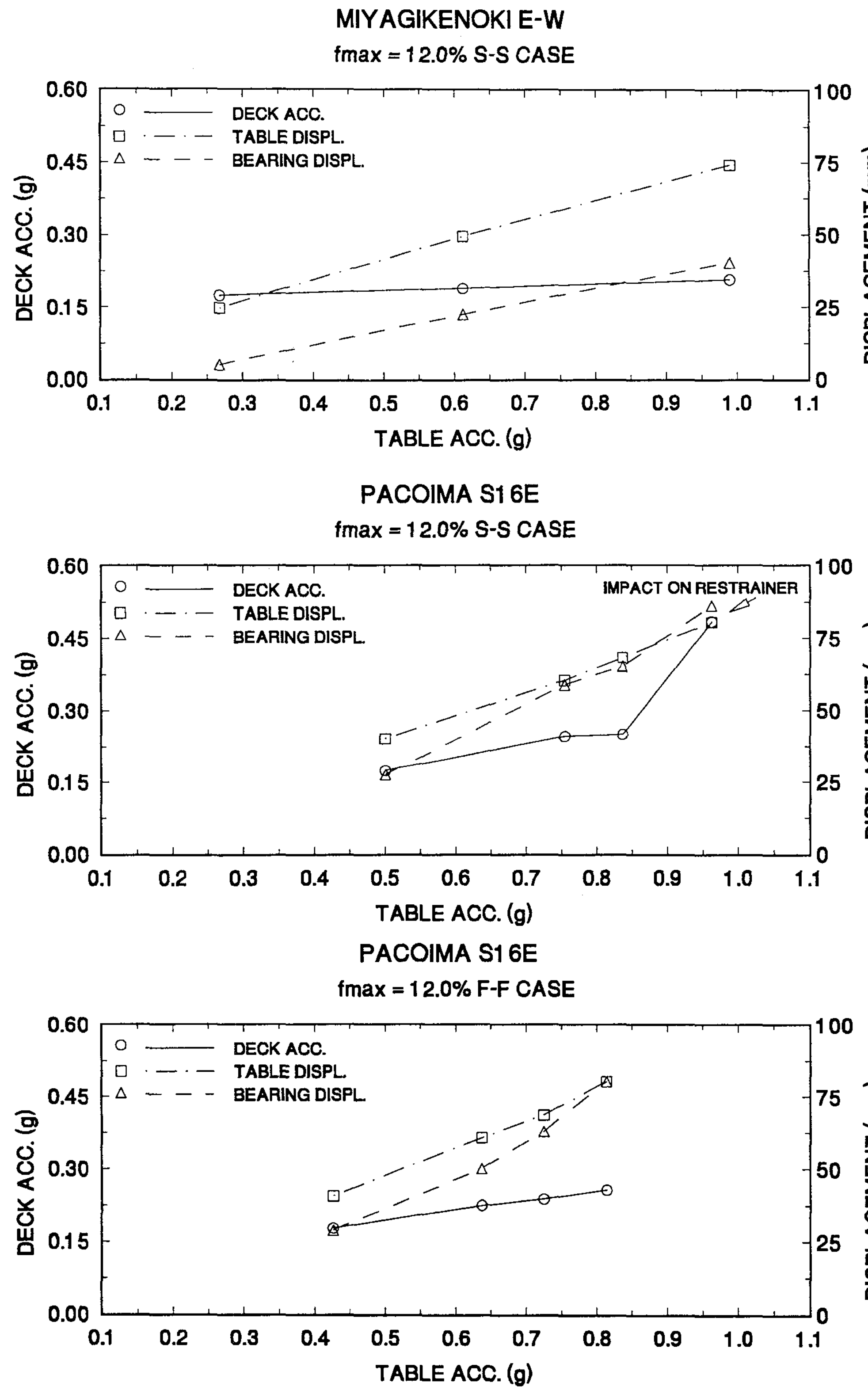

Figure 5-4 **Response of Isolated Bridge Model under Increasing Earthquake Intensity (S-S:case of stiff piers, F-F:case of flexible piers).**

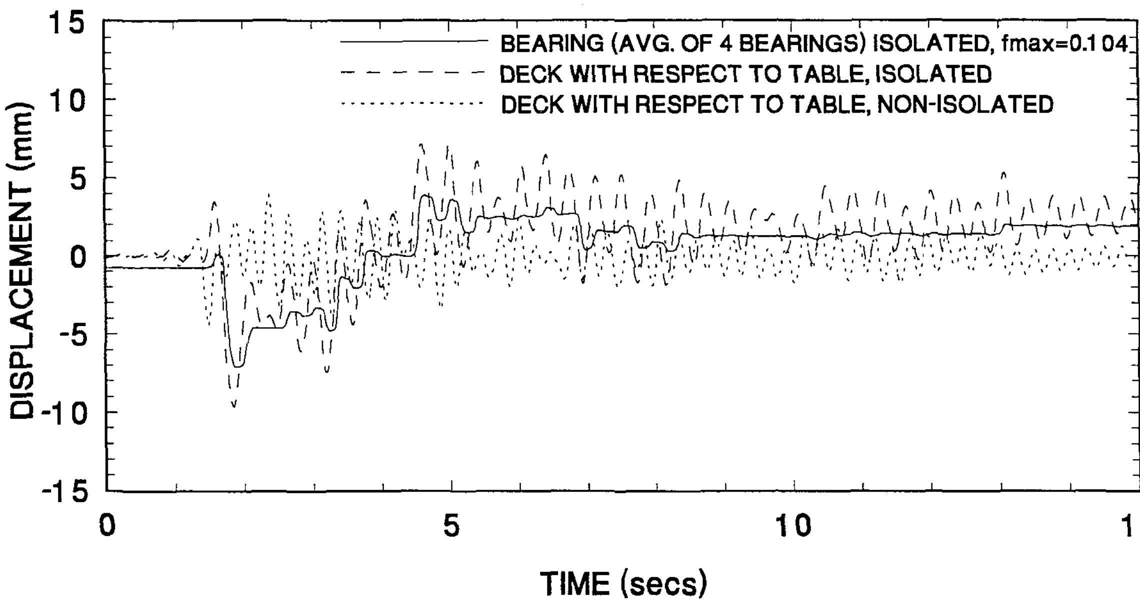

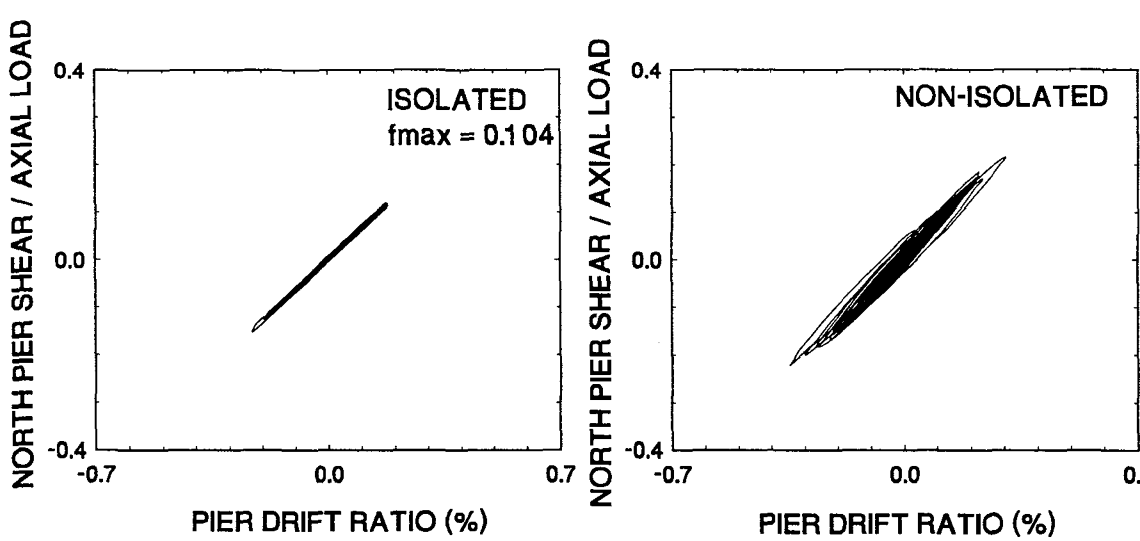

Figure 5-5 Comparison of Response of Isolated Bridge (case of flexible piers) to Response of Non-isolated Bridge for Japanese Level 1, Ground Condition 1 Input

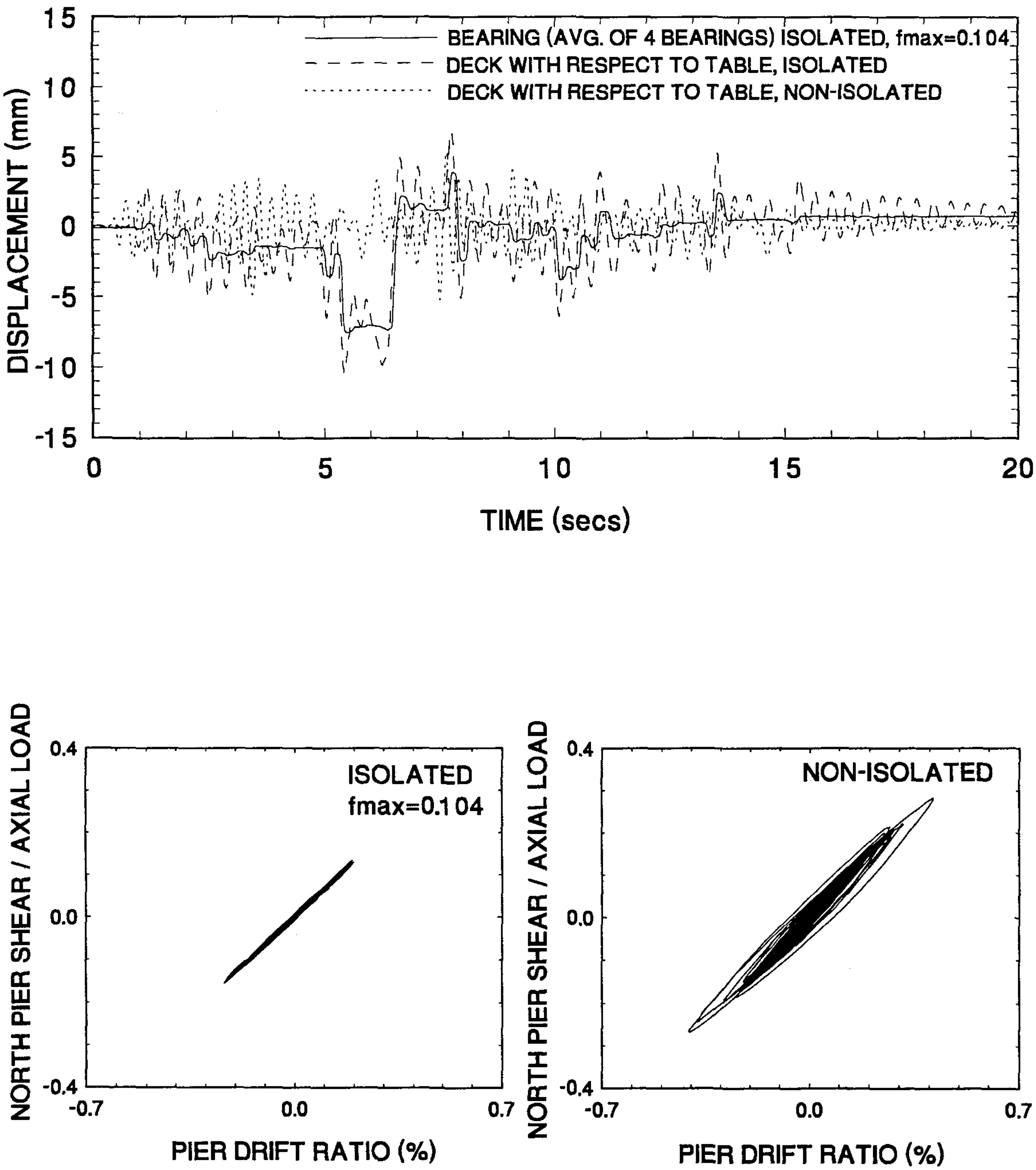

Figure 5-6 Comparison of Response of Isolated Bridge (case of flexible piers) to Response of Non-isolated Bridge for Japanese Level 1, Ground Condition 2 Input

5.5 Effect of Vertical Ground Motion

The force-displacement of an FPS bearing is described by Equation (3-9). Under vertical ground motion the load on the bearing varies, so that Equation (3-9) is modified to

$$F = (1 + \frac{\ddot{u}_{gv}}{g})\,[\frac{W}{R}u + \mu W sgn(\dot{u})\,] \tag{5-1}$$

where $\ddot{u}_{gv}$ = vertical ground acceleration and g = acceleration of gravity. In effect, the vertical ground acceleration modifies the load on the bearing and, thus, modifies both the restoring force and the friction force. A second indirect effect of the vertical ground motion is the modification of bearing pressure at the sliding interface. This, in turn, modifies the coefficient of sliding friction which is pressure dependent.

It appears, in a casual review of these effects, that the vertical ground motion has significant effects. The experimental results provide evidence to the contrary. Figures 5-8 and 5-9 compare the response of the isolated bridge (case of flexible piers, f_{max}=0.104) to the El Centro S00E 200% and Taft N21E 400% input, with and without the vertical ground component. Evidently, the vertical input has a minor effect which is primarily seen in the wavy form of the isolation system hysteresis loop. The observed differences in the loops of pier shear force versus pier deformation are not real but rather a result of the vertical motion effect on the displacement transducer which measured the pier deformation.

The reason for the rather minor effect of vertical motion on the response of the isolated bridge is that the vertical ground motion contains frequencies different than those of the horizontal ground motion and that the two motions are not in phase. The peaks of the horizontal and vertical ground motions occur at different times so that their effects do not coincide.

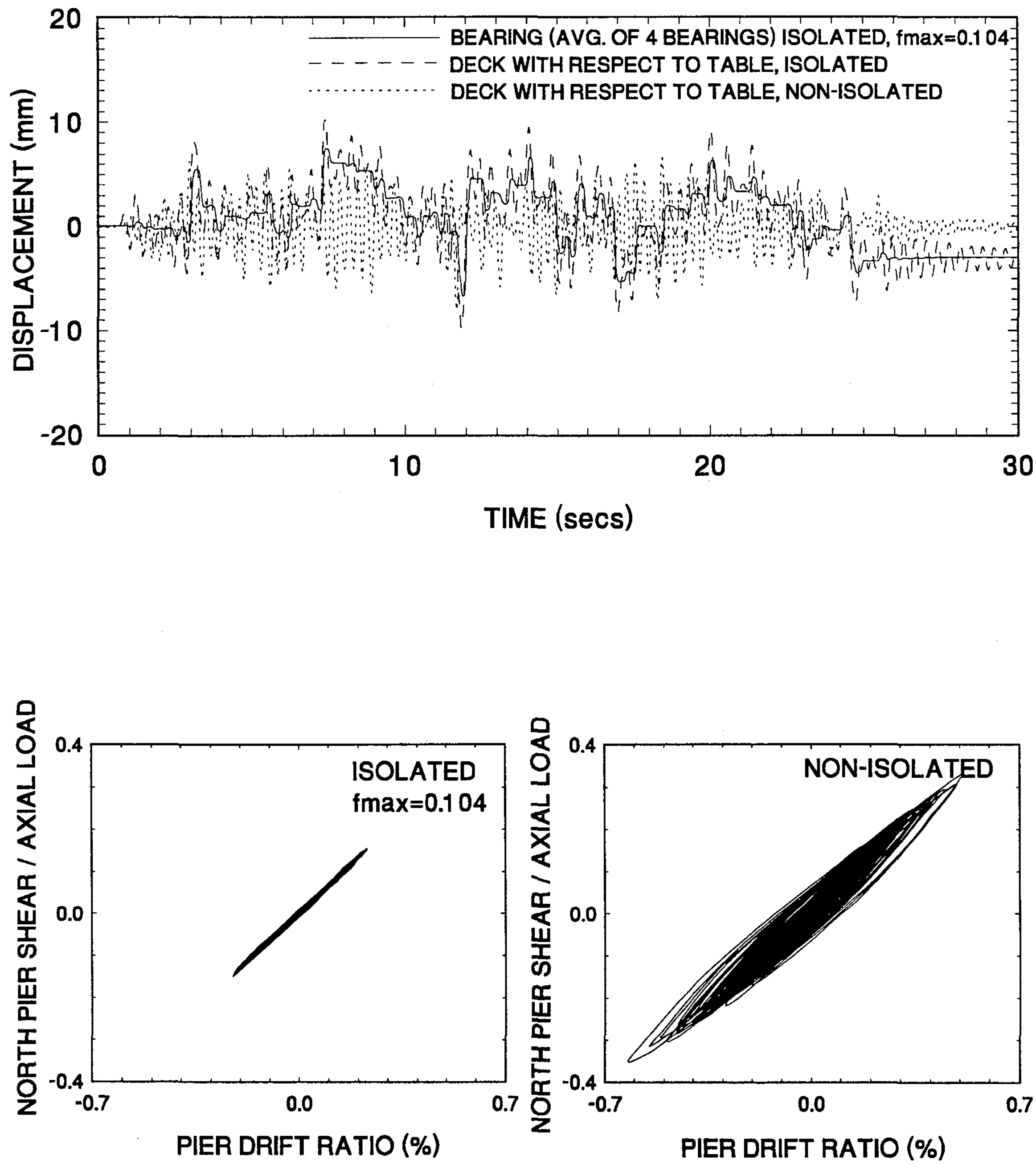

Figure 5-7 **Comparison of Response of Isolated Bridge (case of flexible piers) to Response of Non-isolated Bridge for Japanese Level 1, Ground Condition 3 Input**

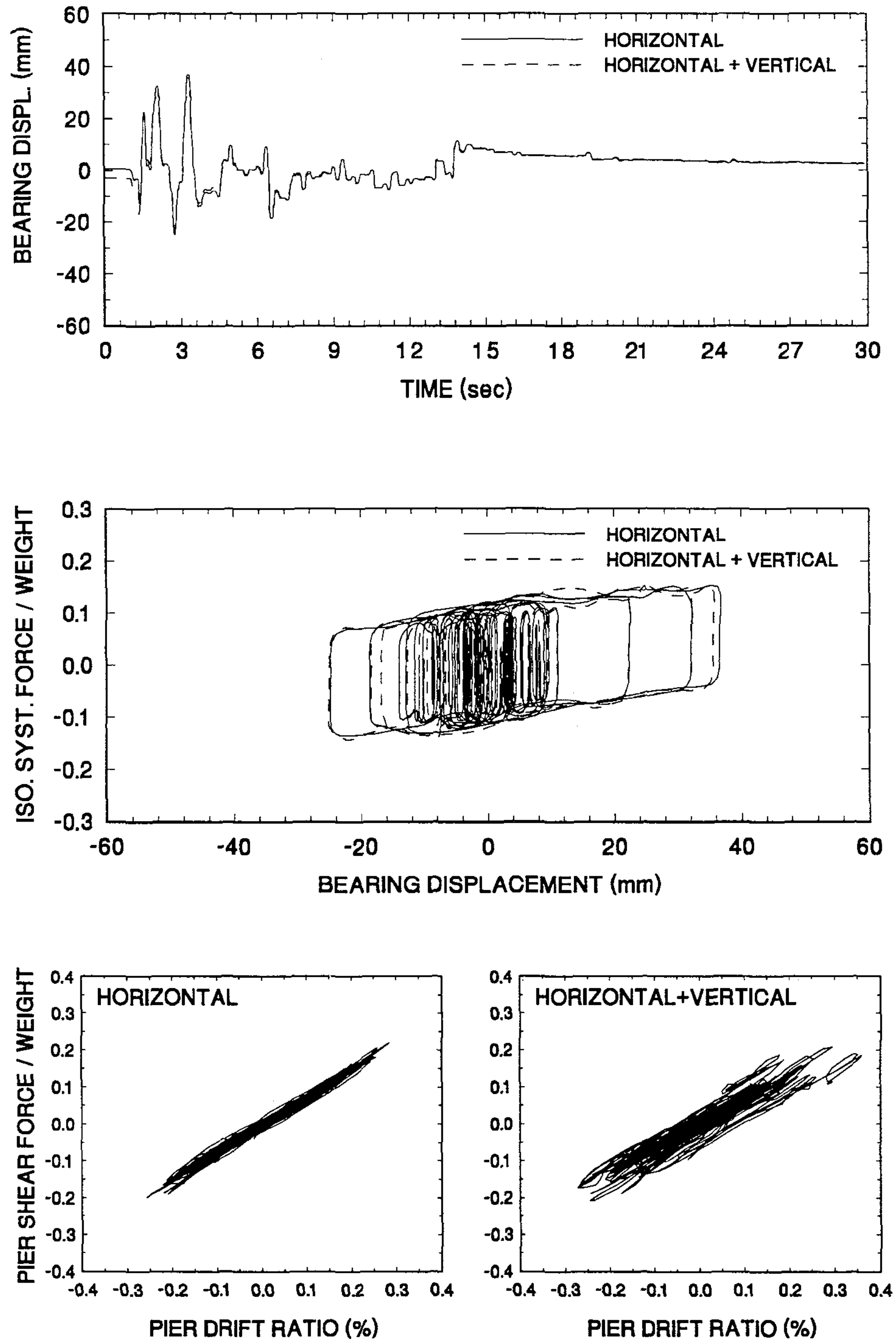

Figure 5-8 Comparison of Response of Isolated Bridge (flexible pier case, material No.1, f_{max}=0.104) for Horizontal Only and Horizontal plus Vertical El Centro S00E 200% Input.

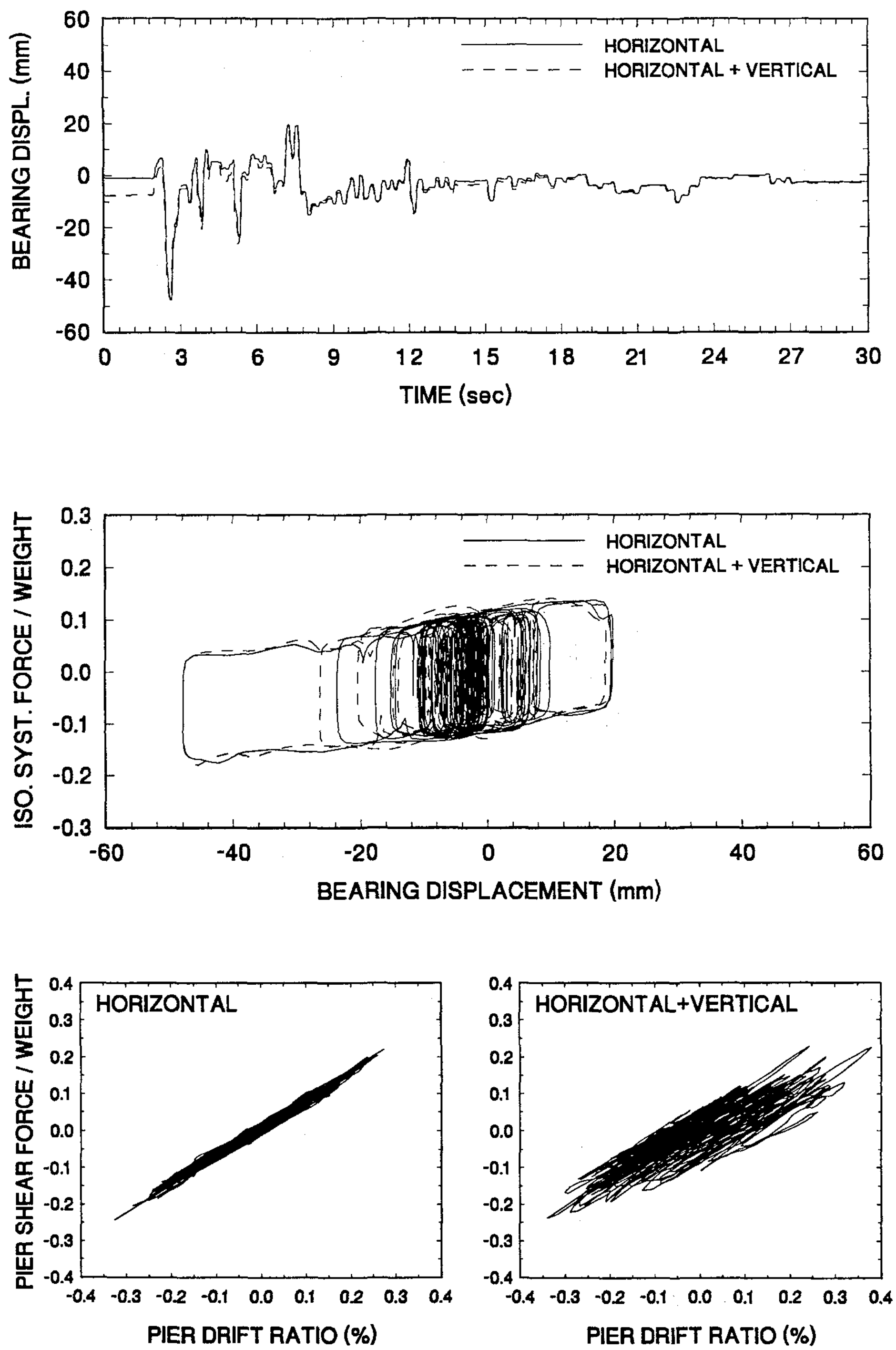

Figure 5-9 Comparison of Response of Isolated Bridge (flexible pier case, material No.1, f_{max}=0.104) for Horizontal Only and Horizontal plus Vertical Taft N21E 400% Input.

5.6 Effect of Impact on the Displacement Restrainer

In some tests with very strong excitation, such as the Pacoima Dam S16E component, or long period excitation, such as the Japanese Level 2, ground condition 3 excitation and the Mexico City (amplified to 120%) excitation, the bearing displacement demand exceeded the bearing displacement capacity. The displacement restrainer of the FPS bearings (see Figure 4-2) was engaged and prevented further displacement at the expense of higher accelerations in the superstructure and higher forces in the substructure. Figure 5-4 provides evidence to the effects of engaging the restrainer in the tests with Pacoima Dam S16E input. In this case, the impact at the engagement of the restrainer is on an essentially rigid pier and the result is an almost 50% increase in deck acceleration.

Evidently, it is a prudent design practice to design the FPS bearings with sufficient displacement capacity to prevent engagement of the restrainer. Nevertheless, the engagement of the displacement restrainer does not result in response values which exceed the values of the non-isolated bridge. An example is provided in Figure 5-10 which compares the response of the isolated bridge (flexible pier case, f_{max}=0.104, test No. FPSAR40) to the response of the non-isolated bridge (extrapolated from the results of test No. FRUN17 assuming linear behavior) for the Japanese level 2, ground condition 3 input.

5.7 System Adequacy

The performance of isolation bearings is assessed by testing as adequate if certain conditions are satisfied. The AASHTO, 1991 requires that in over three cycles of testing at five different amplitudes of displacement (0.25, 0.50, 0.75, 1.0 and 1.25 times the total design displacement) the effective stiffness of the specimen differs by not more than 10 percent from the average effective stiffness. Furthermore, the AASHTO, 1991 requires that in tests with at least 10 cycles of motion at the total design displacement, there is no

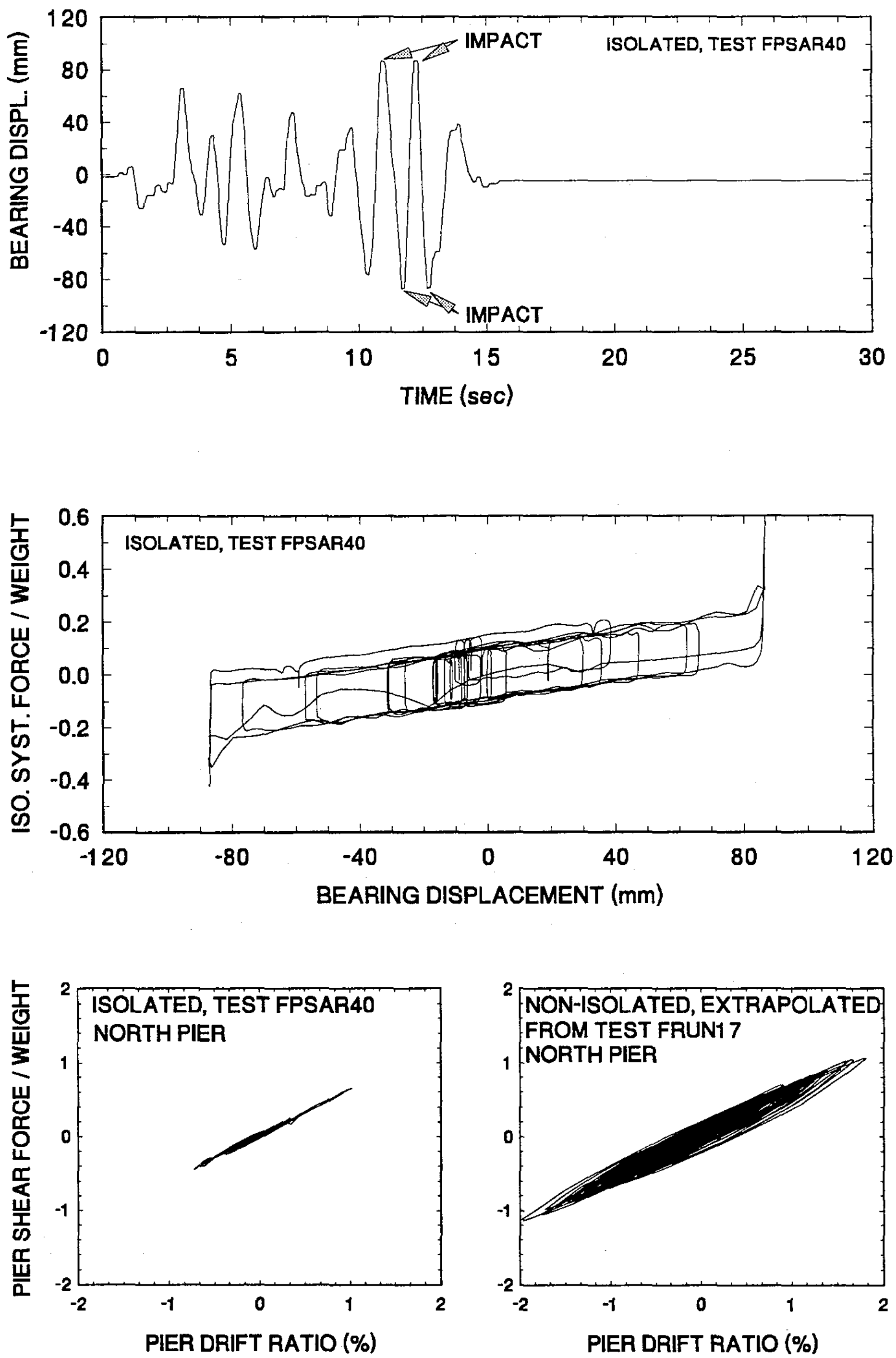

Figure 5-10 Comparison of Response of Isolated Bridge with Engagement of Displacement Restrainer to Response of Non-isolated Bridge under the Japanese Level 2, Ground Condition 3 Input

greater than 20 percent change in either the effective stiffness or the effective damping between the first and any subsequent cycle.

In FPS bearings, the stiffness is entirely controlled by the radius of curvature of the spherical sliding surface (see Equation 3-8). Thus, the stiffness cannot change with repeated testing. However, the coefficient of friction may change and this will affect both the effective stiffness and the effective damping.

Evidence for the exceptional stability of the frictional properties of the sliding interface in the tested FPS bearings is provided in Figure 5-11. The figure shows recorded force-displacement loops of all four bearings in identification tests using the model configuration 2 in Figure 4-9. The bearing material is No.1 under pressure of 17.2 MPa (see Figure 4-4). Five cycles of harmonic motion with 75mm amplitude and 0.4 Hz frequency were imposed. The peak velocity of sliding exceeded 188 mm/s. One test was conducted prior to the seismic testing. The other identical test was conducted following 58 seismic tests (test No. FPSAR01 to FPSAR58 in Tables 5-II and 5-III). It may be observed that the loops prior and following the 58 seismic tests are identical. The friction coefficient remained unchanged after at least 30 cycles at approximately the displacement capacity of the bearings and over 100 cycles at lower displacement.

5.8 Permanent Displacements

Permanent displacements may develop in all hysterestic isolation systems. The AASHTO (AASHTO 1991) and UBC (ICBO 1991) specifications attempt to account for this possibility by either specifying minimum stiffness requirements or by penalizing systems which lack sufficient stiffness. Particularly, the AASHTO, 1991 specifications require that the restoring force of an isolation system at the design displacement, d_i, be at least 0.025W (W=total seismic dead load) greater than the restoring force at displacement equal to $d_i/2$. Systems which do not meet this criterion need to be configured to accommodate displacements equal to at least $3d_i$.

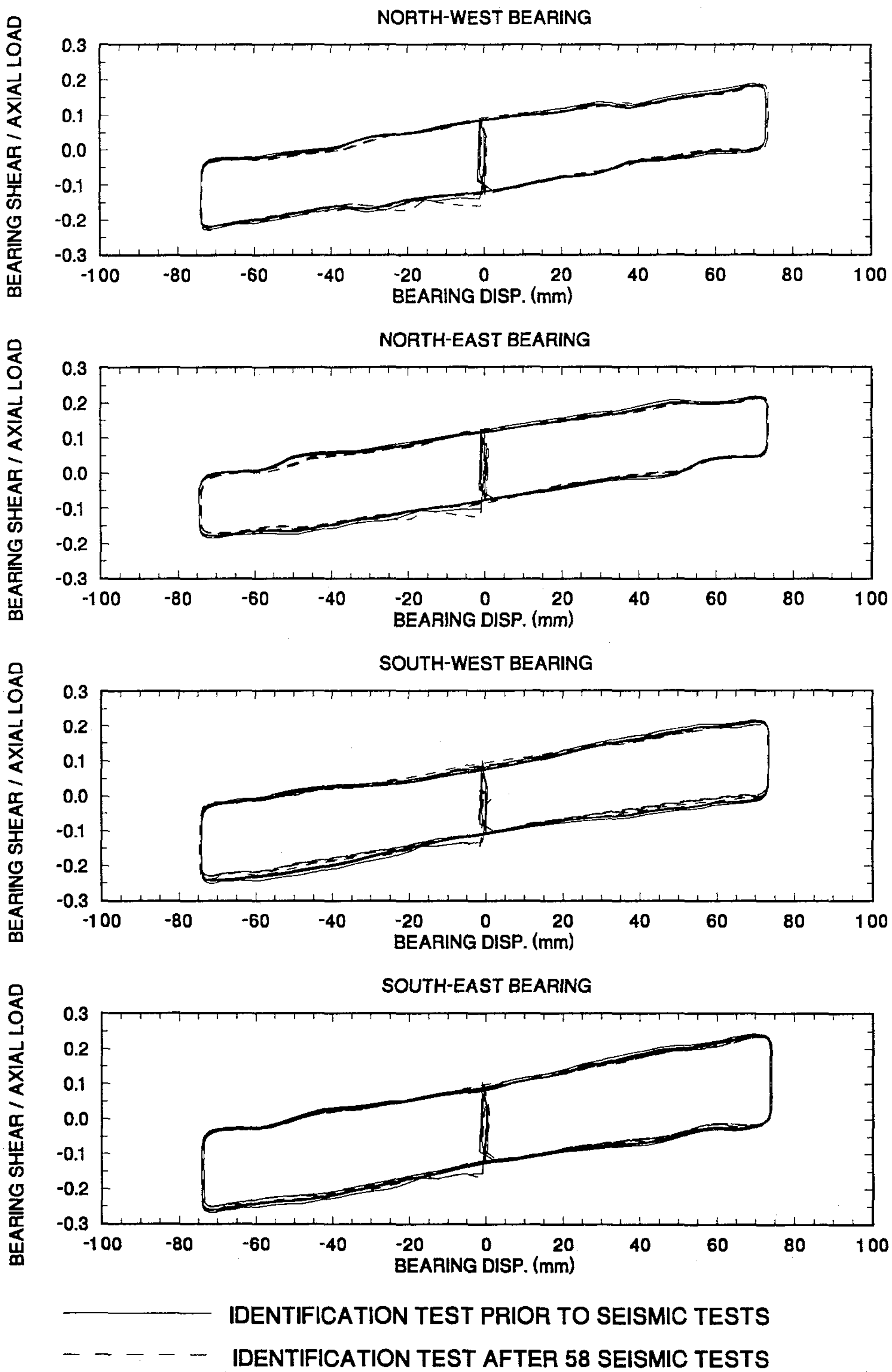

Figure 5-11 Recorded FPS Bearing Force-Displacement Loops for Five Cycles of Harmonic Motion of Amplitude=75mm and Frequency=0.4 Hz. Material No.1, Pressure=17.2 MPa.

The assumption in AASHTO is that systems which do not meet the aforementioned criteria will have large permanent displacements (of the order of d_i) which will accumulate in successive earthquakes. Indeed, this may be the case in systems which completely lack restoring force. Evidence for this was provided by Constantinou, 1990b and 1991b in tests of a sliding isolation system without restoring force.

The tested isolation system had a force-displacement relation expressed by Equations (3-9) and (4-1). The force developed at displacement d_i is, thus, given by

$$F_i = f_{max} W + \frac{d_i W}{R} \tag{5-2}$$

The requirement of AASHTO on the lateral restoring force is equivalent to

$$\frac{d_i}{R} > 0.05 \tag{5-3}$$

For the tested FPS bearings, R=558.8mm, so that Equation (5-3) is equivalent to d_i>27.9mm. Therefore according to AASHTO, it would be expected that in the tests with peak bearing displacement exceeding this limit, the permanent displacements are small and not cumulative. Indeed this has been the case. An inspection of Table 5-III reveals that the permanent displacements were small and not cumulative.

However, the same behavior was also observed in tests with weak excitation when the bearing displacements were less than the limit of 27.9mm. Particularly interesting is the sequence of tests FPSBR (see Table 5-III). In nine of the ten conducted tests the bearing displacements were less than this limit. Yet, the permanent displacements were small and not cumulative.

SECTION 6

ANALYTICAL PREDICTION OF RESPONSE

6.1 Introduction

Analytical techniques for predicting the dynamic response of sliding isolation systems are available (Mokha 1988, 1990b and 1991; Constantinou 1990a, 1990b, 1991a and 1991b). These analytical techniques are employed herein in the prediction of the response of the tested bridge model. The analytical model accounts for the pier flexibility, pier top rotation and vertical motion effects on the properties of the FPS bearings.

6.2 Analytical Model

Figure 6-1 shows the analytical model in the case of the bridge with flexible piers. The degrees of freedom are selected to be the deck displacement with respect to the table, U_d, the pier displacements with respect to the table, U_{p1} and U_{p2}, and the pier rotations, ϕ_{p1} and ϕ_{p2}.

Each pier is modeled by a beam element of length L_i, moment of inertia I_i and modulus of elasticity E_i (i=1 or 2). The beam element is fixed to the table and connected at its top to a rigid block of height h, mass m_{pi} and mass moment of inertia about the center of mass (C.M.) I_{pi}. The center of mass is located at distance h_i from the bottom of the block. This block represents the pier top.

Free body diagrams of the deck and pier tops of the bridge model are shown in Figure 6-2. It should be noted that there is no transfer of moment between the deck and the supporting pier top. The equations of motion are derived by consideration of dynamic equilibrium of the deck and piers in the horizontal direction and of the piers in the rotational direction:

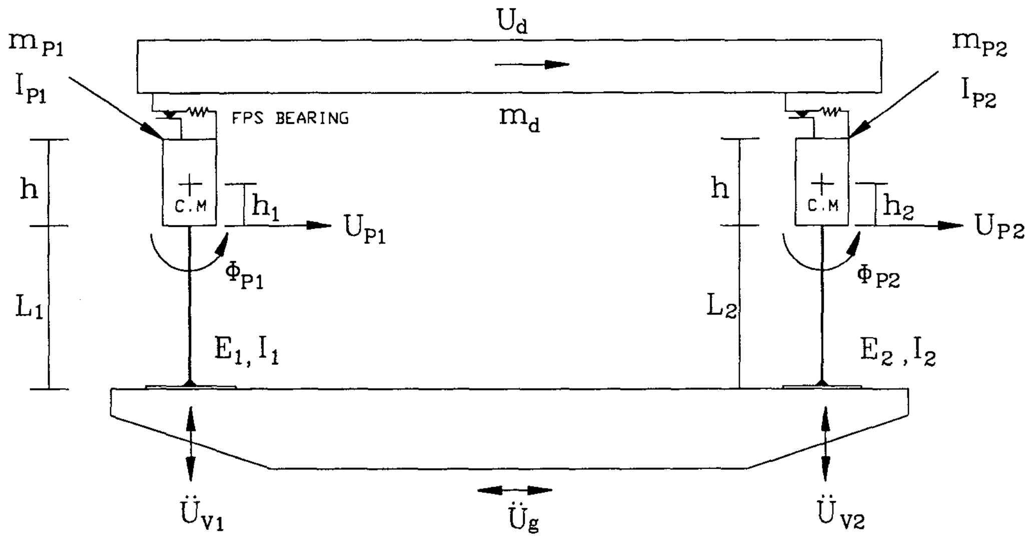

Figure 6-1 Longitudinal Direction Model of Isolated Bridge

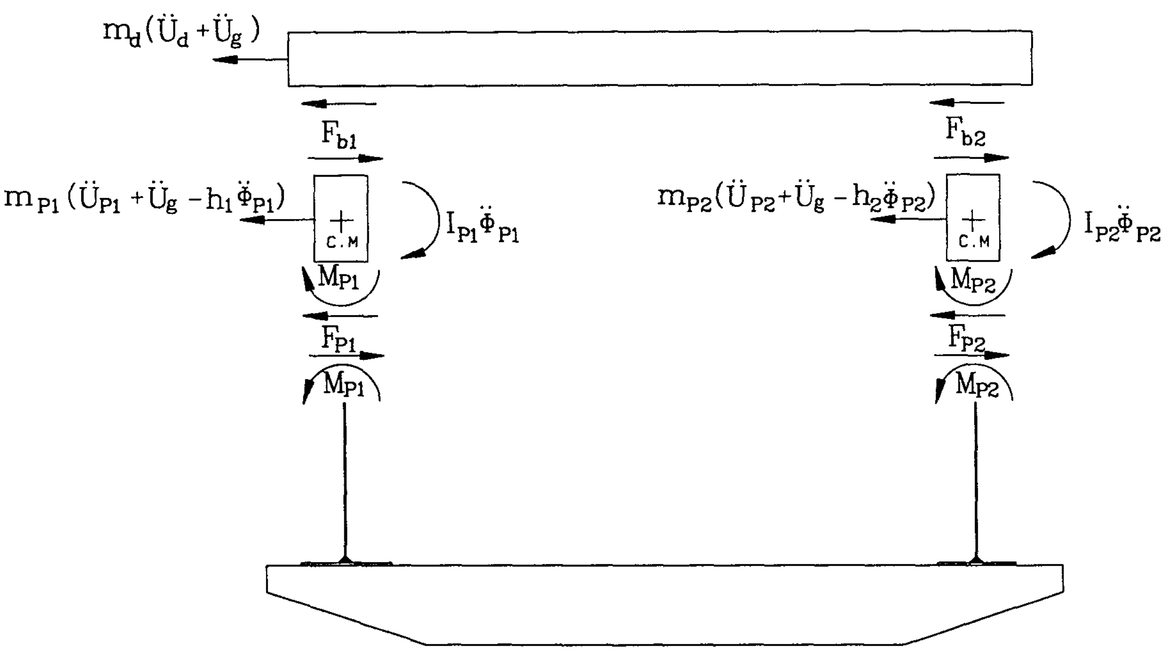

Figure 6-2 Free Body Diagram of Bridge Model

$$m_d(\ddot{U}_d + \ddot{U}_g) + F_{b1} + F_{b2} = 0 \tag{6-1}$$

$$m_{p1}(\ddot{U}_{p1} + \ddot{U}_g - h_1\ddot{\phi}_{p1}) + F_{p1} - F_{b1} = 0 \tag{6-2}$$

$$m_{p2}(\ddot{U}_{p2} + \ddot{U}_g - h_2\ddot{\phi}_{p2}) + F_{p2} - F_{b2} = 0 \tag{6-3}$$

$$I_{p1}\ddot{\phi}_{p1} + M_{p1} + F_{p1}h_1 + F_{b1}(h - h_1) = 0 \tag{6-4}$$

$$I_{p2}\ddot{\phi}_{p2} + M_{p2} + F_{p2}h_2 + F_{b2}(h - h_2) = 0 \tag{6-5}$$

where F_{b1} and F_{b2} are the lateral forces in the FPS bearings, and F_{pi} and M_{pi} are the lateral force and bending moment at the connection of the pier top to the end of the column:

$$\begin{Bmatrix} F_{pi} \\ M_{pi} \end{Bmatrix} = E_i I_i \begin{bmatrix} \frac{12}{L_i^3} & \frac{6}{L_i^2} \\ \frac{6}{L_i^2} & \frac{4}{L_i} \end{bmatrix} \begin{Bmatrix} U_{pi} \\ \phi_{pi} \end{Bmatrix} + \begin{bmatrix} C_{pi}^1 & 0 \\ 0 & C_{pi}^2 \end{bmatrix} \begin{Bmatrix} \dot{U}_{pi} \\ \dot{\phi}_{pi} \end{Bmatrix} \tag{6-6}$$

The first part of Equation (6-6) describes the elastic forces, whereas the second part is used to account for linear viscous energy dissipation in the piers.

The lateral force in the FPS bearings is given by (see section 3)

$$F_{bi} = \frac{W_i^*}{R} U_{bi} + \mu_i(\dot{U}_{bi}) W_i^* Z_i \tag{6-7}$$

$$U_{bi} = U_d - U_{pi} + h\phi_{pi} \tag{6-8}$$

$$W_i^* = W_i\left(1 + \frac{\ddot{U}_{vi}}{g}\right) \tag{6-9}$$

where W_i=weight carried by pier i(i=1,2), W_i^*=normal load on the sliding interface, U_{bi}=bearing displacement, μ_i=coefficient of sliding friction and Z_i= variable describing essentially rigid-plastic behavior. Variable Z_i satisfies the following equation (Constantinou 1990a):

$$Y_i\dot{Z}_i + \gamma\,|\dot{U}_{bi}|Z_i|Z_i| + \beta\,\dot{U}_{bi}Z_i^2 - \dot{U}_{bi} = 0 \tag{6-10}$$

In this equation, Y_i="yield" displacement (=0.25 mm) and β and γ=parameters satisfying the condition $\beta+\gamma=1$.

The coefficient of sliding friction follows the relation (Constantinou 1990a, see also section 4)

$$\mu_i = f_{maxi} - (f_{maxi} - f_{mini})\exp(-a_i|\dot{U}_{bi}|) \tag{6-11}$$

in which f_{max} and f_{min} are, in general, functions of the bearing pressure.

6.3 Comparison of Analytical and Experimental Results

Analytical results are compared to experimental results in the test series FPSAR (see Table 5-II and 5-III). In these tests, the sliding interface consisted of composite material No.1 (see section 4) at bearing pressure of 17.2 MPa. Analyses were performed for the case flexible piers. The dynamic response of the isolated bridge model is described by Equations (6-1) to (6-11). Solution of these equations was obtained by first reducing these equations to a system of 12 first order differential equations (variables: U_d, $\dot{U}_d$, U_{pi},

$\dot{U}_{pi}$, ϕ_{pi}, $\dot{\phi}_{pi}$ and Z_i, i=1,2), and then numerically integrating the system by using an adaptive integration scheme with truncation error control (Gear 1971).

The data used in the analytical model were: deck weight $m_d g$=140 kN, pier weight $m_{pi}g$=8.9 kN, L_1=L_2=1.6 m, h_1=h_2=98mm, h=413 mm, I_{p1}=I_{p2}=38.22 kN·s²·mm, E_1=E_2=200000 MPa, I_1=I_2=3.022x10^{-5}m^4 (2 AISC tubes Ts 6x6x5/16). Based on these data the fundamental period of each pier, in its cantilever position, was calculated to be 0.092s. This is in close agreement with the experimentally determined value of 0.096s. The second mode of the cantilever pier had a calculated frequency of 102 Hz. This frequency could neither be detected in the tests nor have any significance in the analysis.

Damping in the piers was described by the second term in Equation (6-6). The fact that the calculated second frequency of the cantilever pier is much larger than the first frequency indicates that the second mode of the pier may be neglected. Accordingly, constant C_{pi}^2 in Equation (6-6) was set equal to zero and constant C_{pi}^1 was assigned a value equal to 0.0062 kNs/mm. Based on this value, the damping ratio in the fundamental mode of the cantilever pier was calculated to be 5% of critical. This is consistent with the experimental data.

The parameters in the model of friction of Equation (6-11) were selected to be f_{mini}=0.04 and a_i=83.1 s/m. Both were assumed to be independent of the bearing pressure. However, the coefficient of friction at high velocity of slicing was described as

$$f_{maxi} = 0.12 - 0.07\tanh(\alpha p_i) \tag{6-12}$$

where α=0.012 (MPa)$^{-1}$ and p_i=bearing pressure in MPa, described by

$$p_i = 17.2\left(1 + \frac{\ddot{U}_{vi}}{g}\right) \tag{6-13}$$

Equation (6-12) is consistent with experimental results on the frictional properties of composite material No.1 in contact with polished stainless steel. This is demonstrated in Figure 6-3. It should be noted that Equations (6-12) and (6-13) give, in the absence of vertical acceleration, p_i=17.2 MPa and f_{maxi}=0.105.

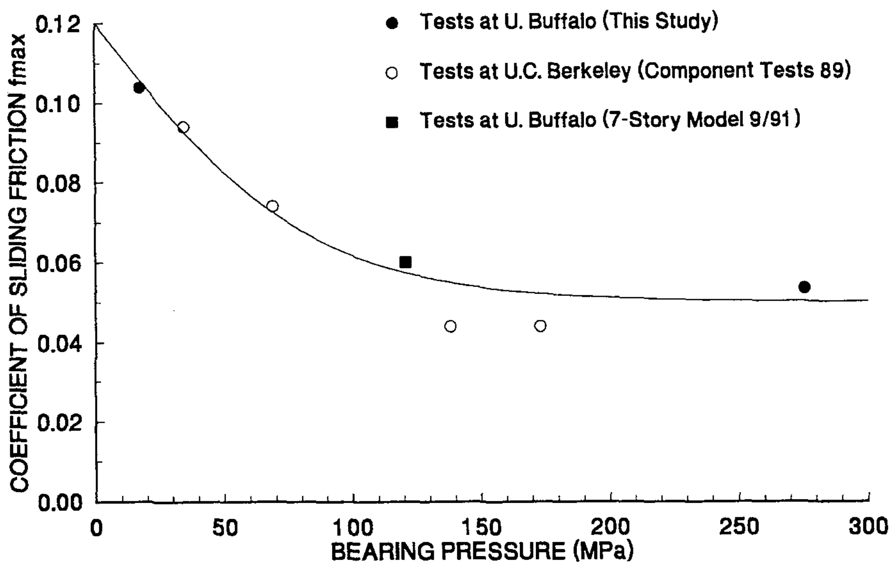

Figure 6-3 Variation of Coefficient of Friction at High Velocity of Sliding (f_{max}) with Pressure (solid line described by equation 6-12)

Equations (6-1) to (6-13) describe the one-directional response of the isolated bridge model, including the full effect of the vertical ground motion. As discussed in section 5, the piers of the model underwent vertical motion even in the case of testing with only horizontal excitation. As an example, Figure 6-4 shows the recorded vertical accelerations at the base of the piers of the isolated model in four tests of the FPSAR series (see Tables 5-II and 5-III), in which the model was excited with the El Centro 200% and Taft 400% motions, without and with the vertical component. In the tests with only horizontal excitation, the two piers have out-of-phase vertical acceleration.

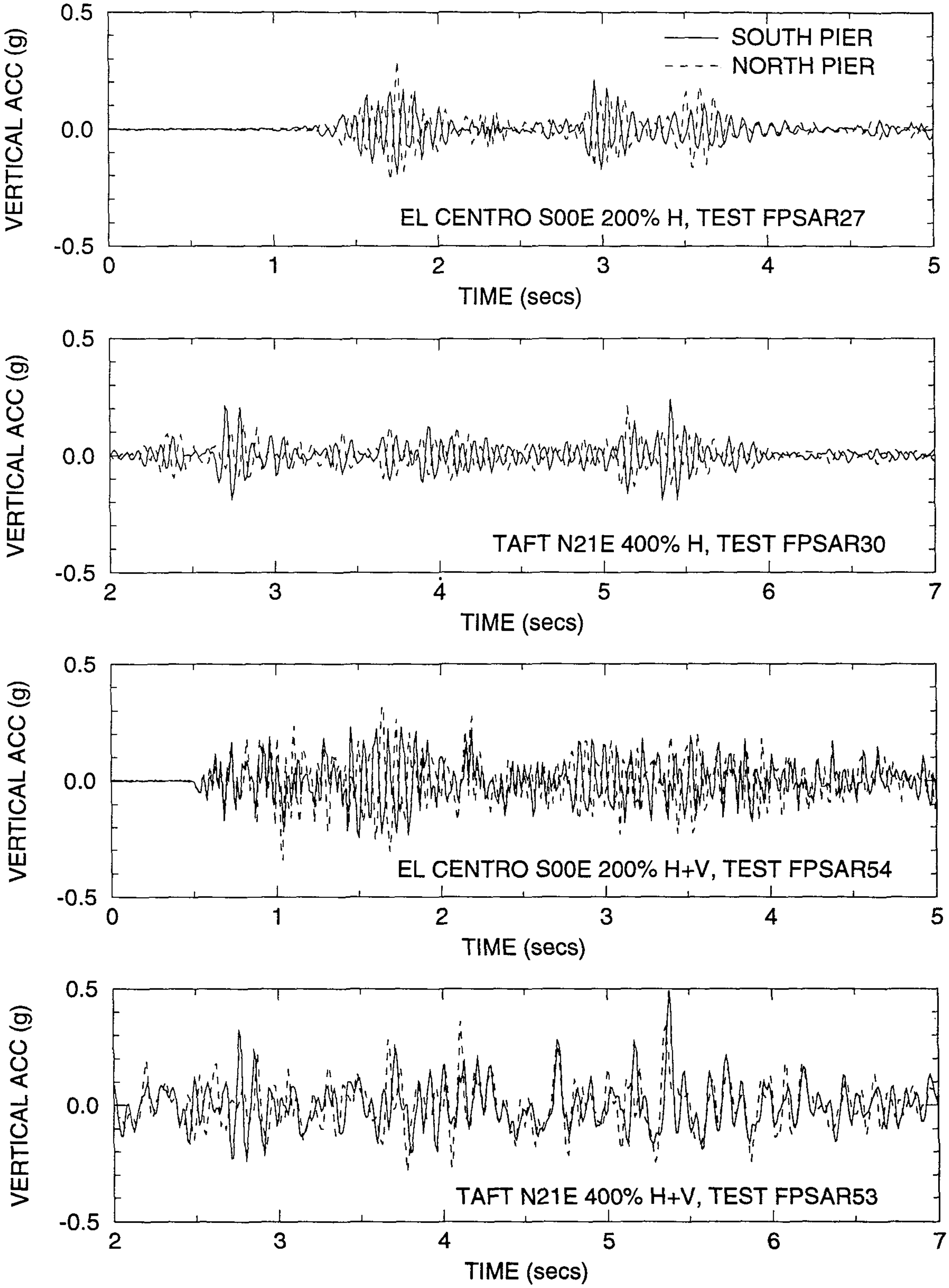

Figure 6-4 Recorded Vertical Acceleration at the Base of Piers in Tests with only Horizontal and with Combined Horizontal-Vertical Excitation

Comparisons of analytical and experimental results are presented in Figures 6-5 to 6-15 in the case of tests with only horizontal excitation. The analysis was based on Equations (6-1) to (6-13) but with $\ddot{U}_{vi}$ set equal to zero (vertical acceleration effects were neglected). Evidently, the analytical results are in very good agreement with the experimental results. This demonstrates that the vertical acceleration effects are not significant.

Figures 6-16 and 6-17 compare experimental and analytical results in the tests with combined horizontal-vertical El Centro 200% and Taft 400% inputs. The analysis accounted for the vertical acceleration effects. The analysis captures correctly the wavy form of the bearing shear force-displacement loops and the two sets of results appear to be in very good agreement.

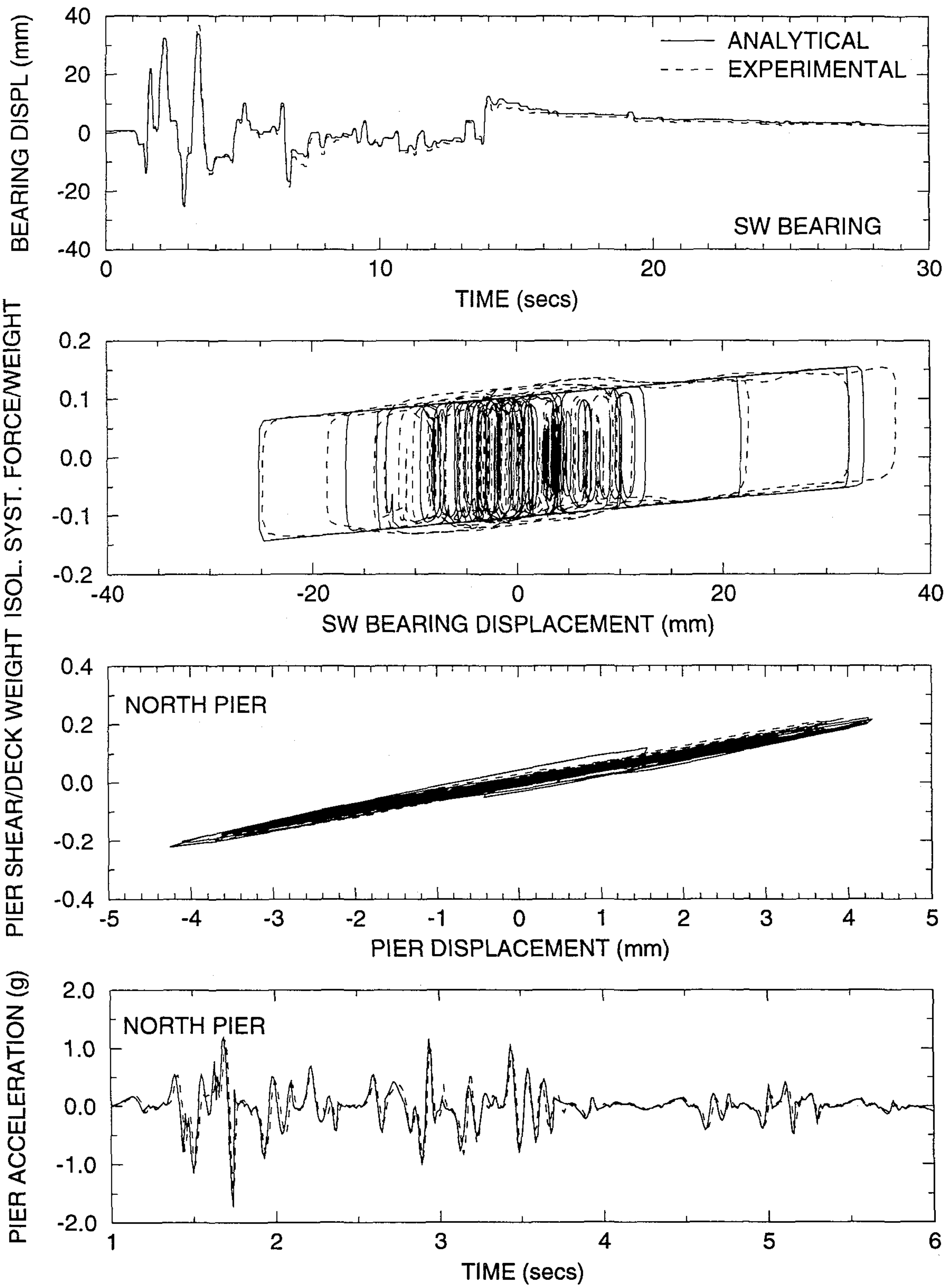

Figure 6-5 Comparison of Experimental and Analytical Results in Tests with El Centro 200% Input (Test No. FPSAR27). Analysis Performed without the Effect of Vertical Pier Acceleration($\ddot{U}_{vi} = 0$)

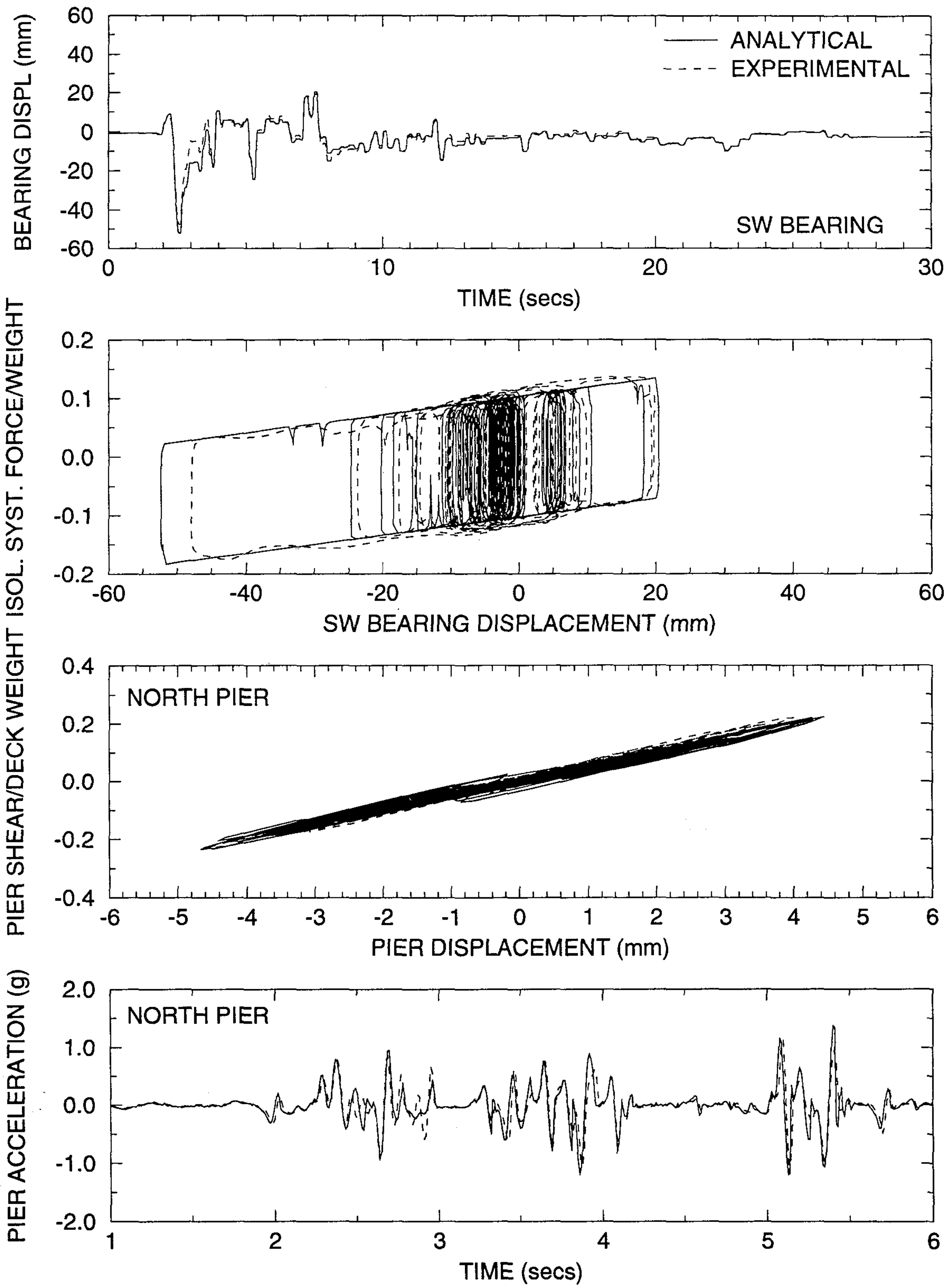

Figure 6-6 **Comparison of Experimental and Analytical Results in Tests with Taft N21E 400% Input (Test No. FPSAR30). Analysis Performed without the Effect of Vertical Pier Acceleration(** $\ddot{U}_{vi} = 0$ **)**

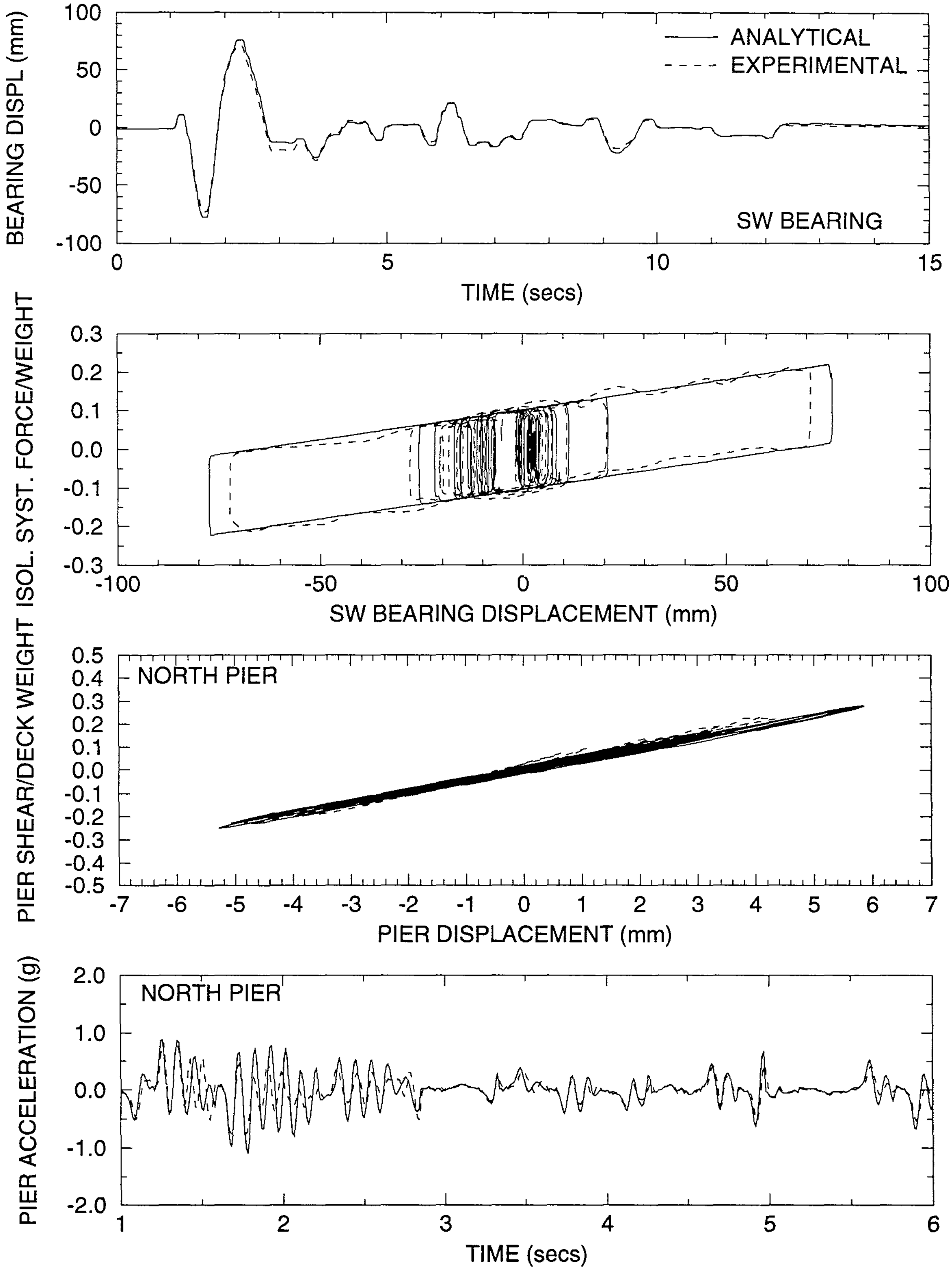

Figure 6-7 Comparison of Experimental and Analytical Results in Tests with Japanese Level 2 G.C.1 100% Input (Test No. FPSAR37). Analysis Performed without the Effect of Vertical Pier Acceleration($\ddot{U}_{vi} = 0$)

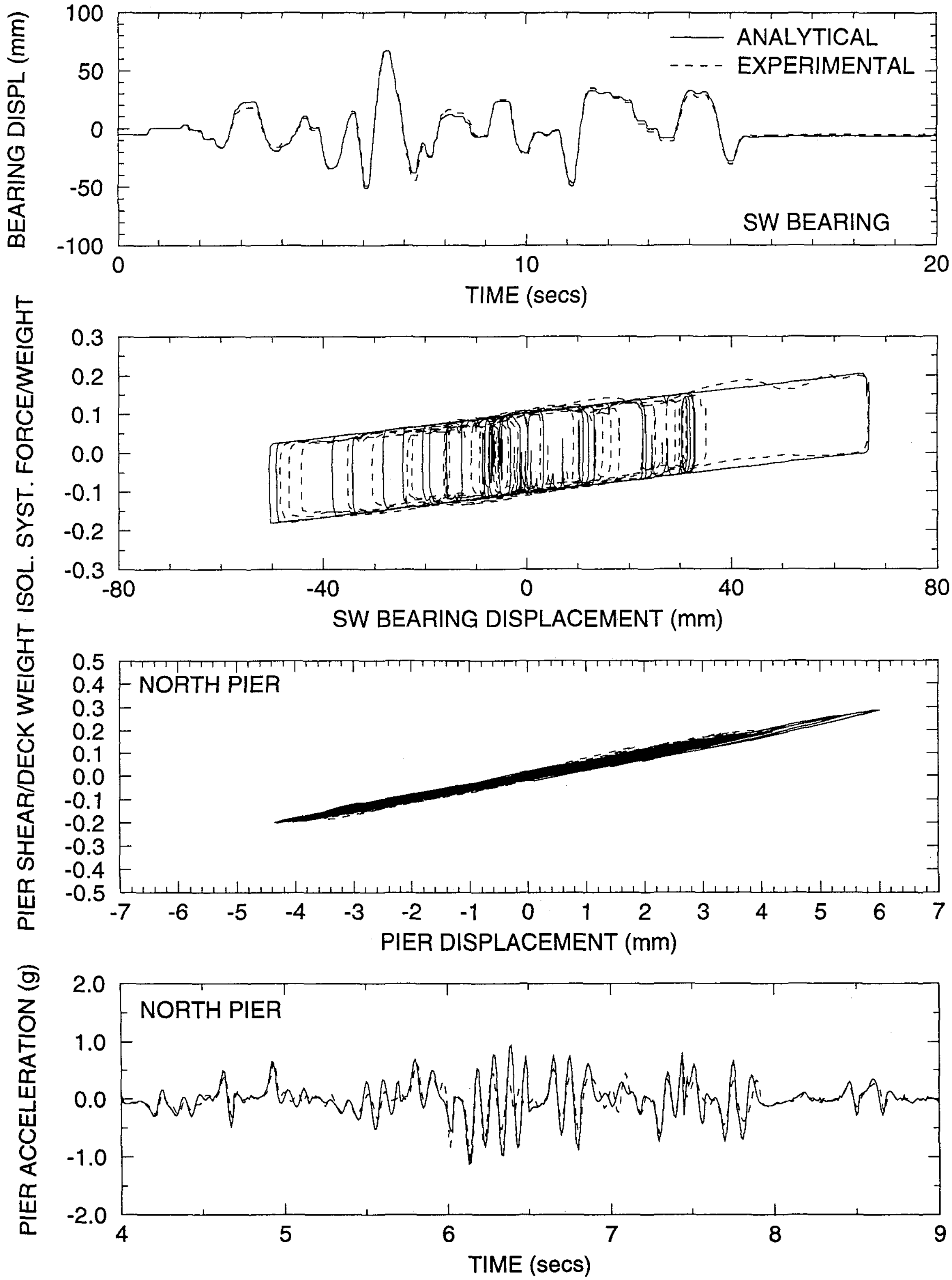

Figure 6-8 **Comparison of Experimental and Analytical Results in Tests with Japanese Level 2 G.C.2 100% Input (Test No. FPSAR38). Analysis Performed without the Effect of Vertical Pier Acceleration($\ddot{U}_{vi} = 0$)**

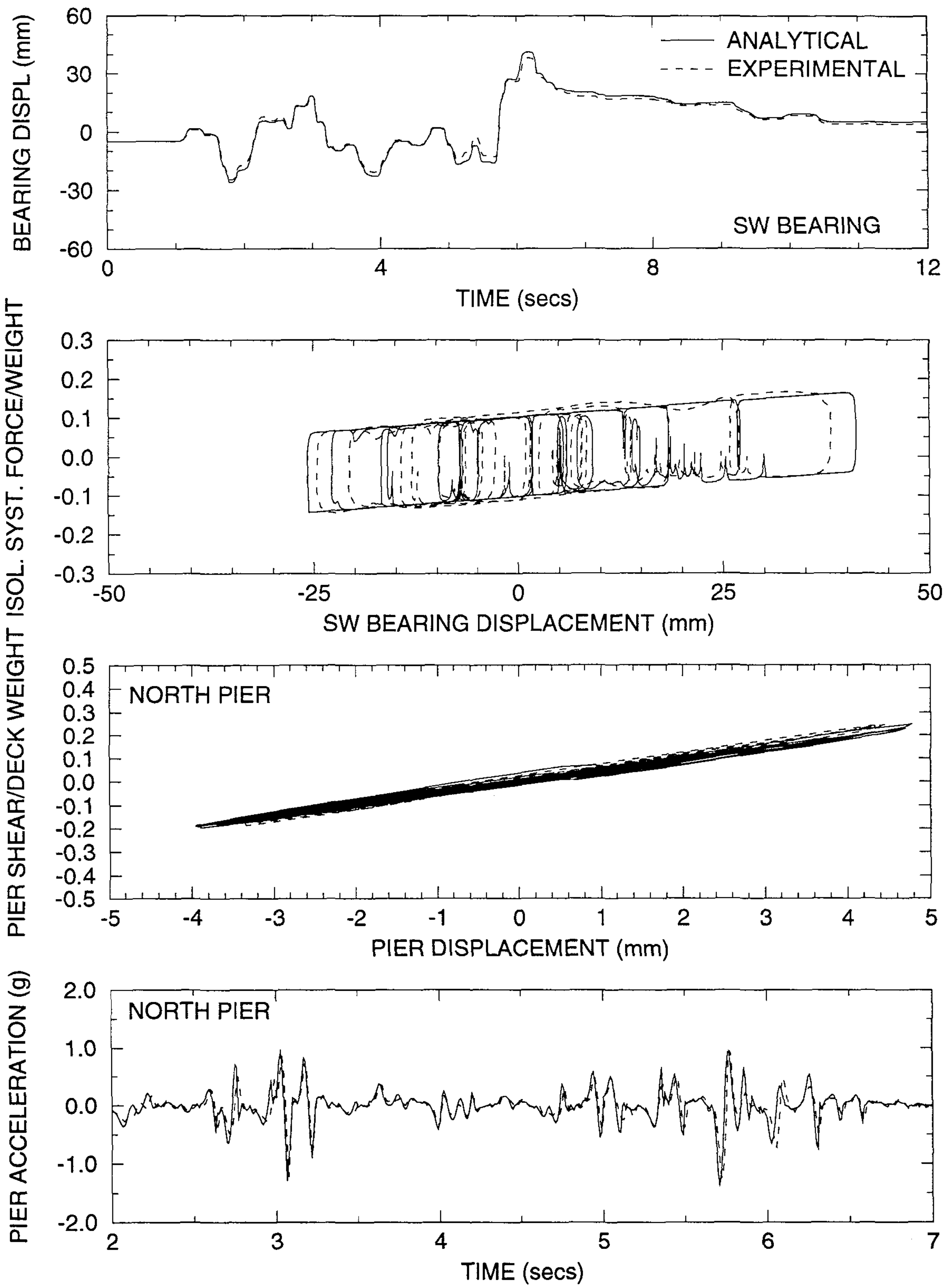

Figure 6-9 **Comparison of Experimental and Analytical Results in Tests with CalTrans R3 0.6g 100% Input (Test No. FPSAR41). Analysis Performed without the Effect of Vertical Pier Acceleration**($\ddot{U}_{vi} = 0$)

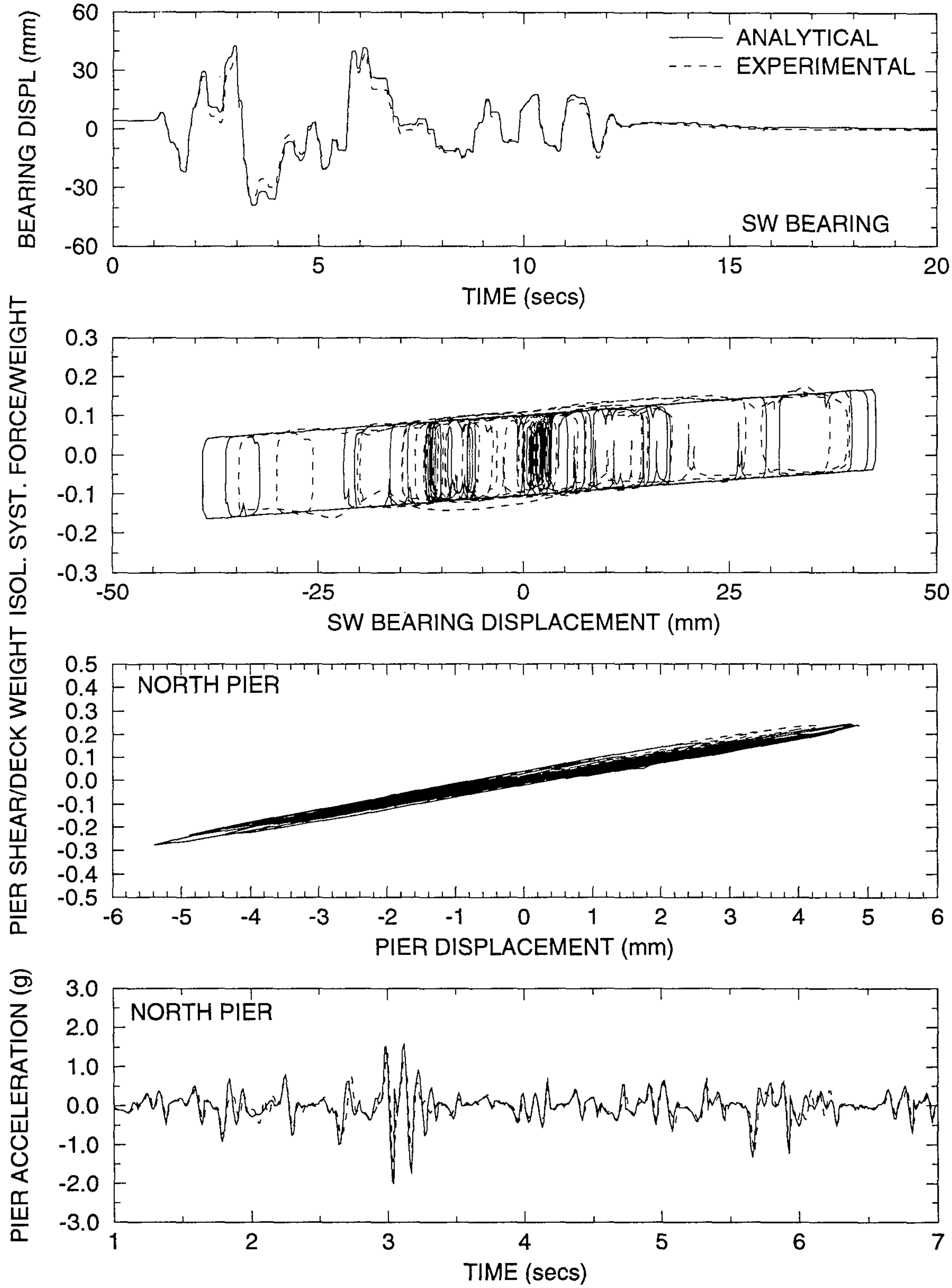

Figure 6-10 Comparison of Experimental and Analytical Results in Tests with CalTrans S3 0.6g 100% Input (Test No. FPSAR42). Analysis Performed without the Effect of Vertical Pier Acceleration($\ddot{U}_{vi} = 0$)

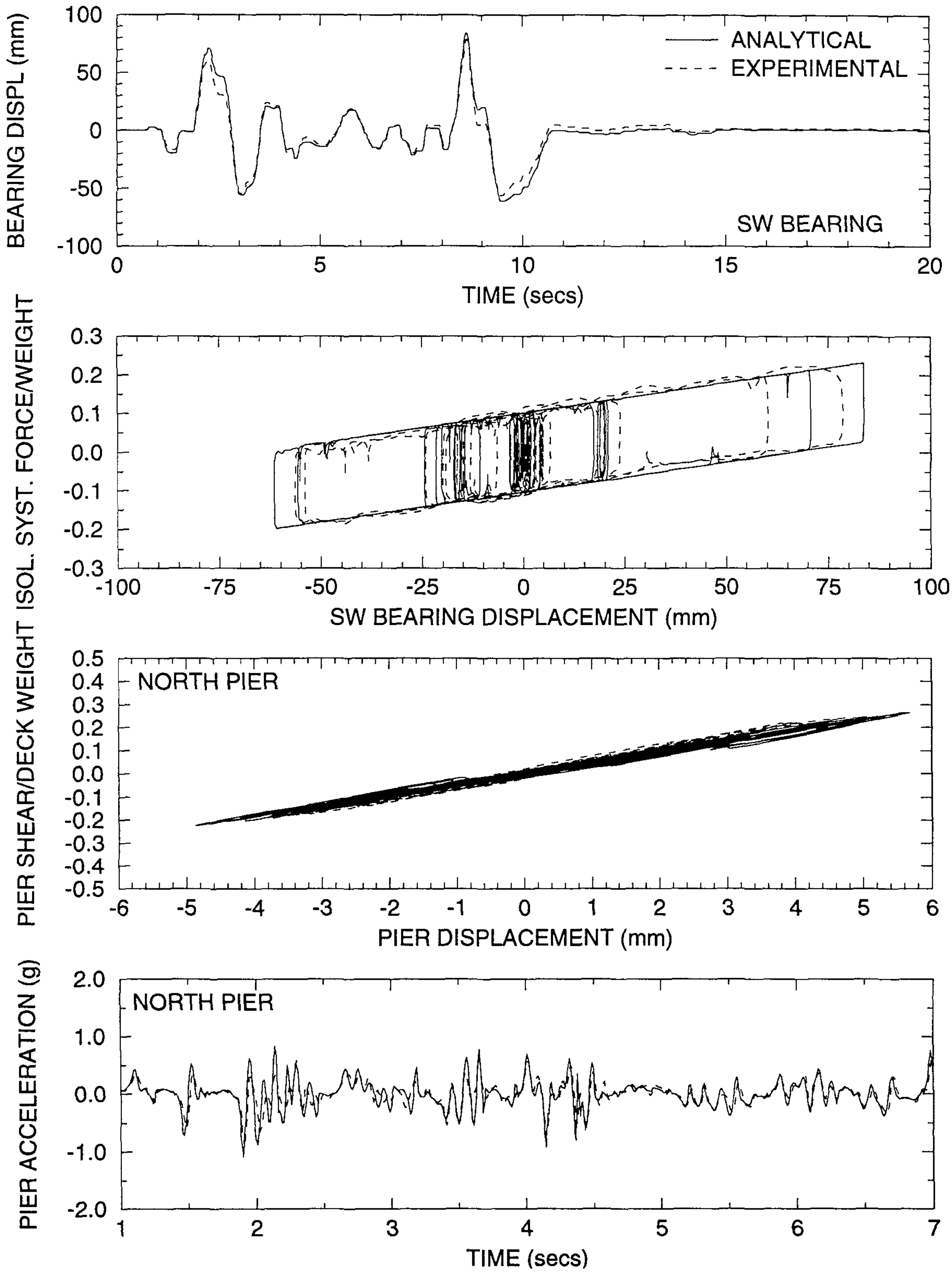

Figure 6-11 Comparison of Experimental and Analytical Results in Tests with CalTrans A2 0.6g 100% Input (Test No. FPSAR43). Analysis Performed without the Effect of Vertical Pier Acceleration($\ddot{U}_{vi} = 0$)

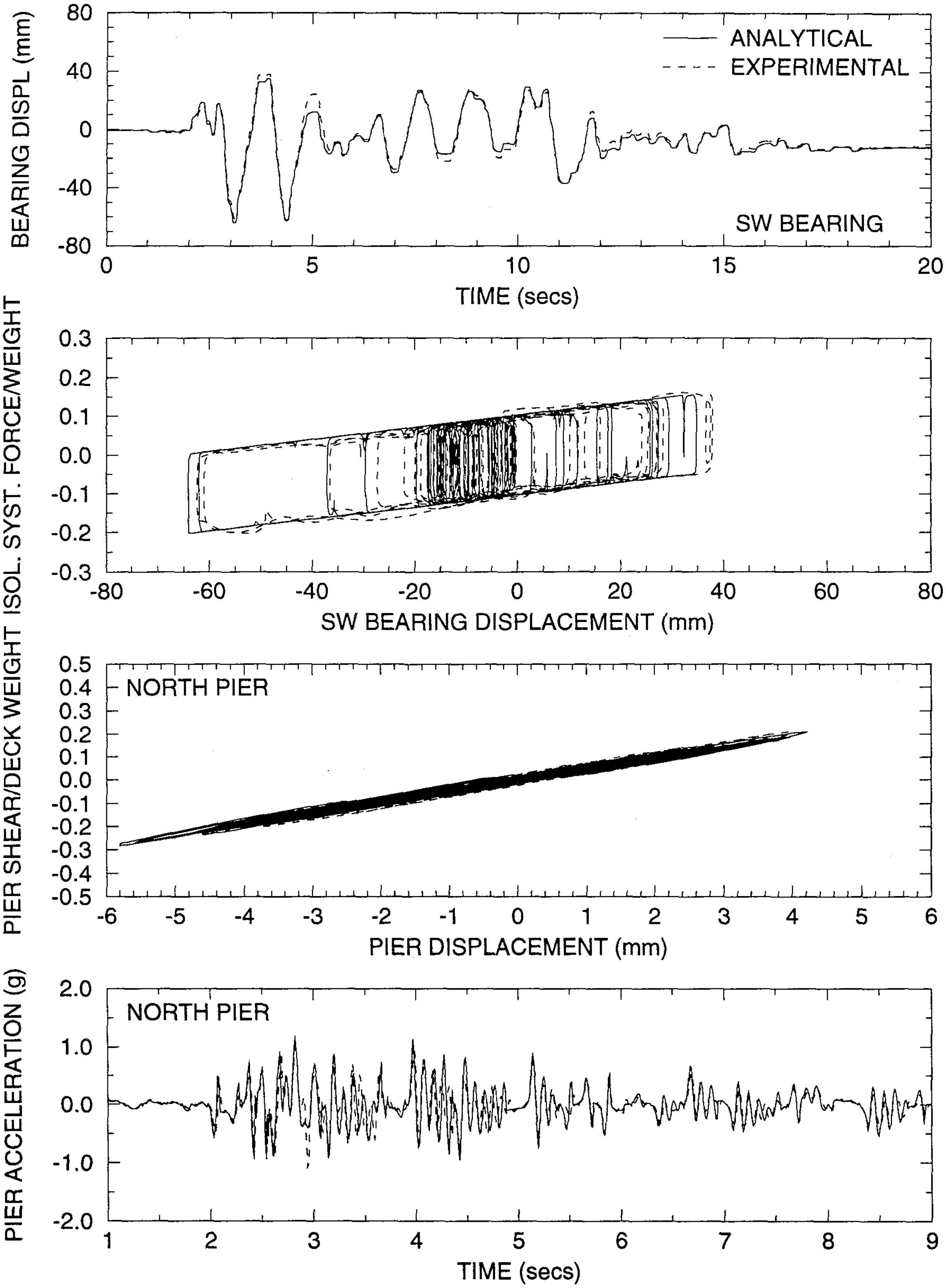

Figure 6-12 Comparison of Experimental and Analytical Results in Tests with Hachinohe N-S 300% Input (Test No. FPSAR45). Analysis Performed without the Effect of Vertical Pier Acceleration($\ddot{U}_{vi} = 0$)

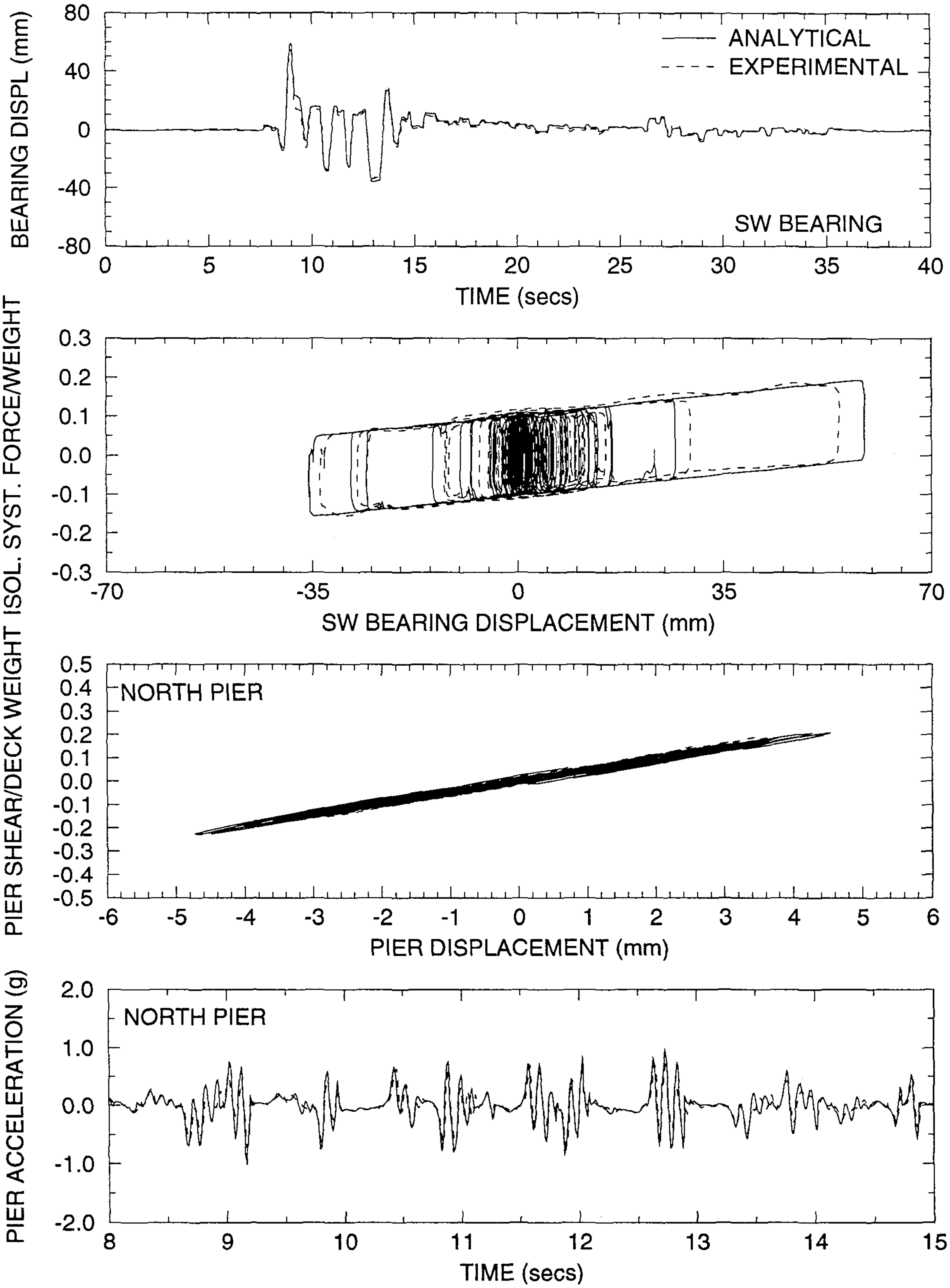

Figure 6-13 Comparison of Experimental and Analytical Results in Tests with Akita N-S 200% Input (Test No. FPSAR47). Analysis Performed without the Effect of Vertical Pier Acceleration($\ddot{U}_{vi} = 0$)

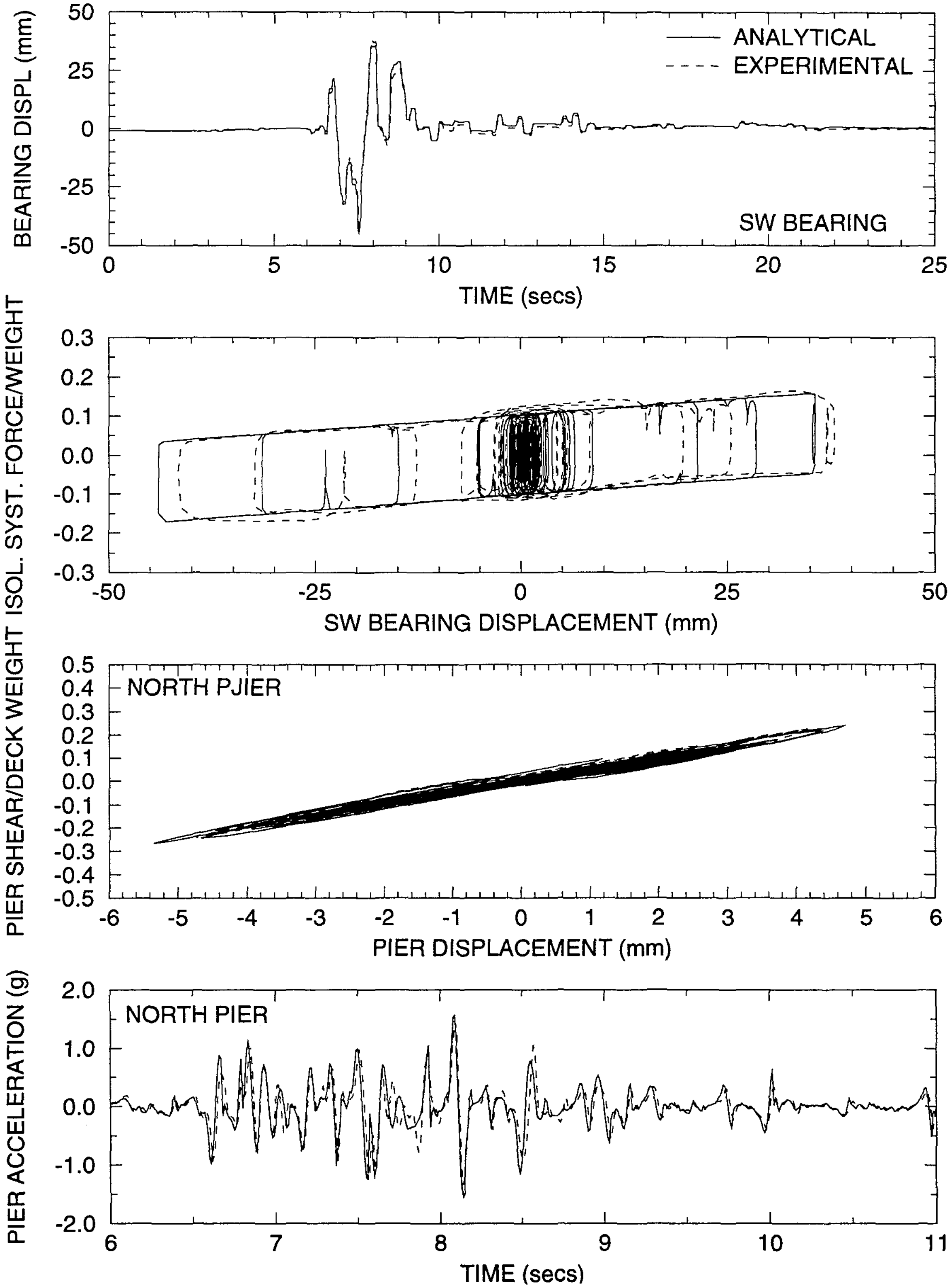

Figure 6-14 Comparison of Experimental and Analytical Results in Tests with Miyagiken Oki 600% Input (Test No. FPSAR49). Analysis Performed without the Effect of Vertical Pier Acceleration($\ddot{U}_{vi} = 0$)

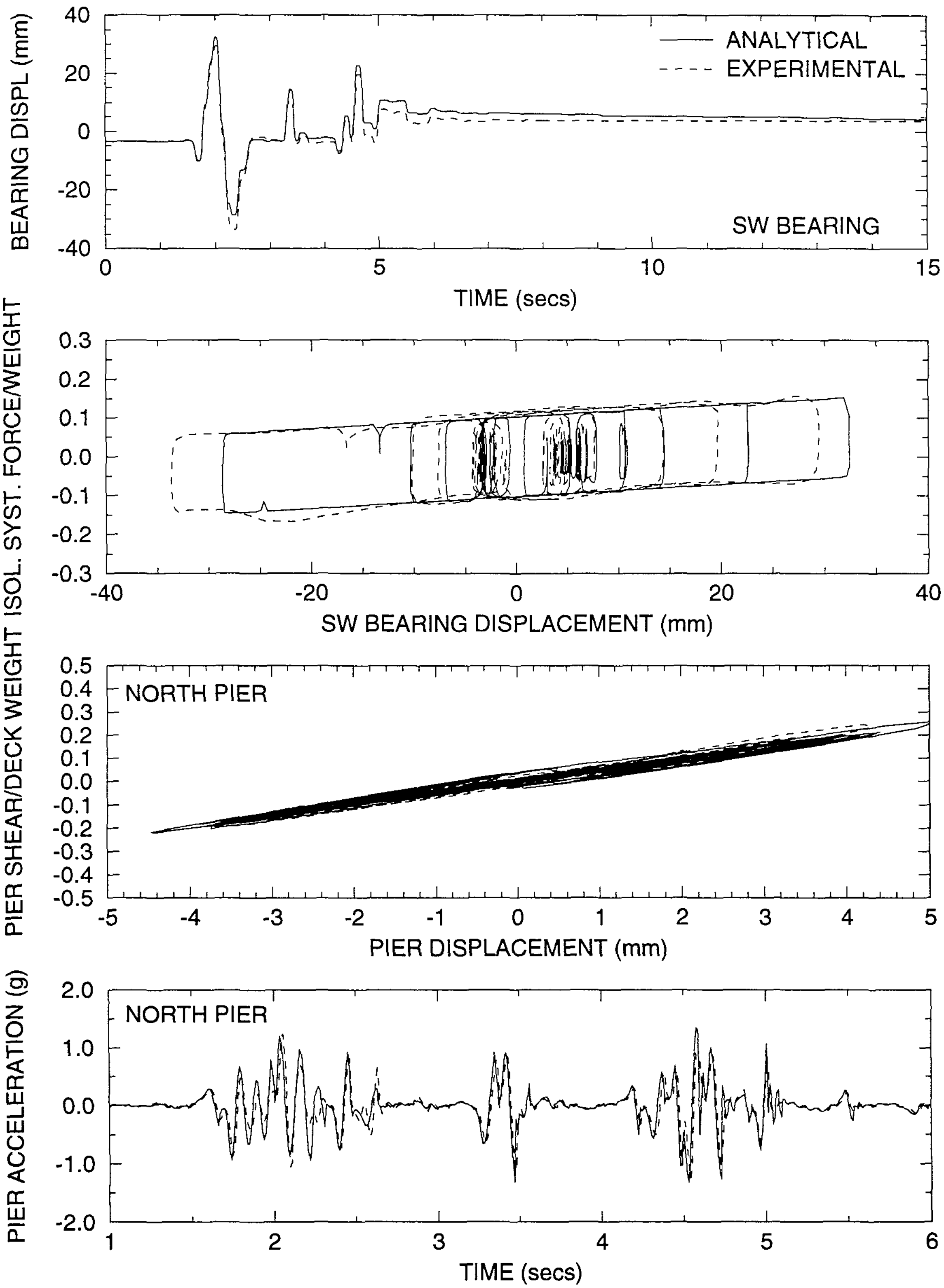

Figure 6-15 Comparison of Experimental and Analytical Results in Tests with Pacoima S74W 100% Input (Test No. FPSAR51). Analysis Performed without the Effect of Vertical Pier Acceleration($\ddot{U}_{vi} = 0$)

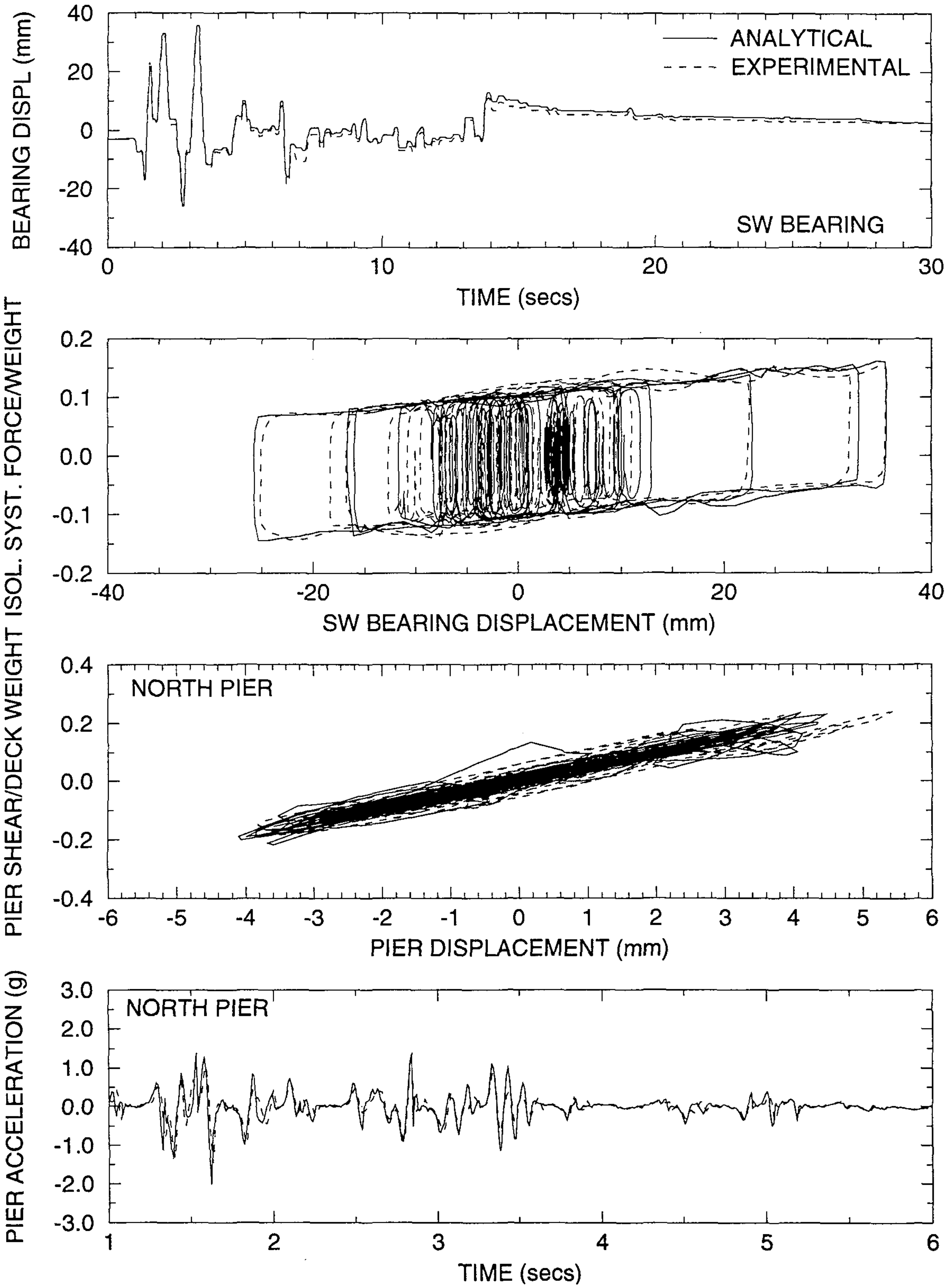

Figure 6-16 Comparison of Experimental and Analytical Results in Tests with El Centro 200% H+V Input (Test No. FPSAR54). Analysis Performed with the Effect of Vertical Pier Acceleration.

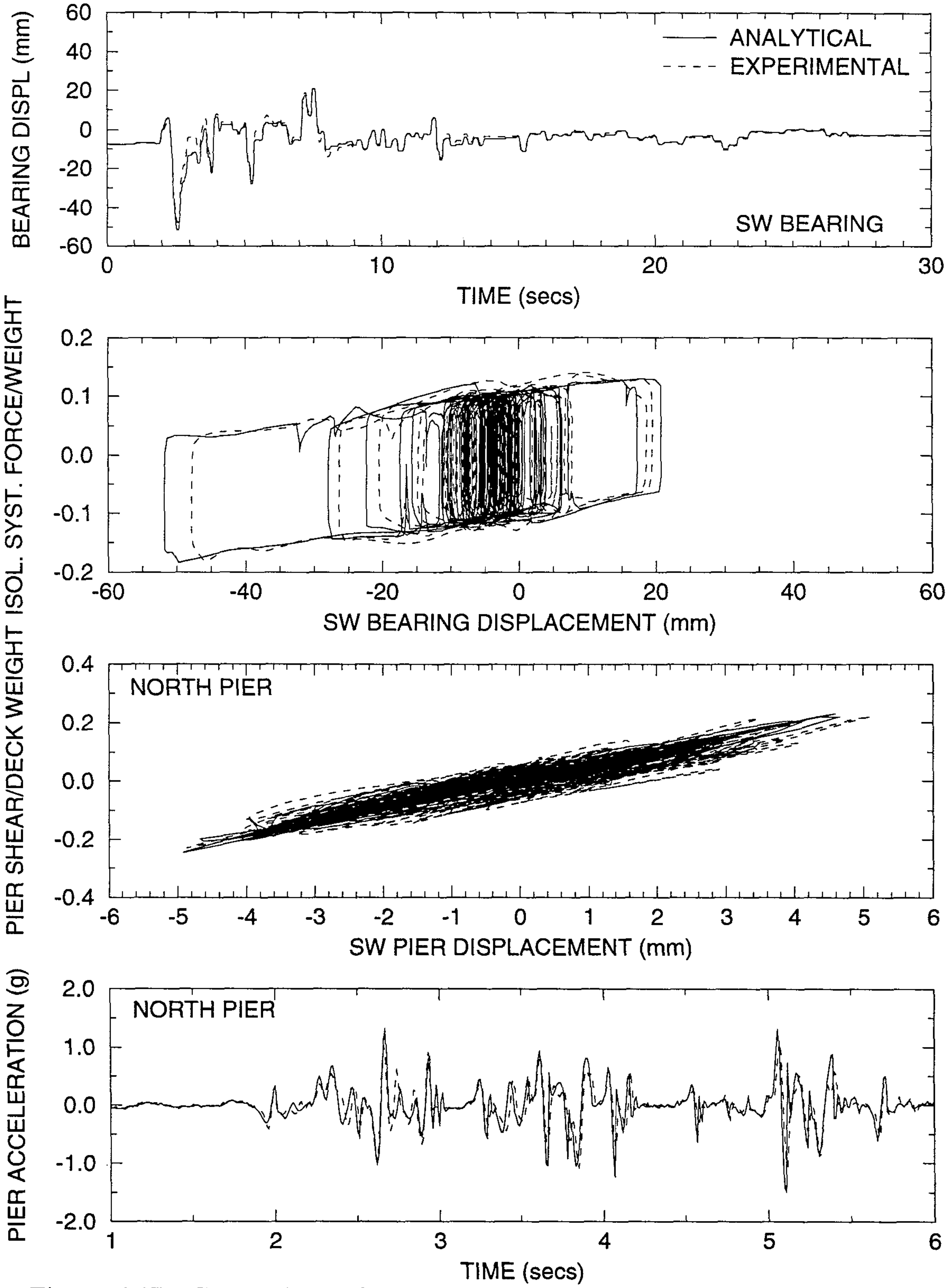

Figure 6-17 Comparison of Experimental and Analytical Results in Tests with Taft N21E 400% H+V Input (Test No. FPSAR53). Analysis Performed with the Effect of Vertical Pier Acceleration.

SECTION 7

CONCLUSIONS

An extensive experimental study of a seismically isolated bridge model with Friction Pendulum (or FPS) bearings was conducted. The conditions of testing allowed the study of a number of effects which were not previously studied in bridge seismic isolation. These effects included the pier flexibility, realistic energy dissipation in the piers, pier top rotation, vertical ground motion and low amplitude excitation. Tests were conducted at two levels of friction, one at low value (f_{max}=0.058) and another at medium value (f_{max}=0.10 to 0.12). The latter case may regarded as appropriate for application in areas of strong seismic excitation, such as California and Japan. The summary and conclusions in this section are for this most interesting case. They are presented below:

(1) The medium friction isolation system was designed for good performance in strong seismic excitation. Indeed, the test results demonstrated substantial reductions of deck acceleration and pier shear force and drift in comparison to the response of a non-isolated comparable (also tested) bridge.

(2) The isolated bridge performed better than the non-isolated bridge in weak seismic excitation, such as the Japanese Level 1 motions. In these motions with peak ground acceleration of only about 0.1g, the piers of the isolated bridge had less than half shear force and drift than the piers of the non-isolated bridge. Figures 5-5 to 5-7 provide vivid illustration of the differences in the pier response in the two cases.

(3) The vertical ground acceleration was found to have a minor effect on the response of the isolated bridge.

(4) The engagement of the displacement restrainer of the FPS bearings resulted in considerable increase in the substructure forces and displacements. Nevertheless, these forces and displacements were much less than those in the non-isolated bridge (see Figure 5-10).

(5) The frictional properties of the bearings remained markedly stable after extensive

testing. Recorded loops of shear force versus displacement of the FPS bearings prior and following 58 seismic tests were identical.

(6) Permanent displacements were found to be very small and not cumulative in successive earthquakes. This was true even in weak excitation in which the bearing displacements were not sufficiently large to mobilize strong restoring force.

An analytical model was presented which was capable of describing the response of the isolated bridge, including the full effects of the vertical ground motion. Comparison of experimental and analytical responses showed very good agreement. This demonstrates that the behavior of FPS bearings is very well understood to allow for accurate prediction of the response of isolated structures with these bearings.

SECTION 8

REFERENCES

American Association of State Highway and Transportation Officials-AASHTO (1991). "Guide specifications for seismic isolation design." Washington, D.C.

Buckle, I.G and Mayes, R.L. (1990). "Seismic isolation history, application, and performance - a world view." Earthquake Spectra, 6(2), 161-201.

Civil Engineering Research Center-CERC (1992). "Temporary manual of design method for base-isolated highway bridges." Japan (in Japanese).

Constantinou, M.C., Mokha, A. and Reinhorn, A.M. (1990a). "Teflon bearings in base isolation II: Modeling." J. Stuct. Engrg., ASCE, 116(2), 455-474.

Constantinou, M.C., Mokha, A. and Reinhorn, A.M. (1990b). "Experimental and analytical study of a combined sliding disc bearing and helical steel spring isolation system." NCEER-90-0019, Nat. Ctr. for Earthquake Engrg. Res., State Univ. of New York, Buffalo, NY.

Constantinou, M.C., Kartoum, A., Reinhorn, A.M. and Bradford, P. (1991a). "Experimental and theoretical study of a sliding isolation system for bridges." Report No. NCEER-91-0027, Nat. Ctr. for Earthquake Engrg. Res., State Univ. of New York, Buffalo, NY.

Constantinou, M.C., Mokha, A. and Reinhorn, A.M. (1991b). "Study of sliding bearing and helical-steel-spring isolation system." J. Struct. Engrg., ASCE, 117(4), 1257-1275.

Constantinou, M.C. Kartoum, A., Reinhorn, A.M. and Bradford, P. (1992a). "Sliding isolation system for bridges:experimental study." Earthquake Spectra, 8(3), 321-344.

Constantinou, M.C. (1992b). "NCEER-Taisei research on sliding isolation systems for bridges." NCEER Bulletin, Nat. Ctr. for Earthquake Engrg. Res., State Univ. of New York, Buffalo, NY, 6(3), 1-4.

Eisenberg J.M., Melentyev, A.M., Smirnov, V.I. and Nemykin, A.N. (1992). "Applications of seismic isolation in the USSR." Proc. 10th WCEE, Madrid, Spain, 4:2039-2046.

Gates, J.H. (1979). "Factors considered in the development of the California seismic design criteria for bridges." Proc. Workshop on Earthquake Resistance of Highway Bridges, Applied Technology Council, Palo Alto, Calif., 141-162.

Gear, C.W. (1971). "The automatic integration of ordinary differential equations." Numer. Math., Commun. of ACM, 14(3), 176-190.

International Conference of Building Officials ICBO (1991). "Uniform building code, earthquake regulations for seismic-isolated structures." Whittier, Calif.

Kartoum, A., Constantinou, M.C. and Reinhorn, A.M. (1992). "Sliding isolation system for bridges: analytical study." Earthquake Spectra, 8(3), 345-372.

Kawamura, S., Kitazawa, K., Hisano, M. and Nagashima, I. (1988). "Study of a sliding-type base isolation system. System composition and element properties." Proceedings of 9th World Conference on Earthquake Engineering, Tokyo-Kyoto, Vol. V, 735-740.

Kawashima, K., Hasegawa, K. and Nagashima, H. (1991). "A perspective of menshin design for highway bridges in Japan" First US-Japan Workshop on Earthquake Protective Systems for Bridges, Buffalo, NY, September.

Kelly, J.M., Buckle, I.G., and Tsai, H-C. (1986). "Earthquake simulator testing of a base-isolated bridge deck." Report No. UCB/EERC-85/09, Earthquake Engrg. Res. Ctr., Univ. of California, Berkeley, Calif., Jan.

Kelly, J. (1993). "State-of-the-art and state-of-the-practice in base isolation." ATC-17-1 Seminar on Seismic Isolation, Passive Energy Dissipation and Active Control, San Francisco, CA, March.

Maison, B.F. and Ventura, C.E. (1992). "Seismic analysis of base-isolated San Bernardino county building." Earthquake Spectra, 8(4), 605-633.

Marioni, A. (1991). "Antiseismic devices for bridges in Italy." 3rd World Congress on joint Sealing and Bearing Systems for Concrete Structures. Vol. 2 of Preprints, 1263-1280, Toronto, Canada.

Martelli, A., Parducci, A. and Forni, M. (1993). "State-of-the-art on development and application of seismic isolation and other innovative seismic design techniques in Italy" ATC-17-1 Seminar on Seismic Isolation, Passive Energy Dissipation and Active Control, San Francisco, CA, March.

Mayes, R.L., Jones, L.R. and Buckle, I.G., (1990). "Impediments to the implementation of seismic isolation" Earthquake Spectra, 6(2), 283-296.

Medeot, R. (1991). "The evolution of aseismic devices for bridges in Italy." 3rd World Congress on Joint Sealing and Bearing Systems for Concrete Structures, Vol. 2 of Preprints, 1295-1320, Toronto, Canada.

Mokha, A., Constantinou, M.C., and Reinhorn, A.M. (1988). "Teflon bearings in aseismic base isolation. Experimental studies and mathematical modeling." Report No. NCEER-88-0038, Nat. Ctr. for Earthquake Engrg. Res., State Univ. of New York, Buffalo, NY.

Mokha, A., Constantinou, M.C. and Reinhorn, A.M. (1990a). "Teflon bearings in base isolation. I: Testing." J. Struct. Engrg., ASCE, 116(2), 438-454.

Mokha, A., Constantinou, M.C. and Reinhorn, A.M. (1990b). "Experimental study and analytical prediction of earthquake response of a sliding isolation system with a spherical surface." Report No. NCEER-90-0020, Nat. Ctr. for Earthquake Engrg. Res., State Univ. of New York, Buffalo, NY.

Mokha, A.,Constantinou, M.C., Reinhorn, A.M., and Zayas, V. (1991). "Experimental study of friction pendulum isolation system." J. Struct. Engrg., ASCE, 117(4), 1201-1217.

Palfalvi, B., Amin, A., Mokha, A., Fatehi, H. and Lee, P. (1993). Implementation issues in seismic isolation retrofit of government buildings." ATC-17-1 Seminar on Seismic Isolation, Passive Energy Dissipation and Active Control, San Francisco, CA, March.

Sabnis, G.M., Harris, H.G., White, R.N. and Mirza, M.S. (1983). "Structural modeling and experimental techniques." Prentice-Hall, Inc., Englewood Cliffs, N.J.

Soong, T.T. and Constantinou, M.C. (1992). "Base isolation and active control technology case studies in the U.S.A." Proc. IDNDR Intl. Symp. on Earthq. Disaster Reduction Technol.-30th Anniv. of IISEE, Tsukuba, Japan, 455-469.

Zayas, V., Low, S.S and Mahin, S.A. (1987). "The FPS earthquake resisting system, experimental report." Report No. UCB/ EERC-87/01, Earthquake Engineering Research Center, University of California, Berkeley, Calif., June.

APPENDIX A

EXPERIMENTAL RESULTS

This appendix contains experimetal results of the tested bridge model in the test series FPSAR (bearing material No.1, f_{max}=0.104) in the configuration with two flexible piers. The recorded time histories of the SW bearing displacement, the loops of isolation force versus SW bearing displacement, and the loops of North pier shear force versus pier deformation are presented for each test. A set of three figures is presented for each test. The set is identified by the input motion and test number.

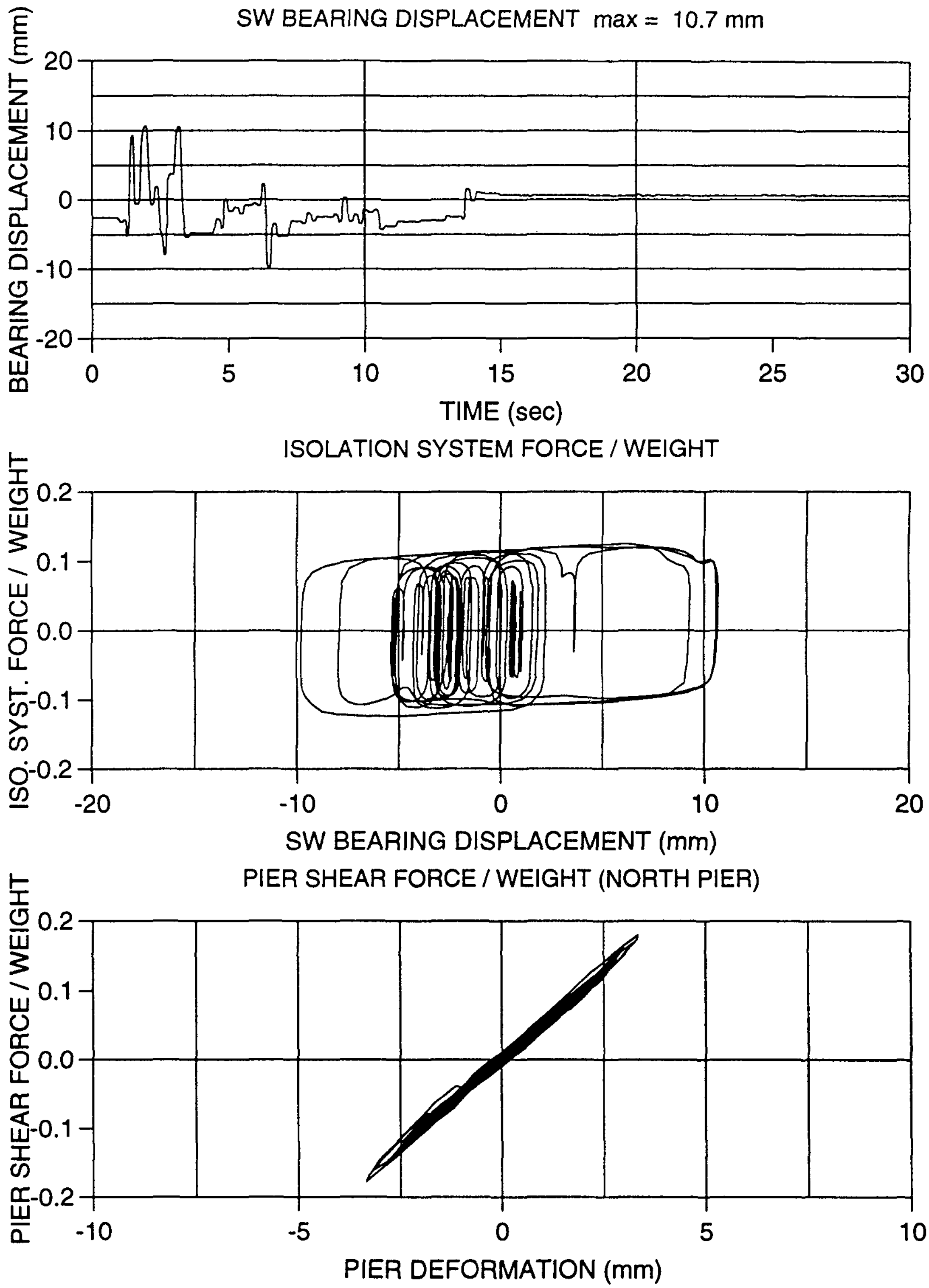

Figure A-1 El Centro S00E 100% (FPSAR26)

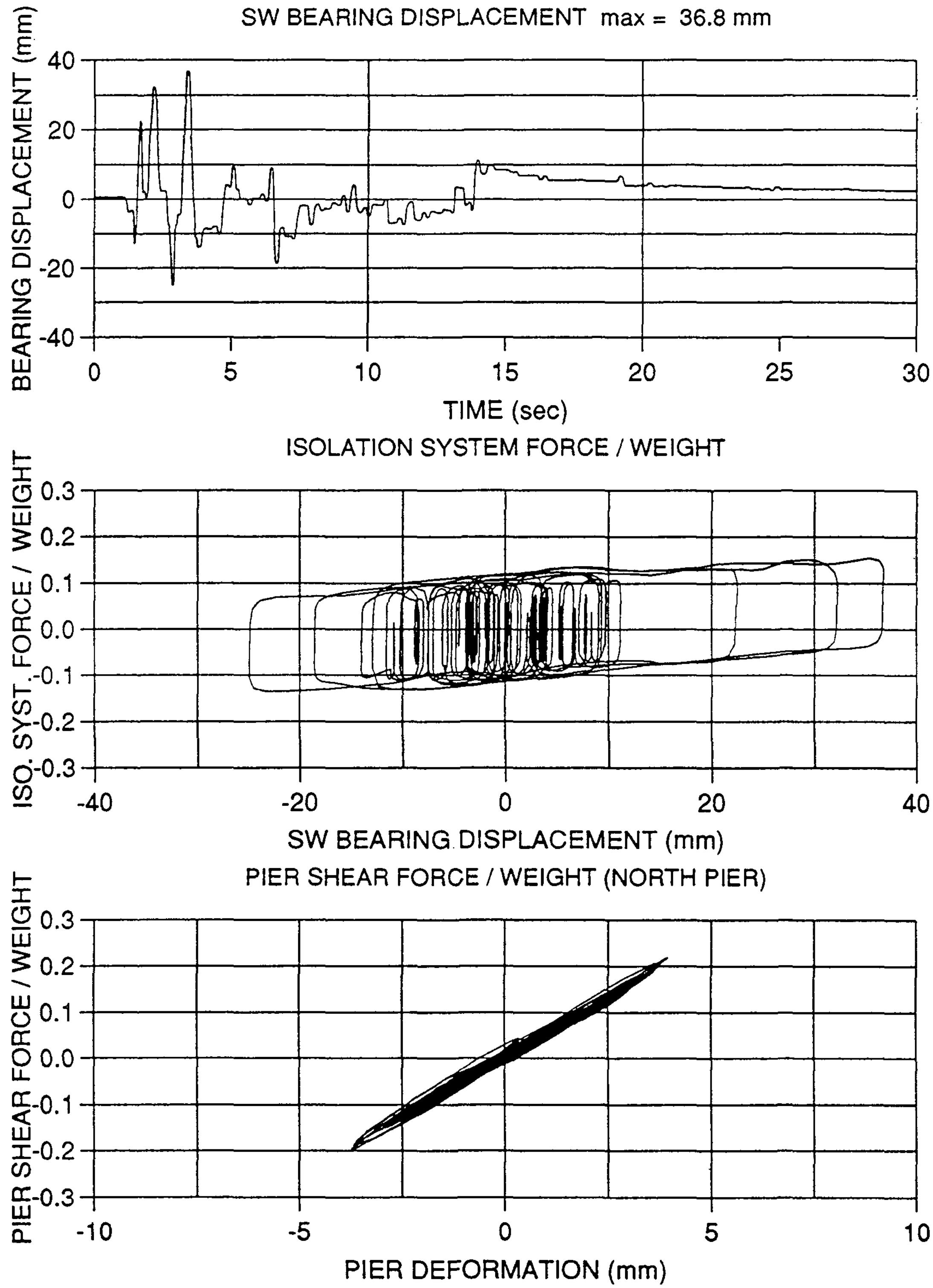

Figure A-2 El Centro S00E 200% (FPSAR27)

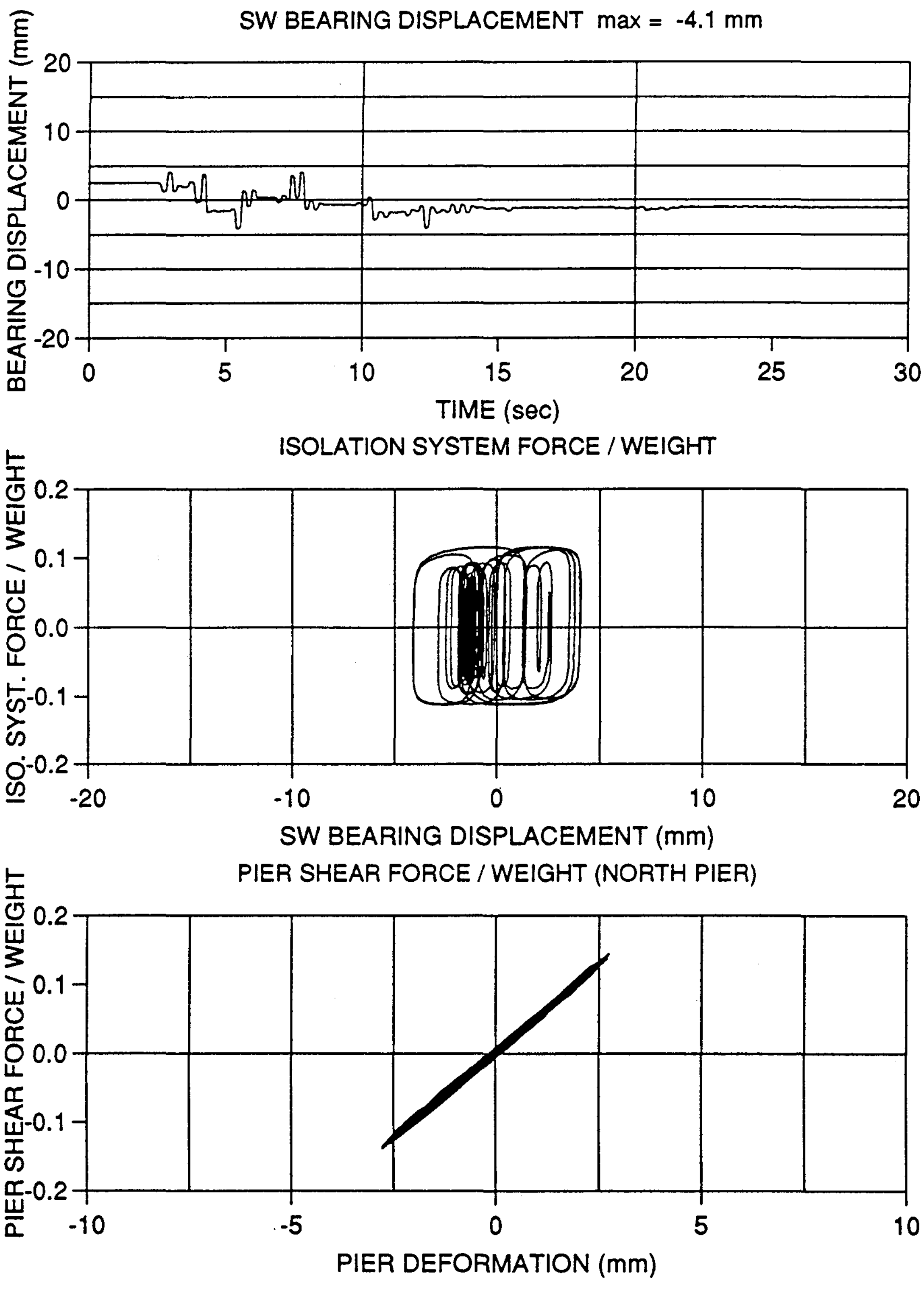

Figure A-3 Taft N21E 100% (FPSAR28)

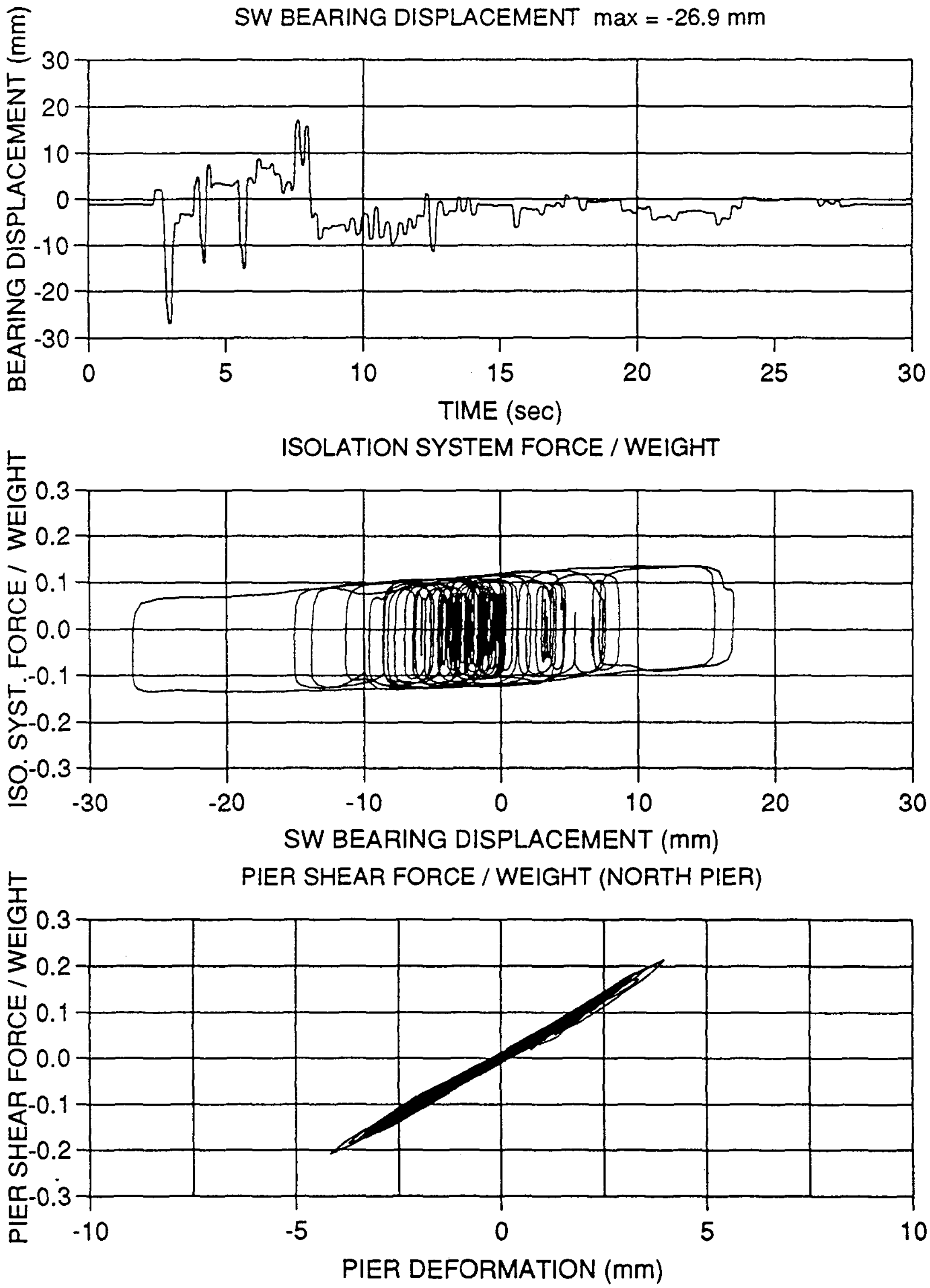

Figure A-4 Taft N21E 300% (FPSAR29)

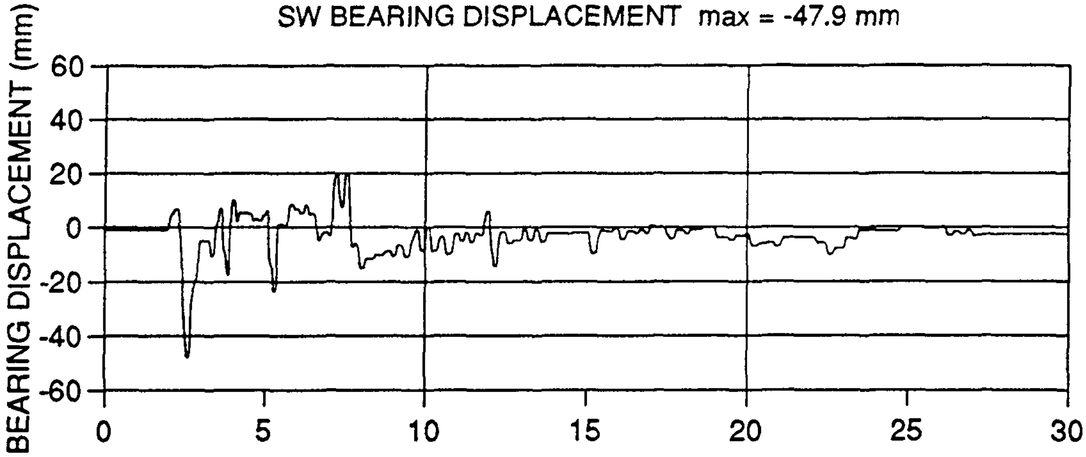

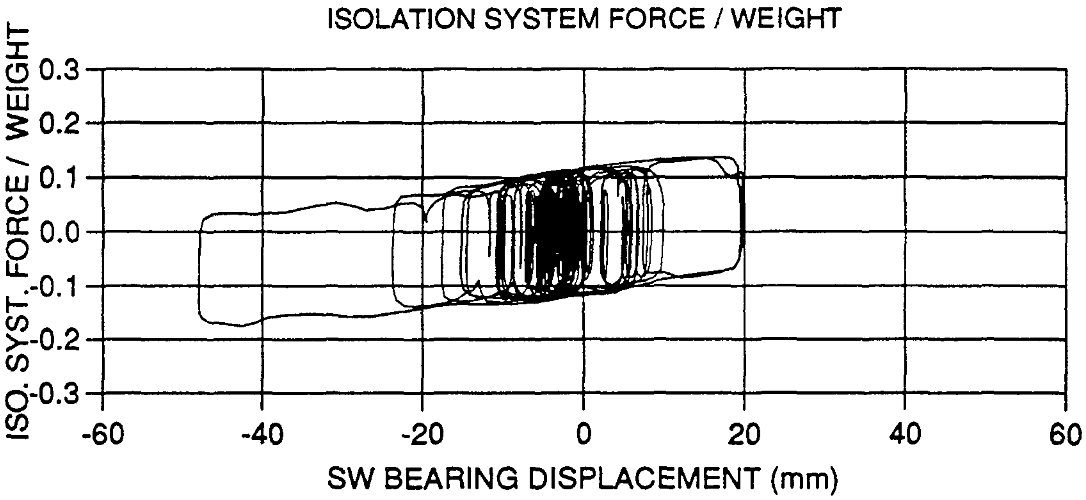

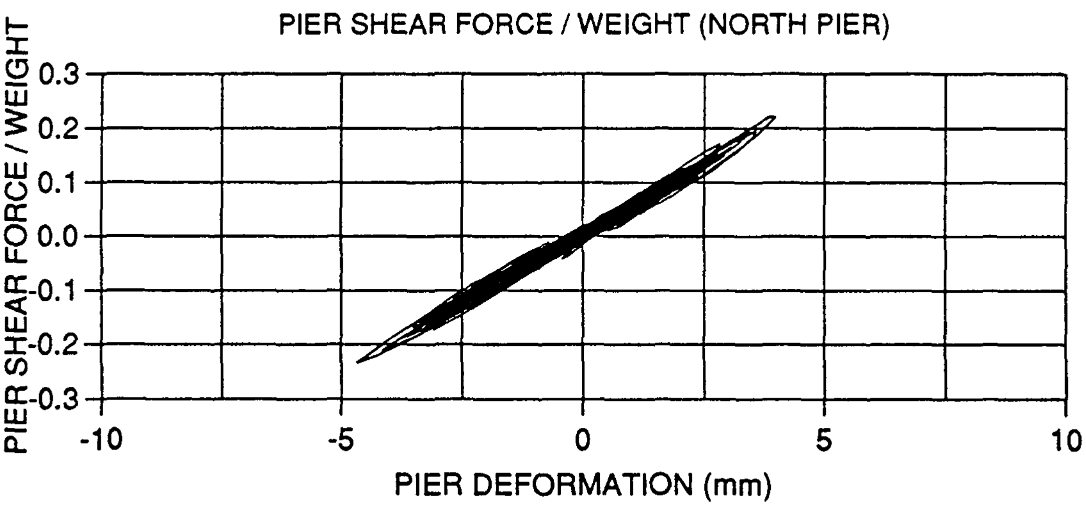

Figure A-5 Taft N21E 400% (FPSAR30)

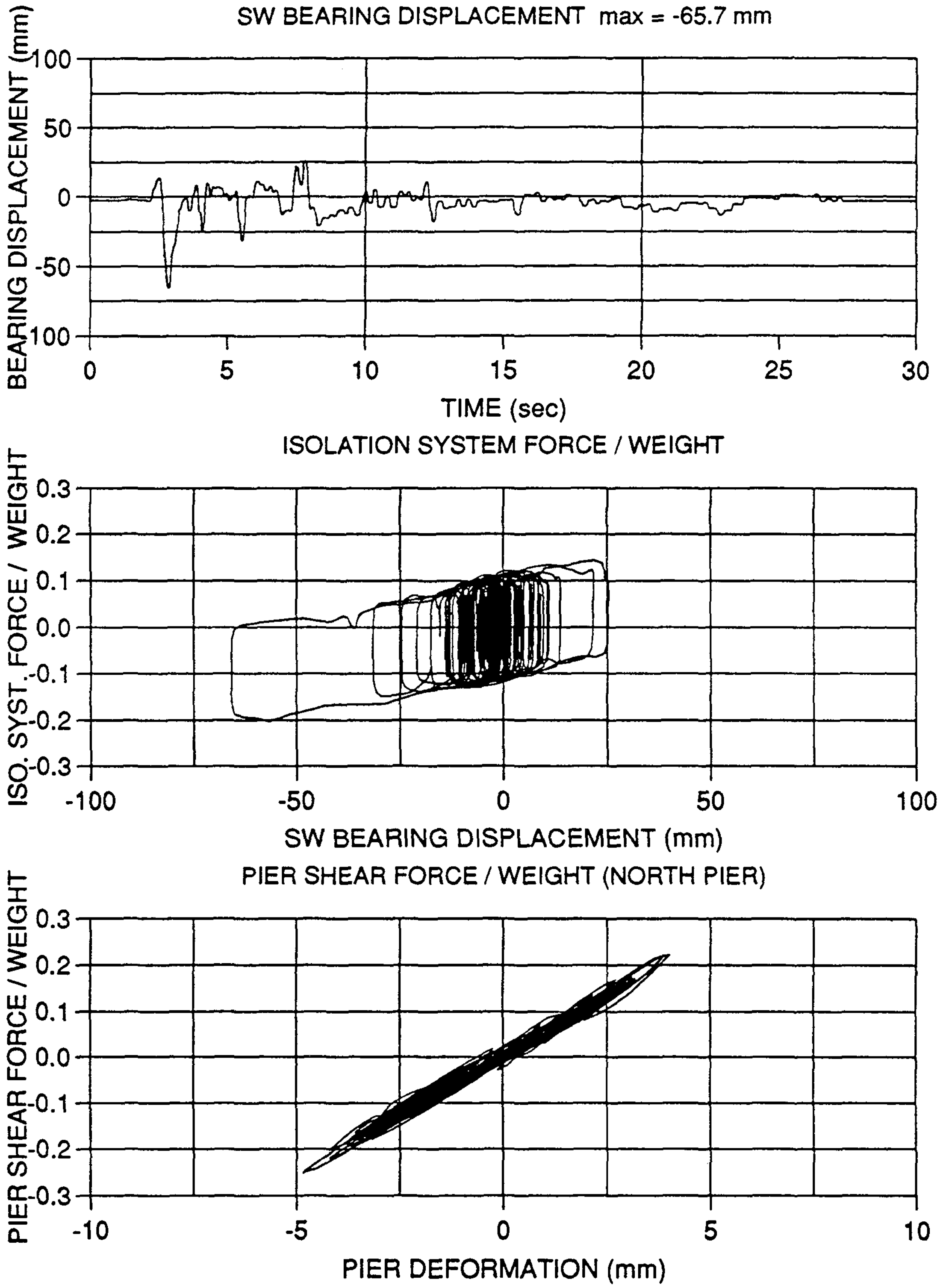

Figure A-6 Taft N21E 500% (FPSAR31)

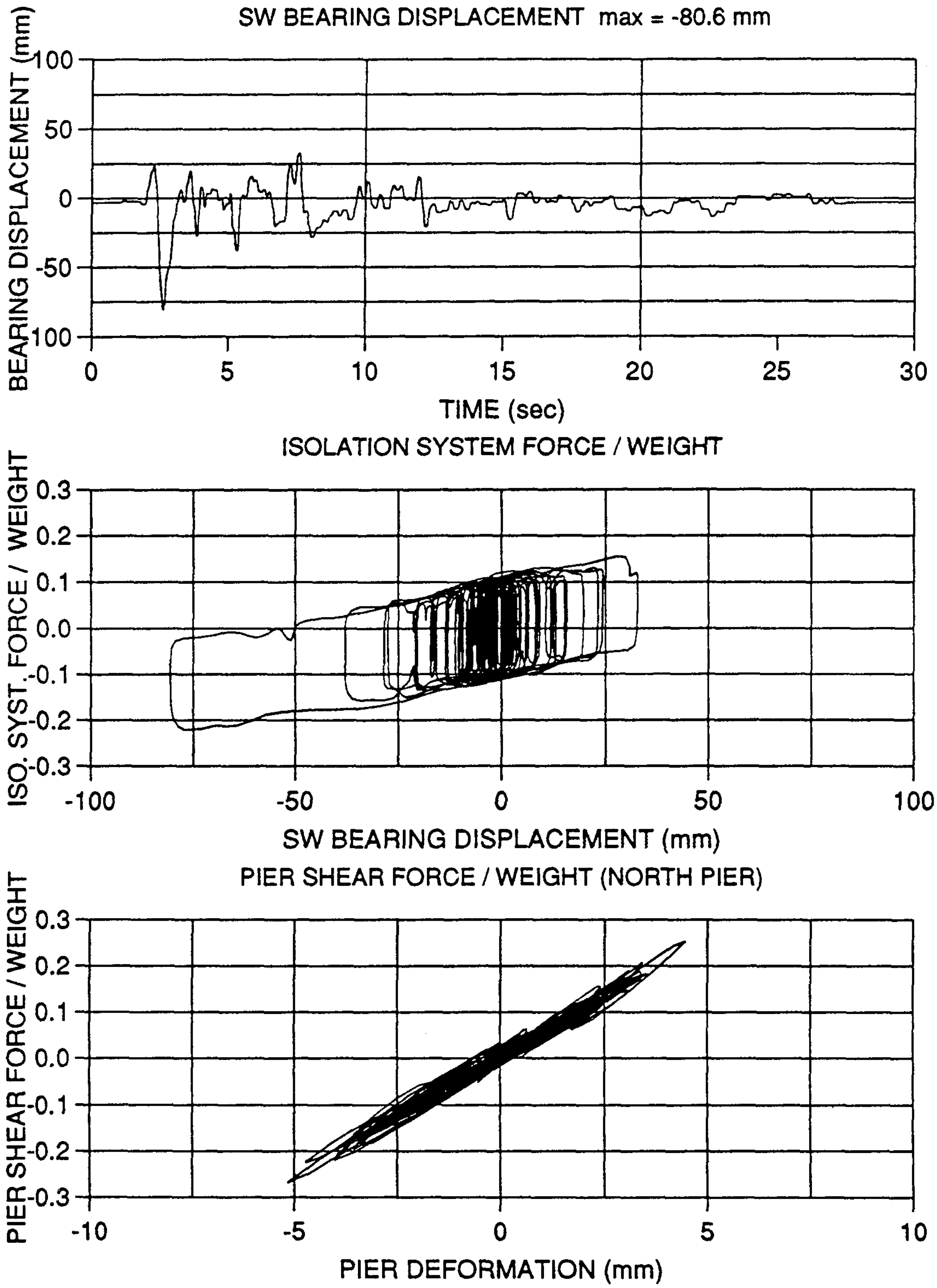

Figure A-7 Taft N21E 600% (FPSAR32)

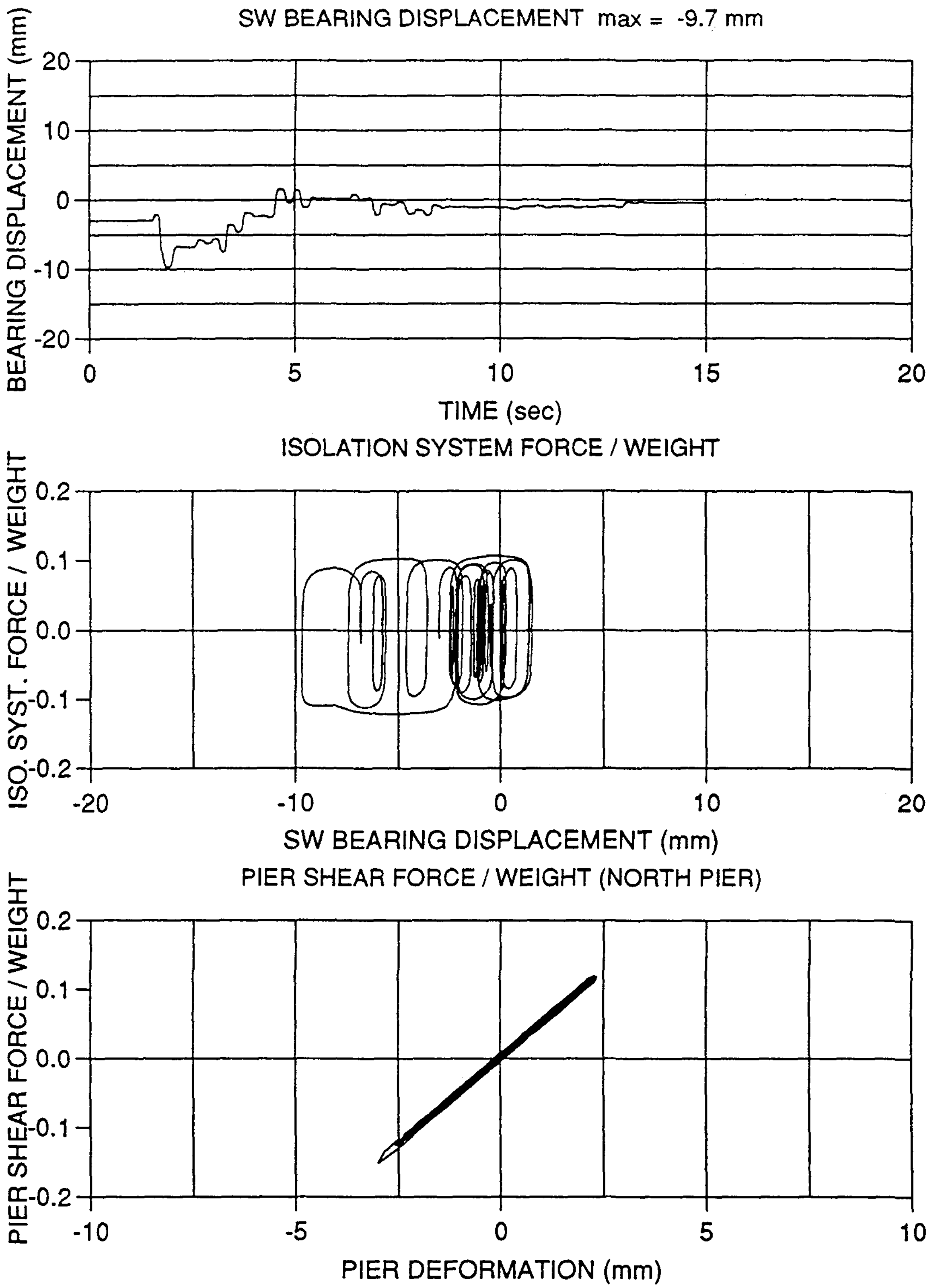

Figure A-8 Japanese Level 1 G.C.1 100% (FPSAR33)

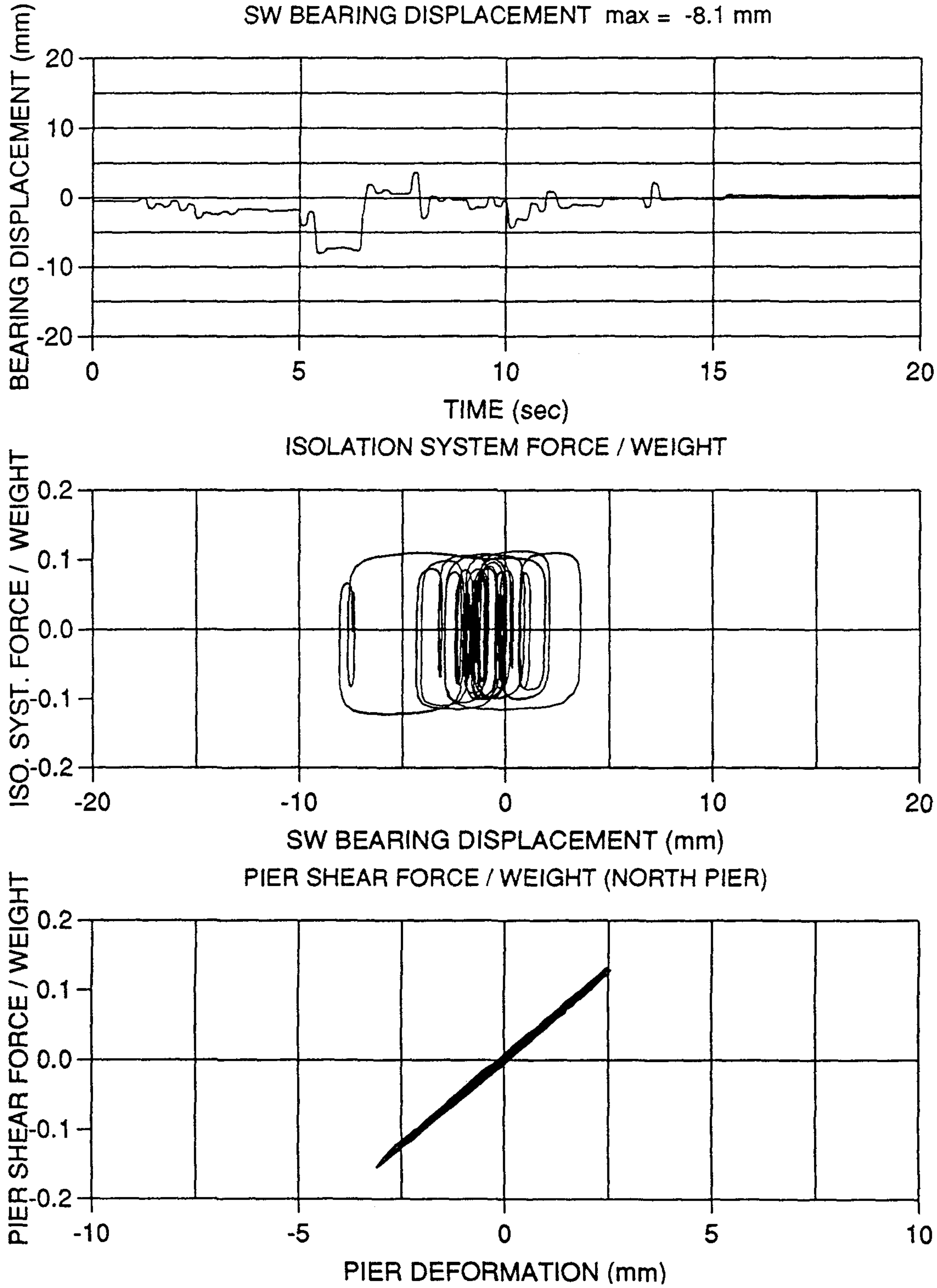

Figure A-9 Japanese Level 1 G.C.2 100% (FPSAR34)

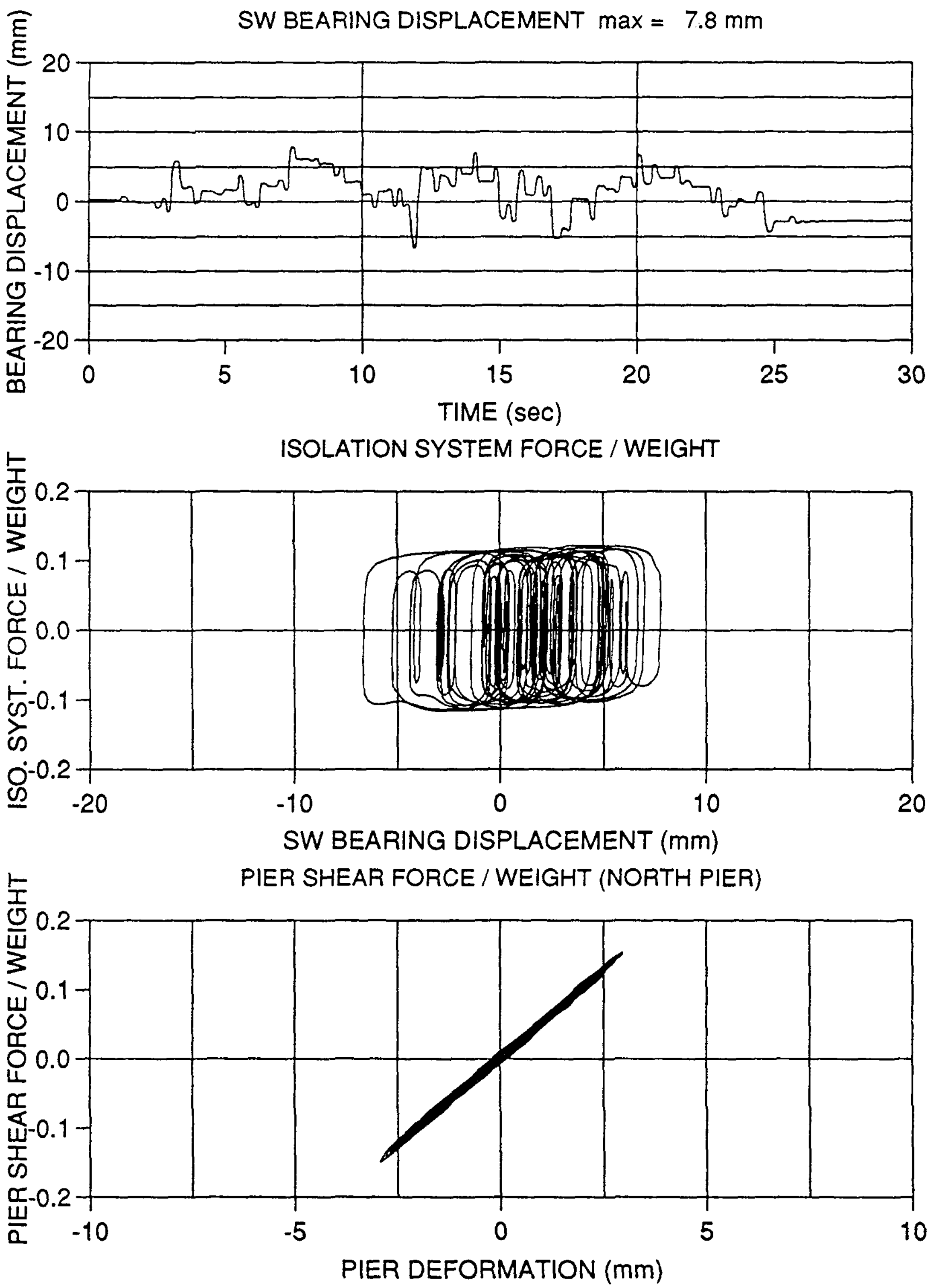

Figure A-10 Japanese Level 1 G.C.3 100% (FPSAR35)

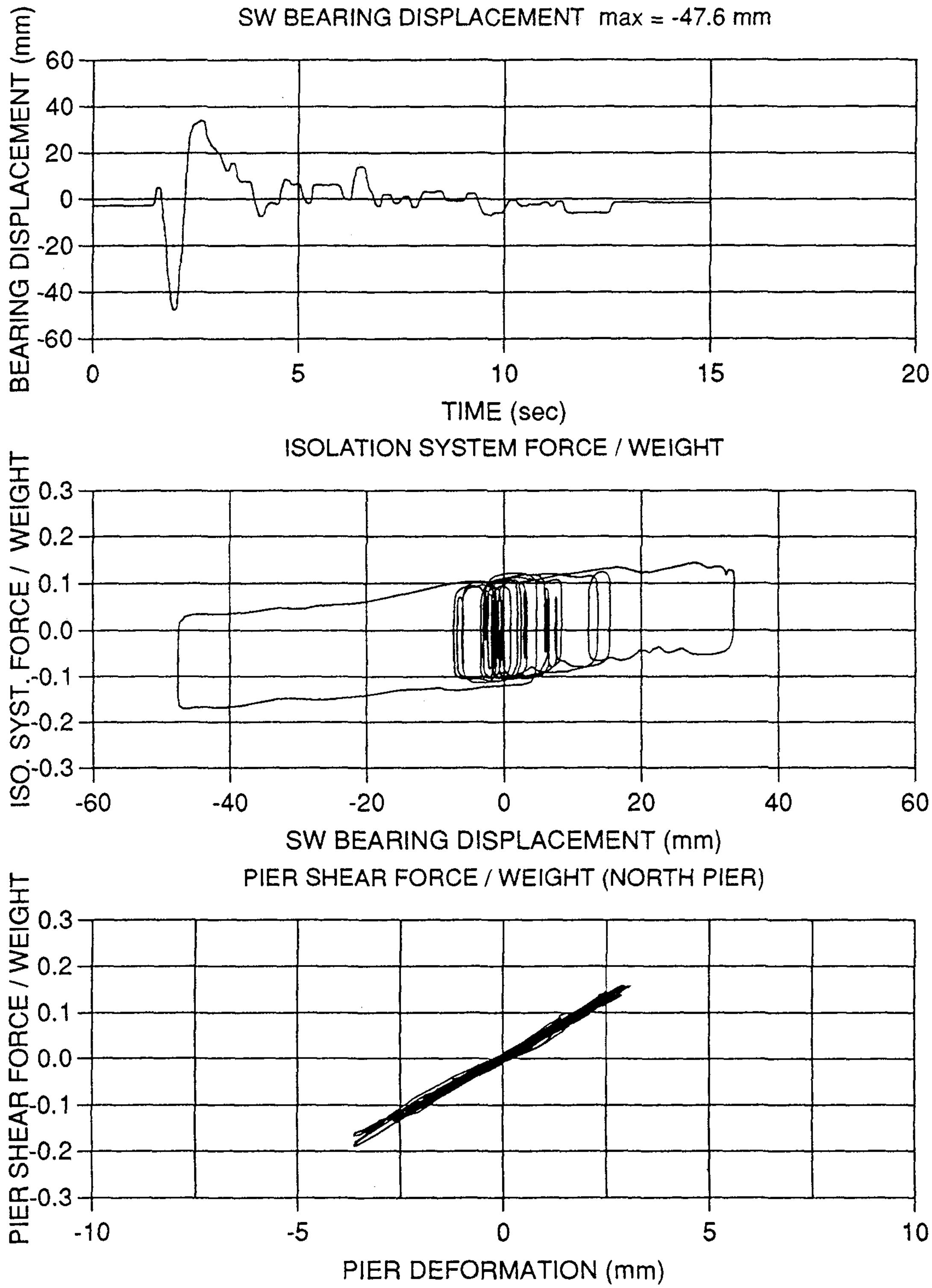

Figure A-11 Japanese Level 2 G.C.1 75% (FPSAR36)

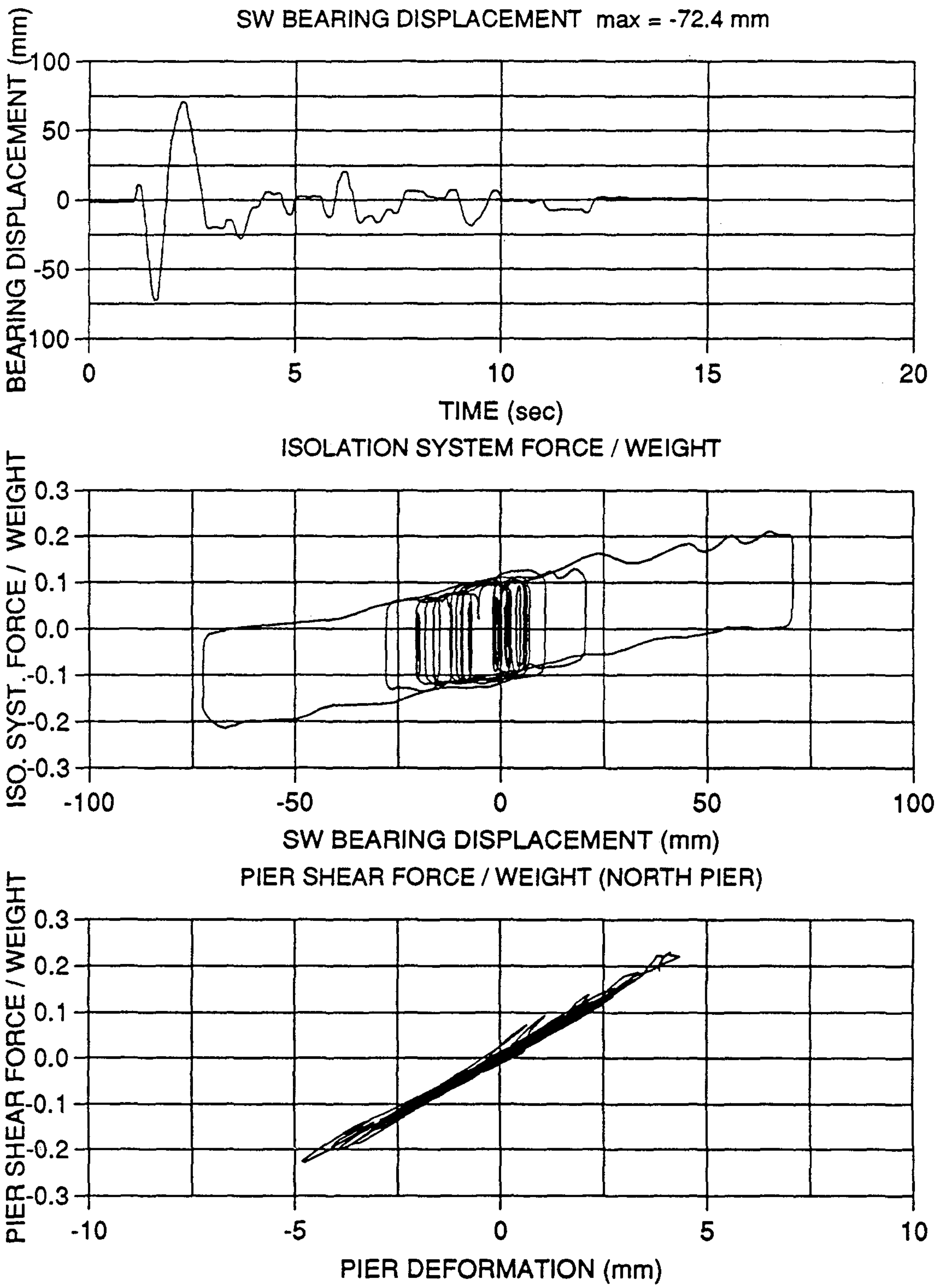

Figure A-12 Japanese Level 2 G.C.1 100% (FPSAR37)

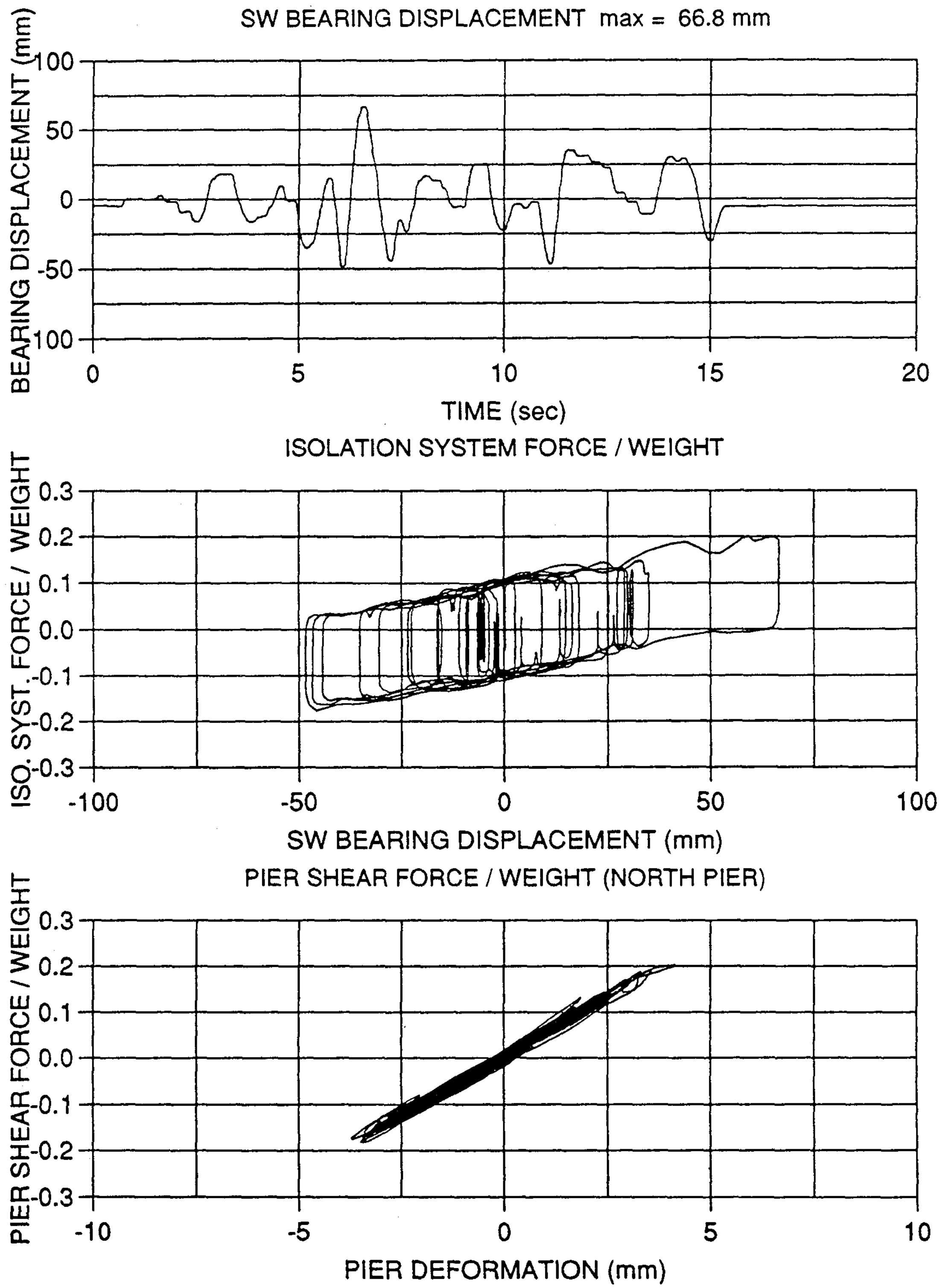

Figure A-13 Japanese Level 2 G.C.2 100% (FPSAR38)

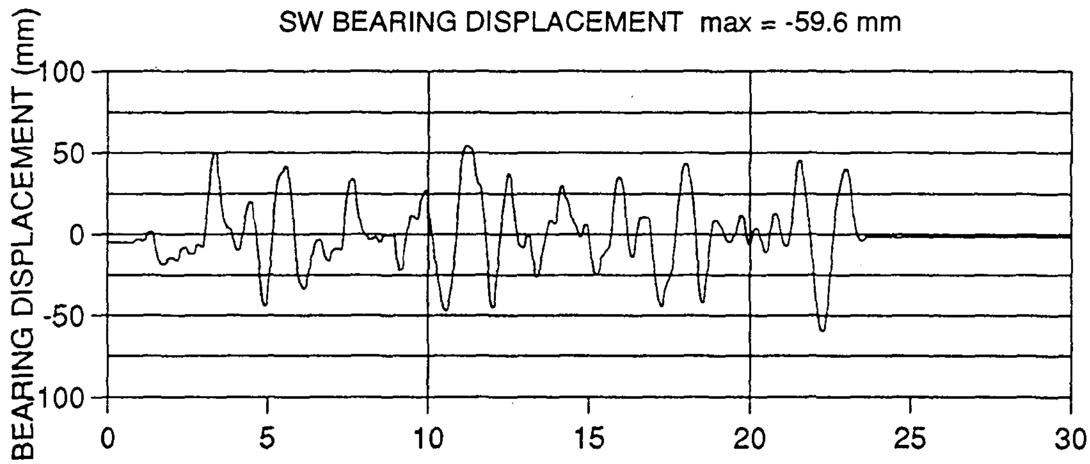

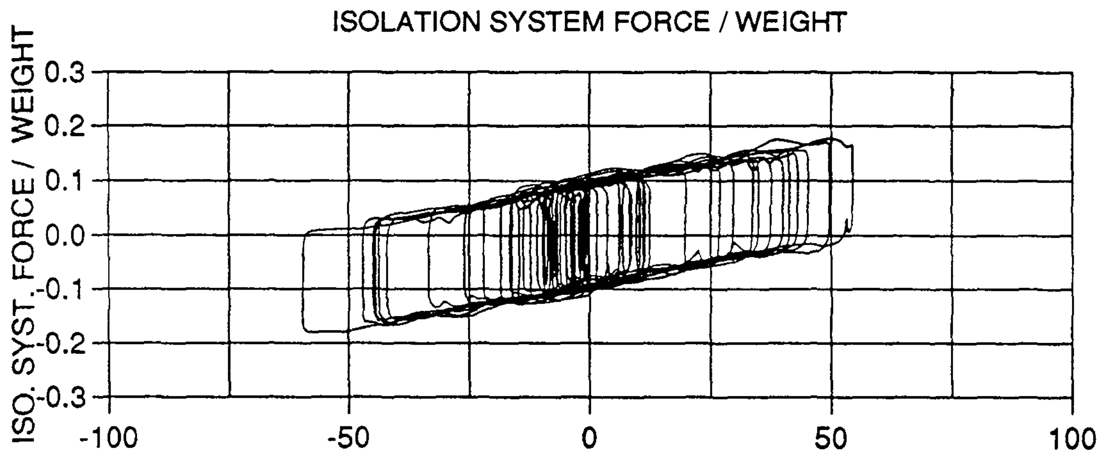

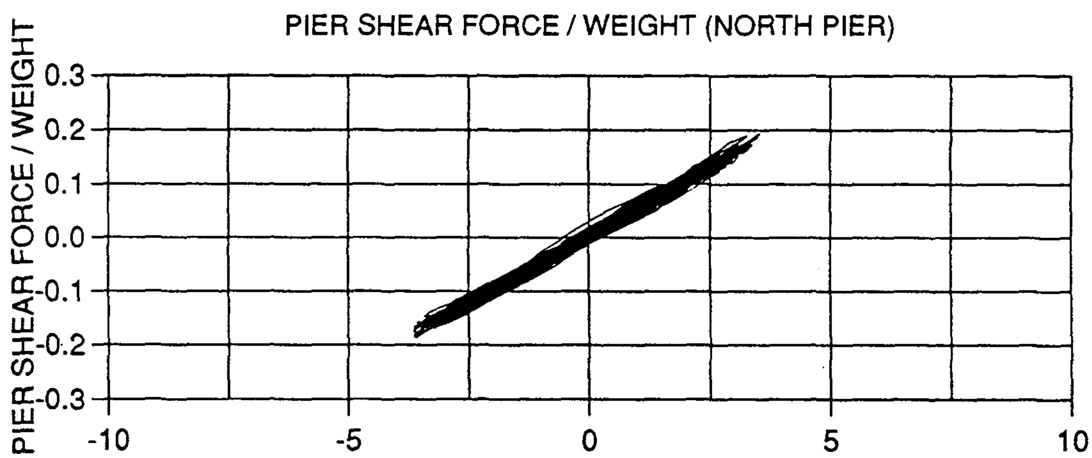

Figure A-14 Japanese Level 2 G.C.3 75% (FPSAR39)

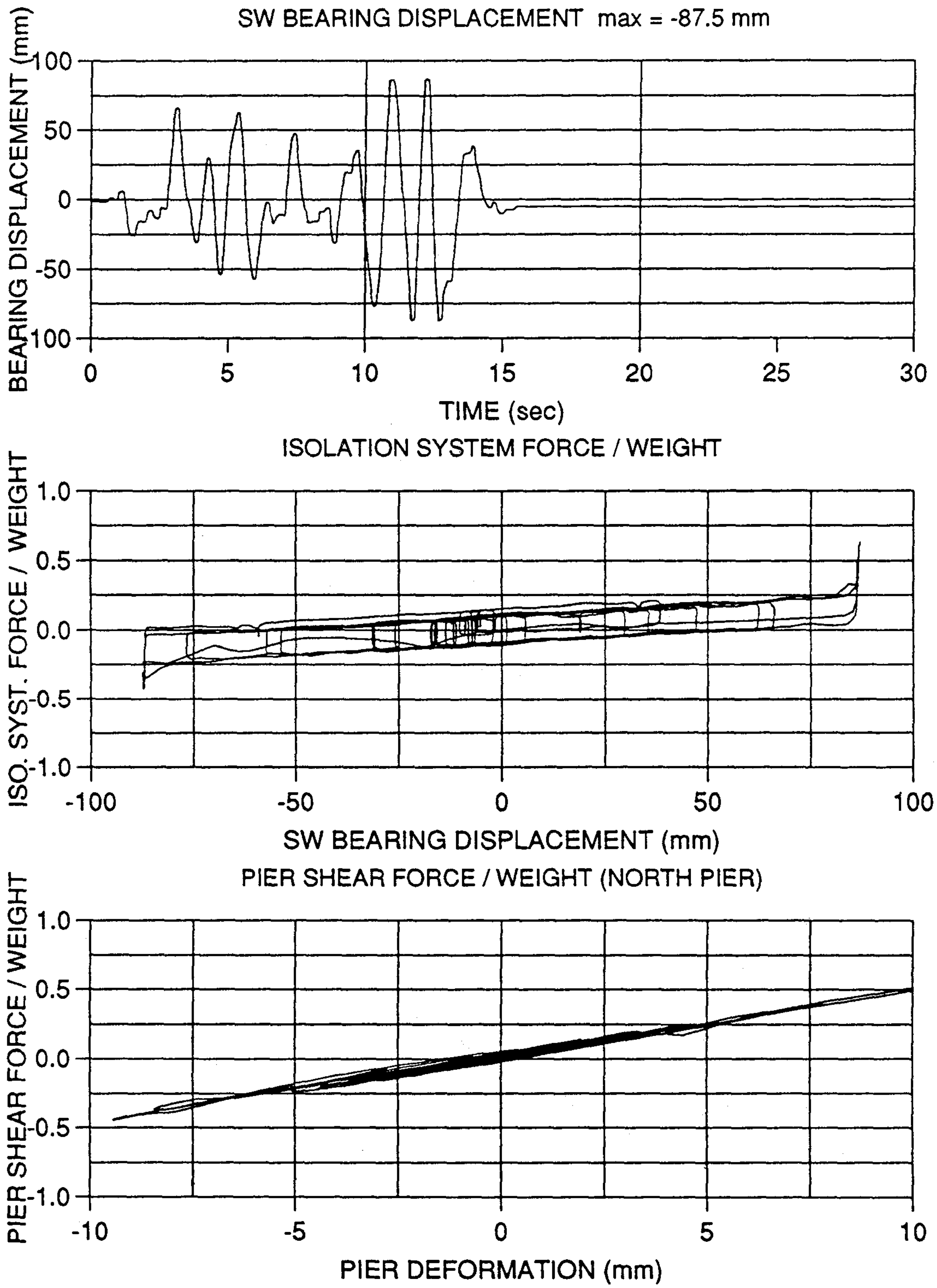

Figure A-15 Japanese Level 2 G.C.3 90% (FPSAR40)

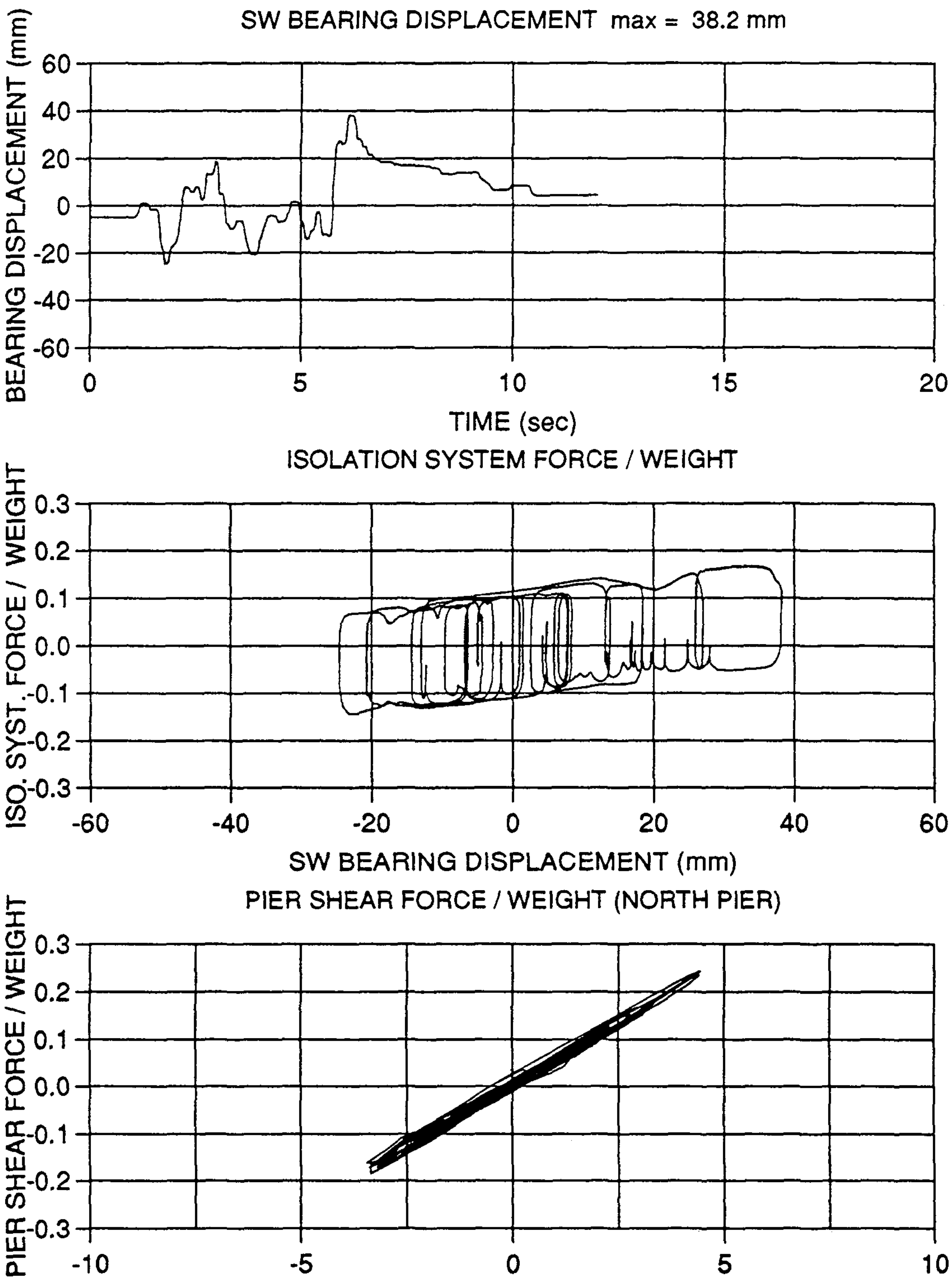

Figure A-16 CalTran R3 0.6g 100% (FPSAR41)

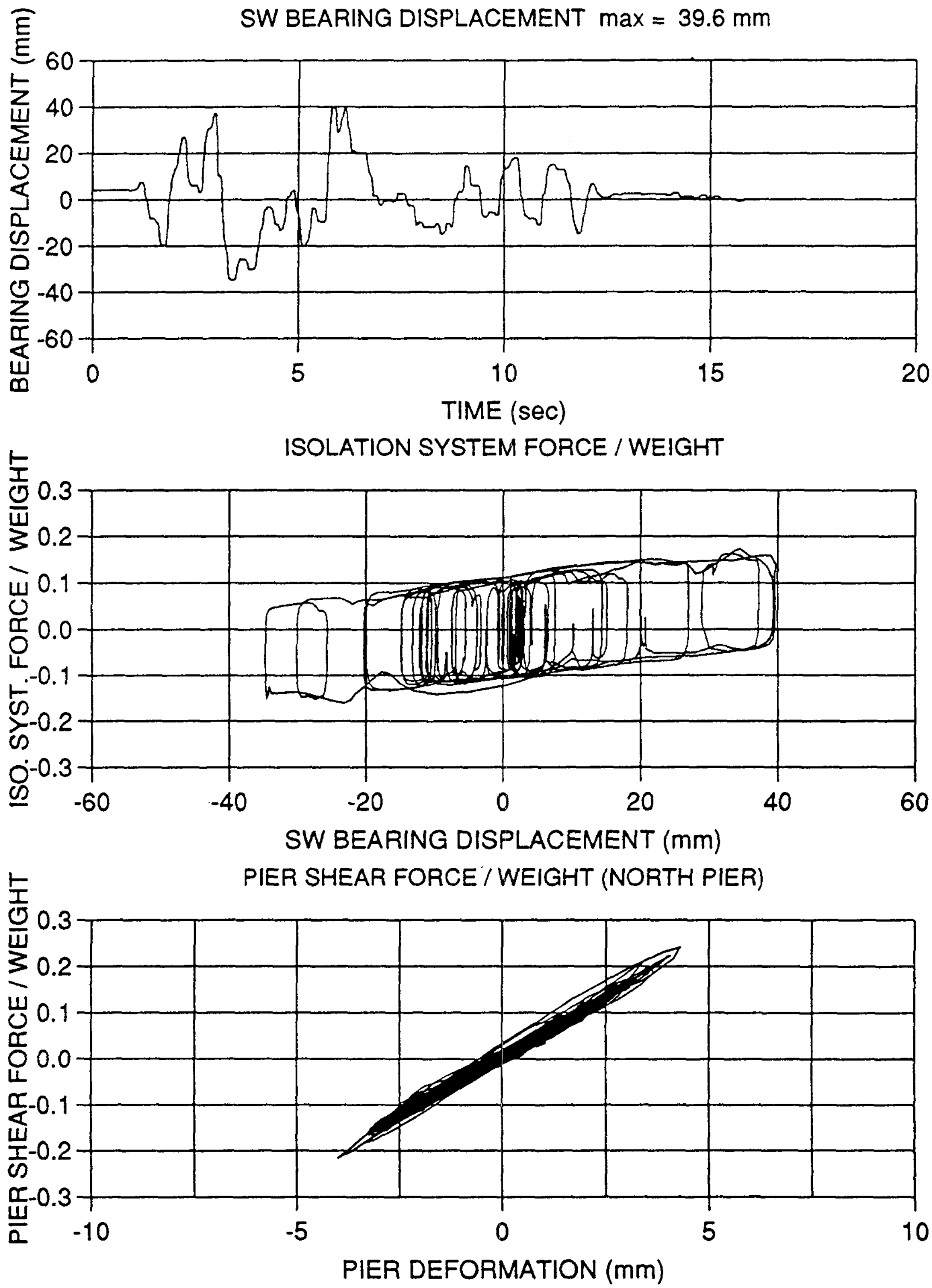

Figure A-17 CalTran S3 0.6g 100% (FPSAR42)

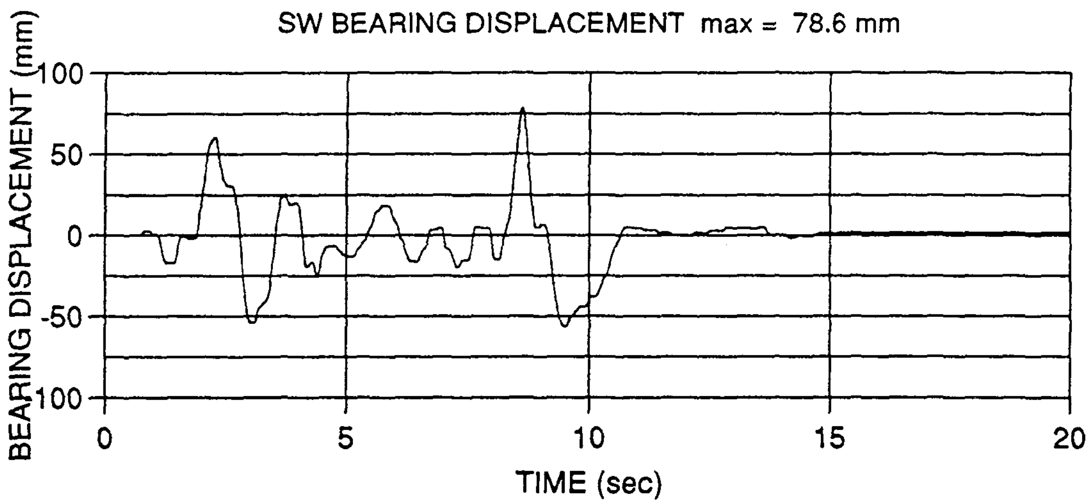

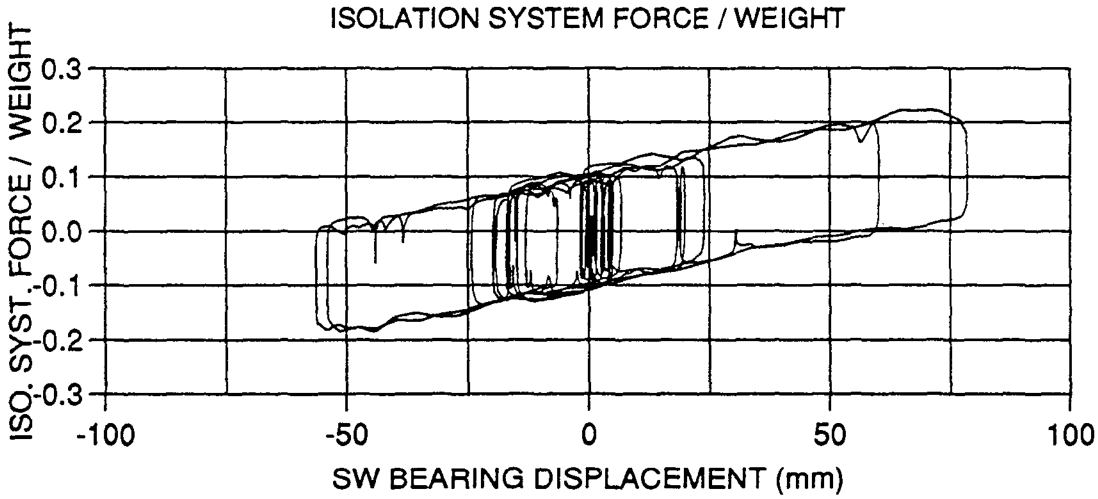

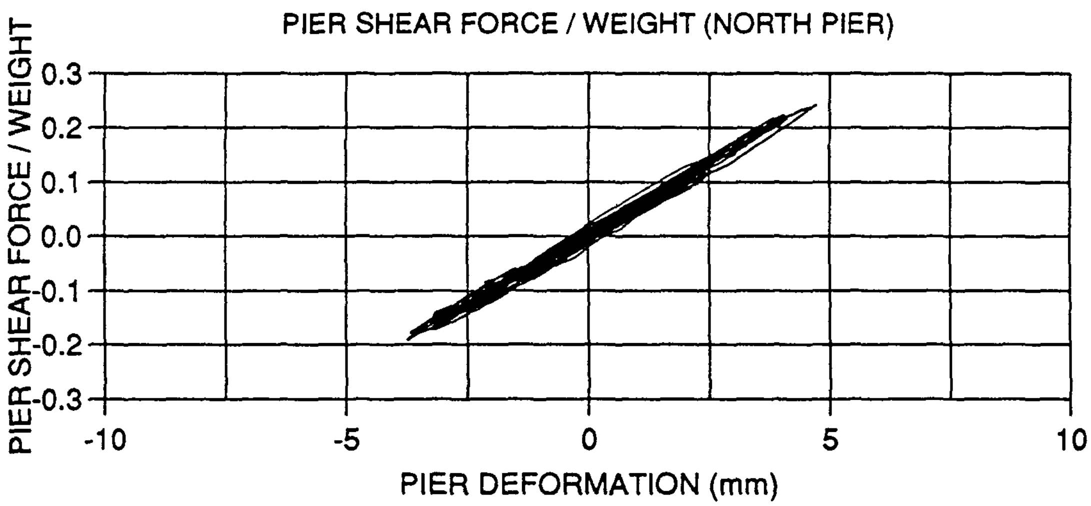

Figure A-18 CalTran A2 0.6g 100% (FPSAR43)

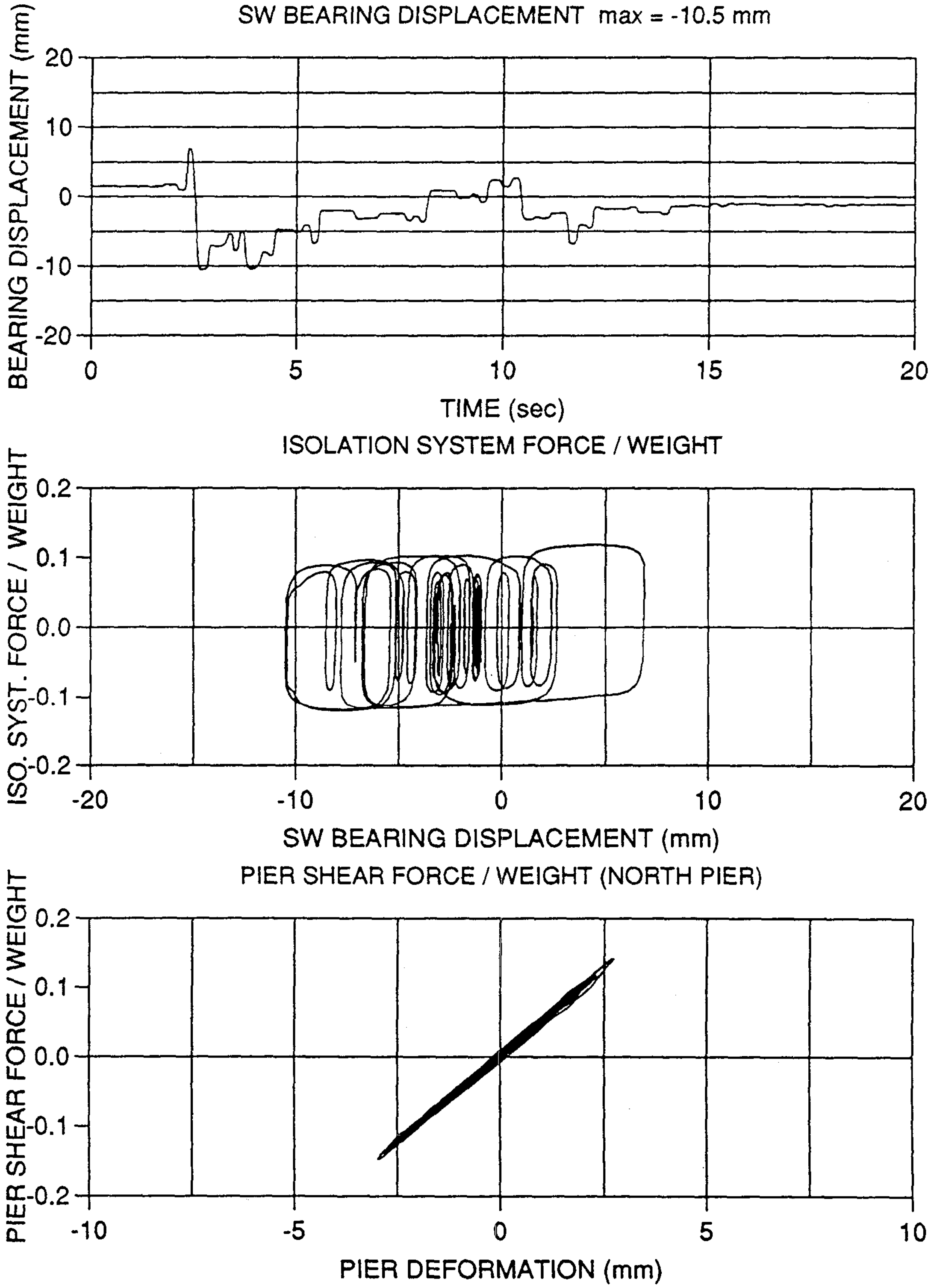

Figure A-19 Hachinohe N-S 100% (FPSAR44)

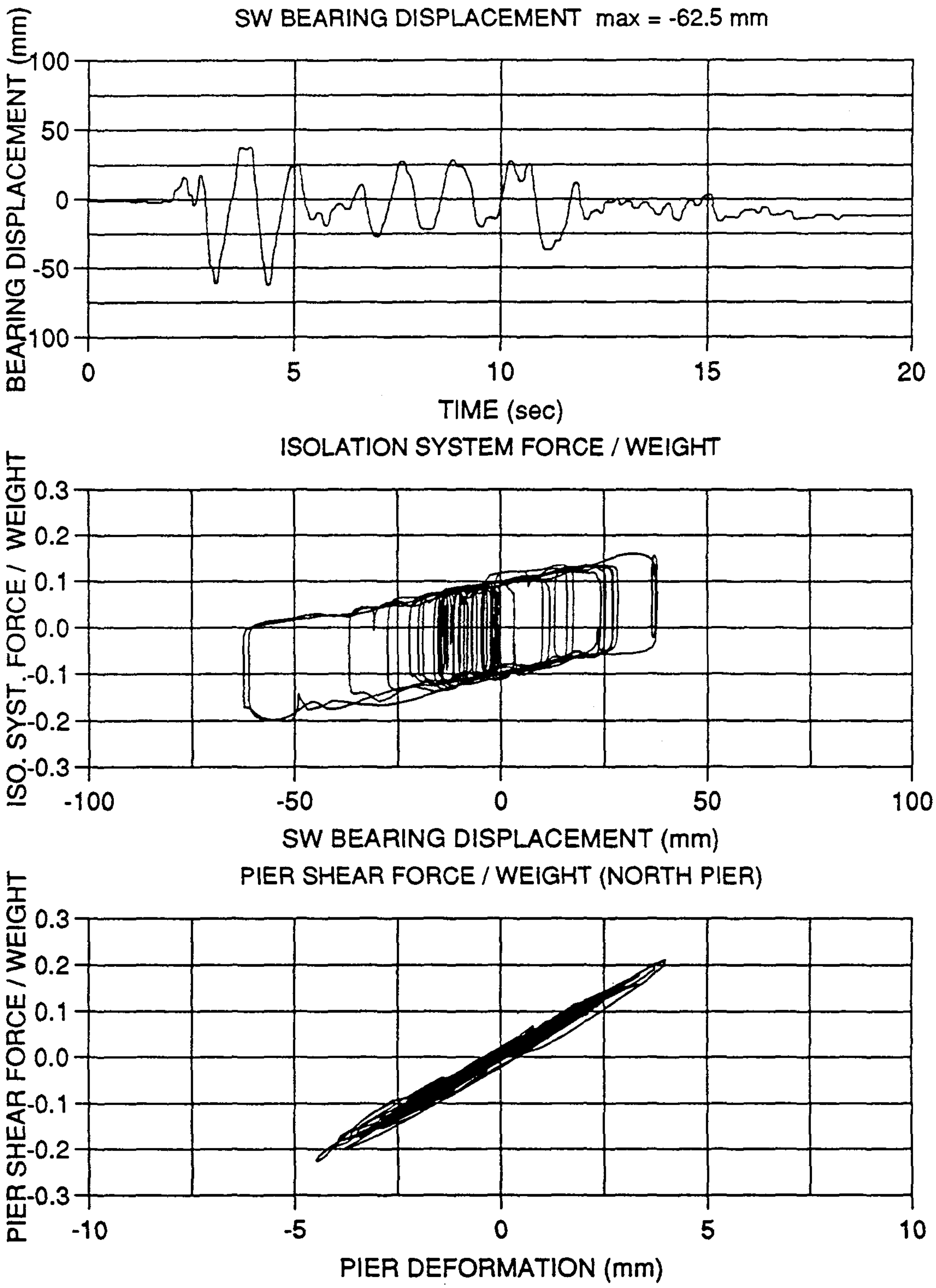

Figure A-20 Hachinohe N-S 300% (FPSAR45)

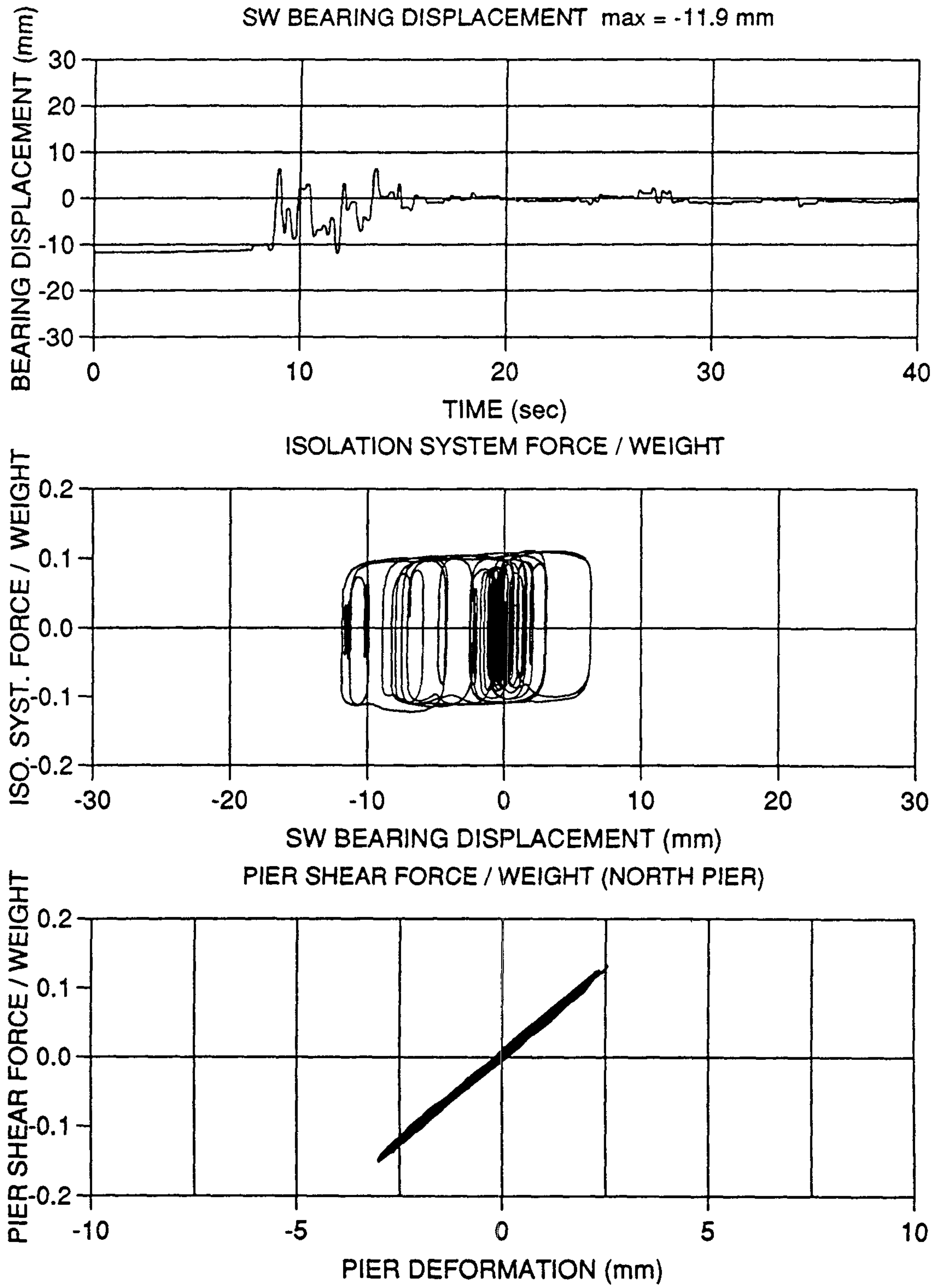

Figure A-21 Akita N-S 100% (FPSAR46)

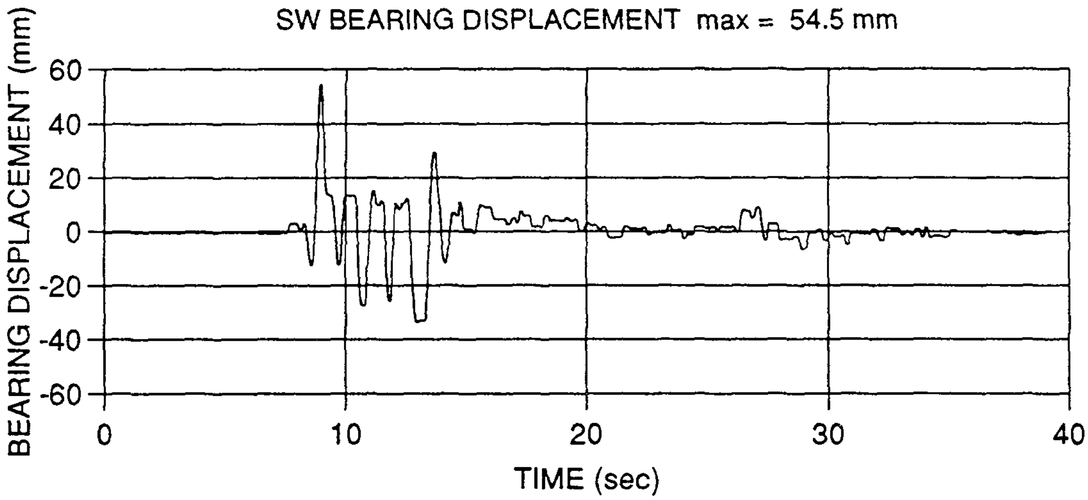

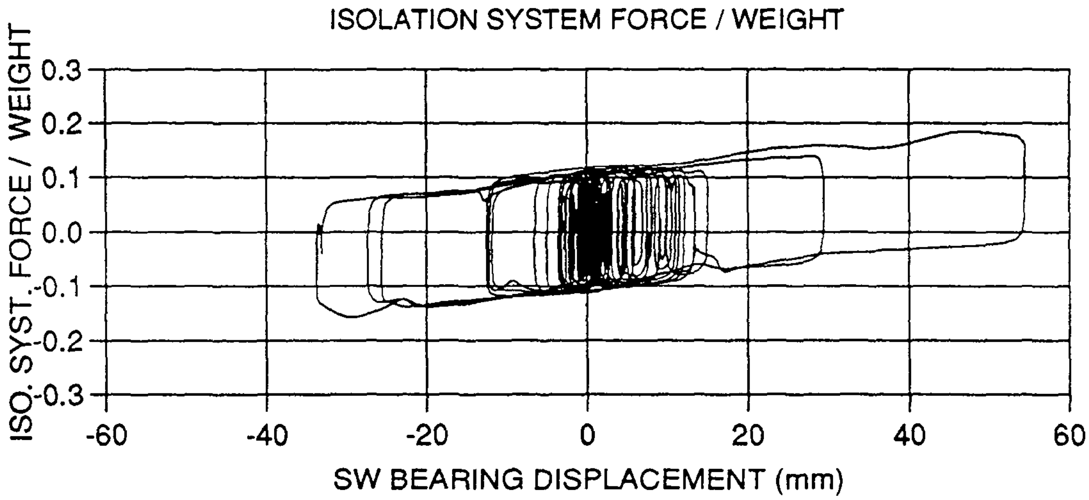

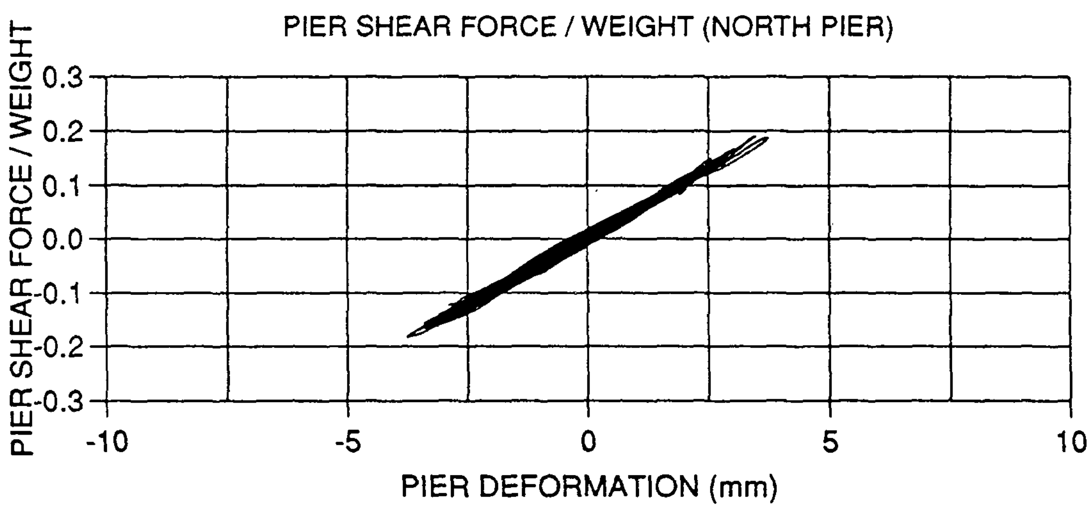

Figure A-22 Akita N-S 200% (FPSAR47)

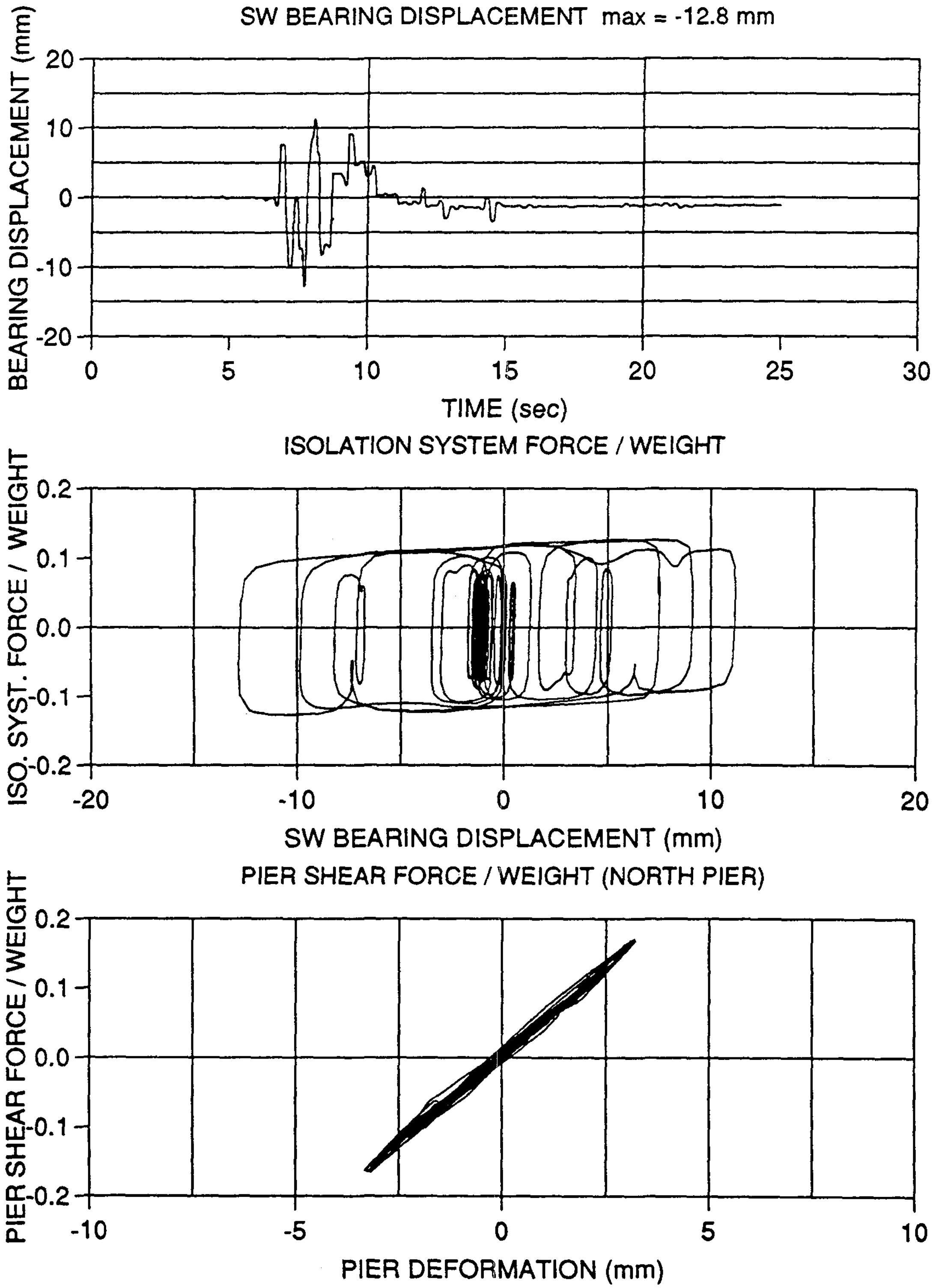

Figure A-23 Miyagiken Oki E-W 300% (FPSAR48)

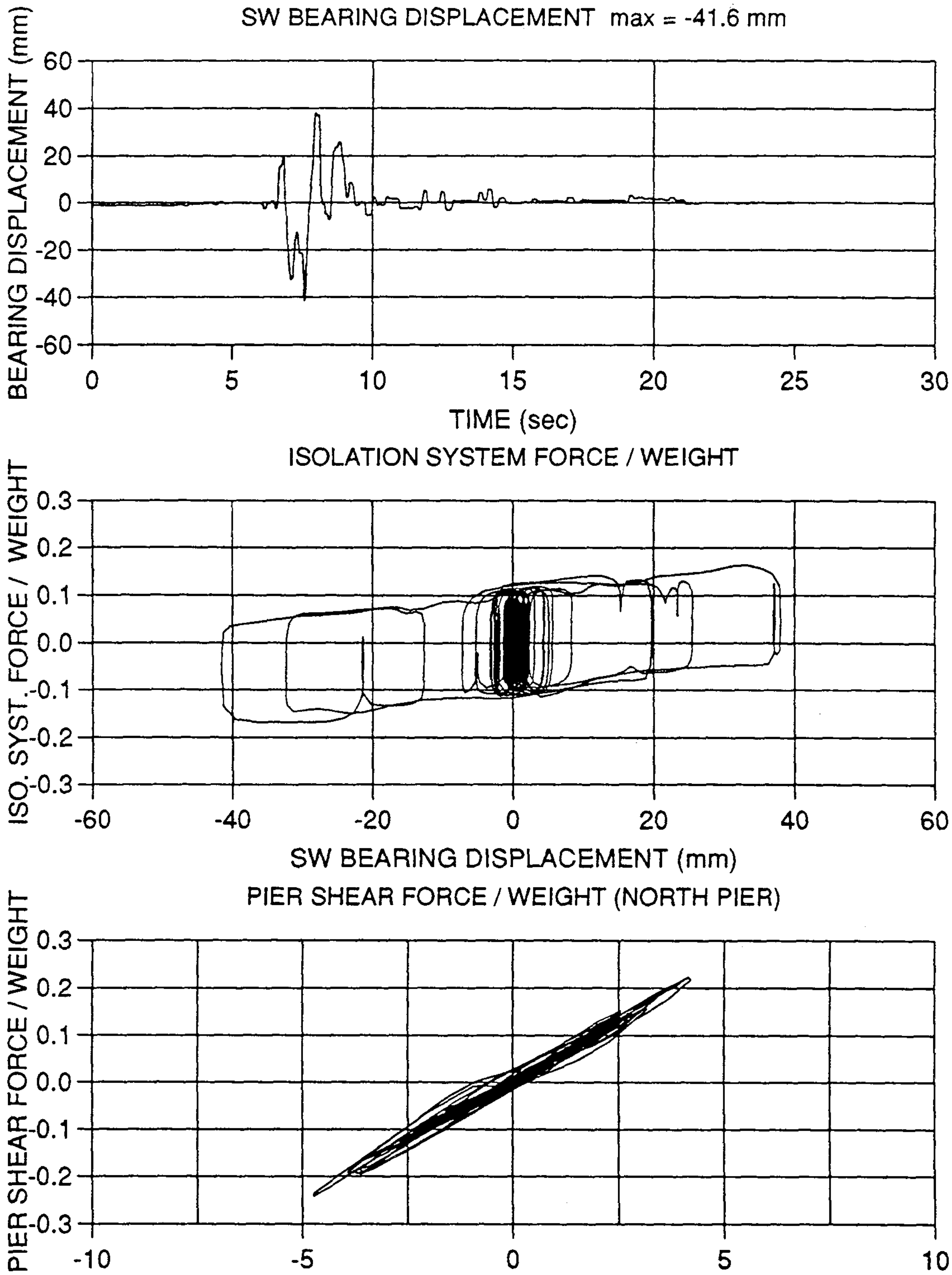

Figure A-24 Miyagiken Oki E-W 600% (FPSAR49)

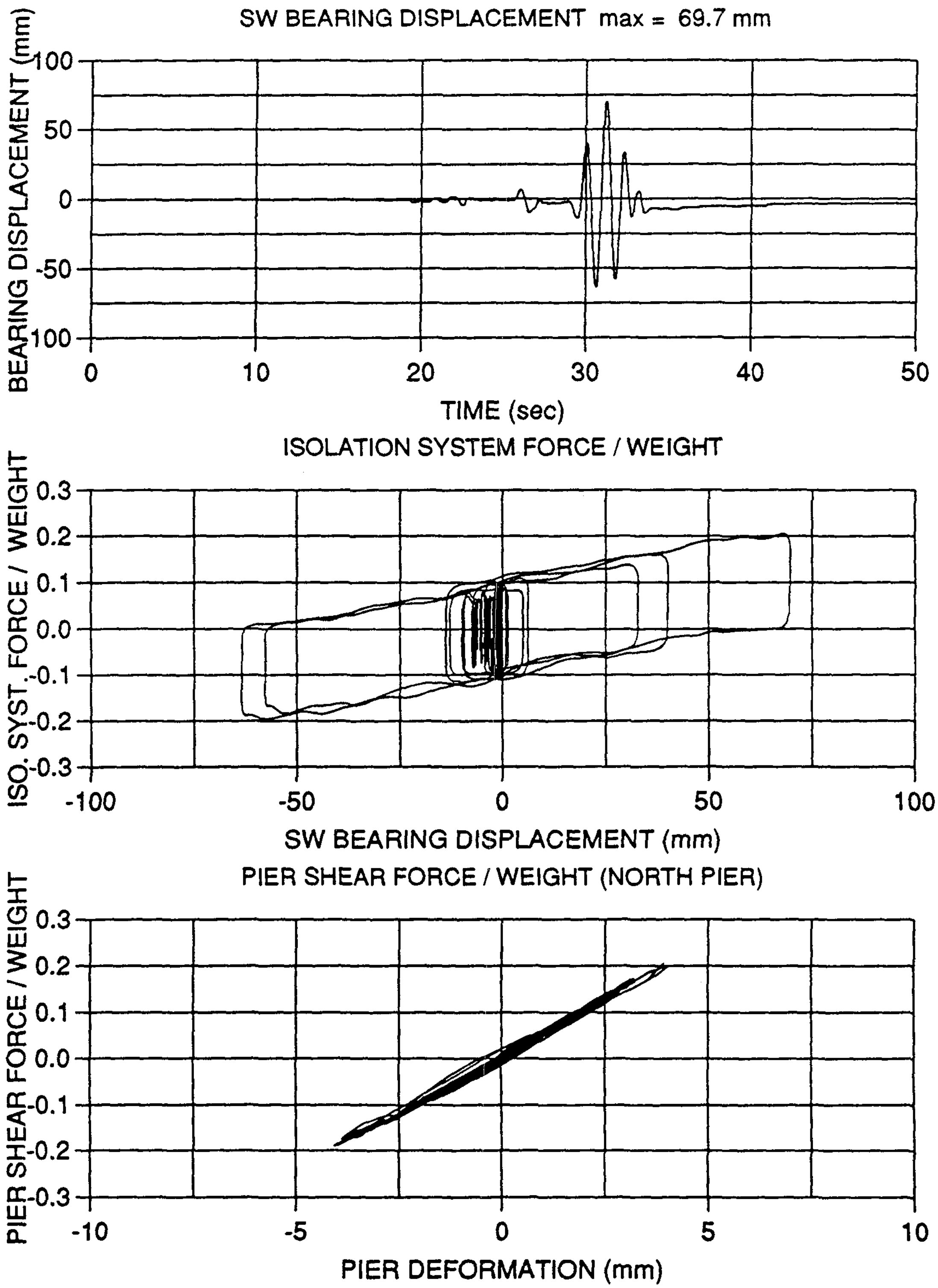

Figure A-25 Mexico City N90W 100% (FPSAR50)

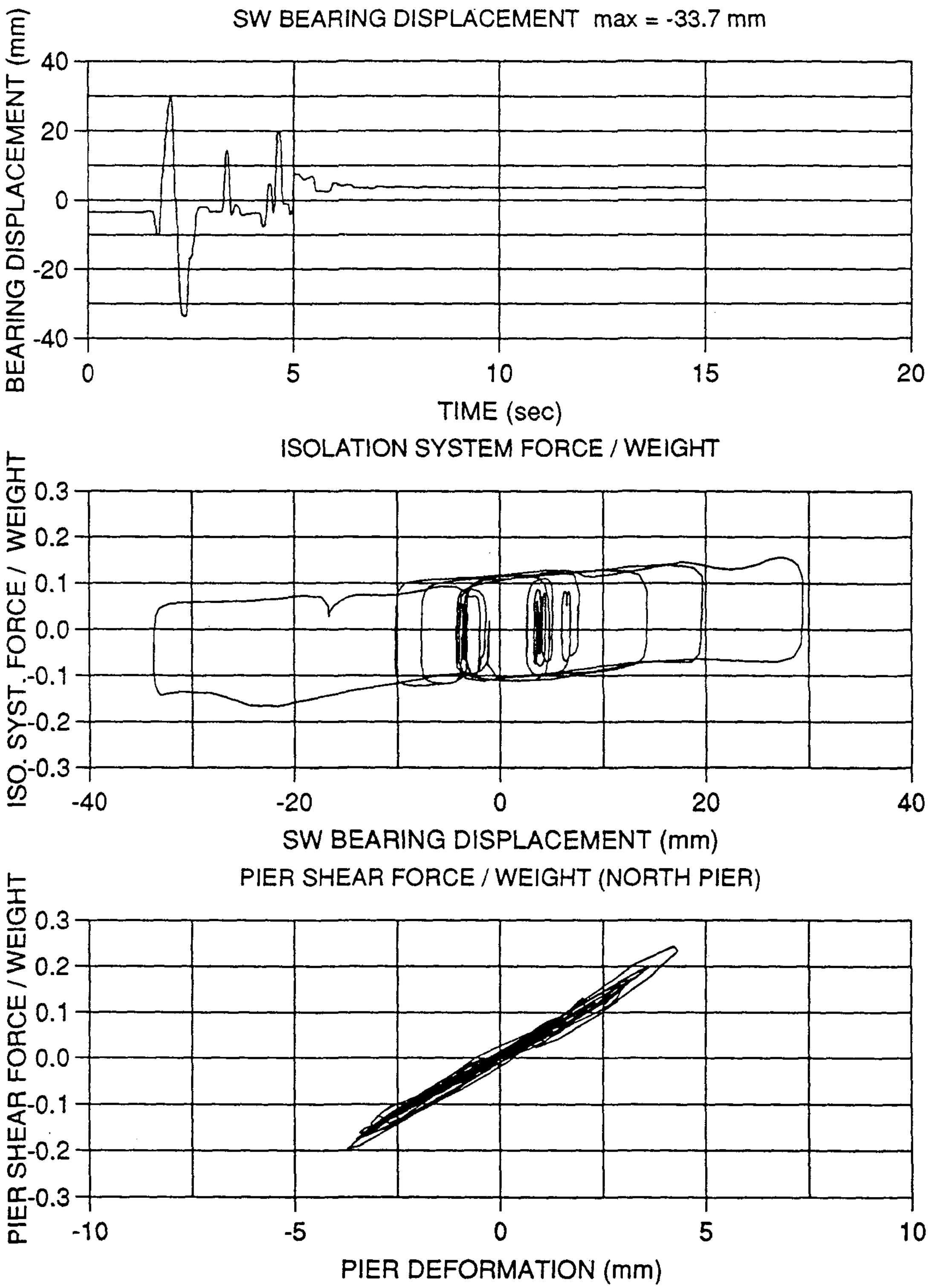

Figure A-26 Pacoima S74W 100% (FPSAR51)

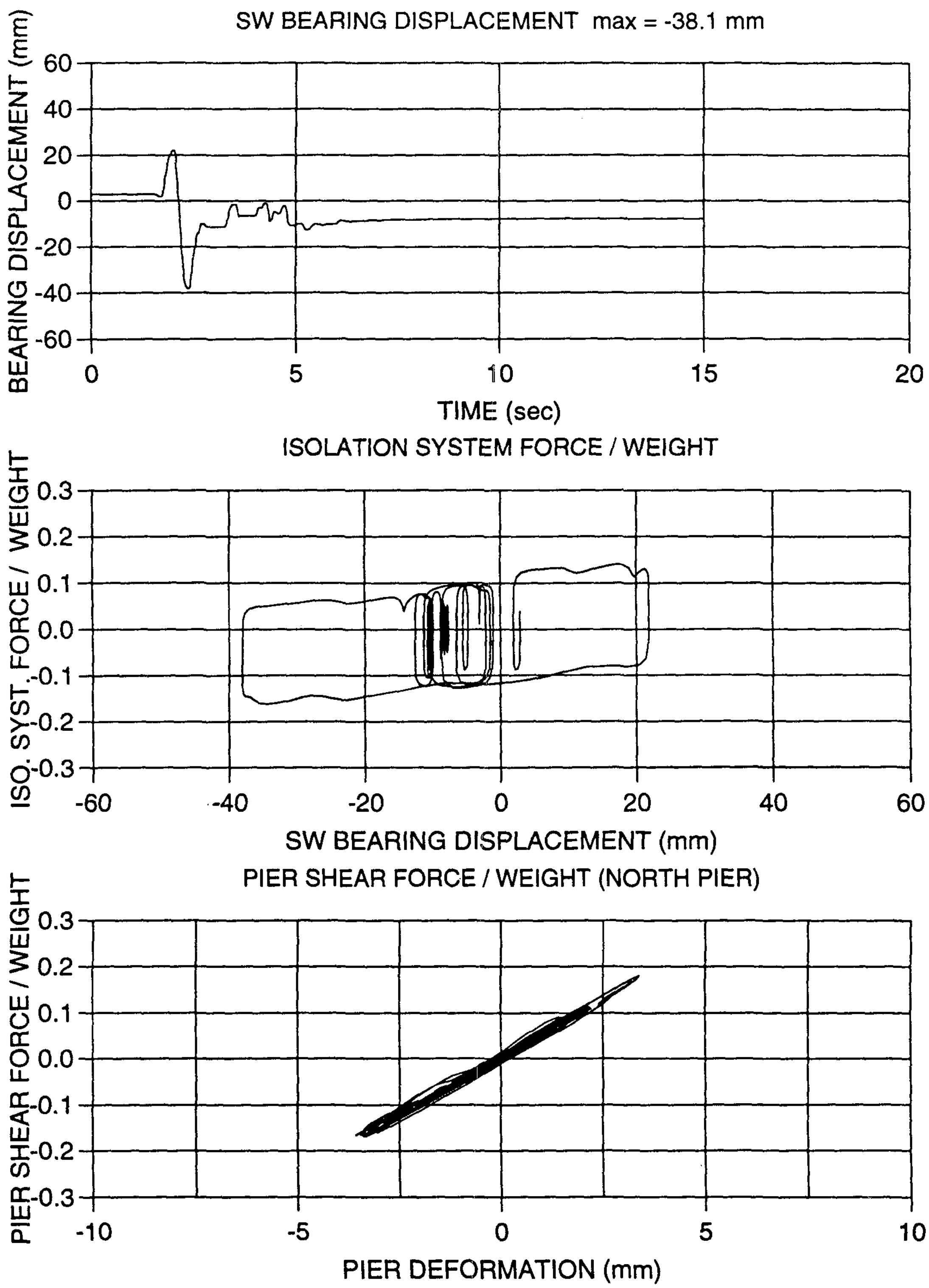

Figure A-27 Pacoima S16E 50% (FPSAR52)

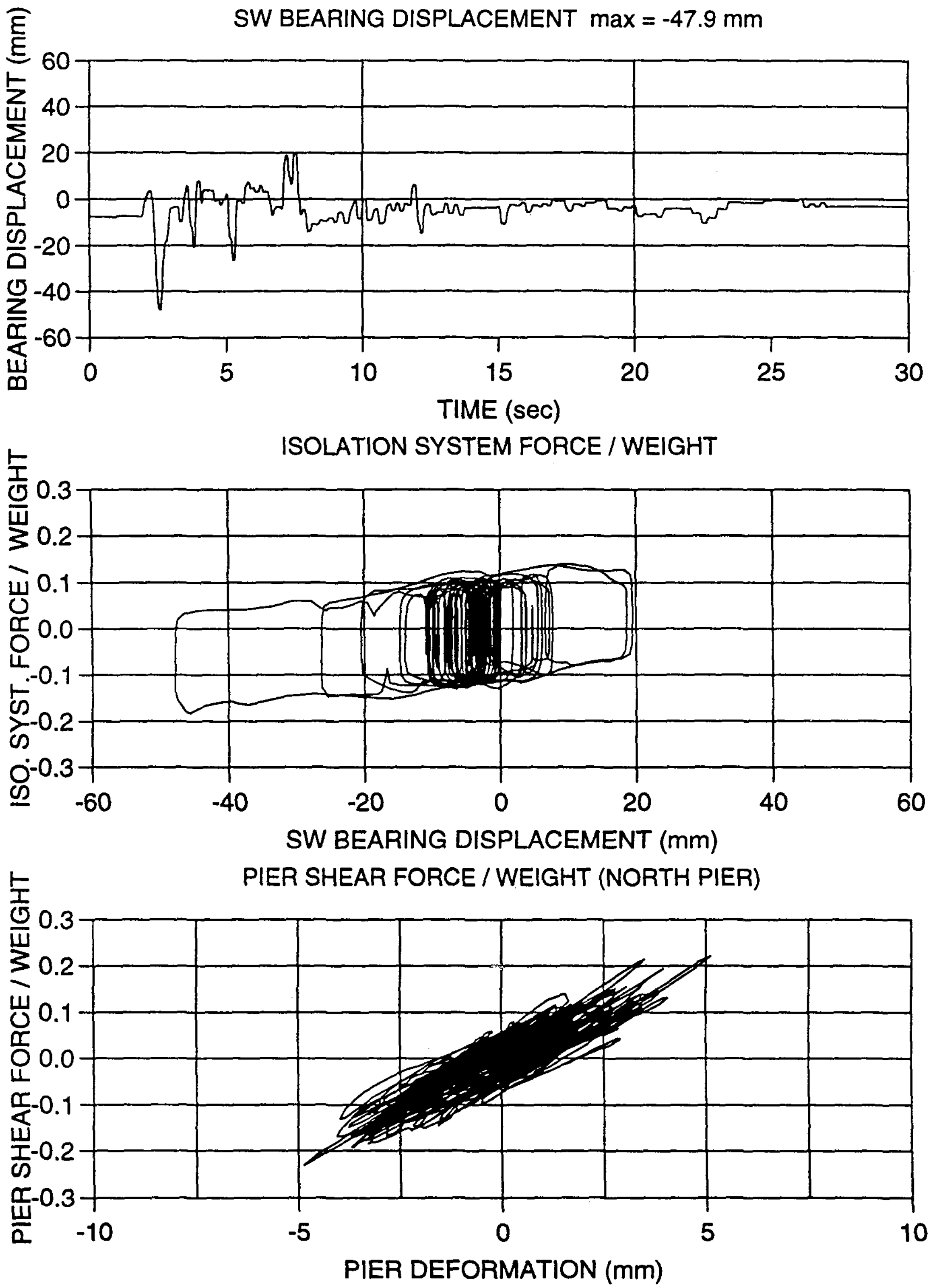

Figure A-28 Taft N21E H+V 400% (FPSAR53)

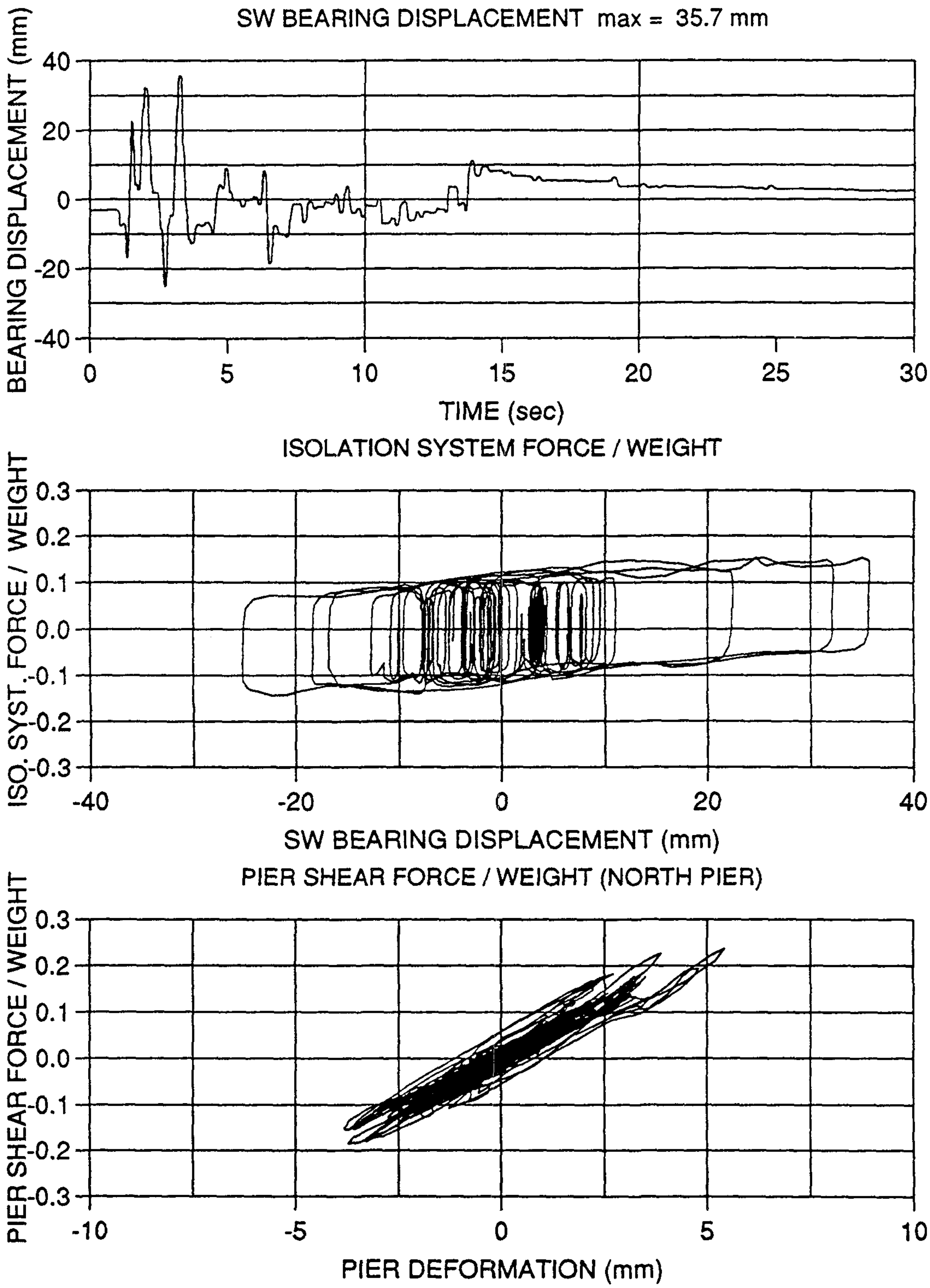

Figure A-29 El Centro S00E H+V 200% (FPSAR54)

NATIONAL CENTER FOR EARTHQUAKE ENGINEERING RESEARCH
LIST OF TECHNICAL REPORTS

The National Center for Earthquake Engineering Research (NCEER) publishes technical reports on a variety of subjects related to earthquake engineering written by authors funded through NCEER. These reports are available from both NCEER's Publications Department and the National Technical Information Service (NTIS). Requests for reports should be directed to the Publications Department, National Center for Earthquake Engineering Research, State University of New York at Buffalo, Red Jacket Quadrangle, Buffalo, New York 14261. Reports can also be requested through NTIS, 5285 Port Royal Road, Springfield, Virginia 22161. NTIS accession numbers are shown in parenthesis, if available.

NCEER-87-0001 "First-Year Program in Research, Education and Technology Transfer," 3/5/87, (PB88-134275).

NCEER-87-0002 "Experimental Evaluation of Instantaneous Optimal Algorithms for Structural Control," by R.C. Lin, T.T. Soong and A.M. Reinhorn, 4/20/87, (PB88-134341).

NCEER-87-0003 "Experimentation Using the Earthquake Simulation Facilities at University at Buffalo," by A.M. Reinhorn and R.L. Ketter, to be published.

NCEER-87-0004 "The System Characteristics and Performance of a Shaking Table," by J.S. Hwang, K.C. Chang and G.C. Lee, 6/1/87, (PB88-134259). This report is available only through NTIS (see address given above).

NCEER-87-0005 "A Finite Element Formulation for Nonlinear Viscoplastic Material Using a Q Model," by O. Gyebi and G. Dasgupta, 11/2/87, (PB88-213764).

NCEER-87-0006 "Symbolic Manipulation Program (SMP) - Algebraic Codes for Two and Three Dimensional Finite Element Formulations," by X. Lee and G. Dasgupta, 11/9/87, (PB88-218522).

NCEER-87-0007 "Instantaneous Optimal Control Laws for Tall Buildings Under Seismic Excitations," by J.N. Yang, A. Akbarpour and P. Ghaemmaghami, 6/10/87, (PB88-134333). This report is only available through NTIS (see address given above).

NCEER-87-0008 "IDARC: Inelastic Damage Analysis of Reinforced Concrete Frame - Shear-Wall Structures," by Y.J. Park, A.M. Reinhorn and S.K. Kunnath, 7/20/87, (PB88-134325).

NCEER-87-0009 "Liquefaction Potential for New York State: A Preliminary Report on Sites in Manhattan and Buffalo," by M. Budhu, V. Vijayakumar, R.F. Giese and L. Baumgras, 8/31/87, (PB88-163704). This report is available only through NTIS (see address given above).

NCEER-87-0010 "Vertical and Torsional Vibration of Foundations in Inhomogeneous Media," by A.S. Veletsos and K.W. Dotson, 6/1/87, (PB88-134291).

NCEER-87-0011 "Seismic Probabilistic Risk Assessment and Seismic Margins Studies for Nuclear Power Plants," by Howard H.M. Hwang, 6/15/87, (PB88-134267).

NCEER-87-0012 "Parametric Studies of Frequency Response of Secondary Systems Under Ground-Acceleration Excitations," by Y. Yong and Y.K. Lin, 6/10/87, (PB88-134309).

NCEER-87-0013 "Frequency Response of Secondary Systems Under Seismic Excitation," by J.A. HoLung, J. Cai and Y.K. Lin, 7/31/87, (PB88-134317).

NCEER-87-0014 "Modelling Earthquake Ground Motions in Seismically Active Regions Using Parametric Time Series Methods," by G.W. Ellis and A.S. Cakmak, 8/25/87, (PB88-134283).

NCEER-87-0015 "Detection and Assessment of Seismic Structural Damage," by E. DiPasquale and A.S. Cakmak, 8/25/87, (PB88-163712).

NCEER-87-0016 "Pipeline Experiment at Parkfield, California," by J. Isenberg and E. Richardson, 9/15/87, (PB88-163720). This report is available only through NTIS (see address given above).

NCEER-87-0017 "Digital Simulation of Seismic Ground Motion," by M. Shinozuka, G. Deodatis and T. Harada, 8/31/87, (PB88-155197). This report is available only through NTIS (see address given above).

NCEER-87-0018 "Practical Considerations for Structural Control: System Uncertainty, System Time Delay and Truncation of Small Control Forces," J.N. Yang and A. Akbarpour, 8/10/87, (PB88-163738).

NCEER-87-0019 "Modal Analysis of Nonclassically Damped Structural Systems Using Canonical Transformation," by J.N. Yang, S. Sarkani and F.X. Long, 9/27/87, (PB88-187851).

NCEER-87-0020 "A Nonstationary Solution in Random Vibration Theory," by J.R. Red-Horse and P.D. Spanos, 11/3/87, (PB88-163746).

NCEER-87-0021 "Horizontal Impedances for Radially Inhomogeneous Viscoelastic Soil Layers," by A.S. Veletsos and K.W. Dotson, 10/15/87, (PB88-150859).

NCEER-87-0022 "Seismic Damage Assessment of Reinforced Concrete Members," by Y.S. Chung, C. Meyer and M. Shinozuka, 10/9/87, (PB88-150867). This report is available only through NTIS (see address given above).

NCEER-87-0023 "Active Structural Control in Civil Engineering," by T.T. Soong, 11/11/87, (PB88-187778).

NCEER-87-0024 "Vertical and Torsional Impedances for Radially Inhomogeneous Viscoelastic Soil Layers," by K.W. Dotson and A.S. Veletsos, 12/87, (PB88-187786).

NCEER-87-0025 "Proceedings from the Symposium on Seismic Hazards, Ground Motions, Soil-Liquefaction and Engineering Practice in Eastern North America," October 20-22, 1987, edited by K.H. Jacob, 12/87, (PB88-188115).

NCEER-87-0026 "Report on the Whittier-Narrows, California, Earthquake of October 1, 1987," by J. Pantelic and A. Reinhorn, 11/87, (PB88-187752). This report is available only through NTIS (see address given above).

NCEER-87-0027 "Design of a Modular Program for Transient Nonlinear Analysis of Large 3-D Building Structures," by S. Srivastav and J.F. Abel, 12/30/87, (PB88-187950).

NCEER-87-0028 "Second-Year Program in Research, Education and Technology Transfer," 3/8/88, (PB88-219480).

NCEER-88-0001 "Workshop on Seismic Computer Analysis and Design of Buildings With Interactive Graphics," by W. McGuire, J.F. Abel and C.H. Conley, 1/18/88, (PB88-187760).

NCEER-88-0002 "Optimal Control of Nonlinear Flexible Structures," by J.N. Yang, F.X. Long and D. Wong, 1/22/88, (PB88-213772).

NCEER-88-0003 "Substructuring Techniques in the Time Domain for Primary-Secondary Structural Systems," by G.D. Manolis and G. Juhn, 2/10/88, (PB88-213780).

NCEER-88-0004 "Iterative Seismic Analysis of Primary-Secondary Systems," by A. Singhal, L.D. Lutes and P.D. Spanos, 2/23/88, (PB88-213798).

NCEER-88-0005 "Stochastic Finite Element Expansion for Random Media," by P.D. Spanos and R. Ghanem, 3/14/88, (PB88-213806).

NCEER-88-0006 "Combining Structural Optimization and Structural Control," by F.Y. Cheng and C.P. Pantelides, 1/10/88, (PB88-213814).

NCEER-88-0007 "Seismic Performance Assessment of Code-Designed Structures," by H.H-M. Hwang, J-W. Jaw and H-J. Shau, 3/20/88, (PB88-219423).

NCEER-88-0008 "Reliability Analysis of Code-Designed Structures Under Natural Hazards," by H.H-M. Hwang, H. Ushiba and M. Shinozuka, 2/29/88, (PB88-229471).

NCEER-88-0009 "Seismic Fragility Analysis of Shear Wall Structures," by J-W Jaw and H.H-M. Hwang, 4/30/88, (PB89-102867).

NCEER-88-0010 "Base Isolation of a Multi-Story Building Under a Harmonic Ground Motion - A Comparison of Performances of Various Systems," by F-G Fan, G. Ahmadi and I.G. Tadjbakhsh, 5/18/88, (PB89-122238).

NCEER-88-0011 "Seismic Floor Response Spectra for a Combined System by Green's Functions," by F.M. Lavelle, L.A. Bergman and P.D. Spanos, 5/1/88, (PB89-102875).

NCEER-88-0012 "A New Solution Technique for Randomly Excited Hysteretic Structures," by G.Q. Cai and Y.K. Lin, 5/16/88, (PB89-102883).

NCEER-88-0013 "A Study of Radiation Damping and Soil-Structure Interaction Effects in the Centrifuge," by K. Weissman, supervised by J.H. Prevost, 5/24/88, (PB89-144703).

NCEER-88-0014 "Parameter Identification and Implementation of a Kinematic Plasticity Model for Frictional Soils," by J.H. Prevost and D.V. Griffiths, to be published.

NCEER-88-0015 "Two- and Three- Dimensional Dynamic Finite Element Analyses of the Long Valley Dam," by D.V. Griffiths and J.H. Prevost, 6/17/88, (PB89-144711).

NCEER-88-0016 "Damage Assessment of Reinforced Concrete Structures in Eastern United States," by A.M. Reinhorn, M.J. Seidel, S.K. Kunnath and Y.J. Park, 6/15/88, (PB89-122220).

NCEER-88-0017 "Dynamic Compliance of Vertically Loaded Strip Foundations in Multilayered Viscoelastic Soils," by S. Ahmad and A.S.M. Israil, 6/17/88, (PB89-102891).

NCEER-88-0018 "An Experimental Study of Seismic Structural Response With Added Viscoelastic Dampers," by R.C. Lin, Z. Liang, T.T. Soong and R.H. Zhang, 6/30/88, (PB89-122212). This report is available only through NTIS (see address given above).

NCEER-88-0019 "Experimental Investigation of Primary - Secondary System Interaction," by G.D. Manolis, G. Juhn and A.M. Reinhorn, 5/27/88, (PB89-122204).

NCEER-88-0020 "A Response Spectrum Approach For Analysis of Nonclassically Damped Structures," by J.N. Yang, S. Sarkani and F.X. Long, 4/22/88, (PB89-102909).

NCEER-88-0021 "Seismic Interaction of Structures and Soils: Stochastic Approach," by A.S. Veletsos and A.M. Prasad, 7/21/88, (PB89-122196).

NCEER-88-0022 "Identification of the Serviceability Limit State and Detection of Seismic Structural Damage," by E. DiPasquale and A.S. Cakmak, 6/15/88, (PB89-122188). This report is available only through NTIS (see address given above).

NCEER-88-0023 "Multi-Hazard Risk Analysis: Case of a Simple Offshore Structure," by B.K. Bhartia and E.H. Vanmarcke, 7/21/88, (PB89-145213).

NCEER-88-0024 "Automated Seismic Design of Reinforced Concrete Buildings," by Y.S. Chung, C. Meyer and M. Shinozuka, 7/5/88, (PB89-122170). This report is available only through NTIS (see address given above).

NCEER-88-0025 "Experimental Study of Active Control of MDOF Structures Under Seismic Excitations," by L.L. Chung, R.C. Lin, T.T. Soong and A.M. Reinhorn, 7/10/88, (PB89-122600).

NCEER-88-0026 "Earthquake Simulation Tests of a Low-Rise Metal Structure," by J.S. Hwang, K.C. Chang, G.C. Lee and R.L. Ketter, 8/1/88, (PB89-102917).

NCEER-88-0027 "Systems Study of Urban Response and Reconstruction Due to Catastrophic Earthquakes," by F. Kozin and H.K. Zhou, 9/22/88, (PB90-162348).

NCEER-88-0028 "Seismic Fragility Analysis of Plane Frame Structures," by H.H-M. Hwang and Y.K. Low, 7/31/88, (PB89-131445).

NCEER-88-0029 "Response Analysis of Stochastic Structures," by A. Kardara, C. Bucher and M. Shinozuka, 9/22/88, (PB89-174429).

NCEER-88-0030 "Nonnormal Accelerations Due to Yielding in a Primary Structure," by D.C.K. Chen and L.D. Lutes, 9/19/88, (PB89-131437).

NCEER-88-0031 "Design Approaches for Soil-Structure Interaction," by A.S. Veletsos, A.M. Prasad and Y. Tang, 12/30/88, (PB89-174437). This report is available only through NTIS (see address given above).

NCEER-88-0032 "A Re-evaluation of Design Spectra for Seismic Damage Control," by C.J. Turkstra and A.G. Tallin, 11/7/88, (PB89-145221).

NCEER-88-0033 "The Behavior and Design of Noncontact Lap Splices Subjected to Repeated Inelastic Tensile Loading," by V.E. Sagan, P. Gergely and R.N. White, 12/8/88, (PB89-163737).

NCEER-88-0034 "Seismic Response of Pile Foundations," by S.M. Mamoon, P.K. Banerjee and S. Ahmad, 11/1/88, (PB89-145239).

NCEER-88-0035 "Modeling of R/C Building Structures With Flexible Floor Diaphragms (IDARC2)," by A.M. Reinhorn, S.K. Kunnath and N. Panahshahi, 9/7/88, (PB89-207153).

NCEER-88-0036 "Solution of the Dam-Reservoir Interaction Problem Using a Combination of FEM, BEM with Particular Integrals, Modal Analysis, and Substructuring," by C-S. Tsai, G.C. Lee and R.L. Ketter, 12/31/88, (PB89-207146).

NCEER-88-0037 "Optimal Placement of Actuators for Structural Control," by F.Y. Cheng and C.P. Pantelides, 8/15/88, (PB89-162846).

NCEER-88-0038 "Teflon Bearings in Aseismic Base Isolation: Experimental Studies and Mathematical Modeling," by A. Mokha, M.C. Constantinou and A.M. Reinhorn, 12/5/88, (PB89-218457). This report is available only through NTIS (see address given above).

NCEER-88-0039 "Seismic Behavior of Flat Slab High-Rise Buildings in the New York City Area," by P. Weidlinger and M. Ettouney, 10/15/88, (PB90-145681).

NCEER-88-0040 "Evaluation of the Earthquake Resistance of Existing Buildings in New York City," by P. Weidlinger and M. Ettouney, 10/15/88, to be published.

NCEER-88-0041 "Small-Scale Modeling Techniques for Reinforced Concrete Structures Subjected to Seismic Loads," by W. Kim, A. El-Attar and R.N. White, 11/22/88, (PB89-189625).

NCEER-88-0042 "Modeling Strong Ground Motion from Multiple Event Earthquakes," by G.W. Ellis and A.S. Cakmak, 10/15/88, (PB89-174445).

NCEER-88-0043 "Nonstationary Models of Seismic Ground Acceleration," by M. Grigoriu, S.E. Ruiz and E. Rosenblueth, 7/15/88, (PB89-189617).

NCEER-88-0044 "SARCF User's Guide: Seismic Analysis of Reinforced Concrete Frames," by Y.S. Chung, C. Meyer and M. Shinozuka, 11/9/88, (PB89-174452).

NCEER-88-0045 "First Expert Panel Meeting on Disaster Research and Planning," edited by J. Pantelic and J. Stoyle, 9/15/88, (PB89-174460).

NCEER-88-0046 "Preliminary Studies of the Effect of Degrading Infill Walls on the Nonlinear Seismic Response of Steel Frames," by C.Z. Chrysostomou, P. Gergely and J.F. Abel, 12/19/88, (PB89-208383).

NCEER-88-0047 "Reinforced Concrete Frame Component Testing Facility - Design, Construction, Instrumentation and Operation," by S.P. Pessiki, C. Conley, T. Bond, P. Gergely and R.N. White, 12/16/88, (PB89-174478).

NCEER-89-0001 "Effects of Protective Cushion and Soil Compliancy on the Response of Equipment Within a Seismically Excited Building," by J.A. HoLung, 2/16/89, (PB89-207179).

NCEER-89-0002 "Statistical Evaluation of Response Modification Factors for Reinforced Concrete Structures," by H.H-M. Hwang and J-W. Jaw, 2/17/89, (PB89-207187).

NCEER-89-0003 "Hysteretic Columns Under Random Excitation," by G-Q. Cai and Y.K. Lin, 1/9/89, (PB89-196513).

NCEER-89-0004 "Experimental Study of 'Elephant Foot Bulge' Instability of Thin-Walled Metal Tanks," by Z-H. Jia and R.L. Ketter, 2/22/89, (PB89-207195).

NCEER-89-0005 "Experiment on Performance of Buried Pipelines Across San Andreas Fault," by J. Isenberg, E. Richardson and T.D. O'Rourke, 3/10/89, (PB89-218440). This report is available only through NTIS (see address given above).

NCEER-89-0006 "A Knowledge-Based Approach to Structural Design of Earthquake-Resistant Buildings," by M. Subramani, P. Gergely, C.H. Conley, J.F. Abel and A.H. Zaghw, 1/15/89, (PB89-218465).

NCEER-89-0007 "Liquefaction Hazards and Their Effects on Buried Pipelines," by T.D. O'Rourke and P.A. Lane, 2/1/89, (PB89-218481).

NCEER-89-0008 "Fundamentals of System Identification in Structural Dynamics," by H. Imai, C-B. Yun, O. Maruyama and M. Shinozuka, 1/26/89, (PB89-207211).

NCEER-89-0009 "Effects of the 1985 Michoacan Earthquake on Water Systems and Other Buried Lifelines in Mexico," by A.G. Ayala and M.J. O'Rourke, 3/8/89, (PB89-207229).

NCEER-89-R010 "NCEER Bibliography of Earthquake Education Materials," by K.E.K. Ross, Second Revision, 9/1/89, (PB90-125352).

NCEER-89-0011 "Inelastic Three-Dimensional Response Analysis of Reinforced Concrete Building Structures (IDARC-3D), Part I - Modeling," by S.K. Kunnath and A.M. Reinhorn, 4/17/89, (PB90-114612).

NCEER-89-0012 "Recommended Modifications to ATC-14," by C.D. Poland and J.O. Malley, 4/12/89, (PB90-108648).

NCEER-89-0013 "Repair and Strengthening of Beam-to-Column Connections Subjected to Earthquake Loading," by M. Corazao and A.J. Durrani, 2/28/89, (PB90-109885).

NCEER-89-0014 "Program EXKAL2 for Identification of Structural Dynamic Systems," by O. Maruyama, C-B. Yun, M. Hoshiya and M. Shinozuka, 5/19/89, (PB90-109877).

NCEER-89-0015 "Response of Frames With Bolted Semi-Rigid Connections, Part I - Experimental Study and Analytical Predictions," by P.J. DiCorso, A.M. Reinhorn, J.R. Dickerson, J.B. Radziminski and W.L. Harper, 6/1/89, to be published.

NCEER-89-0016 "ARMA Monte Carlo Simulation in Probabilistic Structural Analysis," by P.D. Spanos and M.P. Mignolet, 7/10/89, (PB90-109893).

NCEER-89-P017 "Preliminary Proceedings from the Conference on Disaster Preparedness - The Place of Earthquake Education in Our Schools," Edited by K.E.K. Ross, 6/23/89, (PB90-108606).

NCEER-89-0017 "Proceedings from the Conference on Disaster Preparedness - The Place of Earthquake Education in Our Schools," Edited by K.E.K. Ross, 12/31/89, (PB90-207895). This report is available only through NTIS (see address given above).

NCEER-89-0018 "Multidimensional Models of Hysteretic Material Behavior for Vibration Analysis of Shape Memory Energy Absorbing Devices, by E.J. Graesser and F.A. Cozzarelli, 6/7/89, (PB90-164146).

NCEER-89-0019 "Nonlinear Dynamic Analysis of Three-Dimensional Base Isolated Structures (3D-BASIS)," by S. Nagarajaiah, A.M. Reinhorn and M.C. Constantinou, 8/3/89, (PB90-161936). This report is available only through NTIS (see address given above).

NCEER-89-0020 "Structural Control Considering Time-Rate of Control Forces and Control Rate Constraints," by F.Y. Cheng and C.P. Pantelides, 8/3/89, (PB90-120445).

NCEER-89-0021 "Subsurface Conditions of Memphis and Shelby County," by K.W. Ng, T-S. Chang and H-H.M. Hwang, 7/26/89, (PB90-120437).

NCEER-89-0022 "Seismic Wave Propagation Effects on Straight Jointed Buried Pipelines," by K. Elhmadi and M.J. O'Rourke, 8/24/89, (PB90-162322).

NCEER-89-0023 "Workshop on Serviceability Analysis of Water Delivery Systems," edited by M. Grigoriu, 3/6/89, (PB90-127424).

NCEER-89-0024 "Shaking Table Study of a 1/5 Scale Steel Frame Composed of Tapered Members," by K.C. Chang, J.S. Hwang and G.C. Lee, 9/18/89, (PB90-160169).

NCEER-89-0025 "DYNA1D: A Computer Program for Nonlinear Seismic Site Response Analysis - Technical Documentation," by Jean H. Prevost, 9/14/89, (PB90-161944). This report is available only through NTIS (see address given above).

NCEER-89-0026 "1:4 Scale Model Studies of Active Tendon Systems and Active Mass Dampers for Aseismic Protection," by A.M. Reinhorn, T.T. Soong, R.C. Lin, Y.P. Yang, Y. Fukao, H. Abe and M. Nakai, 9/15/89, (PB90-173246).

NCEER-89-0027 "Scattering of Waves by Inclusions in a Nonhomogeneous Elastic Half Space Solved by Boundary Element Methods," by P.K. Hadley, A. Askar and A.S. Cakmak, 6/15/89, (PB90-145699).

NCEER-89-0028 "Statistical Evaluation of Deflection Amplification Factors for Reinforced Concrete Structures," by H.H.M. Hwang, J-W. Jaw and A.L. Ch'ng, 8/31/89, (PB90-164633).

NCEER-89-0029 "Bedrock Accelerations in Memphis Area Due to Large New Madrid Earthquakes," by H.H.M. Hwang, C.H.S. Chen and G. Yu, 11/7/89, (PB90-162330).

NCEER-89-0030 "Seismic Behavior and Response Sensitivity of Secondary Structural Systems," by Y.Q. Chen and T.T. Soong, 10/23/89, (PB90-164658).

NCEER-89-0031 "Random Vibration and Reliability Analysis of Primary-Secondary Structural Systems," by Y. Ibrahim, M. Grigoriu and T.T. Soong, 11/10/89, (PB90-161951).

NCEER-89-0032 "Proceedings from the Second U.S. - Japan Workshop on Liquefaction, Large Ground Deformation and Their Effects on Lifelines, September 26-29, 1989," Edited by T.D. O'Rourke and M. Hamada, 12/1/89, (PB90-209388).

NCEER-89-0033 "Deterministic Model for Seismic Damage Evaluation of Reinforced Concrete Structures," by J.M. Bracci, A.M. Reinhorn, J.B. Mander and S.K. Kunnath, 9/27/89.

NCEER-89-0034 "On the Relation Between Local and Global Damage Indices," by E. DiPasquale and A.S. Cakmak, 8/15/89, (PB90-173865).

NCEER-89-0035 "Cyclic Undrained Behavior of Nonplastic and Low Plasticity Silts," by A.J. Walker and H.E. Stewart, 7/26/89, (PB90-183518).

NCEER-89-0036 "Liquefaction Potential of Surficial Deposits in the City of Buffalo, New York," by M. Budhu, R. Giese and L. Baumgrass, 1/17/89, (PB90-208455).

NCEER-89-0037 "A Deterministic Assessment of Effects of Ground Motion Incoherence," by A.S. Veletsos and Y. Tang, 7/15/89, (PB90-164294).

NCEER-89-0038 "Workshop on Ground Motion Parameters for Seismic Hazard Mapping," July 17-18, 1989, edited by R.V. Whitman, 12/1/89, (PB90-173923).

NCEER-89-0039 "Seismic Effects on Elevated Transit Lines of the New York City Transit Authority," by C.J. Costantino, C.A. Miller and E. Heymsfield, 12/26/89, (PB90-207887).

NCEER-89-0040 "Centrifugal Modeling of Dynamic Soil-Structure Interaction," by K. Weissman, Supervised by J.H. Prevost, 5/10/89, (PB90-207879).

NCEER-89-0041 "Linearized Identification of Buildings With Cores for Seismic Vulnerability Assessment," by I-K. Ho and A.E. Aktan, 11/1/89, (PB90-251943).

NCEER-90-0001 "Geotechnical and Lifeline Aspects of the October 17, 1989 Loma Prieta Earthquake in San Francisco," by T.D. O'Rourke, H.E. Stewart, F.T. Blackburn and T.S. Dickerman, 1/90, (PB90-208596).

NCEER-90-0002 "Nonnormal Secondary Response Due to Yielding in a Primary Structure," by D.C.K. Chen and L.D. Lutes, 2/28/90, (PB90-251976).

NCEER-90-0003 "Earthquake Education Materials for Grades K-12," by K.E.K. Ross, 4/16/90, (PB91-251984).

NCEER-90-0004 "Catalog of Strong Motion Stations in Eastern North America," by R.W. Busby, 4/3/90, (PB90-251984).

NCEER-90-0005 "NCEER Strong-Motion Data Base: A User Manual for the GeoBase Release (Version 1.0 for the Sun3)," by P. Friberg and K. Jacob, 3/31/90 (PB90-258062).

NCEER-90-0006 "Seismic Hazard Along a Crude Oil Pipeline in the Event of an 1811-1812 Type New Madrid Earthquake," by H.H.M. Hwang and C-H.S. Chen, 4/16/90(PB90-258054).

NCEER-90-0007 "Site-Specific Response Spectra for Memphis Sheahan Pumping Station," by H.H.M. Hwang and C.S. Lee, 5/15/90, (PB91-108811).

NCEER-90-0008 "Pilot Study on Seismic Vulnerability of Crude Oil Transmission Systems," by T. Ariman, R. Dobry, M. Grigoriu, F. Kozin, M. O'Rourke, T. O'Rourke and M. Shinozuka, 5/25/90, (PB91-108837).

NCEER-90-0009 "A Program to Generate Site Dependent Time Histories: EQGEN," by G.W. Ellis, M. Srinivasan and A.S. Cakmak, 1/30/90, (PB91-108829).

NCEER-90-0010 "Active Isolation for Seismic Protection of Operating Rooms," by M.E. Talbott, Supervised by M. Shinozuka, 6/8/9, (PB91-110205).

NCEER-90-0011 "Program LINEARID for Identification of Linear Structural Dynamic Systems," by C-B. Yun and M. Shinozuka, 6/25/90, (PB91-110312).

NCEER-90-0012 "Two-Dimensional Two-Phase Elasto-Plastic Seismic Response of Earth Dams," by A.N. Yiagos, Supervised by J.H. Prevost, 6/20/90, (PB91-110197).

NCEER-90-0013 "Secondary Systems in Base-Isolated Structures: Experimental Investigation, Stochastic Response and Stochastic Sensitivity," by G.D. Manolis, G. Juhn, M.C. Constantinou and A.M. Reinhorn, 7/1/90, (PB91-110320).

NCEER-90-0014 "Seismic Behavior of Lightly-Reinforced Concrete Column and Beam-Column Joint Details," by S.P. Pessiki, C.H. Conley, P. Gergely and R.N. White, 8/22/90, (PB91-108795).

NCEER-90-0015 "Two Hybrid Control Systems for Building Structures Under Strong Earthquakes," by J.N. Yang and A. Danielians, 6/29/90, (PB91-125393).

NCEER-90-0016 "Instantaneous Optimal Control with Acceleration and Velocity Feedback," by J.N. Yang and Z. Li, 6/29/90, (PB91-125401).

NCEER-90-0017 "Reconnaissance Report on the Northern Iran Earthquake of June 21, 1990," by M. Mehrain, 10/4/90, (PB91-125377).

NCEER-90-0018 "Evaluation of Liquefaction Potential in Memphis and Shelby County," by T.S. Chang, P.S. Tang, C.S. Lee and H. Hwang, 8/10/90, (PB91-125427).

NCEER-90-0019 "Experimental and Analytical Study of a Combined Sliding Disc Bearing and Helical Steel Spring Isolation System," by M.C. Constantinou, A.S. Mokha and A.M. Reinhorn, 10/4/90, (PB91-125385).

NCEER-90-0020 "Experimental Study and Analytical Prediction of Earthquake Response of a Sliding Isolation System with a Spherical Surface," by A.S. Mokha, M.C. Constantinou and A.M. Reinhorn, 10/11/90, (PB91-125419).

NCEER-90-0021 "Dynamic Interaction Factors for Floating Pile Groups," by G. Gazetas, K. Fan, A. Kaynia and E. Kausel, 9/10/90, (PB91-170381).

NCEER-90-0022 "Evaluation of Seismic Damage Indices for Reinforced Concrete Structures," by S. Rodriguez-Gomez and A.S. Cakmak, 9/30/90, PB91-171322).

NCEER-90-0023 "Study of Site Response at a Selected Memphis Site," by H. Desai, S. Ahmad, E.S. Gazetas and M.R. Oh, 10/11/90, (PB91-196857).

NCEER-90-0024 "A User's Guide to Strongmo: Version 1.0 of NCEER's Strong-Motion Data Access Tool for PCs and Terminals," by P.A. Friberg and C.A.T. Susch, 11/15/90, (PB91-171272).

NCEER-90-0025 "A Three-Dimensional Analytical Study of Spatial Variability of Seismic Ground Motions," by L-L. Hong and A.H.-S. Ang, 10/30/90, (PB91-170399).

NCEER-90-0026 "MUMOID User's Guide - A Program for the Identification of Modal Parameters," by S. Rodriguez-Gomez and E. DiPasquale, 9/30/90, (PB91-171298).

NCEER-90-0027 "SARCF-II User's Guide - Seismic Analysis of Reinforced Concrete Frames," by S. Rodriguez-Gomez, Y.S. Chung and C. Meyer, 9/30/90, (PB91-171280).

NCEER-90-0028 "Viscous Dampers: Testing, Modeling and Application in Vibration and Seismic Isolation," by N. Makris and M.C. Constantinou, 12/20/90 (PB91-190561).

NCEER-90-0029 "Soil Effects on Earthquake Ground Motions in the Memphis Area," by H. Hwang, C.S. Lee, K.W. Ng and T.S. Chang, 8/2/90, (PB91-190751).

NCEER-91-0001 "Proceedings from the Third Japan-U.S. Workshop on Earthquake Resistant Design of Lifeline Facilities and Countermeasures for Soil Liquefaction, December 17-19, 1990," edited by T.D. O'Rourke and M. Hamada, 2/1/91, (PB91-179259).

NCEER-91-0002 "Physical Space Solutions of Non-Proportionally Damped Systems," by M. Tong, Z. Liang and G.C. Lee, 1/15/91, (PB91-179242).

NCEER-91-0003 "Seismic Response of Single Piles and Pile Groups," by K. Fan and G. Gazetas, 1/10/91, (PB92-174994).

NCEER-91-0004 "Damping of Structures: Part 1 - Theory of Complex Damping," by Z. Liang and G. Lee, 10/10/91, (PB92-197235).

NCEER-91-0005 "3D-BASIS - Nonlinear Dynamic Analysis of Three Dimensional Base Isolated Structures: Part II," by S. Nagarajaiah, A.M. Reinhorn and M.C. Constantinou, 2/28/91, (PB91-190553).

NCEER-91-0006 "A Multidimensional Hysteretic Model for Plasticity Deforming Metals in Energy Absorbing Devices," by E.J. Graesser and F.A. Cozzarelli, 4/9/91, (PB92-108364).

NCEER-91-0007 "A Framework for Customizable Knowledge-Based Expert Systems with an Application to a KBES for Evaluating the Seismic Resistance of Existing Buildings," by E.G. Ibarra-Anaya and S.J. Fenves, 4/9/91, (PB91-210930).

NCEER-91-0008 "Nonlinear Analysis of Steel Frames with Semi-Rigid Connections Using the Capacity Spectrum Method," by G.G. Deierlein, S-H. Hsieh, Y-J. Shen and J.F. Abel, 7/2/91, (PB92-113828).

NCEER-91-0009 "Earthquake Education Materials for Grades K-12," by K.E.K. Ross, 4/30/91, (PB91-212142).

NCEER-91-0010 "Phase Wave Velocities and Displacement Phase Differences in a Harmonically Oscillating Pile," by N. Makris and G. Gazetas, 7/8/91, (PB92-108356).

NCEER-91-0011 "Dynamic Characteristics of a Full-Size Five-Story Steel Structure and a 2/5 Scale Model," by K.C. Chang, G.C. Yao, G.C. Lee, D.S. Hao and Y.C. Yeh," 7/2/91, (PB93-116648).

NCEER-91-0012 "Seismic Response of a 2/5 Scale Steel Structure with Added Viscoelastic Dampers," by K.C. Chang, T.T. Soong, S-T. Oh and M.L. Lai, 5/17/91, (PB92-110816).

NCEER-91-0013 "Earthquake Response of Retaining Walls; Full-Scale Testing and Computational Modeling," by S. Alampalli and A-W.M. Elgamal, 6/20/91, to be published.

NCEER-91-0014 "3D-BASIS-M: Nonlinear Dynamic Analysis of Multiple Building Base Isolated Structures," by P.C. Tsopelas, S. Nagarajaiah, M.C. Constantinou and A.M. Reinhorn, 5/28/91, (PB92-113885).

NCEER-91-0015 "Evaluation of SEAOC Design Requirements for Sliding Isolated Structures," by D. Theodossiou and M.C. Constantinou, 6/10/91, (PB92-114602).

NCEER-91-0016 "Closed-Loop Modal Testing of a 27-Story Reinforced Concrete Flat Plate-Core Building," by H.R. Somaprasad, T. Toksoy, H. Yoshiyuki and A.E. Aktan, 7/15/91, (PB92-129980).

NCEER-91-0017 "Shake Table Test of a 1/6 Scale Two-Story Lightly Reinforced Concrete Building," by A.G. El-Attar, R.N. White and P. Gergely, 2/28/91, (PB92-222447).

NCEER-91-0018 "Shake Table Test of a 1/8 Scale Three-Story Lightly Reinforced Concrete Building," by A.G. El-Attar, R.N. White and P. Gergely, 2/28/91, (PB93-116630).

NCEER-91-0019 "Transfer Functions for Rigid Rectangular Foundations," by A.S. Veletsos, A.M. Prasad and W.H. Wu, 7/31/91.

NCEER-91-0020 "Hybrid Control of Seismic-Excited Nonlinear and Inelastic Structural Systems," by J.N. Yang, Z. Li and A. Danielians, 8/1/91, (PB92-143171).

NCEER-91-0021 "The NCEER-91 Earthquake Catalog: Improved Intensity-Based Magnitudes and Recurrence Relations for U.S. Earthquakes East of New Madrid," by L. Seeber and J.G. Armbruster, 8/28/91, (PB92-176742).

NCEER-91-0022 "Proceedings from the Implementation of Earthquake Planning and Education in Schools: The Need for Change - The Roles of the Changemakers," by K.E.K. Ross and F. Winslow, 7/23/91, (PB92-129998).

NCEER-91-0023 "A Study of Reliability-Based Criteria for Seismic Design of Reinforced Concrete Frame Buildings," by H.H.M. Hwang and H-M. Hsu, 8/10/91, (PB92-140235).

NCEER-91-0024 "Experimental Verification of a Number of Structural System Identification Algorithms," by R.G. Ghanem, H. Gavin and M. Shinozuka, 9/18/91, (PB92-176577).

NCEER-91-0025 "Probabilistic Evaluation of Liquefaction Potential," by H.H.M. Hwang and C.S. Lee," 11/25/91, (PB92-143429).

NCEER-91-0026 "Instantaneous Optimal Control for Linear, Nonlinear and Hysteretic Structures - Stable Controllers," by J.N. Yang and Z. Li, 11/15/91, (PB92-163807).

NCEER-91-0027 "Experimental and Theoretical Study of a Sliding Isolation System for Bridges," by M.C. Constantinou, A. Kartoum, A.M. Reinhorn and P. Bradford, 11/15/91, (PB92-176973).

NCEER-92-0001 "Case Studies of Liquefaction and Lifeline Performance During Past Earthquakes, Volume 1: Japanese Case Studies," Edited by M. Hamada and T. O'Rourke, 2/17/92, (PB92-197243).

NCEER-92-0002 "Case Studies of Liquefaction and Lifeline Performance During Past Earthquakes, Volume 2: United States Case Studies," Edited by T. O'Rourke and M. Hamada, 2/17/92, (PB92-197250).

NCEER-92-0003 "Issues in Earthquake Education," Edited by K. Ross, 2/3/92, (PB92-222389).

NCEER-92-0004 "Proceedings from the First U.S. - Japan Workshop on Earthquake Protective Systems for Bridges," Edited by I.G. Buckle, 2/4/92.

NCEER-92-0005 "Seismic Ground Motion from a Haskell-Type Source in a Multiple-Layered Half-Space," A.P. Theoharis, G. Deodatis and M. Shinozuka, 1/2/92, to be published.

NCEER-92-0006 "Proceedings from the Site Effects Workshop," Edited by R. Whitman, 2/29/92, (PB92-197201).

NCEER-92-0007 "Engineering Evaluation of Permanent Ground Deformations Due to Seismically-Induced Liquefaction," by M.H. Baziar, R. Dobry and A-W.M. Elgamal, 3/24/92, (PB92-222421).

NCEER-92-0008 "A Procedure for the Seismic Evaluation of Buildings in the Central and Eastern United States," by C.D. Poland and J.O. Malley, 4/2/92, (PB92-222439).

NCEER-92-0009 "Experimental and Analytical Study of a Hybrid Isolation System Using Friction Controllable Sliding Bearings," by M.Q. Feng, S. Fujii and M. Shinozuka, 5/15/92, (PB93-150282).

NCEER-92-0010 "Seismic Resistance of Slab-Column Connections in Existing Non-Ductile Flat-Plate Buildings," by A.J. Durrani and Y. Du, 5/18/92.

NCEER-92-0011 "The Hysteretic and Dynamic Behavior of Brick Masonry Walls Upgraded by Ferrocement Coatings Under Cyclic Loading and Strong Simulated Ground Motion," by H. Lee and S.P. Prawel, 5/11/92, to be published.

NCEER-92-0012 "Study of Wire Rope Systems for Seismic Protection of Equipment in Buildings," by G.F. Demetriades, M.C. Constantinou and A.M. Reinhorn, 5/20/92.

NCEER-92-0013 "Shape Memory Structural Dampers: Material Properties, Design and Seismic Testing," by P.R. Witting and F.A. Cozzarelli, 5/26/92.

NCEER-92-0014 "Longitudinal Permanent Ground Deformation Effects on Buried Continuous Pipelines," by M.J. O'Rourke, and C. Nordberg, 6/15/92.

NCEER-92-0015 "A Simulation Method for Stationary Gaussian Random Functions Based on the Sampling Theorem," by M. Grigoriu and S. Balopoulou, 6/11/92, (PB93-127496).

NCEER-92-0016 "Gravity-Load-Designed Reinforced Concrete Buildings: Seismic Evaluation of Existing Construction and Detailing Strategies for Improved Seismic Resistance," by G.W. Hoffmann, S.K. Kunnath, A.M. Reinhorn and J.B. Mander, 7/15/92.

NCEER-92-0017 "Observations on Water System and Pipeline Performance in the Limón Area of Costa Rica Due to the April 22, 1991 Earthquake," by M. O'Rourke and D. Ballantyne, 6/30/92, (PB93-126811).

NCEER-92-0018 "Fourth Edition of Earthquake Education Materials for Grades K-12," Edited by K.E.K. Ross, 8/10/92.

NCEER-92-0019 "Proceedings from the Fourth Japan-U.S. Workshop on Earthquake Resistant Design of Lifeline Facilities and Countermeasures for Soil Liquefaction," Edited by M. Hamada and T.D. O'Rourke, 8/12/92, (PB93-163939).

NCEER-92-0020 "Active Bracing System: A Full Scale Implementation of Active Control," by A.M. Reinhorn, T.T. Soong, R.C. Lin, M.A. Riley, Y.P. Wang, S. Aizawa and M. Higashino, 8/14/92, (PB93-127512).

NCEER-92-0021 "Empirical Analysis of Horizontal Ground Displacement Generated by Liquefaction-Induced Lateral Spreads," by S.F. Bartlett and T.L. Youd, 8/17/92, (PB93-188241).

NCEER-92-0022 "IDARC Version 3.0: Inelastic Damage Analysis of Reinforced Concrete Structures," by S.K. Kunnath, A.M. Reinhorn and R.F. Lobo, 8/31/92, (PB93-227502, A07, MF-A02).

NCEER-92-0023 "A Semi-Empirical Analysis of Strong-Motion Peaks in Terms of Seismic Source, Propagation Path and Local Site Conditions, by M. Kamiyama, M.J. O'Rourke and R. Flores-Berrones, 9/9/92, (PB93-150266).

NCEER-92-0024 "Seismic Behavior of Reinforced Concrete Frame Structures with Nonductile Details, Part I: Summary of Experimental Findings of Full Scale Beam-Column Joint Tests," by A. Beres, R.N. White and P. Gergely, 9/30/92, (PB93-227783, A05, MF-A01).

NCEER-92-0025 "Experimental Results of Repaired and Retrofitted Beam-Column Joint Tests in Lightly Reinforced Concrete Frame Buildings," by A. Beres, S. El-Borgi, R.N. White and P. Gergely, 10/29/92, (PB93-227791, A05, MF-A01).

NCEER-92-0026 "A Generalization of Optimal Control Theory: Linear and Nonlinear Structures," by J.N. Yang, Z. Li and S. Vongchavalitkul, 11/2/92, (PB93-188621).

NCEER-92-0027 "Seismic Resistance of Reinforced Concrete Frame Structures Designed Only for Gravity Loads: Part I - Design and Properties of a One-Third Scale Model Structure," by J.M. Bracci, A.M. Reinhorn and J.B. Mander, 12/1/92.

NCEER-92-0028 "Seismic Resistance of Reinforced Concrete Frame Structures Designed Only for Gravity Loads: Part II - Experimental Performance of Subassemblages," by L.E. Aycardi, J.B. Mander and A.M. Reinhorn, 12/1/92.

NCEER-92-0029 "Seismic Resistance of Reinforced Concrete Frame Structures Designed Only for Gravity Loads: Part III - Experimental Performance and Analytical Study of a Structural Model," by J.M. Bracci, A.M. Reinhorn and J.B. Mander, 12/1/92, (PB93-227528, A09, MF-A01).

NCEER-92-0030 "Evaluation of Seismic Retrofit of Reinforced Concrete Frame Structures: Part I - Experimental Performance of Retrofitted Subassemblages," by D. Choudhuri, J.B. Mander and A.M. Reinhorn, 12/8/92.

NCEER-92-0031 "Evaluation of Seismic Retrofit of Reinforced Concrete Frame Structures: Part II - Experimental Performance and Analytical Study of a Retrofitted Structural Model," by J.M. Bracci, A.M. Reinhorn and J.B. Mander, 12/8/92.

NCEER-92-0032 "Experimental and Analytical Investigation of Seismic Response of Structures with Supplemental Fluid Viscous Dampers," by M.C. Constantinou and M.D. Symans, 12/21/92, (PB93-191435).

NCEER-92-0033 "Reconnaissance Report on the Cairo, Egypt Earthquake of October 12, 1992," by M. Khater, 12/23/92, (PB93-188621).

NCEER-92-0034 "Low-Level Dynamic Characteristics of Four Tall Flat-Plate Buildings in New York City," by H. Gavin, S. Yuan, J. Grossman, E. Pekelis and K. Jacob, 12/28/92, (PB93-188217).

NCEER-93-0001 "An Experimental Study on the Seismic Performance of Brick-Infilled Steel Frames With and Without Retrofit," by J.B. Mander, B. Nair, K. Wojtkowski and J. Ma, 1/29/93, (PB93-227510, A07, MF-A02).

NCEER-93-0002 "Social Accounting for Disaster Preparedness and Recovery Planning," by S. Cole, E. Pantoja and V. Razak, 2/22/93, to be published.

NCEER-93-0003 "Assessment of 1991 NEHRP Provisions for Nonstructural Components and Recommended Revisions," by T.T. Soong, G. Chen, Z. Wu, R-H. Zhang and M. Grigoriu, 3/1/93, (PB93-188639).

NCEER-93-0004 "Evaluation of Static and Response Spectrum Analysis Procedures of SEAOC/UBC for Seismic Isolated Structures," by C.W. Winters and M.C. Constantinou, 3/23/93, (PB93-198299).

NCEER-93-0005 "Earthquakes in the Northeast - Are We Ignoring the Hazard? A Workshop on Earthquake Science and Safety for Educators," edited by K.E.K. Ross, 4/2/93, (PB94-103066, A09, MF-A02).

NCEER-93-0006 "Inelastic Response of Reinforced Concrete Structures with Viscoelastic Braces," by R.F. Lobo, J.M. Bracci, K.L. Shen, A.M. Reinhorn and T.T. Soong, 4/5/93, (PB93-227486, A05, MF-A02).

NCEER-93-0007 "Seismic Testing of Installation Methods for Computers and Data Processing Equipment," by K. Kosar, T.T. Soong, K.L. Shen, J.A. HoLung and Y.K. Lin, 4/12/93, (PB93-198299).

NCEER-93-0008 "Retrofit of Reinforced Concrete Frames Using Added Dampers," by A. Reinhorn, M. Constantinou and C. Li, to be published.

NCEER-93-0009 "Seismic Applications of Viscoelastic Dampers to Steel Frame Structures," by K.C. Chang and T.T. Soong, to be published.

NCEER-93-0010 "Seismic Performance of Shear-Critical Reinforced Concrete Bridge Piers," by J.B. Mander, S.M. Waheed, M.T.A. Chaudhary and S.S. Chen, 5/12/93, (PB93-227494, A08, MF-A02).

NCEER-93-0011 "3D-BASIS-TABS: Computer Program for Nonlinear Dynamic Analysis of Three Dimensional Base Isolated Structures," by S. Nagarajaiah, C. Li, A.M. Reinhorn and M.C. Constantinou, 8/2/93.

NCEER-93-0012 "Effects of Hydrocarbon Spills from an Oil Pipeline Break on Ground Water," by O.J. Helweg and H.H.M. Hwang, 8/3/93.

NCEER-93-0013 "Simplified Procedures for Seismic Design of Nonstructural Components and Assessment of Current Code Provisions," by M.P. Singh, L.E. Suarez, E.E. Matheu and G.O. Maldonado, 8/4/93.

NCEER-93-0014 "An Energy Approach to Seismic Analysis and Design of Secondary Systems," by G. Chen and T.T. Soong, 8/6/93.

NCEER-93-0015 "Proceedings from School Sites: Becoming Prepared for Earthquakes - Commemorating the Third Anniversary of the Loma Prieta Earthquake," Edited by F.E. Winslow and K.E.K. Ross, 8/16/93, to be published.

NCEER-93-0016 "Reconnaissance Report of Damage to Historic Monuments in Cairo, Egypt Following the October 12, 1992 Dahshur Earthquake," by D. Sykora, D. Look, G. Croci, E. Karaesmen and E. Karaesmen, 8/19/93.

NCEER-93-0017 "The Island of Guam Earthquake of August 8, 1993," by S.W. Swan and S.K. Harris, 9/30/93.

NCEER-93-0018 "Engineering Aspects of the October 12, 1992 Egyptian Earthquake," by A.W. Elgamal, M. Amer, K. Adalier and A. Abul-Fadl, 10/7/93.

NCEER-93-0019 "Development of an Earthquake Motion Simulator and its Application in Dynamic Centrifuge Testing," by I. Krstelj, Supervised by J.H. Prevost, 10/23/93.

NCEER-93-0020 "NCEER-Taisei Corporation Research Program on Sliding Seismic Isolation Systems for Bridges: Experimental and Analytical Study of a Friction Pendulum System (FPS)," by M.C. Constantinou, P. Tsopelas, Y-S. Kim and S. Okamoto, 11/1/93.